The University Of Sheffield.

Access To Thesis.

- A bound copy of every thesis which is accepted as worthy for a higher degree, must be deposited in the University of Sheffield Library, where it will be made available for borrowing or consultation in accordance with University Regulations.
- All students registering from 2008–09 onwards are also required to submit an electronic copy of their final, approved thesis. Students who registered prior to 2008–09 may also submit electronically, but this is not required.

Author: Saila Ismail Dept: Infection and Immunity

Thesis Title: The regulation of inflammatory responses of airway e Registration No: 90253333

For completion by all students:

Submit in print form only (for deposit in the University Library): ☐

Submit in print form and also upload to the *White Rose eTheses Online* server: In full ☑

Edited eThesis ☐

Please indicate if there are any embargo restrictions on this thesis. Please note that if no boxes are ticked, you will have consented to your thesis being made available without any restrictions.

Embargo details: (complete only if requesting an embargo to either your print and/or eThesis)	Embargo required?		Length of embargo (in years)
Print Thesis	Yes ☐	No ☑	_____
eThesis	Yes ☐	No ☑	_____

Supervisor: I, the supervisor, agree to the named thesis being made available under the conditions specified above.

Name: Prof. Ian Sabroe Dept: Infection and Immunity

Signed: Signed electronically Ian Sabroe Date: Sunday, 27 September 2015

Student: I, the author, agree to the named thesis being made available under the conditions specified above.

I give permission to the University of Sheffield to reproduce the print thesis in whole or in part in order to supply single copies for the purpose of research or private study for a non-commercial purpose.

I confirm that this thesis is my own work, and where materials owned by a third party have been used copyright clearance has been obtained. I am aware of the University's *Guidance on the Use of Unfair Means* (www.sheffield.ac.uk/lets/design/unfair)

I confirm that all copies of the thesis submitted to the University (including electronic copies on CD/DVD) are identical in content.

Name: Saila Ismail Dept: Infection and Immunity

Signed: Signed electronically Saila Ismail Date: 22 September 2015

For completion by students also submitting an electronic thesis (eThesis):

I, the author, agree that the University of Sheffield's eThesis repository (currently WREO) will make my eThesis available over the internet via an entirely non-exclusive agreement and that, without changing content, WREO may convert my thesis to any medium or format for the purpose of future preservation and accessibility.

I, the author, agree that the metadata relating to the eThesis will normally appear on both the University's eThesis server and the British Library's EThOS service, even if the thesis is subject to an embargo. I agree that a copy of the eThesis may be supplied to the British Library.

I confirm that the upload is identical to the final, examined and awarded version of the thesis as submitted in print to the University for deposit in the Library (unless edited as indicated above).

Name: Saila Ismail Dept: Infection and Immunity

Signed: Signed electronically Saila Ismail Date: 22 September 2015

THIS SHEET MUST BE BOUND IN THE FRONT OF THE PRINTED THESIS BEFORE IT IS SUBMITTED

The University Of Sheffield.

The regulation of inflammatory responses of airway epithelial cells and fibroblasts to rhinoviral infection

Saila Ismail

Thesis submitted for the degree of Doctor of Philosophy

Department of Infection and Immunity

September 2015

Abstract

Human rhinoviral (RV) infection is a major trigger of exacerbations of airway diseases such as asthma and COPD. Whilst many studies have shown that RV-infected airway epithelial cells secrete many proinflammatory cytokines that may exacerbate airway inflammation, limited studies have sought to investigate the potential role of airway fibroblasts in mediating RV-induced inflammation in airway diseases. Furthermore, the signalling pathways involved in the regulation of cytokine responses of structural airway cells to RV infection remain unclear, particularly with regard to signalling via PI3K, and the PI3K-dependent pathway, autophagy.

The first aim of this thesis was to investigate the innate immune responses of human airway fibroblasts to RV infection, and to compare those responses with those of airway epithelial cells. It was found that RV infection induced differential responses in normal human airway fibroblasts and epithelial cells. In comparison to airway epithelial cells, the lack of viral-detecting PRRs TLR3, RIG-I, MDA5 and virally-induced transcription factors IRF1 and IRF7 in fibroblasts may be a potential explanation as to why the fibroblasts do not secrete the IFN-stimulated cytokines CCL5 and CXCL10 (indicating that the RV-infected fibroblasts do not produce IFNs), therefore providing no antiviral response to limit viral replication, with concomitant cell death. The work presented here demonstrated the permissiveness of lung fibroblasts isolated from idiopathic pulmonary fibrosis (IPF) patients to RV infection. This study also showed the ability of IL-1β to enhance proinflammatory responses of RV-infected epithelial cells. Furthermore, it was demonstrated that in the presence of monocytes, RV and bacterial-derived LPS coinfections could act in synergy to augment the proinflammatory responses of airway tissue cells.

The second aim of this thesis was to determine whether the PI3K-dependent pathway autophagy is involved in the detection of RV infection, and therefore regulates the RV-induced responses of airway epithelial cells. It was found that the PI3K pharmacological inhibitor 3-MA, typically used to inhibit autophagy, suppressed RV-induced cytokine production in airway epithelial cells. In contrast to the actions of 3-MA, specific targeting of the autophagy proteins Bec1, LC3, Atg7, or the autophagy-specific class III PI3K Vps34 by siRNA had very modest effects on RV-induced cytokine responses. Knockdown of autophagy proteins by siRNA also had minimal effects on RV replication. However, it was found that RV infection induced autophagy in the airway epithelial cells, although additional

work is required to confirm this finding. Subsequent experiments performed using a panel of broad and class I-selective PI3K small-molecule inhibitors demonstrated functional redundancy of class I PI3K isoforms in modulating the RV-induced inflammation. The PI3K inhibitors 3-MA and LY294002 also remarkably reduced viral replication, suggesting that PI3Ks exert their roles in controlling RV infection via multiple mechanisms. Moreover, preliminary data suggests a potential role for mTOR in regulating the proinflammatory responses to RV infection.

In conclusion, the work outlined in this thesis demonstrates two major findings: (i) a potential role for lung fibroblasts in mediating airway inflammation following RV infection and (ii) the involvement of PI3Ks and mTOR in induction of proinflammatory cytokines in response to RV infection, and that autophagy plays a limited role in the cytokine response to RV infection or control of RV replication.

Acknowledgements

First and foremost, I would like to express my deep gratitude and thanks to my supervisors, Dr. Lisa Parker and Prof. Ian Sabroe, for their expert guidance, teachings and continued support throughout my journey of a PhD studentship. I would like to say thank you for having constant faith in me and encouraging me when I felt that there was no hope. I am really grateful to have had to work with you.

I would also like to thank everyone in the Department of Infection and Immunity, particularly everybody in the Sabroe lab, past or present, who have offered their help and expertise. I would especially like to thank Dr. Clare Stokes, Claudia Paiva and Dr. Linda Kay for helping me with various laboratory techniques. Also, thanks to my personal tutor, Dr. Lynne Prince, for her support and encouragement.

Special thanks go to my parents, my siblings and my fiancée in Malaysia. Despite being over the other side of the world, their unconditional love and support are the strongest motivation. Also, thank you to my housemates and friends for the great times we had here in Sheffield!

Las but not least, I would like to thank the University of Sheffield, UK and Putra University, Malaysia, for funding this project and giving me the financial support.

Publications and Conference Abstract

Publications arising from this thesis

Stokes, C. A., **Ismail, S.**, Dick, E.P., Bennett, J.A. Johnston, S.L., Edwards, M.R., Sabroe, I., Parker, L.C. (2011). "Role of interleukin-1 and MyD88-dependent signaling in rhinovirus infection." *Journal of Virology*. 85(15): 7912-7921.

Ismail, S., Stokes, C.A., Prestwich, E.C., Roberts, R.L., Juss, J.K., Sabroe, I., Parker, L.C. (2014). "Phosphoinositide-3 kinase inhibition modulates responses to rhinovirus by mechanisms that are predominantly independent of autophagy." *PLoS One*. 9(12): e116055.

Conference abstract

Ismail, S., Stokes, C.A., Juss, J.K., Sabroe, I., Parker, L.C. "Phosphoinositide-3 kinase inhibition modulates responses to rhinovirus by mechanisms that are predominantly independent of autophagy." Gordon Research Conference: Viruses and Cells. Lucca, Italy. May 5-10, 2013.

Table of Contents

List of Figures

List of Tables

List of Abbreviations

3-MA	3-methyladenine
Abs	Antibodies
AMPK	Adenosine 5’-monophosphate-activated protein kinase
AP-1	Activator protein-1
ASMCs	Airway smooth muscle cells
Atg	Autophagy-related gene
Baf	Bafilomycin A1
BALF	Bronchoalveolar lavage fluid
BEAS-2B	Human bronchial epithelial cell line
BEBM	Bronchial Epithelial Basal Media
Bec1	Beclin-1
BEGM	Bronchial Epithelial Growth Media
BMDCs	Bone marrow-derived dendritic cells
CARD	Caspase recruitment domain
CCL	CC-chemokine ligand
COPD	Chronic obstructive pulmonary disease
CSE	Cigarette smoke extract
CTD	C-terminal domain
DAMPs	Damage-associated molecular patterns
DAPI	4',6-diamidino-2-phenylindole
DCs	Dendritic cells
DNA	Deoxyribonucleic acid
dsRNA	Double-stranded RNA
ER	Endoplasmic reticulum
ECM	Extracellular matrix
ELISA	Enzyme-linked immunosorbent assay
FADD	Fas-associated death domain
FCS	Fetal calf serum
Fig.	Figure
h	hour
GBD	Global burden of disease

GFP	Green fluorescent protein
GOLD	Global Initiative for Obstructive Lung Disease
HBECs	Human bronchial epithelial cells
HBSS	Hank's balanced salt solution
HEK293	Human embryonic kidney 293 cells
HeLa	Human cervical epithelial cell line
HIV-1	Human immunodeficiency virus type 1
HLFs	Human lung fibroblasts
HMGB1	High-mobility group box 1
HSV	Herpes simplex virus
IC_{50}	Concentration of an inhibitor where the response is reduced by half
ICAM-1	Intercellular adhesion molecule-1
ICS	Inhaled corticosteroid
IFN	Interferon
IFNAR	IFN-α/β receptor
IFNLR	IFN-λ receptor
Ig	Immunoglobulin
IκB	Inhibitory κB
IKK	IκB kinase
IL-1R	IL-1 receptor
IL-1ra	IL-1 receptor antagonist
IL-1RAacp	IL-1 receptor accessory protein
IPF	Idiopathic pulmonary fibrosis
IPFFs	Idiopathic Pulmonary Fibrosis patient fibroblasts
IRAK	IL-1R-associated kinase
IRF	IFN regulatory factor
ISGs	IFN-stimulated genes
ISGF3	IFN-stimulated gene factor 3
Jak	Janus kinase
LC3	Light chain 3
LD	Limit of detection
LDLR	Low-density lipoprotein receptor
LFBM	Lung Fibroblast Basal Media

LFGM	Lung Fibroblast Growth Media
LPS	Lipopolysaccharide
LRR	Leucine-rich repeat
MAPK	Mitogen-activated protein kinase
MAVS	Mitochondrial antiviral signaling protein
MDA5	Melanoma differentiation associated gene 5
MEFs	Mouse embryonic fibroblasts
min	minutes
MMP	Matrix metalloproteinase
MOI	Multiplicity of infection
mTOR	Mammalian target of rapamycin
MyD88	Myeloid Differentiation factor 88
NAP1	NF-κB-activating kinase (NAK)-associated protein 1
NF-κB	Nuclear factor-κB
NLR	NOD-like receptor
NOD	Nucleotide-binding oligomerisation domain
OD	Optical density
PAMPs	Pathogen-associated molecular patterns
PBMC	Peripheral Blood Mononuclear Cell
PCR	Polymerase chain reaction
PDPK1	3-phosphoinositide dependent protein kinase 1
PE	Phosphatidylethanolamine
p.i.	post-infection
PI3K	Phosphoinositide 3-kinase
Poly(I:C)	Polyinosinic : polycytidylic acid
PRR	Pattern recognition receptor
PtdIns	Phosphatidylinositol
RIG-I	Retinoic acid-inducible gene 1
RIP1	Receptor-interacting protein 1
RLR	RIG-I-like receptor
RNA	Ribonucleic acid
ROS	Reactive oxygen species
RSV	Respiratory syncytial virus
RV	Rhinovirus

sec	seconds
SINTBAD	TBK1 adaptor
siRNA	small interfering RNA
ssRNA	single-stranded RNA
STAT	Signal transducer and activator of transcription
STING	Stimulator of IFN genes
TAK1	TGF-β-activated kinase 1
TBK1	TRAF-family member associated NF-κB activator (TANK)-binding kinase 1
TEM	Transmission electron microscopy
TGF-β	Transforming growth factor-beta
TIR	Toll/interleukin-1 receptor
TLR	Toll-like receptor
TNF	Tumour necrosis factor
TRADD	TNF receptor-associated death domain
TRAF	TNF receptor-associated factor
TRIF	TIR-domain-containing adaptor protein inducing IFN-β
UV	Ultraviolet light
VPS34	Vacuolar protein sorting 34
VSV	Vesicular stomatitis virus
WHO	World health organisation

Chapter 1: Introduction

1.1. Chronic inflammatory diseases of the lung

Chronic inflammatory airway diseases are diseases of the lung that are characterised by chronic airway inflammation and increased airway hyperresponsiveness, and include asthma, chronic obstructive pulmonary disease (COPD) and idiopathic pulmonary fibrosis (IPF). Asthma and COPD are both very common worldwide; by which according to the Global Burden of Disease (GBD) study, a collaborative project between several organisations including the World Health Organisation (WHO), it was estimated that currently 235 million people suffer from asthma and 64 million people have COPD (reviewed in Royce et al., 2014).

1.1.1. Chronic Obstructive Pulmonary Disease (COPD)

Chronic obstructive pulmonary disease (COPD) is a major and growing global health problem, resulting in an increasing burden on healthcare expenditure in industrialised and developing countries (reviewed in Heffner, 2011, Mannino and Buist, 2007). The GBD study conducted by the WHO predicted that by 2020, COPD will be the third most common cause of death in the world (Lopez and Murray, 1998). A relatively recent worldwide epidemiological study reported that COPD is already the fourth most common cause of death in the world, and in the USA, it is the only common cause of death that has increased over the last 40 years (Lopez et al., 2006).

COPD is an inflammatory airway disease characterised by chronic development of airflow limitation, and in contrast to asthma, this condition is not easily reversed. It is predominantly caused by years of cigarette smoking, particularly in developed countries. Meanwhile, in developing countries, there are other common causes of COPD such as indoor air pollution from burning fuels and occupational exposure to hazardous gases (reviewed in Barnes, 2004b, Pauwels et al., 2001). COPD comprises two different conditions of the lung, chronic bronchitis and emphysema (reviewed in MacNee, 2005, Barnes, 2008). Chronic bronchitis is characterised by inflammation, mucus hypersecretion and fibrosis of the bronchioles. Emphysema is the destruction of alveolar walls, which consequently limits the transfer of oxygen into the bloodstream (Hogg, 2008, reviewed in Barnes, 2004b, Lane et al., 2010). Figure 1.1 portrays the mechanisms of airflow limitation in COPD.

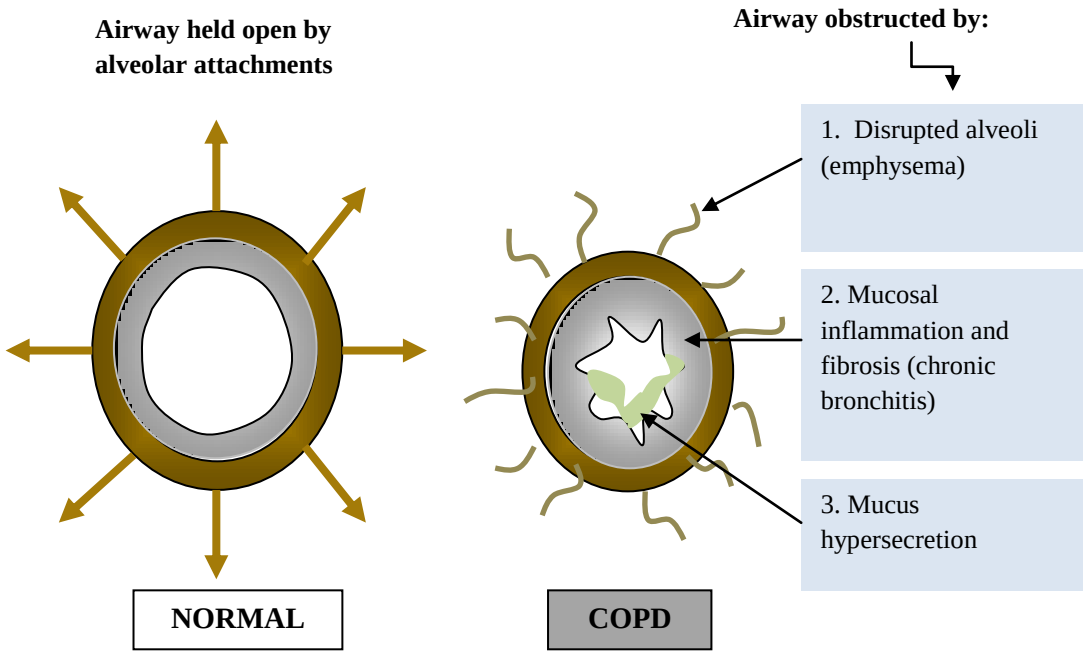

Figure 1. 1 Mechanisms of airflow limitation in chronic obstructive pulmonary disease.

In normal individuals, the airway is held open by alveolar attachments. In COPD patients, the alveoli are destroyed (emphysema). Peripheral airways are also blocked and deformed by mucosal inflammation and fibrosis (chronic bronchitis) as well as mucus hypersecretion.

[Adapted from (Barnes, 2004b)]

Existing therapies used for reducing the symptoms of COPD, such as inhaled corticosteroids (ICSs), are found to be effective in reducing the rate of exacerbations; however, ICSs do not reduce the long-term chronic decline of lung function in COPD patients (Burge et al., 2000, Pauwels et al., 1999, Vestbo et al., 1999). Bronchodilators, another commonly used drug therapy, relieve breathlessness and may reduce exacerbation rate (particularly with long-acting anticholinergics), though they may be associated with an increased risk of cardiovascular problems (Salpeter et al., 2004). Since there are no effective treatments currently available to treat chronic progression of COPD, there has been a renewed interest in understanding the cellular and molecular mechanisms of COPD; where a combination of different approaches, including *in vitro* modelling of human tissues, together with the use of animal models is needed (Sabroe et al., 2007a).

1.1.2. Asthma

Similar to COPD, asthma is another respiratory disease that poses a major and growing healthcare and economic burden worldwide. According to the WHO, asthma is the most common chronic disease of children (reviewed in Royce et al., 2014, Lambrecht and Hammad, 2013). Asthma is a chronic inflammatory airway disorder characterised by airflow obstruction and bronchial hyperresponsiveness that leads to recurrent episodes of coughing, wheezing, breathlessness and chest tightness (reviewed in Holt, 2012, Barnes, 2008). Risk factors for the development of asthma include both genetic and environmental factors, including genes pre-disposing individuals to allergy and airway hyperresponsiveness (atopy), allergens, viral infections and occupational sensitisers (reviewed in Bateman et al., 2008, Barnes, 2008). The strongest risk factor linked to the development of asthma is a family history of atopic asthma, by which increased levels of allergen-specific immunoglobulin E (IgE) antibodies are commonly detected in the affected individuals (reviewed in Holt and Sly, 2012, Bateman et al., 2008). More recently, studies have shown that children who have lower respiratory viral infections such as rhinovirus (RV) infection during the first 3 years of life are at a higher risk for the development of childhood asthma (Jackson et al., 2012, Jackson et al., 2008).

To date, there is no cure for asthma which is believed to be due to the complexity of the underlying pathological mechanisms of asthma. Similar to what is used to alleviate the symptoms of COPD (Section 1.1.1), ICSs are commonly used to effectively reduce the symptoms of asthma (reviewed in Holt and Sly, 2012, Bateman et al., 2008). Long-acting

inhaled β2-agonists such as formoterol and salmeterol are also used to control asthma exacerbations, although they are more effective when used in combination with ICSs (Gibson et al., 2007, Lazarus et al., 2001, reviewed in Bateman et al., 2008).

Whilst asthma and COPD have some common clinical and pathological features, this thesis will focus on the immunopathology of COPD.

1.2. Innate immunity and inflammation in COPD

Chronic inflammation of the lower respiratory tract in COPD is mediated by the affected structural tissue cells as well as the recruited immune cells, all of which have the capacity to release multiple inflammatory proteins including proinflammatory cytokines, chemokines and proteases (reviewed in Barnes, 2004b, Lane et al., 2010).

Although the adaptive immune response also contributes to chronic inflammation in COPD, the sections below focus on inflammation caused by the innate immune response, which is the first line of immune defence against any foreign agent, as innate immunity is the focus of this thesis.

1.2.1. Structural tissue cells involved in COPD

1.2.1.1. Airway epithelial cells

Airway epithelial cells are important tissue cells involved in the development of COPD as they are able to secrete various mediators of COPD including proinflammatory cytokines and reactive oxygen species (ROS) (Discussed in Section 1.2.3) (Rusznak et al., 2000, Rahman and MacNee, 1996, Schulz et al., 2004). Epithelial cells are activated by cigarette smoke components to release inflammatory cytokines such as tumour necrosis factor (TNF)-alpha (TNF-α), interleukin-1 beta (IL-1β) and CXC-chemokine ligand (CXCL) 8 (Discussed in Section 1.2.4) (Mio et al., 1997, Floreani et al., 2003, Hellermann et al., 2002). In COPD, along with immune cells, airway epithelial cells contribute to the occurrence of local fibrosis (excessive fibroblast proliferation) in the small airways by producing transforming growth factor (TGF)-β and fibroblast growth factors (FGFs) (Takizawa et al., 2001, Kranenburg et al., 2002).

1.2.1.2. Fibroblasts

Lung fibroblasts have been documented to play central roles in the fibrotic component of COPD, where their excessive proliferation results in fibrosis in the small airways (reviewed in Araya and Nishimura, 2010). An essential role of fibroblasts is to mediate tissue repair and modulation via production of extracellular matrix (ECM) proteins, which is partly stimulated by TGF-β (reviewed in Dunsmore and Rannels, 1996). However, in patients with COPD, the production of ECM proteoglycans such as decorin and versican are altered, which may partly contribute to disease development (Noordhoek et al., 2005, Hallgren et al., 2010).

Apart from producing ECM, fibroblasts have been proposed to participate in the inflammatory response through secretion of several cytokines and direct interaction with inflammatory cells; although very little is known about the exact mechanisms of fibroblast-triggered inflammation (reviewed in Buckley et al., 2001).

1.2.2. Innate immune cells involved in COPD

Clinical studies have shown that there are increased numbers of $CD8^+$ (cytotoxic) lymphocytes, neutrophils and macrophages in bronchial biopsies, small airways, and lung parenchyma from COPD patients (Hogg et al., 2004, Jeffery, 2001).

1.2.2.1. Macrophages and monocytes

In response to chemoattractants such as CC-chemokine ligand (CCL) 2 released by cigarette smoke-activated alveolar macrophages, circulating monocytes migrate to the lung and differentiate to macrophages (Traves et al., 2004, reviewed in Barnes, 2009). Alveolar macrophages contribute to the orchestration of inflammation in COPD by releasing chemokines that attract additional innate immune cells such as neutrophils, and also T cells which participate in adaptive immunity (reviewed in Barnes, 2004a). Macrophages have also been shown to contribute to emphysema occurrence via secretion of macrophage elastase MMP12 (Hautamaki et al., 1997, reviewed in Shapiro, 1999).

1.2.2.2. Neutrophils

Neutrophils have been found to be increased in the sputum, bronchoalveolar lavage fluid (BALF) and airway smooth muscle of patients with COPD, believed to be consequent upon increased levels of chemoattractants such as CXCL1 and CXCL8 (Discussed in Section

1.2.4) (Keatings et al., 1996, Baraldo et al., 2004). Indeed, higher neutrophil numbers in bronchial biopsies correlates with more severe airway inflammation and increased decline in lung function, further supporting the evidence that neutrophils may play an important role in the pathogenesis of COPD (Stanescu et al., 1996).

Apart from their capability to attract other immune cells through their secreted cytokines, neutrophils are able to secrete a number of proteases such as matrix metalloproteinase (MMP9) and neutrophil elastase, as well as ROS (Discussed in the next section) (Takeyama et al., 2000, reviewed in Barnes, 2009, Lane et al., 2010).

1.2.3. Mediators of COPD

Development of COPD is often reported to be mediated by orchestrated activity of reactive oxygen species (ROS), proteases and cytokines, all of which are secreted by leukocytes as well as structural tissue cells (reviewed in Barnes, 2004b, MacNee, 2005).

1.2.3.1. Reactive Oxygen Species (ROS)

ROS, such as superoxide anion and the hydroxyl radical, are unstable molecules with unpaired electrons. Excessive production of ROS may cause oxidative stress (reviewed in MacNee, 2001). This oxidative stress is a vital condition in COPD, as intensified oxidative stress leads to oxidation of DNA, lipids and proteins, consequently causing lung injury (reviewed in Henricks and Nijkamp, 2001, MacNee, 2001, Gutteridge and Halliwell, 2000). In COPD, ROS are produced by cigarette smoke-activated immune cells and structural cells, such as alveolar macrophages and epithelial cells, respectively (reviewed in MacNee, 2001, Rahman and MacNee, 1996).

1.2.3.2. Proteases

In COPD, proteases, especially neutrophil elastase (a serine protease) play crucial roles in causing emphysema wherein they cause elastin degradation in the alveolar walls (Majo et al., 2001, Gottlieb et al., 1996). Together with MMP9, neutrophil elastase produced by leukocytes such as neutrophils, T-lymphocytes and macrophages may also trigger mucus hypersecretion in COPD (Ohnishi et al., 1998, reviewed in Barnes, 2009). Apart from neutrophil elastase, neutrophils may also secrete two other serine proteases, called cathepsin

G and proteinase 3, which are both capable of inducing mucus secretion (Rao et al., 1993, Witko-Sarsat et al., 1999, Sommerhoff et al., 1990).

1.2.3.3. Cytokines

To date, over 50 cytokines have been recognised to be involved in the pathophysiology of COPD (reviewed in Barnes, 2004b). Not only are cytokines responsible for inflammation caused by the innate immune cells infiltration, they also play a crucial role in regulating the induction of adaptive immunity. The major cytokines involved in COPD are discussed in detail in the next section below.

1.2.4. Proinflammatory cytokines and chemokines involved in COPD

Proinflammatory cytokines play a vital role in inducing inflammation. Recognition of cytokines by their specific receptors present on the target cells leads to acute leukocyte influx, which consequently amplifies the secretion of additional cytokines by the recruited immune cells.

Chemokines (chemoattractant cytokines) are a family of cytokines that cause the movement of particularly targeted cells via directed chemotaxis. In COPD, chemokines are responsible for recruiting inflammatory cells from the circulation into the lung.

Three proinflammatory cytokines that are known to have a major role in COPD are discussed below.

1.2.4.1. Interleukin-1 beta (IL-1β)

IL-1β has been heavily implicated in the pathology of COPD (reviewed in Barnes, 2004b, Sabroe et al., 2007b, Curtis et al., 2007). Sapey and co-workers found that IL-1β levels were higher in the sputum samples taken from COPD patients compared with healthy individuals, although it was not statistically different. Furthermore, they revealed that patients with COPD had significantly reduced levels of IL-1β antagonists, namely IL-1 receptor antagonist (IL-1RA) and IL-1 soluble receptor 2 (IL-1sRII) (Sapey et al., 2009). In addition, following stimulation with cigarette smoke, cultured bronchial epithelial cells obtained from patients with COPD secrete higher amounts of IL-1β compared with epithelial cells from normal controls (Rusznak et al., 2000). IL-1β is also released by monocytes (Morris et al., 2005, Morris et al., 2006).

IL-1β has been shown to significantly increase the secretion of CXCL8 from alveolar macrophages taken from patients with COPD (Culpitt et al., 2003). IL-1β also triggers the recruitment of circulating monocytes and neutrophils (Rider et al., 2011). Using IL-1β-overexpressed transgenic mice, Lappalainen and colleagues showed that IL-1β plays a function in inducing emphysema and airway fibrosis (Lappalainen et al., 2005).

A humanised IL-1β blocking antibody, canakinumab is currently being clinically tested for the treatment of several inflammatory diseases, including COPD (reviewed in Dhimolea, 2010, Church and McDermott, 2009).

1.2.4.2. CXC-chemokine ligand 8 (CXCL8)

CXCL8, previously known as interleukin-8 (IL-8), was the first chemokine to be identified in COPD (Keatings et al., 1996). CXCL8 is a potent chemoattractant for neutrophils, and this therefore partly explains its ability to drive inflammation in COPD (reviewed in Barnes, 2004b).

Keatings and colleagues showed that the concentration of CXCL8 was increased in induced sputum of COPD patients compared with smokers with normal lung function and non-smokers, which was associated with neutrophil infiltration in patients with COPD (Keatings et al., 1996). This is consistent with a more recent finding by Culpitt and colleagues where they found that alveolar macrophages from patients with COPD secrete almost five-fold greater concentration of CXCL8 compared with the macrophages from normal cigarette smokers (Culpitt et al., 2003).

1.2.4.3. Interleukin-6 (IL-6)

Similar to the previously mentioned cytokines, interleukin-6 (IL-6) levels have also been found to be higher in induced sputum, BALF and exhaled breath condensate of patients with COPD compared with the healthy controls, especially during exacerbations (Bhowmik et al., 2000, Bucchioni et al., 2003, Song et al., 2001). Furthermore, Aldonyte and co-workers reported that monocytes from COPD patients which are stimulated with lipopolysaccharide (LPS) release more IL-6 in comparison with the LPS-stimulated monocytes from normal individuals, thus implying the important role of IL-6 in magnifying inflammation in COPD (Aldonyte et al., 2003).

Despite a wealth of evidence showing the high levels of IL-6 in COPD patients, the exact mechanisms of how IL-6 contributes to inflammation in COPD remains unclear.

1.2.5. Summary: Inflammatory mechanisms in COPD

Figure 1.2 illustrates the inflammatory mechanisms generated by several immune cells and structural tissue cells known to be important in the pathogenesis of COPD.

Although we now have a reasonably solid knowledge of various cytokines that are increased in patients with COPD, our understanding of how these cytokines work together to cause the immunopathology in COPD is very poor. It is important to note that many cytokines are redundant in their functions, thus studies using *in vivo* models such as murine models of COPD could be misleading. The fact that there are differences in lung structure and immune responses between mice and humans also makes interpretation of the findings obtained from these *in vivo* murine studies difficult (Sabroe et al., 2007a). Therefore, our current efforts of investigating the interactions of various cytokines produced by the immune cells as well as the structural tissue cells *in vitro* are crucial to enable a better understanding of the complex cytokine networking in COPD.

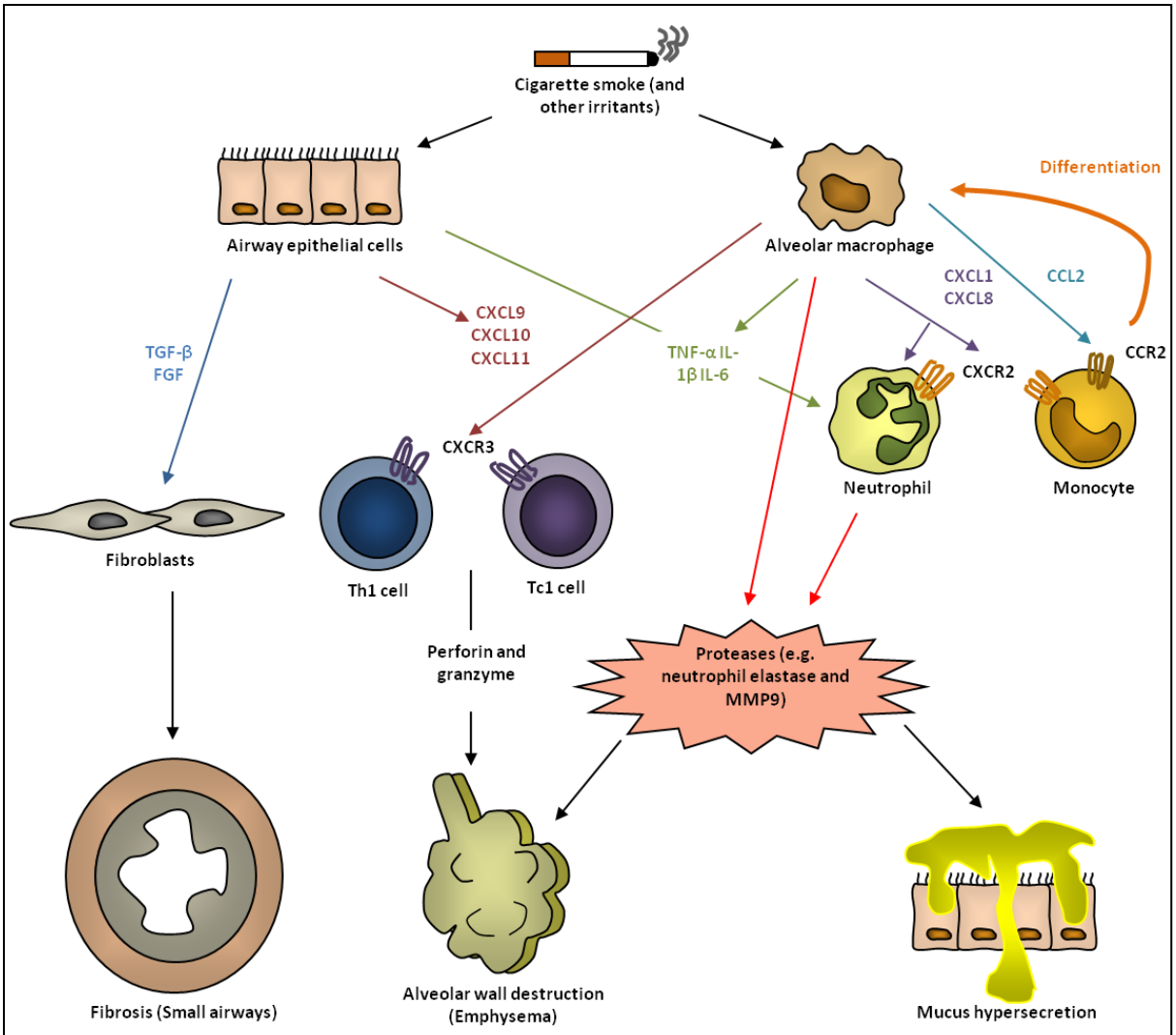

Figure 1. 2 Inflammatory mechanisms in chronic obstructive pulmonary disease.
Inhaled cigarette smoke or other irritants trigger airway epithelial cells and alveolar macrophages to secrete several cytokines, leading to recruitment of other immune cells to the lungs. Released CC-chemokine ligand (CCL) 2 by macrophages attracts monocytes via its binding to CC-chemokine receptor (CCR) 2, consequently leading to monocyte differentiation into macrophages within the lungs. Secreted CXC-chemokine ligand (CXCL) 1 and CXCL8, which act on CXC-chemokine receptor (CXCR) 2 attract neutrophils and monocytes. CXCL9, CXCL10 and CXCL11 released by epithelial cells and macrophages bind to CXCR3 present on T helper (Th) 1 cells and type 1 cytotoxic (Tc1) cells. Neutrophils and macrophages are able to release proteases such as neutrophil elastase (which causes elastin degradation, leading to emphysema) and matrix metalloproteinase (MMP) 9 (which causes mucus hypersecretion). Emphysema occurrence is also mediated by perforin and granzyme secreted by activated Tc1 cells. Epithelial cells and macrophages also produce tumour necrosis factor-α (TNF-α), interleukin-1 beta (IL-1β) and IL-6, which further intensify inflammation in the lung airways. Fibrosis (narrowing of the small airways) occurs as a result of excessive fibroblast proliferation, which is stimulated by transforming growth factor beta (TGF-β) and fibroblast growth factors (FGFs) secreted by airway epithelial cells.

[Information gathered from (Barnes, 2009, Lane et al., 2010)]

1.3. The role of Rhinoviruses (RVs) in COPD exacerbations

COPD exacerbations can be triggered by multiple factors such as common pollutants, allergens and bacteria, however, respiratory viruses are the most common cause of COPD exacerbations (reviewed in Barnes, 2008, Papi et al., 2007). These respiratory viruses include RV, coronavirus, influenza A and B, parainfluenza, adenovirus and respiratory syncytial virus (RSV) (reviewed in Wedzicha, 2004). Among these viruses, RVs have been found to be the predominant cause of virus-induced COPD exacerbations (Seemungal et al., 2001, Rohde et al., 2003).

1.3.1. RV serotypes and cellular entry

RVs are the major cause of the common cold. They are members of the virus family *Picornaviridae* (Hughes, 2004). Like all other picornaviruses, RVs are small (about 30nm in diameter), non-enveloped, positive-sense single-stranded RNA (ssRNA) viruses (Arnold and Rossmann, 1990, Kim et al., 1989). Except for RV-14, which has a genome length of 7212 bases, most RVs have a genome of 7102-7152 bases in length (Stanway et al., 1984, Lee et al., 1995). At the 5' end of the genome is a virus-encoded protein, and there is a poly-A tail at the 3’ end of the genome (Stanway et al., 1984, Lee et al., 1995).

To date, 148 RV serotypes have been discovered (Harvala et al., 2012, Arden et al., 2010). There are two ways by which these serotypes can be classified: The first, which is the traditional method, is based upon the host-cell receptor used for viral entry; and the second method is based upon the sequence homology. According to the receptor usage method, RV serotypes are categorised into two groups; major and minor. Major group RVs (88 serotypes) infect cells via intercellular adhesion molecule 1 (ICAM-1) whereas minor group RVs (12 serotypes) utilise low-density lipoprotein receptor (LDLR) for cellular entry (Greve et al., 1989, Staunton et al., 1989, Hofer et al., 1994, Gruenberger et al., 1995). Meanwhile, using the genetic analysis method, RV serotypes are divided into three phylogenetic groups; RV-A (74 serotypes), RV-B (25 serotypes) and a newly identified RV-C (> 50 serotypes) (reviewed in Palmenberg et al., 2009). Over 90% of the known RV-A and RV-B serotypes bind to ICAM-1 to enter host cells, 12 serotypes of RV-A utilise LDLR, whilst the receptor that is used for internalisation by the new group RV-C remains unknown (Arden et al., 2010, reviewed in Bochkov et al., 2011).

1.3.2. Life cycle of RVs

Attachment of RV to the receptor present on the host cell elicits conformational changes in the virus capsid, eventually leading to the release of the RV ssRNA genome into the cytoplasm (Casasnovas and Springer, 1994, Schober et al., 1998, Prchla et al., 1994). In the cytoplasm the viral genomic RNA is translated by host ribosomes to produce viral proteins necessary for viral replication (reviewed in Andino et al., 1999, Jackson and Kaminski, 1995). The same genomic RNA is then amplified in a two step process: first, the positive-sense genomic RNA is reverse transcribed by the viral RNA-dependent RNA polymerase, hence generating a complementary negative-sense RNA; by which replication intermediate double-stranded RNA (dsRNA) is formed. Second, the negative-sense RNA is subsequently used as a template to generate many copies of the viral genome, which are then used for the latter cycles of viral protein synthesis. The new infectious virions are assembled in the cytoplasm and finally released from the cell (reviewed in Bedard and Semler, 2004, Andino et al., 1999). Figure 1.3 shows an overview of the RV life cycle.

1.3.3. RV-induced exacerbations of COPD

Many clinical studies report that RVs are the most common virus found in sputum and nasal lavage of patients with acute exacerbations of COPD (Wark et al., 2013, Perotin et al., 2013, McManus et al., 2008, Rohde et al., 2003, Greenberg et al., 2000, Seemungal et al., 2001). Furthermore, Mallia and colleagues have recently shown direct experimental evidence that RV infection induces the clinical features of acute COPD exacerbations (Mallia et al., 2011).

RVs have been shown to potentiate the production of several inflammatory cytokines in COPD patients including CXCL8 and IL-6 (Baines et al., 2013, Seemungal et al., 2000, Wedzicha et al., 2000, Schneider et al., 2010). These increased cytokine levels partly explain the mechanisms of RV-induced acute airway inflammation during COPD exacerbations. Figure 1.4 depicts the epithelial and innate immune cell responses to RV infection that may lead to exacerbations of COPD.

It has been suggested that patients with COPD are more susceptible to RV infections (Seemungal et al., 2001, Schneider et al., 2010, Mallia et al., 2011). Schneider and co-workers demonstrated that RV infection of airway epithelial cells from patients with COPD yields higher viral load as compared to that of normal controls, although the mechanisms were not determined (Schneider et al., 2010). Meanwhile, a separate study showed that

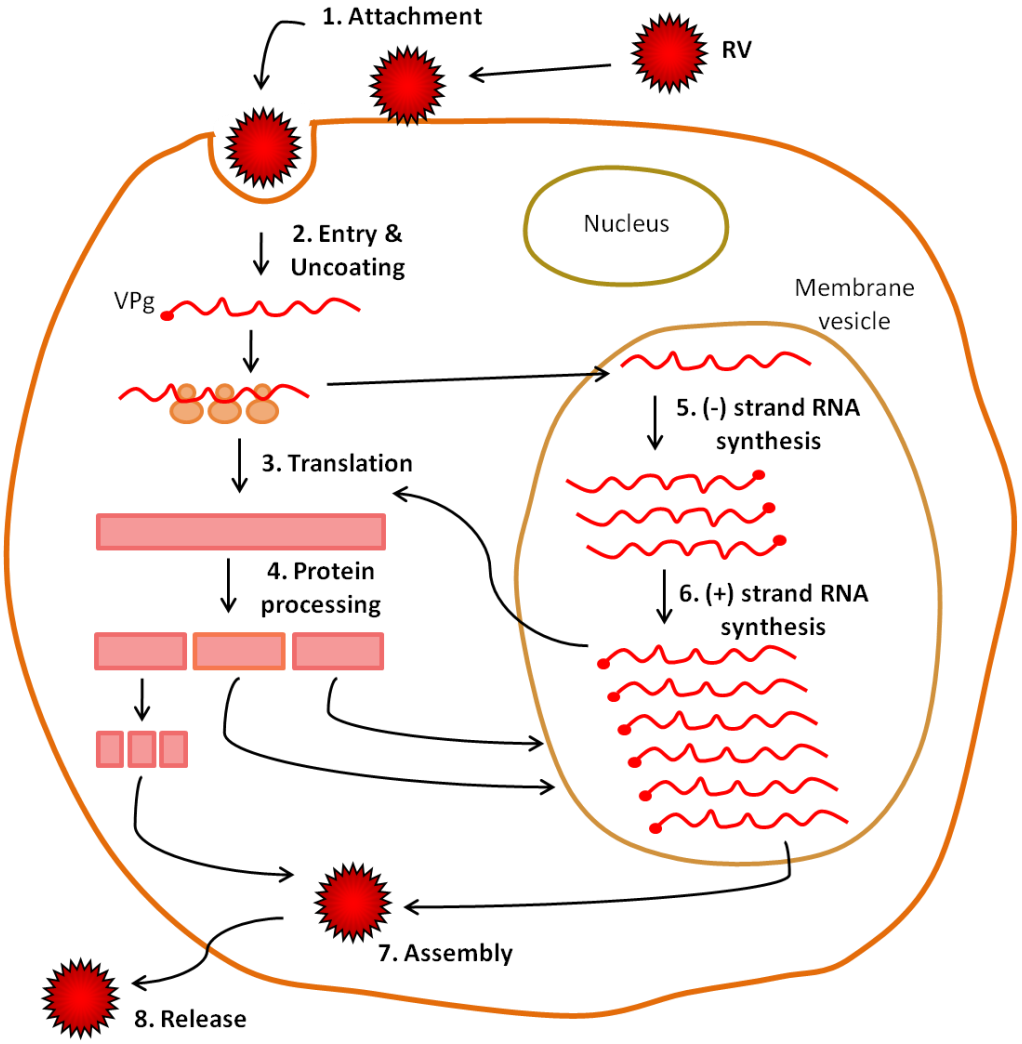

Figure 1. 3 Overview of the RV life cycle.

RV binds to a specific receptor on the cell surface. The viral RNA is then unpackaged and delivered into the cytoplasm of the cell. The genome-linked protein VPg is removed from the viral RNA, which is then translated. The newly formed polyprotein is then cleaved to produce individual viral proteins. RNA synthesis occurs on membrane vesicles. Genomic (+) strand RNA is copied by the viral RNA polymerase to form full-length (-) strand RNAs, which are then copied to produce additional (+) strand RNAs. Early in infection, the newly synthesised (+) strand RNA is translated to produce additional viral proteins. Later in infection, the (+) strand RNAs are packaged into virions. Finally, the virions are released from the host cell by lysis.

[Information gathered from (De Palma et al., 2008, Andino et al., 1999)]

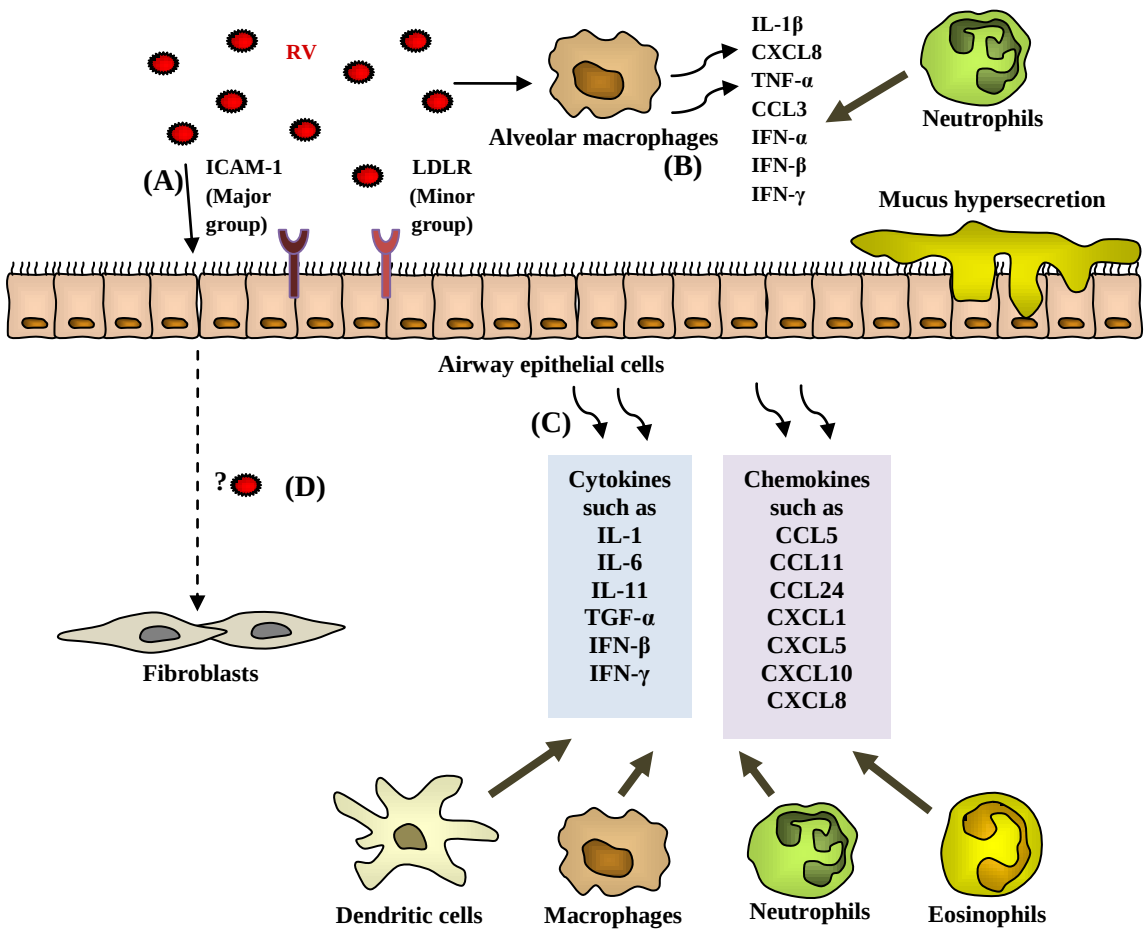

Figure 1. 4 Epithelial and innate immune cell responses to rhinovirus (RV) infection that may lead to COPD exacerbations.

(A) RVs infect epithelial cells either via intercellular adhesion molecule-1 (ICAM-1) or low-density lipoprotein (LDL) receptor, depending on the RV group. (B) Interaction between RVs and macrophages stimulates production of proinflammatory cytokines (such as interleukin-1 beta (IL-1β), CXC-chemokine ligand (CXCL) 8, tumour necrosis factor-α (TNF-α) and CC-chemokine ligand (CCL) 3) as well as interferons (IFNs) (including IFN-α, IFN-β and IFN-γ). Some of these cytokines such as CXCL8 and TNF-α produced by alveolar macrophages may cause neutrophil infiltration. (C) RV-infected epithelial cells release cytokines and chemokines that consequently lead to neutrophilic, eosinophilic and lymphocytic inflammation, as well as mucus hypersecretion and potentially airway remodelling. (D) RVs potentially pass through epithelial cell layers and infect neighbouring fibroblasts. [Other abbreviations used in the schematic diagram: TGF-α, transforming growth factor-α; CXCL, CXC-chemokine ligand]

[Adapted from (Jackson and Johnston, 2010)]

production of the important antiviral cytokine, interferon (IFN) -β (Discussed in Section 1.7), was impaired in cells taken from patients with COPD, which may be a crucial mechanism underlying the increased susceptibility of patients with COPD to RV infection (Mallia et al., 2011). Another possible reason is that RVs induce up-regulation of their own receptor ICAM-1 (the receptor for major group of RVs) (Papi and Johnston, 1999). Studies also revealed that the presence of adenoviral E1A protein in alveolar epithelial cells and bronchial epithelial cells of patients with emphysema intensifies expression of ICAM-1, thus adding in to the possible causes of higher susceptibility of COPD patients to RV infections (Higashimoto et al., 2002, Keicho et al., 1997). Nonetheless, the nature of this susceptibility remains to be fully determined.

1.4. Viral detection by Pattern-Recognition Receptors (PRRs)

The innate immune system responds to microbial infections and endogenous molecules via a group of germ-line encoded receptors termed pattern-recognition receptors (PRRs). Members of this family of receptors specifically detect microbial pathogens, which are called pathogen-associated molecular patterns (PAMPs) and endogenous molecules released from damaged cells, termed damage-associated molecular patterns (DAMPs) (reviewed in Sparrer and Gack, 2015, Takeuchi and Akira, 2010). The PRRs responsible for detecting viruses are discussed below.

Three main PRR families have been described to play a major role in the detection of viral infections; Toll-like receptors (TLRs), which recognise viral DNA or RNA in intracellular vesicles of the infected cells, retinoic acid inducible gene-I (RIG-I)-like receptors (RLRs), which detect viral RNA in the cytoplasm, and uncharacterised DNA sensor molecules, which detect cytoplasmic viral DNA (reviewed in Chow et al., 2015, Yoneyama and Fujita, 2010). Apart from the TLR- and RLR-mediated pathways, different other sensing pathways have been recently identified to recognise viral nucleic acids, including the nucleotide-binding oligomerisation domain (NOD)-like receptors (NLRs) pathway and the stimulator of IFN genes (STING) pathway (Summarised in Section 1.6.1 and 1.6.2, respectively).

1.4.1. Toll-like Receptors (TLRs)

TLRs are a family of single-transmembrane receptors which consist of an extracellular leucine-rich repeat (LRR) domain, which is responsible for detection of specific PAMPs, a transmembrane-spanning domain, and a cytoplasmic signal-transduction domain known as the toll/interleukin-1 receptor (TIR) domain (reviewed in Carty and Bowie, 2010, Yoneyama and Fujita, 2010). TLRs recognise a range of microbes including bacteria and viruses, leading to activation of the innate immune system and subsequent orchestration of the adaptive immune response.

To date, four TLRs have been identified to be responsible for recognition of viral nucleic acids which are TLR 3, 7, 8 and 9; and unlike the other TLRs (which are present on the plasma membrane), all these virus-sensing TLRs are mainly located within the endosomal compartments (reviewed in Kawai and Akira, 2011, Carty and Bowie, 2010). Except for TLR9 which detects viral DNA, the other three TLRs play an important role in recognising RNA viruses.

As previously discussed (Section 1.3.1), RV is an RNA virus therefore, this review will only discuss on TLRs that detect viral RNA (i.e. TLR 3, 7 and 8) (Section 1.4.1.1-2). Of relevance to the current study, a new role for TLR2 (which commonly detects lipoproteins of bacteria and fungi) in recognising RV protein capsid will also be briefly discussed in Section 1.4.1.3.

1.4.1.1. Recognition of viral double-stranded RNA by TLR3

TLR3 senses dsRNA, which is found in the genome of dsRNA viruses, or during the replication-intermediates of ssRNA viruses (Alexopoulou et al., 2001, Tabeta et al., 2004). Like the other TLRs that detect viral nucleic acids, TLR3 is mainly expressed in the endosomal compartments of cells such as in myeloid dendritic cells (DCs) and macrophages; however, in fibroblasts and epithelial cells, TLR3 is also observed on the cell surface (Matsumoto and Seya, 2008).

Of relevance to this project, Wang and co-workers recently demonstrated that in a human bronchial epithelial cell line (BEAS-2B cells), RV is exclusively detected by TLR3 and MDA5, but not RIG-I (see Section 1.4.2 for RLRs). The authors claimed that although RV is an ssRNA virus, its presence is detected via its dsRNA replication-intermediate (Wang et al., 2009). Similarly, Slater and colleagues demonstrated that TLR3 and MDA5 (see Section

1.4.2 for RLRs) are required for the induction of innate cytokine responses of primary human bronchial epithelial cells (HBECs) to RV infection (Slater et al., 2010). Furthermore, a separate study also revealed that RV infection increases the expression of TLR3 mRNA and TLR3 protein on the cell surface of the BEAS-2B cells (Hewson et al., 2005).

As for all viral nucleic acid-sensing TLRs, recognition of dsRNA by TLR3 will activate specific downstream signalling cascades that lead to the transcription of proinflammatory cytokines as well as type I IFN genes (Discussed in Section 1.5).

1.4.1.2. Recognition of viral single-stranded RNA by TLR7/8

TLR7 and TLR8 are structurally homologous, and both are responsible in detecting ssRNA (Lund et al., 2004, Melchjorsen et al., 2005, Triantafilou et al., 2005). Like TLR3 (Section 1.4.1.1), TLR7 and TLR8 are primarily localised within the intracellular endosomal compartments (Triantafilou et al., 2005, reviewed in He et al., 2013). In humans, TLR7 is mainly observed in plasmacytoid DCs whilst TLR8 is predominantly expressed in myeloid DCs and monocytes (reviewed in He et al., 2013, Kawai and Akira, 2011).

Although many studies have shown that RV infection is predominantly recognised by TLR3 (where RV dsRNA replication-intermediate acts as the key PAMP) (Wang et al., 2009, Slater et al., 2010) (Section 1.4.1.1), a recent publication has demonstrated that RV genomic ssRNA can also be detected by TLR7/8 in primary HBECs (Triantafilou et al., 2011). However, our group (Parker et al., 2008) and others (Slater et al., 2010, Sadik et al., 2009) have shown that primary HBECs as well as A459 and BEAS-2B lung epithelial cell lines do not respond to TLR7/8 agonists. Furthermore, a study has also demonstrated that TLR7 and TLR8 are not expressed in human A549 lung epithelial cell line (Tissari et al., 2005). These discrepancies concerning the involvement of TLR7/8 in detecting RV infection in human lung epithelial cells warrant further study. The possibility that TLR7/8 respond to natural viral infections distinctly to synthetic ligands remains to be investigated.

1.4.1.3. Recognition of viral protein capsid by TLR2

As discussed earlier, early detection of RV infection of airway epithelial cells is believed to mainly be via recognition of RV dsRNA replication-intermediate by the endosomal TLR3 (Section 1.4.1.1). However, two recent publications have shown that RV protein capsid can also be detected by TLR2 on the epithelial cell surface (Triantafilou et al., 2011, Unger et al.,

2012). Triantafilou and co-workers demonstrated that knockdown of TLR2 (by RNA interference) resulted in reduction of cytokine secretion following RV-6 infection in primary HBECS (Triantafilou et al., 2011).

1.4.2. Retinoic acid inducible gene-I (RIG-I)-like receptors (RLRs)

As noted earlier, RLRs are a family of PRRs that detect viral RNA present in the cytoplasm of infected cells. All members of RLRs contain an RNA helicase domain (reviewed in Yoneyama and Fujita, 2010). To date, three distinct groups of RLRs have been identified which are retinoic acid inducible gene-I (RIG-I), melanoma differentiation associated gene 5 (MDA5) and laboratory of genetics and physiology 2 (LGP2) (Satoh et al., 2010, reviewed in Yoneyama and Fujita, 2010, Takeuchi and Akira, 2010). RLRs recognise viral dsRNA or synthetic dsRNA analogue such as polyinosinic:polycytidylic acid (poly I:C), consequently inducing the production of type I IFNs as well as proinflammatory cytokines (reviewed in Yoneyama and Fujita, 2010).

A recent study by Kato and his colleagues showed that the length of the dsRNAs determine their differential recognition by RIG-I and MDA5. They discovered that a relatively long poly I:C (> 1 kbp) was selectively detected by MDA5, whilst a shorter form of poly I:C created by enzyme digestion (<1 kbp) was exclusively recognised by RIG-I (Kato et al., 2008). Furthermore, presence of 5'-triphosphate moiety of viral RNA is crucial for RIG-I but not for MDA5 (Hornung et al., 2006, Pichlmair et al., 2006).

Of relevance to viral detection, studies revealed that the 5' end of picornaviruses is protected by the covalent attachment of a viral protein, called VPg, allowing picornaviruses to evade recognition by RIG-I (Shen et al., 2008, Habjan et al., 2008). In fact, several reports propose that MDA5 is exclusively responsible for the detection of picornaviruses (Kato et al., 2006, Gitlin et al., 2006). Using RIG-I-knockout mice, Kato and colleagues discovered that recognition of viral dsRNA by RIG-I is a cell-type specific as they found that RIG-I is critical in detecting RNA viruses (i.e. Newcastle Disease Virus, Vesicular Stomatitis Virus and Sendai Virus) in fibroblasts and conventional DCs, but not in plasmacytoid DCs, where in these particular type of DCs, the viral RNA is sensed by TLRs (Kato et al., 2005).

As mentioned above, MDA5 plays a crucial role in detecting picornaviruses. Again, although picornaviruses are ssRNA viruses, they are known to synthesise long replication intermediate dsRNAs, thus allowing MDA5 to sense their presence (Wang et al., 2009).

1.5. TLR and RLR signalling pathways

Following recognition of PAMPs and DAMPs by PRRs, specific intracellular downstream signalling cascades are activated, which subsequently lead to production of proinflammatory cytokines (reviewed in Takeuchi and Akira, 2010). However, in response to viral infections, the infected cells also produce type I IFNs which direct the antiviral immune response (reviewed in Yoneyama and Fujita, 2010). The two major pathways associated with viral infections; the TLR and RLR signalling pathways are discussed below.

TLR and RLR signalling pathways have been extensively studied and reviewed by many groups (Loiarro et al., 2010, Takeuchi and Akira, 2010, Yoneyama and Fujita, 2010, Chaudhuri et al., 2005, Carty and Bowie, 2010), thus only a brief description of the main components are described here. TLR signalling is generally categorised into two different pathways depending on the type of adaptor molecule used which is either MyD88 (Myeloid Differentiation factor 88) or TRIF (TIR-domain-containing adaptor protein inducing IFN-β). Production of proinflammatory cytokines is commonly described to be generated through MyD88-dependent signalling pathway (reviewed in Loiarro et al., 2010, Takeuchi and Akira, 2010) (Discussed in Section 1.5.1). Of relevance to this project, IL-1β (which plays a crucial role in mediating inflammation in COPD; Section 1.2.4.1) also induces production of proinflammatory cytokines via the typical MyD88-dependent signalling pathway. However, TLR3 induces proinflammatory cytokine production via a MyD88-independent pathway, where it only requires TRIF as its adaptor protein (Yamamoto et al., 2002) (Discussed in Section 1.5.2). As a result of viral infections, type I IFNs can be produced either via TRIF- (for TLR3), or via MyD88- (for TLR7/8/9) dependent signalling pathway. Figure 1.5 shows the TLR/IL-1 receptor (IL-1R) signalling pathways activated following detections of IL-1β and RV dsRNA by IL-1R/IL-1 receptor accessory protein (IL-1RAcp) and TLR3, respectively.

1.5.1. The MyD88-dependent signalling pathway

All TLRs and IL-1R utilise the adaptor protein MyD88 for signal transduction following ligand binding; with the exception of TLR3 which signals via TRIF (See Section 1.5.2) (reviewed in Takeuchi and Akira, 2010, Loiarro et al., 2010). In the MyD88-dependent pathway, binding of ligand to TLR/IL-1R leads to the recruitment of MyD88 to the cytoplasmic domain of the receptor complex (See Figure 1.5A). MyD88 then interacts with

IL-1R-associated kinase (IRAK)-4 via the N-terminal death domain. Activated IRAK-4 in turn activates other IRAK family members, IRAK-1 and IRAK-2. The IRAKs next dissociate from MyD88 and interact with TNF receptor-associated factor (TRAF) 6. Activated TRAF6 then interacts and activates TGF-β-activated kinase 1 (TAK1). TAK1 binds and activates the inhibitory κB (IκB) kinase (IKK) complex that subsequently phosphorylates the NF-κB binding protein IκBα/β. The phosphorylated IKBα/β is then targeted by ubiquitin-mediated proteasome degradation, making the transcription factor NF-κB free to translocate from the cytoplasm to the nucleus and consequently initiate transcription of proinflammatory cytokine genes such as CXCL8. The activated TAK1 also activates mitogen-activated protein kinase (MAPK) cascades leading to activation of activator protein-1 (AP-1), which also participates in the induction of proinflammatory cytokine genes (reviewed in Takeuchi and Akira, 2010, Loiarro et al., 2010).

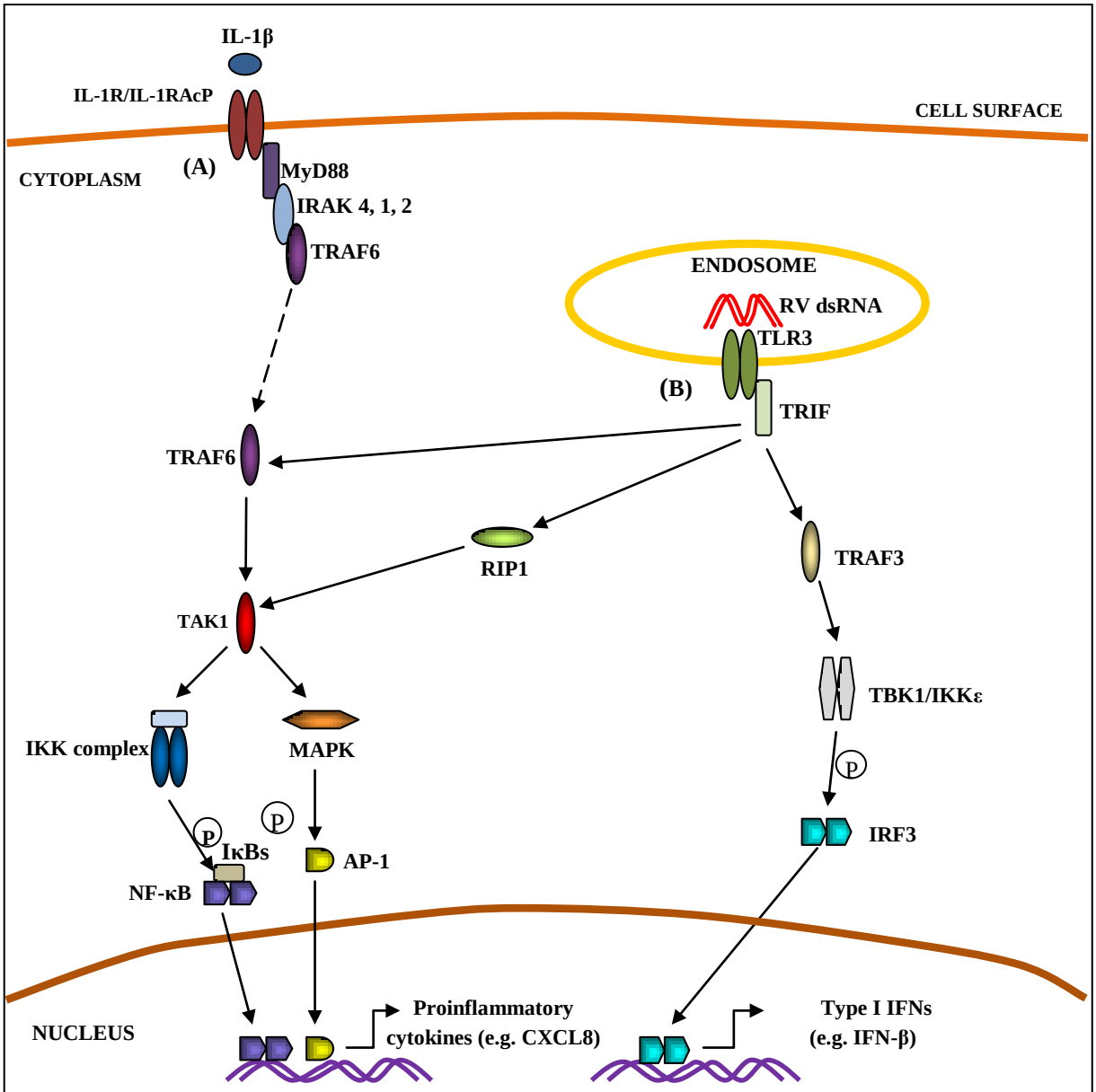

Figure 1. 5 TLR/IL-1R signalling pathways activated following recognitions of IL-1β and RV dsRNA by IL-1R/IL-1RAcP and TLR3, respectively.

(A) In the MyD88-dependent pathway, ligand stimulation recruits MyD88 to the cytoplasmic domain of IL-1R/IL-1RAcP. In turn, MyD88 recruits a family of IRAK proteins (i.e. IRAK 4, 1, 2) and TRAF6. TRAF6 subsequently activates TAK1 resulting in the activation of an IKK complex. The IKK complex then phosphorylates IκBα/β, an NF-κB inhibitory protein. Phosphorylated IκBα/β is then degraded, making the transcription factor complex NF-κB free to translocate from the cytosol to the nucleus and consequently initiates transcription of proinflammatory cytokine genes such as CXCL8. The activated TAK1 also activates MAPK cascades leading to activation of AP-1, which also participates in the induction of proinflammatory cytokine genes. (B) Ligand-bound TLR3 activates TRIF-dependent pathway. TRIF interacts with TRAF6 and RIP1 subsequently activating NF-κB and MAPK pathways responsible for expression of proinflammatory cytokines genes. TRIF also interacts with TRAF3, which then activates TBK1/IKKε resulting in the activation of transcription factor IRF3. Activated IRF3 translocates into the nucleus to induce transcription of type I IFNs such as IFN-β. (See List of Abbreviations for the abbreviations used in this figure legend.)

[Information gathered from (Loiarro et al., 2010, Takeuchi and Akira, 2010)]

1.5.2. The TRIF-dependent signalling pathway

Activation of TLR3 by dsRNA results in the recruitment of the adaptor protein TRIF (reviewed in Kawai and Akira, 2011, Takeuchi and Akira, 2010) (See 1.5B). TRIF interacts with TRAF3, which then activates TBK1/IKKε. The activated TBK1/IKKε then phosphorylates IRF3, and the activated IRF3 in turn translocates into the nucleus to induce transcription of type I IFNs such as IFN-β. TRIF also interacts with TRAF6 and receptor-interacting protein 1 (RIP1), which leads to the activation of the transcription factors NF-κB and AP-1 that are responsible for expression of proinflammatory cytokines genes (reviewed in Kawai and Akira, 2011, Takeuchi and Akira, 2010).

1.5.3. The RLR signalling pathway

As previously discussed (Section 1.4), the RLR signalling pathway is involved in the detection of viral dsRNA such as RV dsRNA in the cytoplasm, which results in the production of proinflammatory cytokines and type I IFNs. Since RV is thought to be exclusively recognised by MDA5 (Section 1.4.1.1 & 1.4.2), the RLR-signalling pathways activated upon detection of RV long dsRNA by MDA5 are described in Figure 1.6. MDA5 detects cytoplasmic viral dsRNA via its positively charged C-terminal domain (reviewed in Takeuchi and Akira, 2010, Yoneyama and Fujita, 2010). Upon detection of the dsRNA, MDA5 interacts with mitochondrial antiviral signalling (MAVS) protein through homophilic interactions between caspase recruitment domains (CARDs), which are ATP-dependent. MAVS then activates TRAF3 and TNF receptor-associated death domain (TRADD). Activated TRAF3 recruits NF-κB-activating kinase (NAK)-associated protein 1 (NAP1)/SINTBAD eventually leading to activation of TBK1 and IKKε. The TBK1/IKKε then phosphorylates IRF3 and IRF7, and the phosphorylated IRF3 and IRF7 in turn translocate to the nucleus to initiate transcription of type I IFN genes. Simultaneously, MAVS-activated TRADD forms a complex with Fas-associated death domain (FADD). FADD in turn interacts with caspase 8 or caspase 10; and the cleaved form of the caspases activates NF-κB allowing translocation of NF-κB from the cytosol to the nucleus to subsequently induce proinflammatory cytokine production (reviewed in Takeuchi and Akira, 2010, Yoneyama and Fujita, 2010).

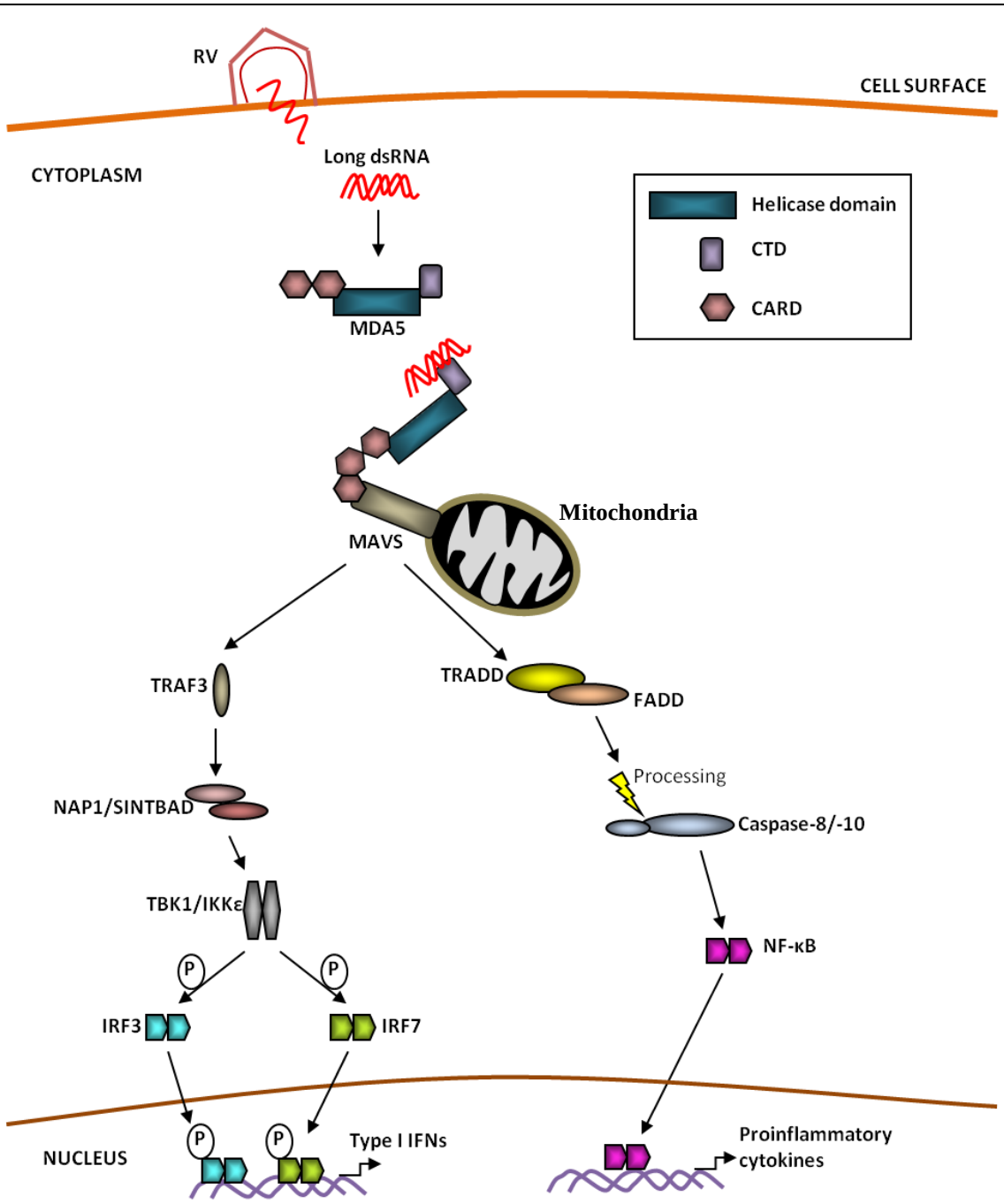

Figure 1. 6 RLR signalling pathway activated following recognition of RV long dsRNA by MDA5.

MDA5 detects cytoplasmic viral dsRNA via positively charged CTD. Upon detection of the dsRNA, MDA5 interacts with a mitochondrial adaptor molecule, MAVS through homophilic interactions between CARD domains, which are ATP-dependent. MAVS then activates TRAF3 and TRADD. Activated TRAF3 recruits NAP1/SINTBAD eventually leading to activation of TBK1/IKKε. The TBK1/IKKε then phosphorylates IRF3 and IRF7, and the phosphorylated IRF3 and IRF7 in turn translocate to the nucleus to initiate transcription of type I IFN genes. Simultaneously, MAVS-activated TRADD forms a complex with FADD. FADD in turn interacts with caspase 8 or caspase 10; and the cleaved form of the caspases activates NF-κB allowing translocation of NF-κB from the cytosol to the nucleus to subsequently induce proinflammatory cytokine production. (See List of Abbreviations for the abbreviations used in this figure legend.)

[Information collected from (Takeuchi and Akira, 2010, Yoneyama and Fujita, 2010)]

1.6. Other cellular systems for detecting viruses

1.6.1. Nucleotide-binding oligomerisation domain (NOD)-like receptors (NLRs)

NLRs are a large cytoplasmic receptor family of more than 20 members including NLRP1, NLRP3, NLRC2, NLRC4 and NLRX1 (reviewed in Lupfer and Kanneganti, 2013). Structurally, NLRs are comprised of 3 domains: a C-terminal LRR-rich domain, a central nucleotide-binding oligomerisation domain (NOD), and an N-terminal effector-binding domain, which is either a CARD, pyrin domain (PYD) or baculovirus inhibitor repeat (BIR) domain (reviewed in Lupfer and Kanneganti, 2013, Jacobs and Damania, 2012).

Besides their established roles in recognising bacterial PAMPs such as peptidoglycan and flagellin, NLRs have also been recently associated with the detection of viral nucleic acids (reviewed in Lupfer and Kanneganti, 2013, Jacobs and Damania, 2012). Recently, NLRP3 has been shown to be involved in recognising influenza virus (ssRNA virus), adenovirus (dsDNA virus) and Sendai virus (ssRNA virus) (Ichinohe et al., 2009, Muruve et al., 2008, Kanneganti et al., 2006). Similarly, NLRC2 (also known as NOD2) has been recently demonstrated to detect several ssRNA viruses including RSV, vesicular stomatitis virus (VSV), influenza virus and parainfluenza virus 3 (Sabbah et al., 2009, Shapira et al., 2009). Additionally, a recent structural analysis study demonstrated that NLRX1 could bind to synthetic ssRNA and dsRNA ligands, indicating that this NLR might be able to bind viral RNA directly (Hong et al., 2012).

1.6.2. Stimulator of IFN genes (STING) pathway

In parallel to early studies identifying multiple cytosolic viral DNA receptors, a new signalling adaptor protein called STING was discovered in 2008 (reviewed in Chow et al., 2015). STING is a membrane resident protein found on the ER or mitochondrion that bridges most viral DNA receptors to downstream signalling events (reviewed in Maringer and Fernandez-Sesma, 2014, Unterholzner, 2013). STING contains four N-terminal transmembrane domains and a globular C-terminal domain, which facilitates interaction of STING with TBK1 (reviewed in Davis and Gack, 2015, Maringer and Fernandez-Sesma, 2014). Upon cytosolic DNA stimulation, STING rapidly dimerises and translocates from the endoplasmic reticulum (ER) through the Golgi apparatus to perinuclear vesicles, where it interacts with TBK1. STING then facilitates the recruitment of IRF3 to TBK1 and subsequent

IRF3 phosphorylation, leading to the nuclear translocation of IRF3 and the induction of type I IFN and other cytokines (reviewed in Chow et al., 2015, Bhat and Fitzgerald, 2014).

STING has been shown to play an important role in the recognition of herpes simplex virus (HSV) (dsDNA virus) (Ishikawa et al., 2009, Ishikawa and Barber, 2008). Furthermore, studies have demonstrated the crucial roles of STING in the production of type I IFN in response to several RNA viruses including VSV and Sendai virus (Zhong et al., 2008, Sun et al., 2009, Zhong et al., 2009).

1.7. Key antiviral cytokines and chemokines induced in response to RV infection

1.7.1. IFNs

IFNs are key cytokines in the antiviral innate immune response. There are three different types of IFNs (type I, II and III); classified based on their structural features, receptor usage and biological functions. Type I IFNs include IFN-α and IFN-β, type II IFN is represented by a single gene product, IFN-γ; and the more recently discovered type III IFNs include IFN-λ1, IFN- λ2 and IFN-λ3 (reviewed in Trinchieri, 2010). Whilst types I and III IFNs play crucial roles in antiviral immunity, studies have shown that IFN-γ (the sole type II IFN) is less involved in antiviral activity, but mainly associated with immune defence against intracellular bacteria and anti-tumour immune response (Dalton et al., 1993, Dorman et al., 2004, reviewed in Donnelly and Kotenko, 2010). Of relevance to the current project, only type I and type III IFNs which exhibit potent antiviral activities are summarised below.

1.7.1.1. Type I

Among all types of IFNs, type I IFNs are the best characterised, and play important roles in antiviral innate immunity. In humans, the type I IFN family consists of 16 members; namely 12 IFN-α subtypes, IFN-β, IFN-ε, IFN-κ and IFN-ω (reviewed in Gonzalez-Navajas et al., 2012). Of all the members of type I IFN family, IFN-α and IFN-β are the best studied and most widely expressed (reviewed in Trinchieri, 2010). Of relevance to the current study, type I IFNs such as IFN-β and IFN-α can be induced following activation of TLR/RLR signalling pathways by RV dsRNA (See Section 1.5). As previously described in Section 1.5,

production of IFNs including type I IFNs is mainly controlled at the gene transcriptional level where IRFs act as major regulators of the IFN gene expression (reviewed in Honda and Taniguchi, 2006). Among nine members of IRF family, IRF3 and IRF7 are believed to be the key regulators of virally-induced type I IFN production.

1.7.1.2. Type III

The type III IFN family was only discovered in 2003, and includes IFN-λ1, IFN-λ2 and IFN-λ3 (Kotenko et al., 2003, Sheppard et al., 2003). Type III IFNs are induced in virally infected cells by mechanisms similar to those for type I IFNs (reviewed in Honda et al., 2006). Although the signalling pathways triggered downstream of type I and type III receptor engagement lead to similar transcriptional responses, the cellular receptors utilised are distinct (reviewed in Levy et al., 2011) (See section 1.7.2 below for details).

1.7.2. IFN-stimulated genes (ISGs)

Upon viral infection, type I (IFN-α and IFN-β) and type III (IFN-λ) IFNs are produced by the virally-infected cells. The newly secreted type I and type III IFNs then trigger expression of over 300 IFN-stimulated genes (ISGs) in neighbouring cells via binding to distinct cell surface receptors (reviewed in Kotenko, 2011). IFN-α and IFN-β bind to a heterodimeric IFN-α/β receptor (IFNAR) composed of two chains, IFNAR1 and IFNAR2. IFN-λs bind to an unrelated receptor consisting of IFN-λ receptor 1 (IFNLR1) chain and a second chain, IL-10R2 which is shared by the IL-10 family of cytokines (reviewed in Levy et al., 2011). Binding of any of these IFNS to their respective receptors leads to activation of the Janus kinase (Jak)/signal transducer and activator of transcription (STAT) signalling pathways, which then activates transcription of hundreds of ISGs (reviewed in Samuel, 2001, Grandvaux et al., 2002). It is the proteins encoded by the ISGs that mediate the antiviral effects of these IFNs. Figure 1.7C shows a brief overview of the Jak/STAT signalling pathways activated following the binding of type I IFN, IFN-β to IFNAR which leads to induction of ISGs in response to RV infection. The main ISGs studied within this thesis (i.e. CCL5 and CXCL10) are described below.

1.7.2.1. CCL5

CCL5, previously known as regulated on activation, normal T cell expressed and secreted (RANTES), is one of the ISGs produced in response to viral infection. CCL5 is produced in a

variety of different cell types including epithelial cells, fibroblasts and T lymphocytes (Smith et al., 1996, Xia et al., 1997). CCL5 is a chemoattractant of monocytes, eosinophils and T lymphocytes, but does not attract neutrophils (Schall et al., 1990). CCL5 has been shown to bind to the chemokine receptors CCR1 (Gao et al., 1993, Neote et al., 1993), CCR3 (Daugherty et al., 1996) and CCR5 (Combadiere et al., 1996, Raport et al., 1996).

1.7.2.2. CXCL10

CXCL10, previously known as IFN-γ-induced protein of 10kDa (IP-10), is another ISG produced in response to viral infection. CXCL10 is produced in a variety of different cell types including endothelial cells, epithelial cells and fibroblasts (Miller and Krangel, 1992, Oppenheim et al., 1991). CXCL10 is a chemokine responsible for recruitment of monocytes and T cells, but has no effect on neutrophils chemotaxis (Dewald et al., 1992, Miller and Krangel, 1992). CXCL10 binds to the G-protein coupled receptor CXCR3 (Loetscher et al., 1996). Of relevance to this project, CXCL10 protein levels are increased in the airways of patients with COPD (Saetta et al., 2002).

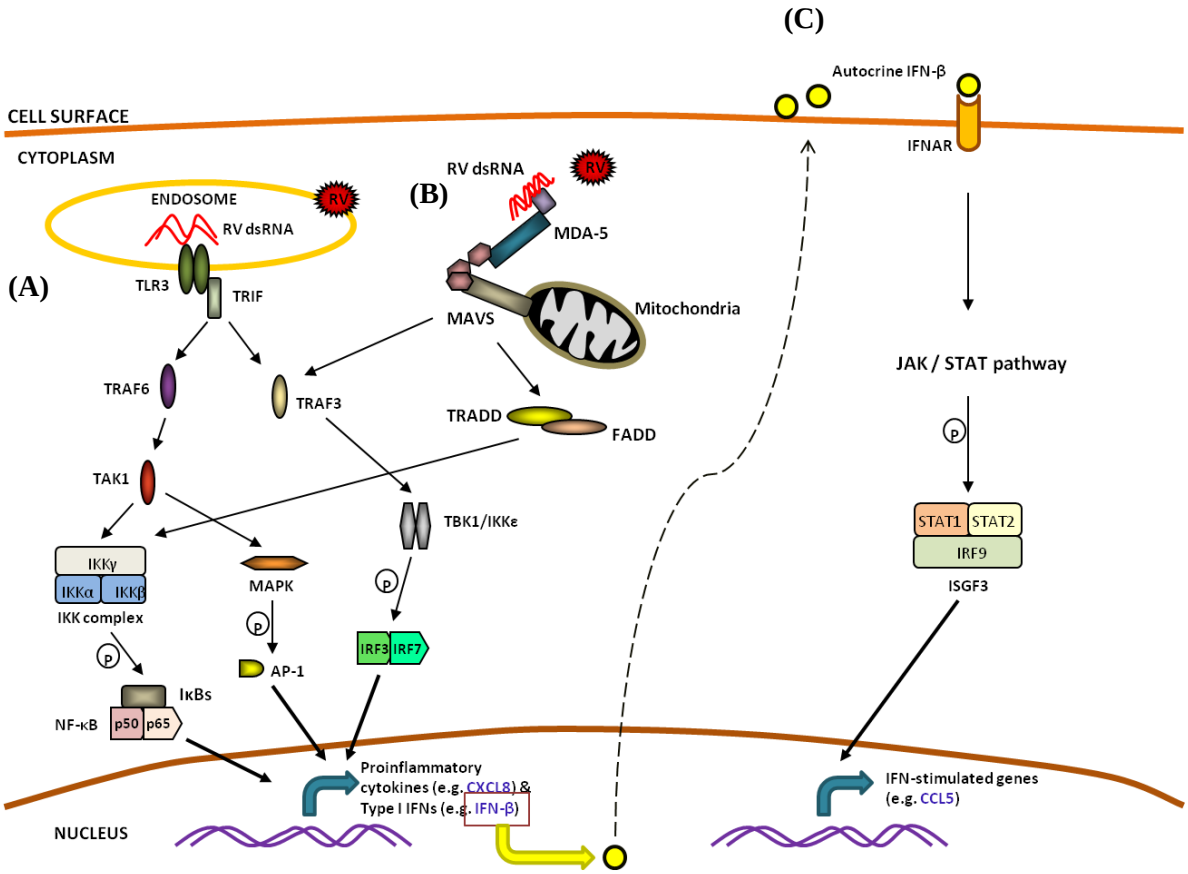

Figure 1. 7 Signalling pathways implicated in the production of type I IFNs and ISGs in response to RV infection.

(A) TLR3- and (B) MDA5- mediated signalling pathways that lead to production of type I IFNs in response to RV infection. See Figure 1.4 & 1.5 for description. (C) IFN-β-bound IFNAR transmits signals downstream via the Jak/STAT pathway. STAT1 and STAT2 are phosphorylated by Jak kinases, translocated to the nucleus, and form a transcription activator, ISGF3 with a DNA-binding subunit, IRF9. ISGF3 activates hundreds of IFN-stimulated genes such as CCL5. (See List of Abbreviations for the abbreviations used in this figure legend.)

1.8. Autophagy

Macroautophagy (referred to herein as autophagy) is a regulated catabolic process by which cytosolic damaged organelles or unused proteins are sequestered in double-membrane vesicles termed autophagosomes. Autophagosomes then fuse with lysosomes to form autolysosomes for subsequent degradation of cytosolic cargos and recycling of amino acid pools (reviewed in Richetta and Faure, 2013, Codogno et al., 2012) [See (Figure 1.8)]. Autophagosomes can also fuse with endosomes to form amphisomes; before fusing with lysosomes (reviewed in Ryter et al., 2011). Autophagy is primarily used as cellular adaptation to a variety of stress conditions, such as nutrient starvation, contributing to cell survival. However, autophagy may also be involved in the cell death pathway (reviewed in Richetta and Faure, 2013, Patel et al., 2013). Beyond its role in homeostasis maintenance, autophagy can also destroy intracellular microorganisms such as viruses and bacteria through their selective targeting (reviewed in Levine et al., 2011).

Autophagy is a complex process involving multiple phases and proteins (See Figure 1.8). To date, over 30 autophagy-related gene (Atg) proteins have been discovered to be involved in the autophagy pathway (reviewed in Nakahira and Choi, 2013). The first phase in the autophagy pathway is the formation of isolation membranes termed phagophores. A phagophore could originate from several sources including the ER, the Golgi apparatus, and the plasma membrane of the mitochondria (reviewed in Nakahira and Choi, 2013, Richetta and Faure, 2013). Following induction of autophagy (as a result of stress conditions such as nutrient depletion), the uncoordinated-51-like autophagy activating kinase 1 (ULK1) complex translocates to the targeted membrane (such as the ER membrane) and subsequently activates the class III phosphoinositide 3-kinase (PI3K) complex. This class III PI3K complex, which is composed of several proteins including Beclin-1, class III PI3K, phosphoinositide 3-kinase regulatory subunit 4 (PIK3R4), Atg14, and activating molecule in Beclin-1-regulated autophagy protein 1 (AMBRA1) is required for the formation of phagophores (reviewed in Ryter et al., 2011, Levine et al., 2011) (Figure 1.8).

During the elongation phase, the phagophore expands to surround and engulf a cytosolic cargo of material targeted for degradation, and eventually forms a double-membrane structure called autophagosome (Figure 1.8). The elongation phase of autophagosome formation requires two conjugation systems. In the first system, Atg12 is conjugated to Atg5. The resulting Atg5-Atg12 complex then forms a complex with Atg16L, which contributes to

elongation of the autophagic membrane (reviewed in Levine et al., 2011, Jordan and Randall, 2011). The second conjugation system requires the microtubule-associated protein-1 light chain 3 (LC3), which exists in two forms, LC3-I and LC3-II. The protease Atg4 cleaves the precursor form of LC3 to generate the LC3-I form, which has an exposed lipid conjugation site at the C-terminal glycine residue. LC3-I can be conjugated with the cellular lipid phosphatidylethanolamine (PE) by Atg7, Atg3 and the Atg5-Atg12-Atg16L complex to form LC3-II. The newly formed LC3-II is then incorporated into both cytoplasmic and luminal faces of the growing autophagosome. In mammals, the conversion of LC3-I (the free form) to LC3-II (the PE-conjugated form) is a crucial regulatory step in autophagosome formation (reviewed in Levine et al., 2011, Jordan and Randall, 2011, Patel et al., 2013).

In the final phases of autophagy, the autophagosome containing the cytosolic components and organelles fuses with the lysosome to become autolysosome (Figure 1.8). Subsequently, the lysosomal degradative enzymes such as acid hydrolases digest the encapsulated contents of autolysosomes. The digested contents are then released to the cytosol for metabolic recycling (reviewed in Nakahira et al., 2011, Levine et al., 2011).

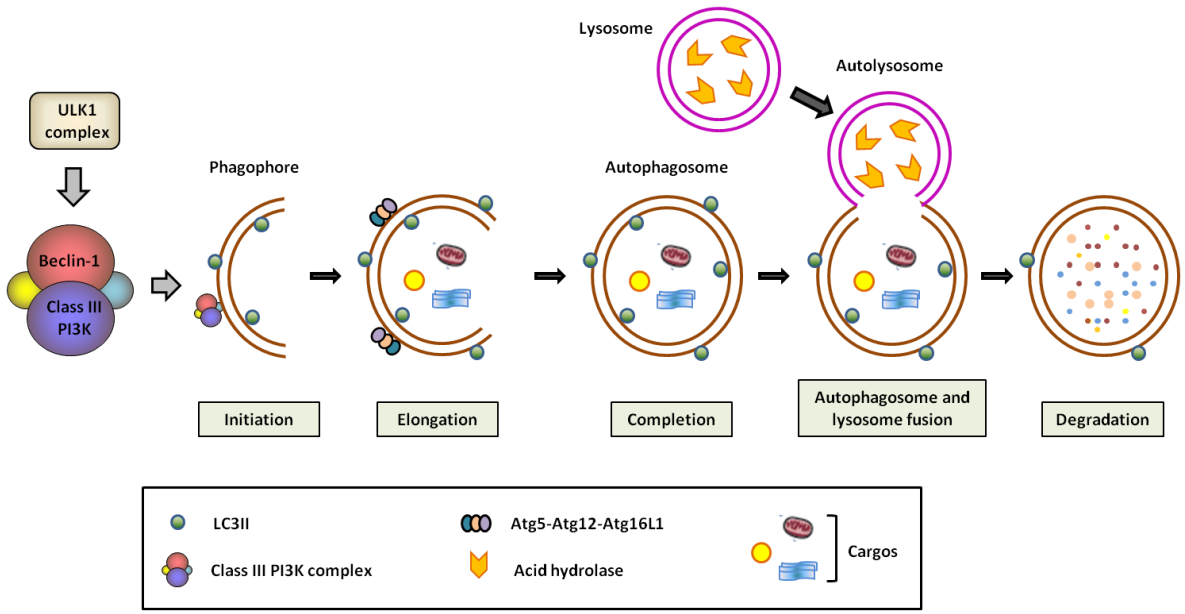

Figure 1. 8 Overview of the autophagy pathway.

Activation of the uncoordinated-51-like autophagy activating kinase 1 (ULK1) complex in response to certain signals initiates the formation of an isolation membrane termed phagophore. Class III phosphoinositide 3-kinase (PI3K) complex composed of Beclin-1, class III PI3K, phosphoinositide 3-kinase regulatory subunit 4 (PIK3R4), Atg14, and activating molecule in Beclin-1-regulated autophagy protein 1 (AMBRA1) is also involved in the phagophore formation. The Atg5-Atg12-Atg16L complex and LC3-II phosphatidylethanolamine (PE) conjugate promote the elongation and enwrap the cytosolic cargos including mitochondria, leading to the formation of autophagosome. Subsequently, lysosome fuses with the autophagosome (the formation of autolysosome) and releases acid hydrolases into the interiors to degrade the cytosolic cargos. [Other abbreviations used in the schematic diagram: Atg, autophagy-related gene protein; LC3, microtubule-associated protein-1 light chain 3]

[Information gathered from (Nakahira and Choi, 2013, Ryter et al., 2011)]

1.8.1. Autophagy in COPD

Increasing evidence suggests that autophagy may play a complex role in COPD by which it may cause either favourable or deleterious phenotype depending in the disease process (reviewed in Mizumura et al., 2012, Haspel and Choi, 2011). Chen and co-workers have shown that autophagy was increased in lung tissue samples derived from patients with COPD at all stages of disease severity (GOLD stage 0 to 4) (Chen et al., 2008). The authors also demonstrated that autophagy was upregulated *in vitro* in primary HBECs exposed to cigarette smoke extract (CSE), and *in vivo* in the lungs of mice that were chronically exposed to cigarette smoke (Chen et al., 2008). The same group also reported that autophagy and apoptosis were concomitantly activated in the BEAS-2B lung epithelial cell line in response to CSE treatment (Kim et al., 2008). Taken together, these studies provide evidence of the adverse effects of autophagy on COPD, by triggering lung epithelial cell death commonly associated with the development of emphysema, a key condition seen in COPD (See Section 1.1.1).

In contrast to the previous findings obtained in CSE-treated-lung epithelial cells (Chen et al., 2008, Kim et al., 2008), a recent study by Monick *et al.* demonstrated that autophagic activity was impaired in alveolar macrophages isolated from either patients with COPD, actively smoking patients without COPD (with a greater than 10 pack-year smoking history) or non-smokers; following CSE treatment (Monick et al., 2010). It is possible that the pathophysiological roles of autophagy is cell-type specific.

1.8.2. Autophagy in antiviral innate immunity

Recently, autophagy has been implicated as one of the mechanisms by which the host cells defend against various viral infections (reviewed in Yordy et al., 2012). Autophagy can contribute to antiviral innate immunity via multiple mechanisms including directly entrapping and degrading virions and virion components (a process termed xenophagy) and by mediating the recognition of viral PAMPs by PRRs (reviewed in Deretic et al., 2013, Jordan and Randall, 2011). Of relevance to the current study, the following section will focus on the role of autophagy in delivering cytosolic viral PAMPs to the endosomal PRRs.

1.8.2.1. Delivery of viral PAMPs to endosomal PRRs by autophagy

As previously discussed in Section 1.4, TLRs that are responsible for the recognition of viral nucleic acids (i.e. TLR 3, 7, 8 and 9) are located in the endosomes, whilst viral-detecting RLRs (i.e. RIG-I and MDA5) are localised in the cytosol. Since many RNA viruses such as RV release their nucleic acid to the cytoplasm for replication, it is clear how the cytoplasmic RLRs are activated by these infections. However, in the case of the endosomal TLRs, it is less apparent since the nucleic acid is protected from the endosomal environment by its capsid during endocytosis. Thus, whilst TLRs are known to play crucial roles in the early detection of many viral infections, the exact mechanisms remain unclear.

For several viruses, autophagy has been recently shown to be responsible for the delivery of cytosolic viral PAMPs to endosomal TLRs, which subsequently leads to the production of proinflammatory and antiviral cytokines (reviewed in Yordy et al., 2012, Richetta and Faure, 2013). In VSV infection, the production of antiviral IFN-α by murine plasmacytoid DCs was shown to be dependent upon the autophagic delivery of viral replication intermediates to endosomal TLR7 (Lee et al., 2007). Similarly, it has been reported that TLR7-dependent secretion of IFN-α by simian virus 5 (SV5) in human plasmacytoid DCs was dependent on autophagy (Manuse et al., 2010). Furthermore, Gorbea and colleagues have demonstrated the autophagy-dependent activation of TLR3 in human kidney fibroblasts infected with coxsackie virus B3 (CVB3) (Gorbea et al., 2010). More recently, Zhou *et al.* have shown that TLR7-dependent IFN-α production requires autophagy in human plasmacytoid DCs following infection with HIV-1 (Zhou et al., 2012).

1.8.2.2. Autophagy and RV infection

Whilst there are no studies to date specifically investigating the roles of autophagy in the induction of inflammatory responses to RV infection, several studies have reported the requirement for autophagy in RV replication, although this remains controversial. In their studies of RV-2 (a minor group of RV), Brabec-Zaruba *et al.* showed that this particular serotype of RV does not induce autophagy and that modulation of autophagy does not affect viral replication (Brabec-Zaruba et al., 2007). In contrast, another group has demonstrated that RV-2 and RV-14 (a major group of RV) induce autophagosome formation and that both RV serotypes exploit the autophagy machinery to promote their replication (Klein and Jackson, 2011, Jackson et al., 2005). However, all these published studies were performed

using HeLa cells, a human cervical epithelial cell line, and since RV is a natural respiratory tract pathogen, it would be of greater relevance to explore the roles of autophagy in RV infection of airway cells.

1.9. Phosphoinositide-3 kinase (PI3K)

Apart from causing the recruitment of signalling adaptor molecules to initiate proinflammatory responses (Section 1.5), TLR activation also leads to the activation of phosphoinositide 3-kinases (PI3Ks) (reviewed in Troutman et al., 2012). PI3Ks have been shown to play important roles in many cellular responses including cell proliferation, cell survival, autophagy and regulation of proinflammatory responses (reviewed in Troutman et al., 2012, Hazeki et al., 2007).

1.9.1. Classes of PI3Ks: A brief overview

PI3Ks are a family of cellular enzymes that phosphorylate the 3-hydroxyl group of the inositol ring of three species of phosphatidylinositol (PtdIns) lipid substrates; namely, PtdIns, PtdIns4phosphate (PtdIns4P) and PtdIns4,5bisphosphate (PtdIns(4,5)P_2) (reviewed in Vanhaesebroeck et al., 2010, Okkenhaug, 2013). The newly generated 3-phosphorylated phosphoinositides act as second messenger molecules, which regulate the intracellular localisation and activity of various effector proteins. The most important downstream effector of PI3K is the serine/threonine kinase Akt. The PI3K/Akt signalling pathway is involved in a wide variety of cellular responses including vesicle trafficking, cell growth, proliferation, autophagy and immunity (reviewed in McNamara and Degterev, 2011, Vanhaesebroeck et al., 2010) (Discussed in Section 1.9.2). There are eight mammalian PI3Ks which have been divided into three classes: class I, II and III; based upon structural characteristics and lipid substrate specificities (See Figure 1.9). Class I PI3Ks can phosphorylate PtdIns, PtdIns4P and PtdIns(4,5)P_2. Class II PI3Ks preferentially phosphorylate PtdIns and PtdIns4P, whilst class III PI3Ks can only phosphorylate PtdIns (reviewed in Vanhaesebroeck et al., 2010, Okkenhaug, 2013).

Amongst the three classes of PI3Ks, class I kinases are the best understood. Members of the class I PI3K family are composed of a catalytic subunit (termed p110) and a regulatory

subunit (p85-type, p101 or p87) (reviewed in Vanhaesebroeck et al., 2010, Okkenhaug, 2013). Class I PI3K isoforms are subdivided into class IA and class IB depending upon which regulatory subunit they employ. The class IA PI3Ks (p110α, p110β and p110δ) bind the p85 type of regulatory subunit, whilst the class IB PI3K (p110γ) binds one of two related regulatory subunits, p101 and p87 (See Figure 1.9). Unlike class II and III, all class I PI3Ks can phosphorylate PtdIns(4,5)P_2, which is converted to PtdIns(3,4,5)P_3 (reviewed in Okkenhaug, 2013, Troutman et al., 2012).

Compared to the other classes of PI3Ks, class II PI3Ks are the least understood. There are three isoforms of class II PI3Ks in mammals: C2α, C2β, andC2γ (See Figure 1.9). It is well accepted that class II PI3Ks can phosphorylate PtdIns and PtdIns4P to the corresponding 3-phosphoinositide lipids. However, whether class II PI3Ks are capable of phosphorylating PtdIns(4,5)P_2 remains unclear (reviewed in Falasca and Maffucci, 2012, Vanhaesebroeck et al., 2010). An *in vitro* study conducted by Gaidarov and colleagues has shown that upon addition of clathrin, PI3K-C2α could alter its substrate specificity, by which it could also convert PtdIns(4,5)P_2 to PtdIns(3,4,5)P_3; apart from synthesising PtdIns(4,5)P_2 from its common substrate PtdIns4P (Gaidarov et al., 2001). However, the exact mechanism of regulation of class II PI3K activity by clathrin remains to be determined.

Class III PI3K has only one member, namely, vacuolar protein sorting 34 (Vps34). The protein kinase Vps15, which forms a complex with Vps34, has been identified as a regulatory protein, however its specific role in Vps34 regulation remains poorly understood (reviewed in Vanhaesebroeck et al., 2010, Okkenhaug, 2013) (See Figure 1.9). Unlike class I and II PI3Ks, the class III PI3K Vps34 has a lipid substrate specificity limited to PtdIns, generating PtdIns4P. In mammals, Vps34 has a well established role in endocytosis, phagocytosis, and autophagy (reviewed in Okkenhaug, 2013, Vanhaesebroeck et al., 2010).

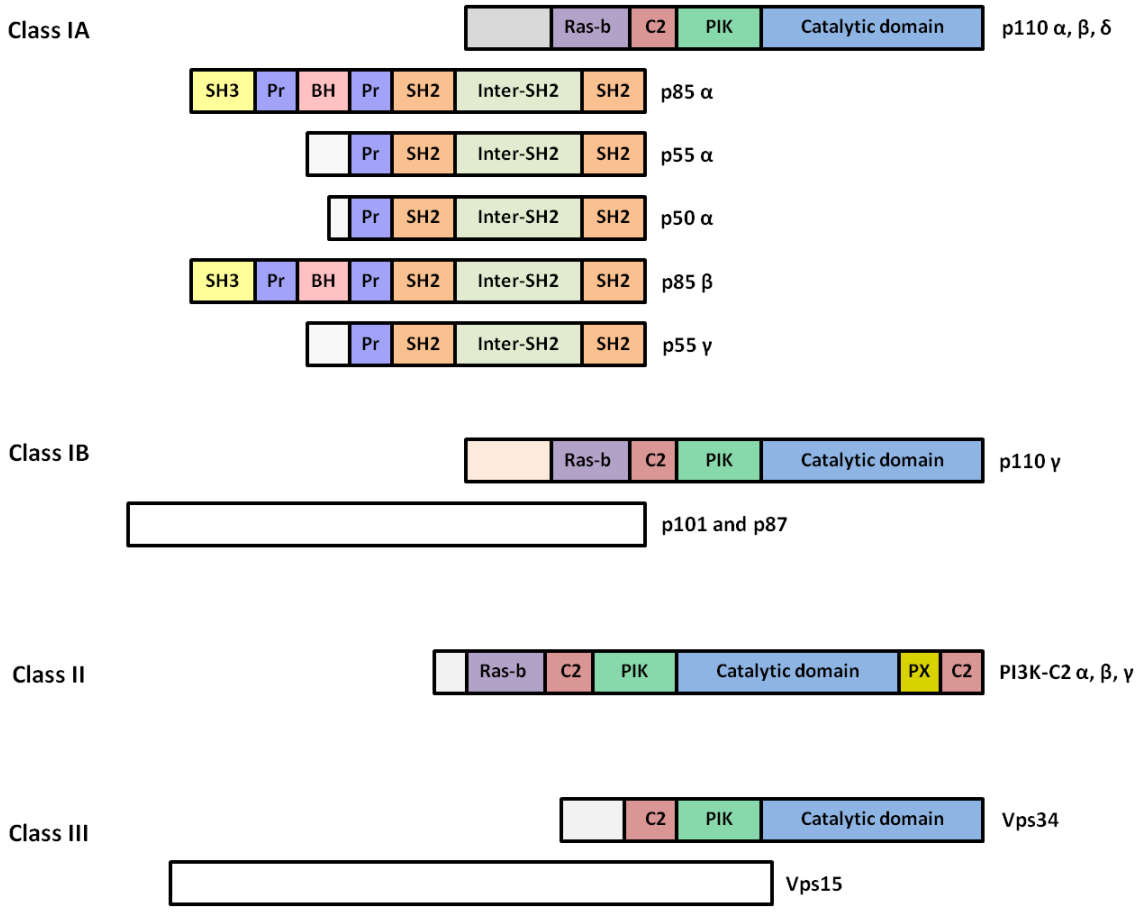

Figure 1. 9 Classification and structural characteristics of the PI3K family.
PI3Ks are divided into three classes based on their structural characteristics and substrate preferences. Each type of PI3K contains a C2 domain and a catalytic domain connected by a helical (PIK) domain. Class I and II, but not class III PI3Ks, also contain a Ras-binding (Ras-b) domain at their N terminal. Class I PI3Ks are subdivided into a class IA group (p110α, p110β and p110δ), which bind the p85 type of regulatory subunit, and a class 1B group (p110γ), which binds one of two related regulatory subunits, p101 and p87. All p85 isoforms have two Src homology 2 (SH2) domains. p101 and p87 lack SH2 domains and have no homology to other proteins or identifiable domain structure. Class II PI3Ks lack regulatory subunits but have two distinct domains at their C terminal, a phox homology (PX) domain and another C2 domain, which could mediate protein-protein interactions. Class III PI3K has only one catalytic member, Vps34 which forms a complex with a serine/threonine kinase, Vps15. (See List of Abbreviations for the abbreviations used in the schematic diagram and the figure legend.)

[Information gathered from (Vanhaesebroeck et al., 2010, Koyasu, 2003)]

1.9.2. The PI3K/Akt signalling pathway

As previously discussed in Section 1.9.1, class I PI3Ks can phosphorylate PtdIns(4,5)P_2 generating PtdIns(3,4,5)P_3. Increased concentrations of PtdIns(3,4,5)P_3 at the plasma membrane leads to the recruitment of the serine/threonine kinase Akt and 3-phosphoinositide dependent protein kinase-1 (PDPK1) (reviewed in Troutman et al., 2012, McNamara and Degterev, 2011). The close proximity of these two proteins at the plasma membrane promotes the phosphorylation of Akt by PDPK1. The activated Akt can phosphorylate and activate a wide range of substrates which mediate many cellular processes including cell growth, proliferation, cell metabolism and protein synthesis (reviewed in Courtney et al., 2010, McNamara and Degterev, 2011). Of relevance to the current study, the role of PI3K/Akt signalling in the regulation of TLR signalling pathway and autophagy are summarised below.

1.9.2.1. The role of PI3K/Akt signalling in the regulation of TLR signalling pathway

The role of PI3K/Akt signalling in the regulation of TLR signalling pathway remains incompletely understood. Studies using pharmacological inhibitors of PI3K have reported contradicting findings. Some studies have shown that PI3K acts as a positive regulator of TLR signalling and therefore the proinflammatory response; whilst other studies have demonstrated that PI3K inhibits the inflammatory response (reviewed in Troutman et al., 2012, Hazeki et al., 2007). Sarkar and colleagues have shown that TLR3-mediated phosphorylation and activation of IRF3 was inhibited by the general PI3K inhibitor LY294002 or wortmannin in human embryonic kidney 293 (HEK293), following stimulation with poly(I:C) (Sarkar et al., 2004). In contrast, a study done by Aksoy *et al.* demonstrated that treatment with LY294002 or wortmannin enhanced the TLR3-dependent NF-κB activation and IFN-β synthesis, in human DCs and HEK293 cells, in response to poly(I:C) stimulation (Aksoy et al., 2005). Furthermore, Ishii and co-workers have reported that wortmannin inhibited the uptake and co-localisation of CpG DNA with TLR9 in endocytic compartments, hence reducing CpG-induced activation of NF-κB and subsequent IL-12 production in mouse bone marrow-derived DCs (BMDCs) (Ishii et al., 2002). On the other hand, using the same cell type (i.e. mouse BMDCs) Fukao and colleagues demonstrated that CpG DNA-induced production of IL-12 was augmented by wortmannin (Fukao et al., 2002).

Studies using transgenic mice lacking PI3K regulatory or catalytic subunits are considered as a more specific approach to examine the role of PI3K in regulating TLR signalling (reviewed in Troutman et al., 2012, Ruse and Knaus, 2006). Similar to the results obtained by pharmacological studies, the findings attained by genetic studies concerning the pro- or anti-inflammatory roles of PI3K/Akt pathway are also contradictory, although it could be due to the cell-type specificity of the PI3K/Akt signalling (reviewed in Hazeki et al., 2007, Ruse and Knaus, 2006). Most studies performed using DCs or macrophages provide evidence that the PI3K/Akt pathway acts as a crucial negative regulator of the proinflammatory response (reviewed in Troutman et al., 2012, Hazeki et al., 2007). Fukao and colleagues have shown that DCs obtained from p85α-deficient mice secreted higher levels of proinflammatory cytokines IL-12, IFN-γ and TNF-α upon TLR2, TLR4, TLR5 and TLR9 stimulation, compared to the wild-type controls (Fukao et al., 2002). Using transient transfection, Pengal and co-workers demonstrated that mouse Raw 264.7 macrophage cell line over-expressing a constitutively active form of Akt generated higher levels of the anti-inflammatory cytokine IL-10, in response to LPS (Pengal et al., 2006). Furthermore, a study has shown that macrophages from Akt1-deficient mice had increased LPS-induced production of the proinflammatory cytokines IL-6, TNF-α and IL-17 (Androulidaki et al., 2009). In contrast, Yum and colleagues have shown that lung neutrophils obtained from p110γ-deficient mice exhibited reduced levels of NF-κB activation and the subsequent production of the proinflammatory cytokines IL-1β and TNF-α, in response to LPS (Yum et al., 2001). Additionally, Rhee *et al.* demonstrated that the non-transformed human colonic epithelial NCM460 cells transiently transfected with the dominant negative form of p85 or Akt showed lower TLR5-mediated IL-8 production (Rhee et al., 2006).

1.9.2.2. A role for PI3K/Akt/mTOR signalling in autophagy modulation

The kinase mammalian target of rapamycin (mTOR) is one of the most studied downstream targets of the PI3K/Akt pathway. mTOR is a serine/threonine kinase which acts as a crucial negative regulator of autophagy. The PI3K/Akt pathway activates mTOR in response to growth factors such as insulin or nutrients such as amino acids (reviewed in Heras-Sandoval et al., 2014, Choi et al., 2013). Suppressing mTOR activity by nutrient starvation or other cellular stresses leads to activation of ULK1 complex and subsequent formation of phagophore (See Section 1.8 for description of the autophagy pathway). Autophagy supplies recycled nutrients to the cells, which in turn reactivates mTOR to inhibit autophagy. Apart

from autophagy, mTOR also plays a vital role in controlling other cellular processes including cell growth and metabolism (reviewed in Shimobayashi and Hall, 2014, Deretic et al., 2013).

In normal physiological condition, mTOR phosphorylates ULK1 (a positive regulator of autophagy) at Ser758, preventing the interaction between ULK1 and adenosine 5'-monophosphate-activated protein kinase (AMPK) (a positive regulator of autophagy that responds to energy depletion), and therefore inhibits autophagy (Kim et al., 2011, reviewed in Shimobayashi and Hall, 2014). Under nutrient depletion, mTOR is inactivated, and hence ULK1 is dephosphorylated, allowing ULK1 to interact with AMPK. AMPK sequentially phosphorylates ULK1 at Ser317 to activate it (Kim et al., 2011, reviewed in Shimobayashi and Hall, 2014). Activated ULK1 then translocates to the targeted membrane (such as the ER membrane) and subsequently activates the class III PI3K complex which is necessary for phagophore nucleation (See Section 1.8) (reviewed in Mizushima et al., 2011, Levine et al., 2011). Furthermore, several studies have shown that mTOR can directly phosphorylate and inhibit Atg13 (a positive regulator of ULK1) at a phosphorylation site (or sites) that is yet to be identified (Hosokawa et al., 2009, Ganley et al., 2009, Jung et al., 2009). More recently, Yuan and colleagues demonstrated that mTOR can also inhibit autophagy by directly phosphorylating Atg14. The phosphorylation of Atg14 impedes PtdIns4P generation by the Atg14-containing class III PI3K complex (Yuan et al., 2013).

1.10. Hypotheses and aims

COPD is an increasing global health problem that needs further attention. Understanding the complex pathological mechanisms in COPD is crucial in order to offer better treatments. The substantial difficulty in translating findings obtained using murine models of COPD makes the *in vitro* human tissues experimental system essential (Sabroe et al., 2007a).

Possible involvement of other tissue cells beyond epithelium, such as fibroblasts in amplifying inflammatory response in COPD remains to be fully determined. There is mounting evidence reporting the effects of respiratory viruses such as RV on the exacerbations of COPD; however, there is still much to learn about the exact mechanisms of RV-induced COPD exacerbations.

Autophagy has been shown to participate in the control of various viral infections (reviewed in Yordy et al., 2012). However, the potential role of autophagy in mediating recognition of dsRNA intermediates by endosomal TLR3 and therefore inflammatory responses is not yet studied.

In this thesis, it was **hypothesised** that:

1. Airway fibroblasts play important roles in COPD exacerbations via TLR/IL-1R signalling pathways; and can affect how viral infections are controlled in health and disease.
2. Autophagy is required for the presentation of cytoplasmic RV dsRNA to the TLR3-containing endosomes, therefore plays a role in the RV-induced innate immune responses.

The **aims** of this thesis were:

1. To investigate the innate immune responses of human airway fibroblasts to RV infection, and to compare those responses with those of airway epithelial cells.
2. To determine whether autophagy is involved in the detection of RV infection, and therefore regulates the RV-induced responses of airway epithelial cells.

2. Materials and Methods

2.1. Materials

2.1.1. Culture media

Table 2. 1 Culture media used in this study listed in alphabetical order.

Name	Composition; (Supplier)	Application
BEAS-2B cell infection media	RPMI 1640 containing 2 mM L-glutamine (Invitrogen), 2% low endotoxin fetal calf serum (FCS)* (PromoCell, Heidelberg, Germany), 100 U/ml penicillin, 100 µg/ml streptomycin (Invitrogen, Paisley, UK).	BEAS-2B cell infection
BEGM complete media	Bronchial Epithelial Basal Media (BEBM) (PromoCell, Heidelberg, Germany) with Bronchial Epithelial Growth Media (BEGM) single quot additives (PromoCell, Heidelberg, Germany)	HBEC culture
BEGM single quot additives	0.004 ml/ml bovine pituitary extract, 10 ng/ml recombinant human epidermal growth factor, 5 µg/ml recombinant human insulin, 0.5 µg/ml hydrocortisone, 0.5 µg/ml adrenaline, 6.7 ng/ml triiodo-L-thyronine, 100.5 µg/ml human transferrin, 0.1 ng/ml retinoic acid (all from PromoCell, Heidelberg, Germany)	HBEC culture
HeLa Ohio cell infection media	DMEM containing 2mM L-glutamine (Invitrogen), 2% low endotoxin FCS (PromoCell, Heidelberg, Germany), 100 U/ml penicillin, 100 µg/ml streptomycin (Invitrogen), 2% 1M HEPES (Invitrogen), 1% sodium bicarbonate (Invitrogen)	HeLa Ohio cell infection
HBEC infection media	BEBM (PromoCell, Heidelberg, Germany)	HBEC infection
HLF infection media	Lung Fibroblast Basal Media (LFBM) (PromoCell, Heidelberg, Germany)	HLF infection
IPFF complete media	DMEM containing 2mM L-glutamine (Invitrogen), 15% low endotoxin FCS (PromoCell, Heidelberg, Germany), 100 U/ml penicillin, 100 µg/ml streptomycin (Invitrogen)	IPFF culture
IPFF infection media	DMEM containing 2mM L-glutamine (Invitrogen), 2% low endotoxin FCS (PromoCell, Heidelberg, Germany), 100 U/ml penicillin, 100 µg/ml streptomycin (Invitrogen)	IPFF infection
LFGM complete media	LFBM (PromoCell, Heidelberg, Germany) with Lung Fibroblast Growth Media (LFGM) single quot additives (PromoCell, Heidelberg, Germany)	HLF culture
LFGM single quot additives	0.02 ml/ml FCS, 1 ng/ml recombinant human fibroblast growth factor, 5 µg/ml recombinant human insulin (all from PromoCell, Heidelberg, Germany)	HLF culture
MEM complete	MEM containing 2mM L-glutamine (Sigma-Aldrich), 10% low endotoxin FCS (PromoCell, Heidelberg, Germany), 100	MRC-5 cell culture

media	U/ml penicillin, 100 µg/ml streptomycin (Invitrogen, Paisley, UK).	
MRC-5 cell infection media	MEM containing 2mM L-glutamine (Sigma), 2% low endotoxin FCS (PromoCell, Heidelberg, Germany), 100 U/ml penicillin, 100 µg/ml streptomycin (Invitrogen, Paisley, UK).	MRC-5 cell infection
RPMI 1640 complete media	RPMI 1640 containing 2mM L-glutamine (Sigma), 10% low endotoxin FCS (PromoCell, Heidelberg, Germany), 100 U/ml penicillin, 100 µg/ml streptomycin (Invitrogen, Paisley, UK).	BEAS-2B cell culture

* NOTE: Endotoxin levels of the FCS used were equal to or less than 0.5 endotoxin units (EU)/ml.

2.1.2. Buffers and reagents

Table 2. 2 Buffers and reagents used in this study listed in alphabetical order.

Reagent	Composition	Application
2X sample buffer	4% sodium dodecyl sulfate (SDS), 0.1M Dithiothreitol (DTT), 20% glycerol, 62.5mM Tris-HCL (pH 6.8), 0.004% bromophenol blue	Western blot
Agarose	Agarose molecular grade powder (National Diagnostics, UK)	Agarose gel electrophoresis
ELISA coating buffer (pH 7.2-7.4)	0.14M NaCl, 2.7mM KCl, 1.5mM KH_2PO_4, 8.1mM Na_2HPO_4	ELISA
ELISA wash buffer (pH 7.2)	0.5M NaCl, 2.5mM NaH_2PO_4, 7.5mM Na_2HPO_4, 0.1% TWEEN-20, pH to 7.2 with NaOH	ELISA
Phosphatase lysis buffer	50mM Tris Base, 50mM NaF, 50mM β -glycerophosphate, 10mM sodium orthovanadate, 1% Triton X-100, 1mM PMSF, 1:100 Protease inhibitor cocktail III (Calbiochem)	Western blot
Resolving gel (10 or 12 %)	0.375M Tris Base (pH 8.8), 0.1% SDS, 10/12% polyacrylamide, 0.1% ammonium persulphate (APS), 0.04% TEMED	Western blot
SDS-PAGE running buffer	20mM Tris Base (pH 8.8), 192mM glycine, 0.1% SDS	Western blot
Stacking gel (5%)	0.125M Tris Base (pH 6.8), 0.1% SDS, 5% polyacrylamide, 0.1% APS, 0.08% TEMED	Western blot

TAE (50X)	242 g Tris Base, 37.2 g EDTA, 57.1 ml acetic acid	Agarose gel electrophoresis
Transfer buffer	20mM Tris Base (pH 8.8), 192mM glycine, 0.01% SDS, 20% methanol	Western blot

2.1.3. Commercially available kits

Table 2. 3 Commercially available kits used in this study listed in alphabetical order.

Name	Components	Application	Supplier
DNA-free™	10X DNase I Buffer, rDNase I, DNase Inactivation Reagent	Genomic DNA removal	Ambion
High-Capacity cDNA Reverse Transcription Kit	10X RT Buffer, 25X dNTP Mix (100mM), 10X RT Random Primers, MultiScribe™ Reverse Transcriptase, RNase Inhibitor, nuclease-free water	cDNA synthesis	Applied Biosystems
RNeasy Mini Kit	Buffer RLT, Buffer RW1, Buffer RPE, RNase-free water, QIAshredder spin columns, RNeasy spin columns, 2ml and 1.5ml collection tubes	Total RNA extraction	Qiagen

Refer to manufacturers' component formulations for detailed component composition.

2.1.4. Antibodies

2.1.4.1. Antibodies for western blot

Table 2. 4 Antibodies for western blot used in this project.

Primary; (Supplier)	Secondary (All from Cell Signaling Technology)
1:2000 anti-Beclin-1 (Abcam)	1:2000 anti-mouse IgG-HRP
1:2000 anti-LC3 (Cell Signaling Technology)	1:2000 anti-rabbit IgG-HRP
1:2000 anti-Atg7 (Cell Signaling Technology)	1:2000 anti-rabbit IgG-HRP
1:1000 anti-VPS34 (Cell Signaling Technology)	1:2000 anti-rabbit IgG-HRP
1:2000 anti-p110 β (Cell Signaling Technology)	1:2000 anti-rabbit IgG-HRP
1:15000 anti-Actin (Sigma-Aldrich)	1:2000 anti-rabbit IgG-HRP

2.1.4.2. Antibodies for Enzyme-Linked Immunoabsorbent Assay (ELISA)

All antibodies for ELISA were purchased from R&D Systems (Abingdon, UK) in a lyophilised form and resuspended, as per manufacturer's recommendations.

Table 2. 5 Antibodies for ELISA used in this project.

Cytokine	ELISA detection limit	Antibody function	Antibody concentration	Isotype
CXCL8	78.1 pg/ml	Capture	1.5 μg/ml	Mouse IgG_1
		Detection	80 ng/ml	Biotinylated goat IgG
CCL5	312.5 pg/ml	Capture	2 μg/ml	Mouse IgG_1
		Detection	20 ng/ml	Biotinylated goat IgG
CXCL10	125 pg/ml	Capture	2.8 μg/ml	Mouse IgG_1
		Detection	0.28 μg/ml	Biotinylated goat IgG
IL-6	39.1 pg/ml	Capture	1 μg/ml	Mouse IgG_1
		Detection	50 ng/ml	Biotinylated goat IgG

2.1.5. DNA oligonucleotides

2.1.5.1. Primers and probes for Real-time PCR

Real-time PCR primer-probe set specific for glyceraldehyde 3-phosphate dehydrogenase (GAPDH) was obtained from Applied Biosystems (Cat. Number: Hs00182082_m1) in a pre-mixed, solution form. The other primers and probes used were from Sigma-Aldrich (Table 2. 6) obtained in a dry pellet form; and were resuspended using nuclease-free water at a stock concentration of 100 μM and stored at -20°C. Primer and probe working stocks were prepared by diluting to 5 μM in nuclease-free water and stored at -20°C. Each probe contains the FAM fluorescent dye and the TAMRA quencher.

Table 2. 6 TaqMan Real-time PCR primers and probes purchased from Sigma-Aldrich.

Name	Sequence (5'-3')
18S forward	CGCCGCTAGAGGTGAAATTCT
18S reverse	CATTCTTGGCAAATGCTTTCG
18S probe	ACCGGCGCAAGACGGACCAGA
IFNβ forward	CGCCGCATTGACCATCTA

IFNβ reverse	TTAGCCAGGAGGTTCTCAACAATAGTCTCA
IFNβ probe	TCAGACAAGATTCATCTAGCACTGGCTGGA
Rhinovirus forward	GTGAAGAGCCSCRTGTGCT
Rhinovirus reverse	GCTSCAGGGTTAAGGTTAGCC
Rhinovirus probe	TGAGTCCTCCGGCCCCTGAATG

2.1.5.2. Primers for end-point PCR

PCR primers used in this study (Table 2. 7) were designed using Primer3 software (available online at http://frodo.wi.mit.edu/primer3/). Genomic and mRNA sequences of the target gene were obtained from NCBI Nucleotide database. The newly-designed primer sequences were run on the NCBI BLAST database to confirm the species-specificity (i.e. human) of the primer. With an exception of GAPDH primers (Eurogentec), all PCR primers were purchased from Sigma-Aldrich in a dry pellet form. Primers were resuspended using nuclease-free water at a stock concentration of 100 µM and stored in 20 µl aliquots at -20°C. GAPDH primers were purchased from Eurogentec in a liquid form.

Table 2. 7 End-point PCR primers used in this project.

Name	Sequence (5'-3')	Annealing Temperature	Product size
TLR3 forward	AGTGCCCCCTTTGAACTCTT	60.0°C	544 bp
TLR3 reverse	GCCAGTTCAAGATGCAGTGA		
TLR7 forward	ACTCCTTGGGGCTAGATGGT	60.0°C	358 bp
TLR7 reverse	GTAGGGACGGCTGTGACATT		
TLR8 forward	TCCTTCAGTCGTCAATGCTG	60.0°C	660 bp
TLR8 reverse	GTAGGGAGCTTGGCAGTTTG		
RIG-I forward	TGCACGAATGAAAGATGCTC	60.0°C	451 bp
RIG-I reverse	TGCAATGTCAATGCCTTCAT		
MDA-5 forward	CTGCTGCAGAAAACAATGGA	60.0°C	614 bp
MDA-5 reverse	TCCAGGCTCAGATGCTTTTT		
MAVS forward	CCTACCACCTTGATGCCTGT	60.0°C	504 bp
MAVS reverse	AAAGGTGCCCTCGGACTTAT		
IRF1 forward	TGGCTGGGACATCAACAAGG	64.0°C	168 bp
IRF1 reverse	TTCCTGCTCTGGTCTTTCACCTCC		
IRF3 forward	CAAGAGGCTCGTGATGGTCAAG	67.5°C	124 bp
IRF3 reverse	TGGGTGGCTGTTGGAAATGTG		
IRF7 forward	TCGTGATGCTGCGGGATAAC	67.5°C	176 bp

IRF7 reverse	ATGTGTGTGTGCCAGGAATGG		
GAPDH forward	ACTTTGGTATCGTGGAAGGAC	50°C	420 bp
GAPDH reverse	TGGTCGTTGAGGGCAATG		

2.2. Maintenance of cell lines

2.2.1. BEAS-2B cell line

The immortalised human bronchial epithelial cell line BEAS-2B (American Type Culture Collection [ATCC], LGC Standards, Teddington, UK) were maintained in 75 cm^2 flasks (Nunc^{TM}, Roskilde, Denmark) in RPMI 1640 complete media (Table 2.1). Cells were passaged when they reached ~95% confluency. The old culture media was removed and the flask washed once with 10 ml of phosphate buffered saline (PBS) (Invitrogen or Lonza), 2 ml of cell dissociation solution (CDS) (Sigma-Aldrich) was placed into the flask and incubated in a humidified incubator at 37°C with 5% CO_2 for 5 minutes (min) until the cell monolayer detached from the flask surface. Once cells had detached the CDS was deactivated by addition of 8 ml of cell culture media. Cells were counted using a haemocytometer and sub-cultured into a new flask at the desired density. Cells were grown in a humidified incubator at 37°C with 5% CO_2.

2.2.2. MRC-5 cell line

The immortalised human lung fibroblast cell line MRC-5 cells (American Type Culture Collection [ATCC], LGC Standards, Teddington, UK) were maintained in 75 cm^2 flasks in MEM complete media (Table 2.1). Cells were passaged when they reached ~95% confluency. The old culture media was removed and the flask washed once with 10 ml of PBS. 2 ml of trypsin-EDTA (TE) (Invitrogen) was added into the flask and incubated in a humidified incubator at 37°C with 5% CO_2 for 5 min until the cell monolayer detached from the flask surface. Once cells had detached the TE was deactivated by addition of 8 ml of cell culture media. Cells were counted using a haemocytometer and sub-cultured into a new flask at the desired density. Cells were grown in a humidified incubator at 37°C with 5% CO_2.

2.3. Maintenance of primary cells

2.3.1. Human bronchial epithelial cells (HBECs)

Primary Human Bronchial Epithelial Cells (HBECs) were purchased from PromoCell (Heidelberg, Germany) who isolated the cells from normal human adult tissue. The cells were maintained in 75 cm^2 flasks (Nunc™, Roskilde, Denmark) in BEGM complete media (Table 2. 1) and grown in a humidified incubator at 37°C with 5% CO_2. Media was replaced every 2-3 days and cells were passaged every 7-12 days using the PromoCell Detach kit (Heidelberg, Germany). Once resuscitated, cells were given the passage number 1 and were typically cultured and used in experiments until passage 6, beyond which point cell growth rate and transfection efficiency was reduced and cells were no longer used.

2.3.2. Human lung fibroblasts (HLFs)

Primary Human Lung Fibroblasts (HLFs) were purchased from PromoCell (Heidelberg, Germany) who isolated the cells from normal human adult tissue. The cells were maintained in 75 cm^2 flasks (Nunc™, Roskilde, Denmark) in LFGM complete media (Table 2. 1) and grown in a humidified incubator at 37°C with 5% CO_2. Media was replaced every 2-3 days and cells were passaged every 5-9 days using the PromoCell Detach kit (Heidelberg, Germany). Once resuscitated, cells were given the passage number 1 and were typically cultured and used in experiments until passage 6, beyond which point cell growth rate was reduced and cells were no longer used.

2.3.3. Idiopathic Pulmonary Fibrosis patient fibroblasts (IPFFs)

Primary Idiopathic Pulmonary Fibrosis patient fibroblasts (IPFFs) were a kind gift from Prof. C.M. Hogaboam, University of Michigan Medical School, USA. The IPFFs were obtained following lung biopsies from patients with idiopathic pulmonary fibrosis (IPF) (slow and rapid progressors). The cells were maintained in 75 cm^2 flasks (Nunc™, Roskilde, Denmark) in IPFF complete media (Table 2. 1) and grown in a humidified incubator at 37°C with 5% CO_2. Media was replaced every 2-3 days and cells were passaged every 5-9 days using trypsin-EDTA (Invitrogen). Once resuscitated, cells were given the passage number 1 and were typically cultured and used in experiments until passage 6, beyond which point cell growth rate was reduced and cells were no longer used. Note that several experiments

involving the use of IPFFs were performed with the assistance of our senior laboratory technician, Dr Linda Kay.

2.4. Mycoplasma testing

The mycoplasma testing was performed by the technicians of our research department using the following protocol.

Cell culture media was tested monthly to detect any presence of mycoplasma contamination using the EZ-PCR mycoplasma test kit, which amplifies specific DNA by PCR (Geneflow, Staffordshire, UK). The test was performed according to the manufacturer's instructions.

2.5. Stimulation of cells with synthetic TLR agonists and cytokines

Cells were grown to ~95% confluence in 12-well plates. At the time of stimulation, cells were washed with media, and stimulated with TLR agonists: poly(I:C) (TLR3) (Invivogen, Toulouse, France), LPS from *Escherichia coli* serotype R515 (TLR4) (Alexis, Nottingham, UK), and/or cytokines: IL-1β, IL-6, TNF-α, IFN-β (cytokines from PeproTech EC, London, UK) at the indicated concentrations. Cells were incubated in a humidified 37°C incubator with 5% CO_2 for the required time (see individual experiments). Cell lysates or cell-free supernatants were harvested and stored at -80°C until required.

2.6. Viral culture

2.6.1. Culture of human rhinovirus (RV) stocks

Human rhinovirus (RV) stocks were prepared by members of the research group using the following protocol.

Human RV minor group serotype 1B (RV-1B) and major group serotype 16 (RV-16) were propagated in HeLa Ohio cell (European Collection of Cell Cultures [ECACC], Sigma-Aldrich, Paisley, UK) monolayers in 175 cm^2 flasks (Nunc^{TM}). Cells were washed twice with 10 ml of HeLa Ohio cell infection media (Table 2.1) and 5 ml of virus stock added to cells with 7.5 ml of infection media. Flasks were gently agitated for 1 hour (h) at room

temperature, 12.5 ml of infection media was then added and incubated in a humidified incubator at 37°C with 5% CO_2 overnight or until approximately 90% cytopathic effect was observed. Flasks were placed in the freezer overnight at -80°C, allowed to defrost and then refrozen at -80°C for at least 1 h (x2) to ensure complete lysis of the HeLa Ohio cells. Cells were pooled and centrifuged at 1500 x *g* for 15 min to pellet cell debris. The resulting RV inoculum was decanted and filtered through a 0.2 µm filter (Millipore, Cork, Ireland) and then aliquoted and stored at -80°C. The 50% tissue culture infective dose ($TCID_{50}$)/ml values were determined via viral cytopathic effect (CPE) assay (Section 2.5.2). Neutralisation using serotype-specific antiserum was carried out to confirm RV-1B (ATCC® VR-1111AS-GP™) and RV16 (ATCC® VR-1126AS/GP™) identities.

2.6.2. Quantification of RV titers by viral cytopathic effect (CPE) assay

The quantification of RV titers was carried out by members of the research group using the following protocol.

50 µl of undiluted RV inoculum, or 50 µl of 10-fold dilutions (up to 10^{-9}) of the RV inoculum, were added to eight replicate wells of a 96-well plate (Nunc™). HeLa Ohio cells were split, resuspended in HeLa Ohio cell infection media (Table 2.1), counted and further diluted in infection media to give $1x10^5$ cells/ml. 150 µl of cells were added to each well, and the plate incubated in a humidified 37°C incubator with 5% CO_2 for 4 days. Viral cytopathic effect (CPE) was determined using light microscopy and infected wells were counted at Day 4. $TCID_{50}$/ml value was determined by scoring the sum of positive wells and using the Spearman-Karber formula.

2.6.3. RV infection of BEAS-2B cells, MRC-5 cells, HBECs, HLFs or IPFFs

BEAS-2B cells, MRC-5 cells, HBECs, HLFs or IPFFs were grown to ~95% confluence in 12-well plates. Cells were serum-starved overnight in their respective cell infection media (Table 2.1) prior to infection. Cells were infected with RV at the indicated $TCID_{50}$/ml for 1 h at room temperature with gentle agitation (80rpm). Filtrate control was obtained by centrifuging viral inocula in 0.2 micron filter tubes (Millipore, Cork, Ireland) at 12000 x *g* for 5 min. UV-inactivated RV was obtained by exposing viral inocula to UV light of 1000 mjoules/cm^2 for 10 min. Following incubation with RV for 1 h, virus was removed, cells were washed twice with media and 1 ml of cell infection media was added to each well. Cells were incubated in a humidified 37°C incubator with 5% CO_2 for the required time (see

individual experiments), after which cell lysates or cell-free supernatants were harvested and stored at -80°C until required.

2.7. Isolation of primary human peripheral blood monocytes

2.7.1. Preparation of Peripheral Blood Mononuclear Cells (PBMCs)

The preparation of PBMCs was performed by members of the research group using the following protocol.

Peripheral venous blood was taken from healthy volunteers, with written informed consent, in accordance with a protocol approved by South Sheffield Local Research Ethics Committee. PBMCs were separated from granulocytes by Optiprep™ (Axis-Shield, Oslo, Norway) density gradient.

2.7.1.1. Cell separation by Optiprep™ (iodixanol) gradient

(1) Whole blood (35.6 ml) was anticoagulated with 3.8% sodium citrate (4.4 ml), and plasma and cells were separated into an upper and lower phase respectively by centrifugation at 320 x *g* for 20 min.
(2) The plasma upper phase was removed and centrifuged at 1000 x *g* for 20 min to give platelet poor plasma (PPP) required in step 5.
(3) 6 ml of 6% Dextran T500, a red cell agglutination agent, was added and gently mixed with the lower cell phase. The mixture was then made up to 50 ml with 0.9% saline, gently mixed, and the air bubbles removed from the top (as this impedes sedimentation) before being allowed to sediment for 30 min.
(4) After 30 min, the upper white cell phase was removed and centrifuged at 221 x *g* for 6 minutes to leave a white cell pellet.
(5) The white cell pellet was re-suspended in 6 ml of Hank's Balanced Salt Solution (HBSS) without calcium and magnesium containing 20% PPP, and 4 ml of OptiPrep™. This cell mixture was gently overlaid with 10 ml of 1.095 g/ml OptriPrep™ (8.374 ml HBSS + 20% PPP and 3 ml OptiPrep™).
(6) 10 ml of 1.080 g/ml OptiPrep™ (10.435 ml HBSS + 20% PPP and 3 ml OptiPrep™) was applied over the 1.095 g/ml layer, and then a final 10 ml of HBSS + 20% PPP was applied over this. To prevent mixing of gradient densities it was important to form the

gradient in a 50-ml tube by gently tipping the tube at an angle of 30° whilst applying the layers with a Pasteur pipette.

(7) The gradient was centrifuged at 1978 x *g* for 30 min without a deceleration brake. This yielded three populations of cells: a red cell layer below the 1.095 g/ml layer, a PMN layer in between the two OptiPrep™ layers and a PBMC layer on top of the 1.080 g/ml Optiprep™ layer (below the HBSS) (Figure 2.1). Cells were washed as in Section 2.7.1.2.

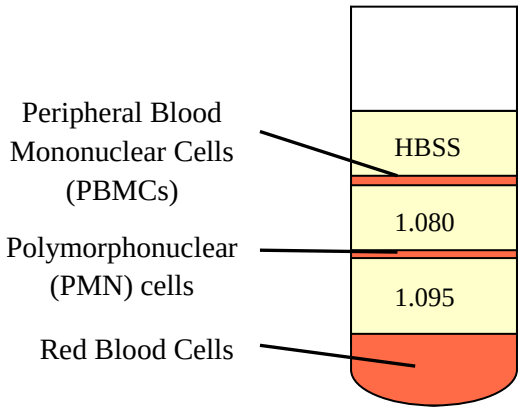

Figure 2. 1 The OptiPrep™ gradient demonstrating separation of cell populations.

2.7.1.2. Cell washes

The PBMCs were resuspended in 10 ml of HBSS + 20% PPP and centrifuged at 511 x g for 6 min. The pellet was then resuspended in RPMI 1640 with 10% low endotoxin FCS and 1% penicillin (100 U/ml) and streptomycin (100 µg/ml).

2.7.2. Negative magnetic selection to obtain purified monocytes

The preparation of highly purified monocytes was performed by other members of the research group using the following protocol.

Monocytes were further purified from PBMCs by negative magnetic selection using the Monocyte Isolation Kit II (Miltenyi Biotec, Audurn, CA, USA) as per manufacturer's instructions. Monocytes were isolated by depletion of non-monocytes (e.g. T and B cells, red blood cells, granulocytes and natural killer cells). Non-monocytes were labelled with a cocktail of biotin-conjugated monoclonal antibodies (monoclonal antibodies against CD3,

CD7, CD16, CD19, CD56, CD123 and Glycophorin A) as primary labelling reagent, and anti-biotin monoclonal antibodies conjugated to MicroBeads^{TM} as a secondary labelling reagent. The magnetically labelled non-monocytes were depleted through retention on a MACS Column in the magnetic field of a MACS separator, whilst the unlabelled monocytes passed through the column.

2.7.3. Treatment of BEAS-2B cells/monocytes cocultures with RV-1B and/or LPS

BEAS-2B cells were grown to ~95% confluence in 12-well plates. Cells were infected with RV-1B as described in Section 2.6.3, and/or stimulated with LPS (0.1 ng/ml). BEAS-2B/monocyte cocultures were created through the addition of 9500 highly purified $CD14^+$ monocytes per well (Section 2.7.2) to the BEAS-2B monolayers, giving a ratio of ~1 monocyte to 5 BEAS-2B cells. Monoculture controls were included in all experiments. The final volume in each well was 1 ml. Cells were then incubated in a humidified 37°C incubator with 5% CO_2 for the required time (see individual experiments). Cell lysates or cell-free supernatants were harvested and stored at -80°C until required.

2.8. Treatment of cells with pharmacological PI3K inhibitors

In indicated experiments, the PI3K inhibitors 3-MA (Sigma-Aldrich), LY294002 (Calbiochem, Merck Millipore, Darmstadt, Germany), PIK-75 (Cayman Chemical, Ann Arbour, MI), TGX-221 (Cayman Chemical), IC87114 (Calbiochem), AS605240 (Cayman Chemical), or PI-103 (Cayman Chemical) were used. The inhibitors were added at the time of stimulation with cytokines or poly(I:C), or immediately after viral infection, and cells were then cultured in a humidified 37°C incubator with 5% CO_2 for the required time (see individual experiments). Cell lysates or cell-free supernatants were harvested and stored at -80°C until required.

2.9. Treatment of cells with autophagy inducers or inhibitors

Cells were grown to ~95% confluence in 12-well plates. At the time of treatment, cells were washed with media, and treated with rapamycin, torin2, bafilomycin A1, starvation media, or

CSE, alone or in combination; at the indicated concentrations (See Section 2.11.1-3 for description of each treatment). Cells were incubated in a humidified 37°C incubator with 5% CO_2 for the required time (see individual experiments). Cell lysates were harvested and stored at -80°C until required. In some experiments, cells were fixed or left to remain alive, prior to visualisation of LC3 puncta (a marker of autophagosome formation) by fluorescence microscopy (See Section 2.13-15 for details).

2.9.1. Pharmacological autophagy inducers or inhibitors

In indicated experiments, pharmacological autophagy inducers rapamycin or torin2 used were from Tocris Bioscience, and the pharmacological autophagy inhibitor bafilomycin A1 used was from Sigma-Aldrich.

2.9.2. Nutrient starvation treatment

For nutrient starvation treatment, cells were cultured in HBSS containing calcium and magnesium (Invitrogen).

2.9.3. Preparation of cigarette smoke extract (CSE)

The preparation of CSE was carried out with the assistance of a member of our research group, Miss Claudia Paiva, using the following protocol.

Two 3R4F research-grade cigarettes (Tobacco and Health Research Institute, University of Kentucky, Lexington) were smoked using a peristaltic pump (Masterflex, USA). The smoke was slowly bubbled into 30 ml of sterile complete culture media in a 50-ml tube. Prior to the experiments, the filters were cut from the cigarettes. Each cigarette was smoked for 6 min. The resulting CSE solution was filtered through a 0.2 μm filter (Millipore, Ireland), designated as a 100% CSE solution, and used within 20 min after preparation. For the treatment, CSE was diluted in culture media for the required percentage.

2.10. Transient gene knockdown using small interfering RNA (siRNA)

Beclin-1, light chain 3 (LC3), autophagy-related protein 7 (Atg7), vacuolar protein sorting 34 (Vps34), p110β, and p110δ were knocked down in BEAS-2B cells or HBECs using a Dharmacon small interfering RNA (siRNA) system (Thermo Scientific, Lafayette, Colorado),

which utilises a pool of four individual siRNA duplexes to lead to gene silencing. The siRNA was delivered into the cells using the lipid-based transfection reagent Lipofectamine^{TM}2000 (Invitrogen). ON-TARGET*plus* SMARTpool siRNAs were used for targeting *Beclin-1*, *Atg7*, *Vps34*, p110β, and p110δ; and siGENOME SMARTpool siRNAs were used for targeting *LC3A* and *LC3B*. ON-TARGET*plus* Non-targeting siRNA #2 (D-001810-02) and siGENOME Non-targeting siRNA #2 (D-001206-14) were also used accordingly as scrambled (scr) controls. The target sequences of each individual siRNA used in this project are shown in Table 2.8.

Table 2. 8 Target sequences of each individual siRNA used in this project.

Target gene (Catalogue number)	Catalogue number of each siRNA duplex	Target sequence (5'-3')
Beclin 1 (L-010552-00)	J-010552-05	GAUACCGACUUGUUCCUUA
	J-010552-06	GGAACUCACAGCUCCAUUA
	J-010552-07	CUAAGGAGCUGCCGUUAUA
	J-010552-08	GAGAGGAGCCAUUUAUUGA
Atg7 (L-020112-00)	J-020112-05	CCAACACACUCGAGUCUUU
	J-020112-06	GAUCUAAACUCAAACUGA
	J-020112-07	GCCCACAGAUGGAGUAGCA
	J-020112-08	GCCAGAGGAUUCAACAUGA
Vps34 (L-005250-00)	J-005250-09	CACCAAAGCUCAUCGACAA
	J-005250-10	AUAGAUAGCUCCCAAAUUA
	J-005250-11	GAACAACGGUUUCGCUCUU
	J-005250-12	GAGAUGUACUUGAACGUAA
LC3A (M-013579-00)	D-013579-01	GGACGGCUUCCUCUAUAUG
	D-013579-02	CGGUGAUCAUCGAGCGCUA
	D-013579-03	ACAUGAGCGAGUUGGUCAA
	D-013579-04	CGCCCAUCGCGGACAUCUA
LC3B (M-012846-01)	D-012846-01	CAAAGUUCCUUGUACCUGA
	D-012846-02	GAUAAUAGAACGAUACAAG
	D-012846-03	GUAGAAGAUGUCCGACUUA
	D-012846-04	AGGAGACGUUCGGGAUGAA
p110β (L-003019-00)	J-003019-10	GGAUUCAGUUGGAGUGAUU
	J-003019-11	GGCGGUGGAUUCACAGAUA
	J-003019-12	GAUUAUGUGUUGCAAGUCA

	J-003019-13	CCAUAGAGGCUGCCAUAAA
p110δ (L-006775-00)	J-006775-09	ACGAUGAGCUGUUCCAGUA
	J-006775-10	CCAAAGACAACAGGCAGUA
	J-006775-11	GCGUGGGCAUCAUCUUUAA
	J-006775-12	CGAGUGAAGUUUAACGAAG

BEAS-2B cells or HBECs were grown to ~70% confluence in 12-well plates. Cells in each well were washed twice with PBS, and media replaced with 800 µl of RPMI 1640 supplemented with 10% FCS but without antibiotics (BEAS-2B cells) or BEBM media (HBECs). siRNA (1 µM in Opti-MEM media [Invitrogen]) and lipofectamine (25 µg/ml in Opti-MEM media) were equilibrated at room temperature for 5 min, and the two solutions were then combined and incubated for a further 20 min. 200 µl of the Lipid-siRNA complexes were added to each well (final concentration of each siRNA = 100 nM) and incubated for 4 h in a humidified incubator at 37°C with 5% CO_2. Cells were then washed with PBS before the addition of 1 ml of RPMI 1640 complete media (BEAS-2B) or BEGM complete media but without bovine pituitary extract (HBECs) (Table 2. 1) for recovery. Cells were incubated in a humidified incubator at 37°C with 5% CO_2 for 24 h before being serum-starved overnight by incubation in infection media (BEAS-2B) (Table 2. 1) or BEBM (HBEC), prior to RV infection. Transfection efficiency was determined by measuring protein expression of the target genes by western blot.

2.11. Transient transfection with GFP-LC3 expressing plasmids

The GFP-LC3 expressing plasmid (plasmid #11546, deposited by K. Kirkegaard research group, Addgene Inc.) was transfected into BEAS-2B cells using the lipid-based transfection reagent Lipofectamine^{TM}2000 (Invitrogen). BEAS-2B cells were grown to ~70% confluence on glass cover slips placed in 6-well plates (for fixed-cell imaging) or 35-mm glass bottom culture dishes (for live-cell imaging). Cells in each well or culture dish were washed twice with PBS, and media replaced with 1.5 ml of RPMI 1640 supplemented with 10% FCS but without antibiotics. The plasmid DNA (4 µg) and lipofectamine (10 µl) were made up to 250 µl with Opti-MEM media (Invitrogen) in two separate microcentrifuge tubes and left to equilibrate at room temperature for 5 min. The two solutions were then combined and

incubated at room temperature for a further 20 min. 500 µl of the lipid-plasmid DNA complexes were added to each well or culture dish and incubated for 6 h in a humidified incubator at 37°C with 5% CO_2. Cells were then washed with PBS before the addition of 2 ml of RPMI 1640 complete media (Table 2. 1) for recovery. Cells were incubated in a humidified incubator at 37°C with 5% CO_2 for 48 h before being treated with autophagy inducers (Section 2.11) for the required time (see individual experiments). Cells were then fixed or left to remain alive, prior to visualisation of GFP-LC3 puncta (a marker of autophagosome formation) by fluorescence microscopy (Section 2.15).

2.12. Immunohistochemistry

BEAS-2B cells were grown on glass cover slips placed in 6-well plates prior to treatment with autophagy inducers (Section 2.11). At the time of staining, cells were fixed with ice-cold 100% methanol and stained for endogenous LC3 using anti-LC3B (Sigma-Aldrich). The secondary antibody used was Alexa Fluor 488 (Molecular Probes). Nuclei were stained with 1x PBS containing 0.5 µg/ml 4',6-diamidino-2-phenylindole (DAPI; Sigma-Aldrich) and mounted on slides with Fluoromount (Southern Biotech). Staining was visualised by fluorescence microscopy (Section 2.15).

2.13. Fluorescence microscopy

Fluorescent images of cells were captured using the Olympus BX61 fluorescence microscope. For live-cell imaging, the microscope was enclosed in an environmental chamber equilibrated to 37°C.

2.14. Western blot analysis

2.14.1. Sample preparation for western blot analysis

Supernatants were removed and cells (~$5x10^5$) washed with PBS. Cells were lysed in 50 µl of phosphatase lysis buffer (Table 2.2). Lysed samples were suspended in an equal volume of

2X sample buffer (Table 2.2) and then heated for 5 min at 95°C. Samples were then stored at -80°C until analysis.

2.14.2. SDS-PAGE

The Bio-Rad mini PROTEIN II electrophoresis cell (Bio-Rad Laboratories Ltd, UK) was used to separate proteins according to size in a 10 or 12% resolving gel (Table 2.2). The resolving gel was poured to within 2 cm of the top of two glass plates separated by 0.75 mm spacers, in a horizontal casting system. The gel was overlaid with a thin layer of butan-2-ol to prevent evaporation, and allowed to set. Once set the butan-2-ol was removed and the gel washed with distilled water. The 5% stacking gel (Table 2.2) was poured on top of the resolving gel and a 15-well 0.75 mM comb inserted. The set gel was placed into the electrophoresis tank and covered with 1L of SDS-PAGE running buffer (Table 2.2). 10 µl of protein sample was loaded into the wells and samples electrophoresed at 60 V through the stacking gel and 200 V through the resolving gel.

2.14.3. Protein transfer and Ponceau S staining

Hybond-C-Extra nitrocellulose transfer membrane (0.45 µm pore size, GE Healthcare Life Sciences, UK) was soaked in transfer buffer (Table 2.2) along with 2 fibre pads and 2 pieces of 3 mm filter paper. A fibre pad and filter paper were placed on the black lower side of a gel cassette. The resolving gel with the samples was then placed onto the filter paper. The nitrocellulose membrane was placed on top of the gel and a piece of filter paper and fibre pad placed above. The cassette was closed and placed in a transfer tank with the black side facing the negative charge. Proteins were transferred to the membrane using the Bio-Rad mini Trans-Blot electrophoretic transfer cell (Bio-Rad laboratories Ltd, UK) for 70 min at 100 V. Protein transfer and equal loading was verified using reversible staining with Ponceau S (Bio-Rad laboratories Ltd, UK). The membrane was incubated with 30 ml Ponceau S for ~40 sec until protein bands were visible. The membrane was de-stained using 0.2% tween-PBS. Non-specific binding sites were then blocked by incubating with 5% non-fat milk in 0.2% tween-PBS for 1 h at room temperature on an orbital shaking platform.

2.14.4. Protein detection by western blot

The nitrocellulose membrane was incubated in primary antibody (Table 2.4) in 5% non-fat milk in 0.2% tween-PBS at 4°C overnight. The membrane was washed 4 times in 0.2%

tween-PBS (5 min per wash) before being incubated with secondary antibody (Table 2.4) in 5% non-fat milk in 0.2% tween-PBS for 1 h at room temperature. The membrane was then washed 4 times in 0.2% tween-PBS (5 min per wash). Labelled proteins were detected using a chemiluminescent kit (Bio-Rad laboratories Inc, UK). The blot image was acquired using a Bio-Rad ChemiDoc^{TM} XRS+ system (Hemel Hempstead, Herts, UK). Densitometric analysis was conducted using ImageJ image analysis software (NIH, United States).

2.14.5. Stripping and re-probing membranes

When required, membranes were stripped of existing primary and secondary antibodies by washing in water for 5 min and then incubating in 0.2M NaOH for 10-12 min on an orbital shaking platform to remove any bound antibodies. Membranes were then washed in water for 5 min followed by 0.2% tween-PBS for 5 min (2X). Membranes were blocked by incubating with 5% non-fat milk in 0.2% tween-PBS for 1 h at room temperature on an orbital shaking platform and then re-probed with alternate antibodies as described in Section 2.14.4.

2.15. Measurement of cytokine release by ELISA

Cell-free supernatants were prepared by centrifugation at 1000 x *g* for 3 min and stored at -80°C until cytokine generation was determined by ELISA using matched antibody pairs (R&D Systems) (Table 2. 5) at previously optimised concentrations. Samples were appropriately diluted in ELISA wash buffer (Table 2.2) to ensure analysis within the linear portions of a log (concentration) / linear (optical density) standard curve. All room temperature incubations were carried out on an orbital shaking platform.

For the ELISA, a 96-well plate (Costar) was coated with respective capture anti-human antibody (Table 2. 5) diluted in ELISA coating buffer (Table 2.2) and incubated overnight at room temperature. The plate was washed using the EL$_X$50 Autostrip Washer (Bio-Tek Instruments Inc.) and blocked with 1% ovalbumin in coating buffer for 1 h. After further washing, 100 µl of standard or sample was loaded per well in duplicate. The plate was incubated for 2 h, washed, and bound cytokine detected using biotinylated detection anti-human antibody (Table 2. 5) and incubated for a further 2 h. After a further wash, bound antibody was visualised using 1:200 streptavidin-HRP (Horse Radish Peroxidise) (Dako, UK) and substrate reagent (R&D Systems) according to the manufacturer's instructions.

Absorbance was measured at 450 nm wavelength using the Varioskan™ Flash multimode plate reader (Thermo Scientific, USA) and ScanIT™ software version 2.4.3 (Thermo Scientific, USA). ELISA detection limits for each cytokine are stated in Table 2. 5.

2.16. RNA extraction and purification

RNA was typically extracted from cells using TRI Reagent® (Sigma-Aldrich). For viral replication qPCR analysis, RNA was extracted using the RNeasy Mini Kit (Table 2. 3).

For RNA extraction using TRI Reagent®, cells in each well of the plate were washed in PBS to remove any residual culture media and 1 ml of TRI Reagent® was added to each well. Samples were incubated for 5 min at room temperature to ensure complete lysis. The lysed cells were then transferred to an Eppendorf tube and 200 µl of chloroform added. After mixing vigorously, the solution was left to separate for 10 min at room temperature, then centrifuged at 12,000 x *g* for 15 min at 4°C. This created three phases, the lower organic phase containing protein, the interphase containing DNA and the upper aqueous phase containing the RNA. The upper aqueous phase was transferred to a fresh tube. To this, 500 µl of isopropanol was added and after mixing vigorously the solution was left to separate for 10 min at room temperature. RNA was pelleted by spinning the solution at 12,000 x *g* for 10 min at 4°C and after removal of the supernatant, the pellet was washed in 75% ethanol and centrifuged at 7500 x *g* for 5 min at 4°C. The ethanol was removed to allow the RNA pellet to air-dry for approximately 10 min and then the RNA pellet was resuspended in 25 µl of sterile water (total volume was approximately 30 µl).

For RNA extraction using the RNeasy Mini Kit (Table 2.3), the cells were lysed using 350 µl per well of Buffer RLT. The lysed sample was mixed with an equal volume of 70% ethanol, added to an RNeasy mini-spin column, and centrifuged at 9000 x *g* for 15 sec. The columns were washed in 700 µl Buffer RW1 with centrifugation at 9000 x *g* for 15 sec. The columns were then washed twice using Buffer RPE. The columns were placed in new 2ml collection tubes and centrifuged again as above to completely remove any residual liquid. The columns were placed in new 1.5 ml collection tubes and RNA was eluted from the spin column using 30 µl nuclease-free water (giving approximately 10 µg RNA/sample extraction).

Following RNA extraction, any genomic DNA contamination was removed using DNA-free™ (Table 2.3) as per manufacturer's instructions. RNA yield and quality was then

determined using the Nanodrop-1000 spectrophotometer (Thermo Fisher Scientific, Loughborough, UK).

2.17. cDNA synthesis

20 µl of RNA (1 µg RNA per sample) was used to synthesise cDNA using the High-Capacity cDNA Reverse Transcription Kit (Table 2.3). The components of the reaction were mixed as shown in Table 2. 9. The reactions were carried out using the Hybaid PCR Express Thermal Cycler (Hybaid, Middlesex, UK), with a thermal cycling condition consisting of 25°C for 10 min, 37°C for 120 min, and 85°C for 5 min.

Table 2. 9 Composition of cDNA reactions.

Component	Volume / reaction
10X RT Buffer	4 µl
25X dNTP Mix (100mM)	1.6 µl
10X RT Random primers	4 µl
MultiScribe™ Reverse Transcriptase	2 µl
RNase Inhibitor	2 µl
Nuclease-free water	6.4 µl
Template RNA	20 µl
Total Volume	**40 µl**

2.18. Real-time PCR

Real-time PCR primers and probes used in this study are listed in Section 2.1.5.1. The primer-probe set specific to GAPDH (Applied Biosystems) are pre-mixed, thus 1 µl of this mixture was added directly to 10 µl of 2X qPCR Master Mix (Eurogentec, Southampton, UK). Primers and probes from Sigma-Aldrich were diluted to 300 nM for forward primers, 900 nM for reverse primers and 175 nM for probes and 1 µl of each was added to 10 µl of 2X qPCR Master Mix. 1 µl of cDNA sample was added to the final master mix containing the relevant primer-probe sets, which was then made up to a final volume of 20 µl with sterile water. The 384-well qPCR plate was sealed with an optical lid and centrifuged at 2000 rpm

for 2 min. The qPCR reactions were carried out using an ABI 7900 Automated TaqMan™ (Applied Biosystems), with an amplification cycle consisting of 50°C for 2 min, 94°C for 10 min, and 45 cycles of 94°C for 15 sec, 60°C for 15 sec. Samples were quantified against serial dilutions of standards of plasmids containing known copy numbers of target genes.

2.19. End-point PCR

2.19.1. PCR conditions

Template cDNA (2 µl) was incubated with the reagents (Promega) stated in Table 2.10. The thermal cycling conditions consisted of an initial denaturing step of 94°C for 2 min followed by 30 cycles consisting a denaturing step at 94°C for 30 sec, annealing step at a primer specific temperature (Table 2. 7) for 1 min and an extension step at 72°C for 30 sec. This was followed by a final extension at 72°C for 2 min and then holding at 4°C. The reaction was performed using a Hybaid PCR Express Thermal Cycler.

Table 2. 10 Composition of end-point PCR reaction.

Component	Volume / reaction
5X Green GoTaq® Flexi Buffer	5 µl
$MgCl_2$ solution (25 mM)	1.5 µl
dNTP Mix (10mM)	1 µl
Forward primer	0.7 µl
Reverse primer	0.7 µl
GoTaq® DNA Polymerase (5U/µl)	0.2 µl
Nuclease-free water	13.9 µl
Template cDNA	2 µl
Total Volume	**25 µl**

2.19.2. Visualisation by Agarose Gel Electrophoresis

A 1L solution of 1X TAE was prepared using TAE stock (50X, Table 2.2) and distilled water. 1.2 % agarose gels were prepared by addition of Agarose (Table 2.2) to 1X TAE solution. The agarose was dissolved by boiling and cooled to approximately 40°C, poured

into a gel-casting tray containing a well forming comb and left to set. The gel was placed into an electrophoresis tank containing 1X TAE and the comb removed. 5 µl of DNA ladder (i.e. HyperLadder IV, 100-1000bp; Bioline) or 10 µl of sample was loaded and samples run at a voltage of 100 V and a current of 100 mA for 1 hour. The gel was visualised using a Bio-Rad ChemiDoc^{TM} XRS+ system (Hemel Hempstead, Herts, UK).

2.20. Lactate dehydrogenase (LDH) assay to measure cell death

LDH release was measured using the CytoTox 96® Non-Radioactive Cytotoxicity Assay (Promega, Madison, USA). This assay utilises a 30-minute coupled enzymatic assay resulting in the conversion of a tetrazolium salt (INT) into a red formazan product. The amount of colour formed is proportional to the number of lysed cells. The general chemical reactions of the CytoTox 96® Assay are as follows:

LDH

$$NAD^+ + \text{lactate} \rightarrow \text{pyruvate} + NADH$$

Diaphorase

$$NADH + INT \rightarrow NAD^+ + \text{formazan (red)}$$

The assay was carried out as per manufacturer's instructions. Cell-free supernatants were prepared by centrifugation at 1000 x *g* for 3 min. Pelleted cells were kept for cell lysate analysis (see below). The cell monolayer was washed once with 500 µl PBS per well to remove any remaining supernatant. Pelleted cells were resuspended in 500 µl of media and transferred into the plate containing the attached cells. Cells were then lysed by freeze-thawing (incubation at -80°C for 40 min followed by thawing at 37°C for 40 min). Following cell lysis, cell-free supernatant containing maximum LDH amount was collected by centrifugation at 1000 x g for 3 min. 50 µl of cell-free supernatant or media from lysed cells was added to 96-well plates. Substrate mix was created by adding 12 ml of assay buffer to a bottle of substrate mix, and inverted gently to dissolve the substrate. Substrate mix was protected from strong direct light and used immediately. 50 µl of reconstituted substrate mix was added to each well. Plates were incubated at room temperature for 30 min in the dark. After 30 min, 50 µl of stop solution was added to each well. Large air bubbles were removed

and absorbance was immediately measured at 492 nm wavelength using an MRX plate reader (ThermoLabsystems, Vantaa, Finland) and Biolinx software version 2.20 (Biolinx, Frankfurt am Main, Germany).

Results from the CytoTox 96® Assay were expressed as the percentage LDH release, calculated as follows:

$$\% \text{ LDH release} = \frac{\text{Minimum release (OD of culture supernatant)}}{\text{Maximum release (OD of culture supernatant + OD of cell lysate)}} \times 100$$

NOTE: In order to correct for any endogenous LDH activity in animal serum, the optical density (OD) reading of "media alone" (media incubated in the absence of cells) was subtracted from all other values.

2.21. Statistics

Data are presented as mean ± SEM (standard error of the mean). Data were analysed using the appropriate statistical test and post-test as stated in the figure legends. A p value of ≤ 0.05 was considered statistically significant. Data were analysed using GraphPad Prism® v6.0 (GraphPad Inc, San Diego, CA, United States).

Chapter 3: Results. Differential responses of human lung fibroblasts and human bronchial epithelial cells to RV infection

3.1 Introduction

Whilst the airway epithelial cells have been considered as the primary site of RV infection, studies have detected the presence of RV in the subepithelial layer of lower airways (using *in situ* hybridisation), although the exact cell type was not determined (Papadopoulos et al., 2000, Wos et al., 2008). Fibroblasts are located just beneath epithelium (Sirianni et al., 2003), and this close contact between airway fibroblasts with airway epithelial cells suggests that RV may also infect fibroblasts. It has been reported that following experimental RV-39 infection, viral replication was higher in airway epithelial cells obtained from COPD subjects compared to that of healthy controls (Schneider et al., 2010). As COPD is associated with the airway tissue damage, this increases the probability of RV to further infect the underlying fibroblasts during a naturally attained RV infection in COPD patients. It is therefore interesting to explore the potential role of lung fibroblasts to amplify inflammation as a result of RV infection.

Apart from contributing to the detrimental airway remodelling in asthma and COPD (reviewed in Araya and Nishimura, 2010), it is known that airway fibroblasts also play major roles in the pathogenesis of idiopathic pulmonary fibrosis (IPF), whereby they are excessively proliferated in IPF lungs (reviewed in Hoo and Whyte, 2012). IPF is a chronic lung disease of unknown aetiology that often leads to respiratory failure and death within 2-5 years of diagnosis (reviewed in Zolak and de Andrade, 2012). Although the cause of IPF is unknown, several potential risk factors have been associated with the disease onset and development including cigarette smoking and other environmental exposures (reviewed in Deretic, 2008). Over the last 5 years, many studies have been reported proposing a role for viruses, such as HSV, Epstein-Barr virus (EBV) and torque teno virus (TTV), in triggering acute exacerbations of IPF (Guenther et al., 2010, Lasithiotaki et al., 2011, Wootton et al., 2011). To date, no study has been reported investigating the ability of RV to induce the inflammatory responses in lung fibroblasts isolated from IPF patients.

Clinical studies have reported increased levels of many proinflammatory cytokines, such as CXCL8, IL-1β and TNFα, in the sputum, bronchial epithelial cells and alveolar macrophages, taken from asthmatic, COPD and IPF patients (Sapey et al., 2009, Rusznak et al., 2000, Zhang et al., 1993, Ordonez et al., 2000). IL-1β has been shown to play a vital role in mediating airway inflammatory diseases (reviewed in Dinarello, 2009). Our group has previously showed that IL-1β could induce CXCL8 (a neutrophil chemoattractant) release from various airway tissue cells including epithelial cells and smooth muscle cells (Morris et al., 2006, Morris et al., 2005). Furthermore, IL-1β could synergistically potentiated cytokine release from cells stimulated with the viral dsRNA mimic poly(I:C) (Morris et al., 2006). However, the potential role of IL-1β to amplify the proinflammatory responses of RV-infected structural airway cells remains to be explored.

Coinfections with viral and bacterial pathogens are common within the airways of asthmatic and COPD patients, and are often associated with severe exacerbations of the diseases (Wilkinson et al., 2006, Louie et al., 2009). Our group has previously demonstrated that costimulation with poly(I:C) and bacterial-derived LPS could enhance CXCL8 release by bronchial epithelial cells in the presence of peripheral blood mononuclear cells (PBMCs) (Morris et al., 2006). Therefore, it is of interest to determine if LPS could potentiate RV-induced inflammatory responses of airway epithelial cells in the presence of innate immune cells.

3.2 Hypothesis and Aims

It was hypothesised that airway fibroblasts play important roles in COPD exacerbations via TLR/IL-1R signalling pathways; and can affect how viral infections are controlled in health and disease.

The specific aims of this chapter were to investigate:

1. The susceptibility of lung fibroblasts to RV infection and their ability to produce proinflammatory cytokines.
2. Whether differences existed between the responses of airway epithelial cells and fibroblasts to RV infection.

3. The potential detrimental effects of RV infection on Idiopathic Pulmonary Fibrosis patient fibroblasts (IPFFs).
4. The potential amplification of inflammatory responses of RV-infected cells in a proinflammatory environment.
5. The ability of viral and bacterial coinfection to potentiate inflammatory responses of airway tissue cells.

3.3 RV induces major cell death in airway fibroblast (MRC-5) cells but not airway epithelial (BEAS-2B) cells

3.3.1 RV-induced cytopathic effects in MRC-5 cells

A recent study investigating the responses of primary bronchial fibroblasts to the minor group RV, RV-1B, showed that fibroblasts were highly susceptible to RV-1B infection, in which viral inocula as low as multiplicity of infection (MOI) 0.08 caused marked cytopathic effects (i.e. cells became rounded and started to detach from the monolayer) (Bedke et al., 2009). Therefore, this study utilised a range of concentrations of RV-1B or RV-16 starting from $3.3x10^4$ $TCID_{50}$/ml (MOI ~0.01) to $2.0x10^7$ (MOI ~6) to infect the human lung fibroblast (MRC-5) cell line. Cells were left uninfected (media control) or infected with RV at the indicated $TCID_{50}$/ml as described in Section 2.6.3. Filtrate and UV-RV control samples ($2x10^7$ $TCID_{50}$/ml) were prepared as described in Section 2.6.3.

Figure 3.1 shows images of MRC-5 fibroblasts infected with RV-1B at a $TCID_{50}$/ml range of $3.3x10^4$ to $1.0x10^7$ for 24 h. RV-1B infection caused pronounced cytopathic effects, as determined by visual observation, in MRC-5 cells at $TCID_{50}$/ml of $2.7x10^5$, $4.0x10^5$, $1.0x10^6$, $2.0x10^6$, $4.0x10^6$, and $1.0x10^7$ (Figure 3.1). These concentrations of RV-1B elicited no obvious cytopathic effects in human bronchial epithelial (BEAS-2B) cells (images not taken). The cytopathic effects of RV-1B were dose-dependent, as the lower $TCID_{50}$/ml of RV-1B ($3.3x10^4$, $6.7x10^4$, $1.3x10^5$) did not result in cytopathic effects in the MRC-5 cells. As expected, filtrate and UV-RV treatment did not result in cell death (Figure 3.1).

The effect of the major group RV, RV-16, on MRC-5 fibroblast and BEAS-2B cell death are shown in Figure 3.2 and Figure 3.3, respectively. Again, similar to the results seen when cells were infected with RV-1B (Figure 3.1), RV-16 infection resulted in higher cytopathic cell

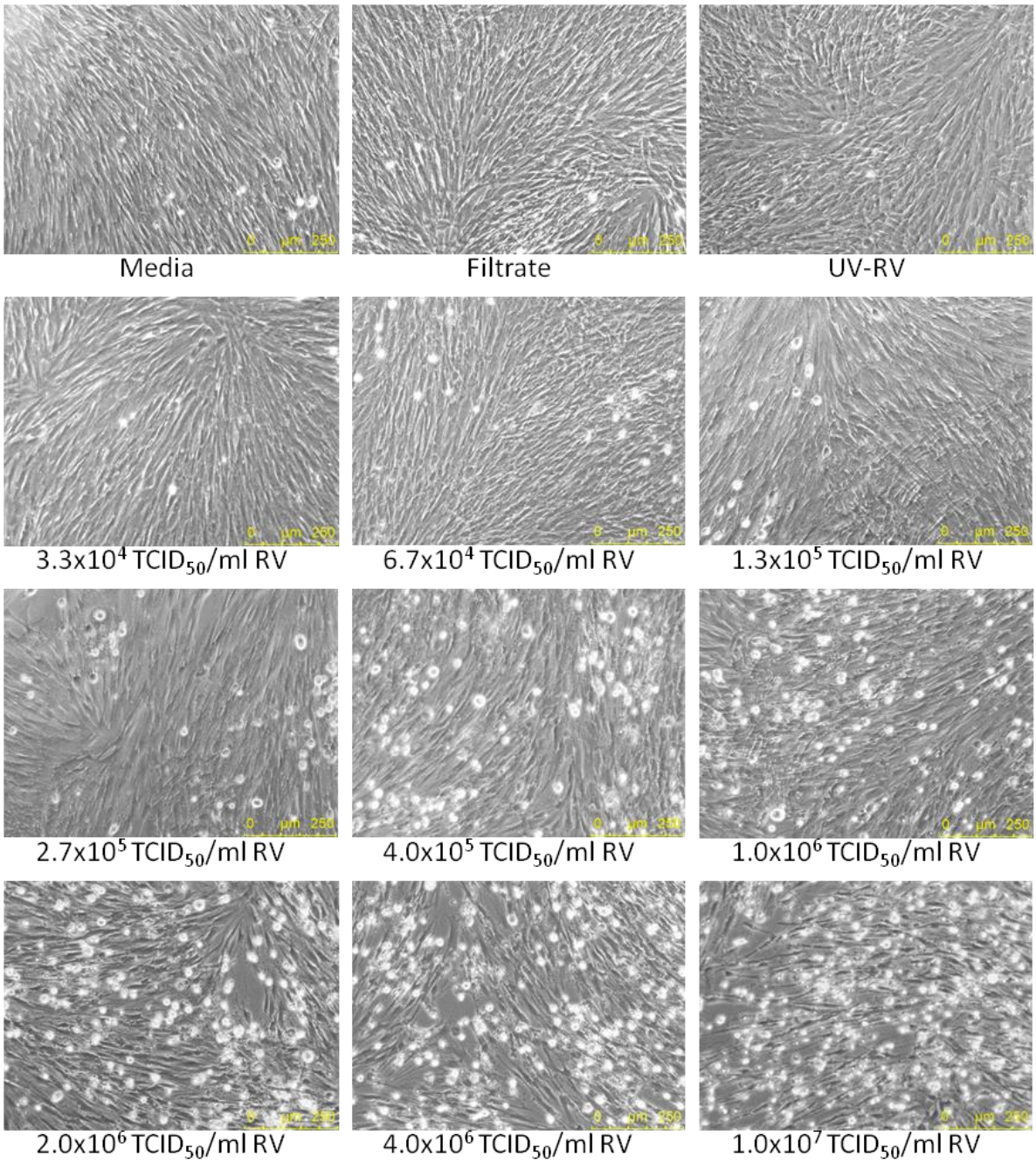

Figure 3. 1 RV-1B-induced cytopathic effects in MRC-5 cells.
MRC-5 cells were infected with RV-1B as described in Section 2.6.3 at the indicated $TCID_{50}$/ml. Filtrate and UV-RV control samples were prepared as described in Section 2.6.3. After 24 h, cell monolayers were observed using a fluorescence and phase contrast Leica DM14000B inverted microscope at 10x magnification. Data shown are representative images of $n = 4$ independent experiments.

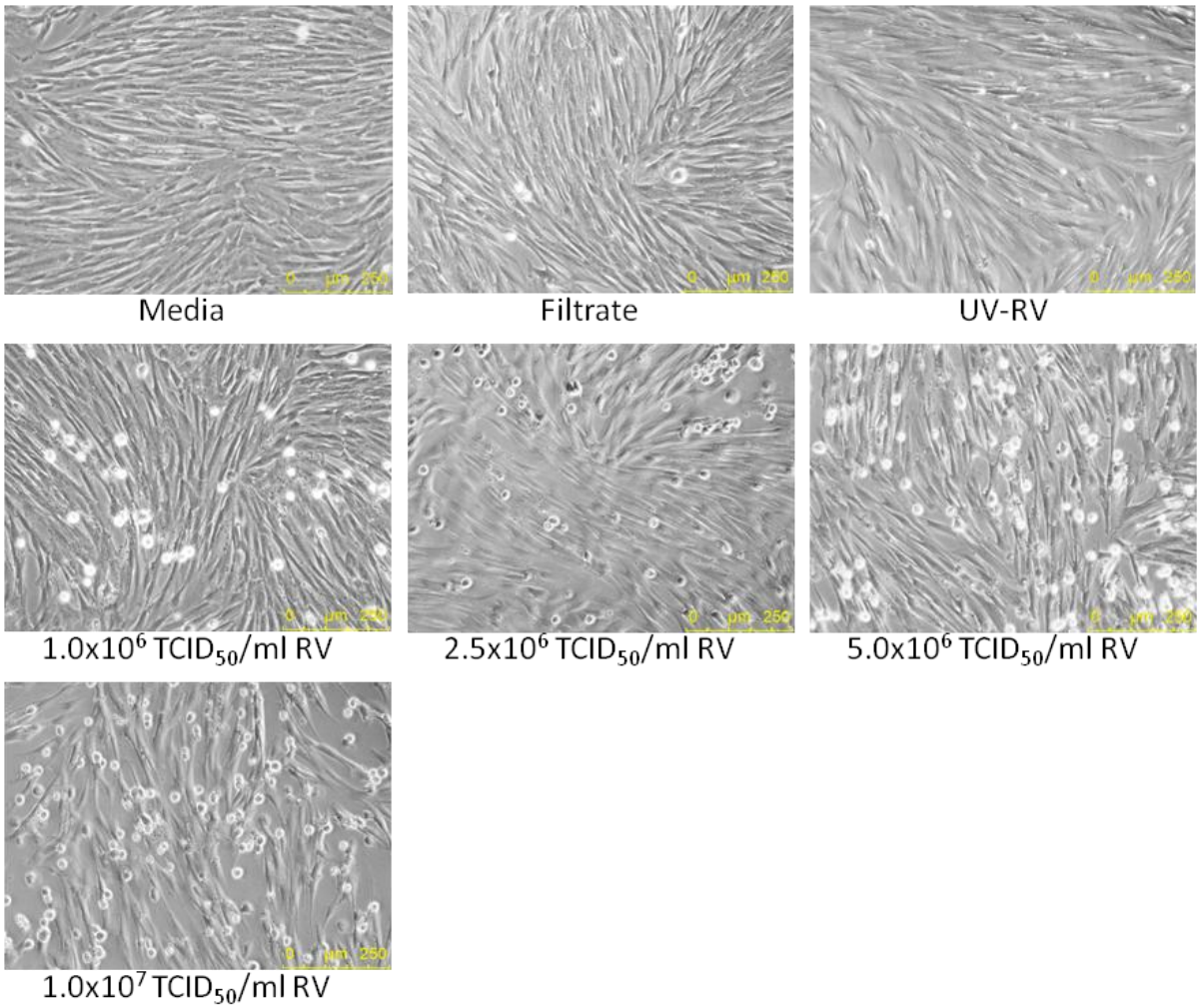

Figure 3. 2 RV-16-induced cytopathic effects in MRC-5 cells.

MRC-5 cells were infected with RV-16 as described in Section 2.6.3 at the indicated $TCID_{50}$/ml. Filtrate and UV-RV control samples were prepared as described in Section 2.6.3. After 24 h, cell monolayers were observed using a fluorescence and phase contrast Leica DM14000B inverted microscope at 10x magnification. Data shown are representative images of $n = 3$ independent experiments.

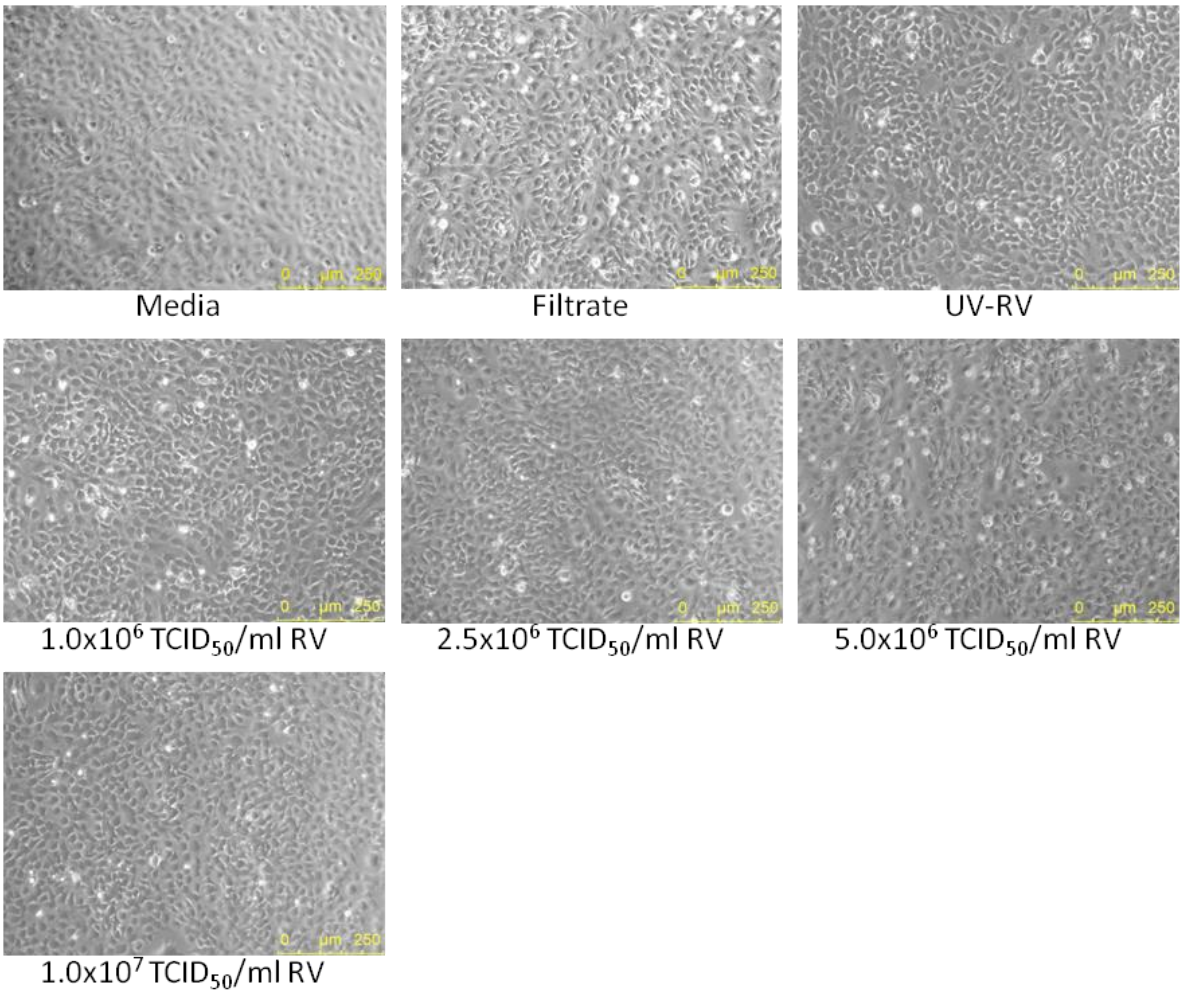

Figure 3. 3 RV-16-induced cytopathic effects in BEAS-2B cells.
BEAS-2B cells were infected with RV-16 as described in Section 2.6.3 at the indicated $TCID_{50}$/ml. Filtrate and UV-RV control samples were prepared as described in Section 2.6.3. After 24 h, cell monolayers were observed using a fluorescence and phase contrast Leica DM14000B inverted microscope at 10x magnification. Data shown are representative images of $n = 3$ independent experiments.

death in MRC-5 cells (Figure 3.2) than in BEAS-2B cells (Figure 3.3). For example, at $5.0x10^6$ $TCID_{50}$/ml, RV-16 caused ~20% rounded/detaching cells in MRC-5 fibroblasts (Figure 3.2) whilst it did not cause obvious rounding/detaching cells in BEAS-2B epithelial cells (Figure 3.3). Interestingly, the same concentration of RV-16 caused less cytopathic effects (Figure 3.2) as compared to RV-1B (Figure 3.1). For example, at $1.0x10^7$ $TCID_{50}$/ml, RV-16 only resulted in ~30% rounded/detaching cells (Figure 3.2), whilst RV-1B caused ~60% rounded/detaching cells (Figure 3.1).

3.3.2 LDH release measured by LDH assay is linearly correlated with cell death

To quantify the cell death observed in RV-infected cells, the LDH cytotoxic assay (Section 2.20) was utilised. LDH is a stable cytosolic enzyme present within all mammalian cells. The normal plasma membrane is impermeable to LDH, but damage to the cell membrane allows leakage of LDH into the extracellular fluid. Prior to using the LDH assay to measure cell death, a pilot experiment was conducted to confirm that the OD readings obtained from the LDH assay were linearly correlated to the amount of LDH released from the dead cells. Supernatant obtained from BEAS-2B cell lysates was serially diluted (1:1, 1:2, 1:4, 1:8, 1:16, 1:32, 1:64, 1:128). 6.1 x 10^5 cells were used to obtain the 1:1 lysate sample, and the remaining dilutions were given putative cell numbers. The LDH assay was then performed as described in Section 2.20. Based on a single experiment, OD readings appeared to be linearly correlated to the amount of LDH released from the dead cells and were therefore could be considered as true representatives of cell viability (Figure 3.4).

3.3.3 RV-1B induces greater cell death in MRC-5 cells than in BEAS-2B cells

After validating the use of the LDH assay in determining the percentage of cell death, MRC-5 and BEAS-2B cell death as a result of RV-1B infection was quantified using the LDH assay. In keeping with the microscopic observations (Figure 3.1), RV-1B infection at the $TCID_{50}$/ml of $1.0x10^7$ induced 50% cell death in MRC-5 cells, whilst only 20% cell death was measured in BEAS-2B cells (Figure 3.5). Furthermore, when cells were infected with $4.0x10^6$ $TCID_{50}$/ml of RV-1B, 30% cell death was seen in MRC-5 cells, whilst only 14% cell death was found in BEAS-2B cells. The RV-1B-induced cell death of MRC-5 fibroblasts started to become minimal (similar to the media control) when the cells were infected with $4.0x10^5$ $TCID_{50}$/ml of RV-1B. Unexpectedly, the UV control sample gave a high percentage of LDH release, as measured by this assay (Figure 3.5), in contrast to what was observed

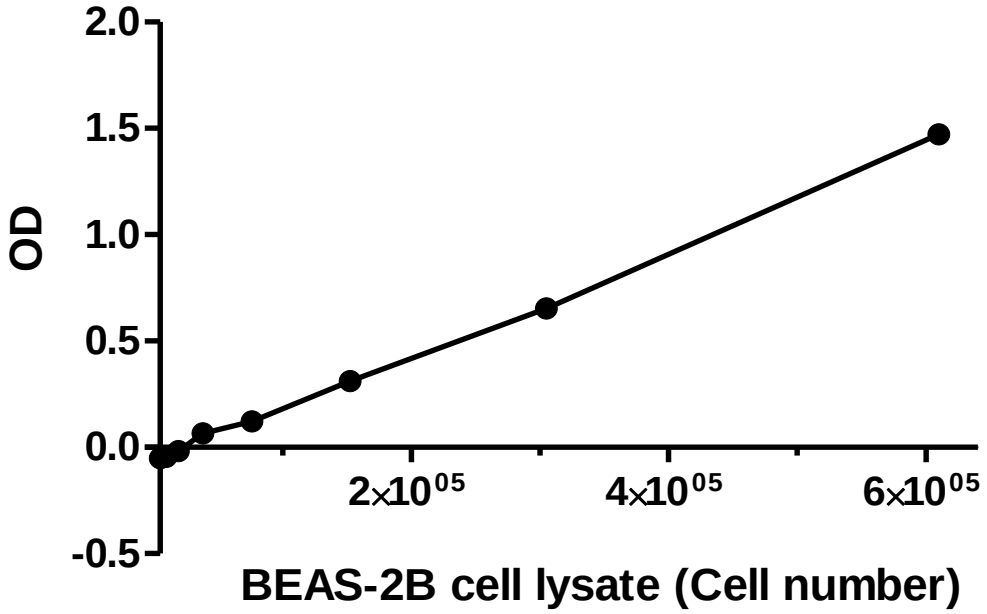

Figure 3. 4 OD readings obtained in LDH assay are linearly correlated with the amount of LDH released by the lysed (dead) cells.

Supernatant obtained from BEAS-2B cell lysates was serially diluted (1:1, 1:2, 1:4, 1:8, 1:16, 1:32, 1:64, 1:128). 6.1 x 10^5 cells were used to obtain the 1:1 lysate sample, and the remaining dilutions were given calculated cell numbers. The LDH assay was performed as described in Section 2.20. Data shown are $n = 1$.

A. MRC-5 cells

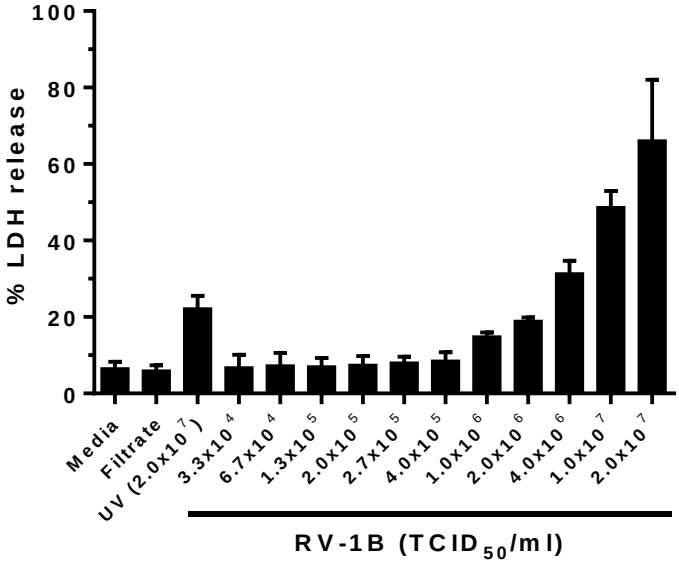

B. BEAS-2B cells

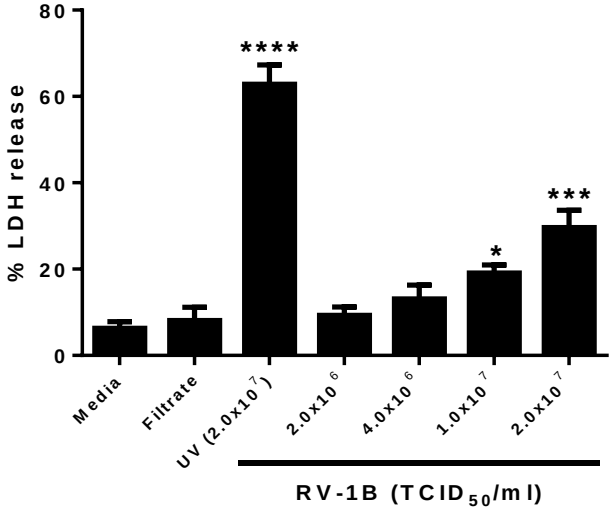

Figure 3. 5 RV-1B induces greater cell death in MRC-5 cells compared to BEAS-2B cells.

Cells were infected with RV-1B as described in Section 2.6.3 at the indicated $TCID_{50}$/ml. At 24 h p.i., cell death was measured as described in Section 2.20 and displayed as % LDH release by dead cells. Data shown are mean ± SD of $n = 2$ (A) or mean ± SEM of $n = 3$ (B) independent experiments. Significant differences are indicated by *p<0.05, ***p<0.001 and ****p<0.0001 (versus media control), as measured by one-way ANOVA with Dunnett's post-test.

microscopically (Figure 3.1). Thus the ability of UV-treated virus to cross-react with the LDH assay was explored further.

3.3.4 UV-treated virus cross-reacts with the LDH assay

Pilot experiments were conducted to investigate the possibility that UV-treated virus cross-reacted with the LDH assay. BEAS-2B cells were exposed to serial dilutions of UV-virus (1:1, 1:2, 1:5, 1:10). The cells were then incubated at 37°C/5% CO_2 for 24 h and LDH release measured by LDH assay. As hypothesised, exposure to UV-virus caused LDH release from BEAS-2B cells in a dilution-dependent manner (Figure 3.6A). As additional confirmation, a cell-free system was then utilised. Viral inoculum was exposed to UV light for 10 min, serially diluted in infection media, and immediately utilised in LDH assay. The UV-virus alone (cell-free system) resulted in high OD readings in a dilution-dependent manner, hence confirming the cross-reactivity of UV-virus with the LDH assay used to measure cell death (Figure 3.6B).

3.3.5 Poly(I:C) does not induce cell death in MRC-5 or BEAS-2B cells

To confirm the visual observation that the synthetic dsRNA poly(I:C) did not cause cell death, and thus the cell death seen in RV-infected cells was not a host-mediated response to PRR activation, the LDH assay was conducted on poly(I:C)-stimulated MRC-5 and BEAS-2B cells. Cells were left untreated or treated with poly(I:C) (10 µg/ml) for 24 h, cell-free supernatants were then collected to measure LDH released from the poly(I:C)-treated cells. Based on two independent experiments, in contrast to RV (Figure 3.5), poly(I:C) did not induce cell death in the MRC-5 fibroblasts (Figure 3.7A) or BEAS-2B epithelial cells (Figure 3.7B). To ascertain that the poly(I:C) utilised was biologically active, the cell-free supernatants were also tested for cytokine release. It was found that the poly(I:C) used could indeed stimulate production of CXCL8 by both MRC-5 and BEAS-2B cells (data not shown).

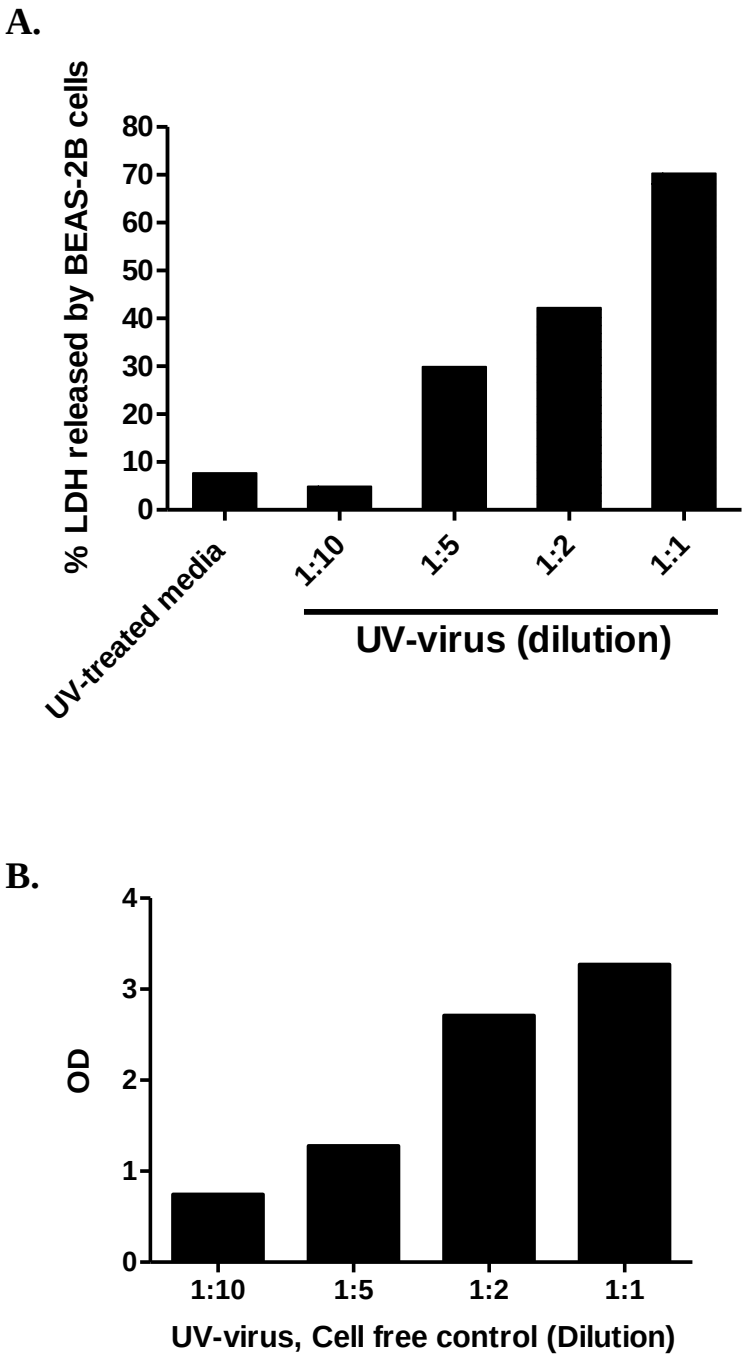

Figure 3. 6 UV-treated virus cross-reacts with LDH assay.

(A) BEAS-2B cells were treated with dilutions of UV-virus (1:1, 1:2, 1:5, 1:10). The cells were then incubated in 37°C/5% CO_2 for 24 h and LDH released from UV-virus-treated BEAS-2B cells determined by LDH assay. (B) Virus was exposed to UV light for 10 min and then serially diluted in infection media. The diluted UV-treated virus was then immediately utilised in LDH assay and the OD values determined. Data shown are $n = 1$.

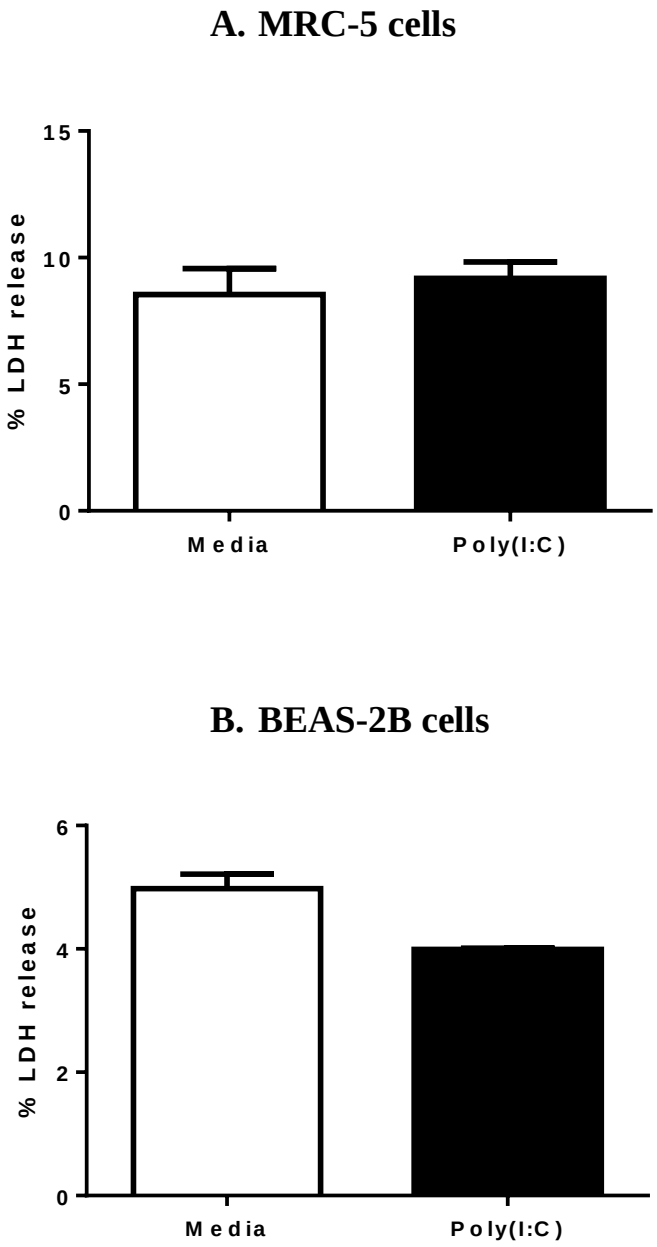

Figure 3. 7 Poly(I:C) does not induce cell death in MRC-5 and BEAS-2B cells.
Cells were stimulated with poly(I:C) (10 µg/ml). After 24 h, cell death was measured as described in Section 2.20 and represented as % of LDH release by dead cells. Data shown are mean ± SD of *n* = 2 independent experiments.

3.4 MRC-5 and BEAS-2B cells express TLR3, RIG-I, MDA5 and MAVS, but not TLR7 and TLR8, as observed at the mRNA level

The innate immune system responds to microbial infections and endogenous molecules via a group of germ-line encoded receptors termed PRRs. The PRRs TLR3, TLR7, TLR8, RIG-I and MDA5 have all been implicated in viral recognition (Section 1.4). Activation of these PRRs by virus leads to the production of type I IFNs and proinflammatory cytokines. Therefore, in this study the expression of these PRRs in MRC-5 fibroblasts and BEAS-2B epithelial cells was determined. The expression of mitochondrial adaptor protein MAVS (which is involved in RLR signalling pathways) was also explored in these cells.

MRC-5 and BEAS-2B cells were grown to ~95% confluence in 12-well plates. As a control, freshly isolated monocytes (Section 2.7) were used. Cells were then lysed and total RNA extracted, followed by cDNA synthesis (Section 2.16, 2.17). The synthesised cDNA were amplified by PCR using primers specific to TLR3, TLR7, TLR8, RIG-I, MDA5 and MAVS (Section 2.19).

Based on two independent experiments, all MRC-5 fibroblasts, BEAS-2B epithelial cells and monocytes appeared to express TLR3, RIG-I, MDA5 and MAVS, although the expression levels of these molecules were much lower in monocytes compared to that in MRC-5 and BEAS-2B cells, as determined at the mRNA level (Figure 3.8). Interestingly, MRC-5 and BEAS-2B cells showed no expression of TLR7 and TLR8, unlike monocytes, which expressed detectable levels of TLR7 and TLR8 (Figure 3.8).

3.5 In contrast to BEAS-2B cells, MRC-5 cells only produce CXCL8 and IL-6, but not CCL5 and CXCL10 in response to RV infection

After confirming that MRC-5 fibroblasts and BEAS-2B epithelial cells express the PRRs involved in recognising RV, the ability of RV infection to induce secretion of the proinflammatory cytokines CXCL8 and IL-6, or the antiviral chemokines CCL5 and CXCL10 in both cell types was explored.

MRC-5 and BEAS-2B cells were infected with RV-1B as described in Section 2.6.3 at several $TCID_{50}$/ml ranging from $3.3x10^4$ to $2.0x10^7$. Filtrate and UV-RV control samples

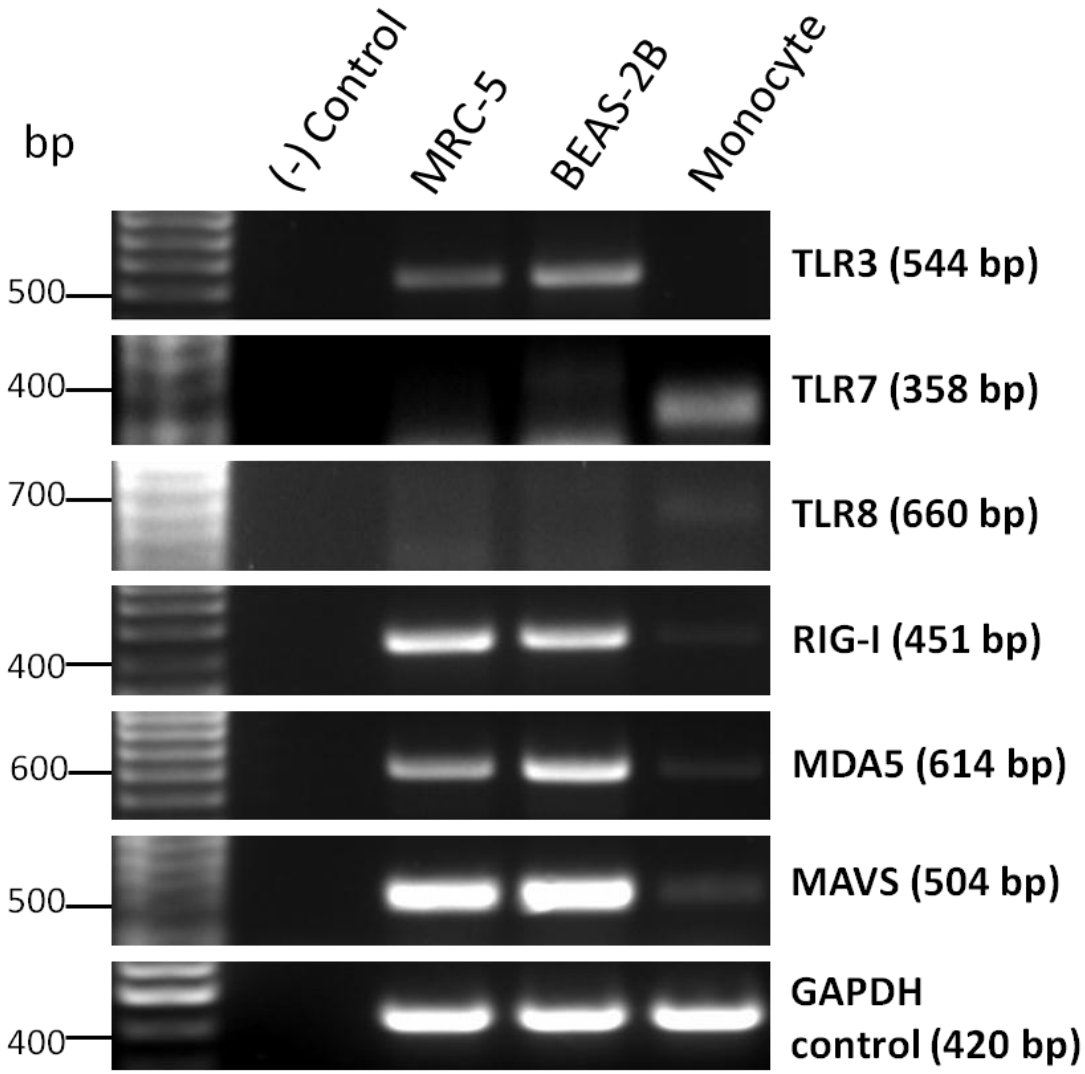

Figure 3. 8 MRC-5 and BEAS-2B cells express TLR3, RIG-I, MDA-5 and MAVS, but not TLR7 and TLR8, as observed at the mRNA level.

Cells were grown to ~95% confluence in 12-well plates (MRC-5 and BEAS-2B cells), or freshly isolated from a donor (monocytes). Cells were then lysed and total RNA extracted. Synthesised cDNA (from 1 µg RNA) of MRC-5 cells, BEAS-2B cells and monocytes were amplified by PCR using primers specific to TLR3, TLR7, TLR8, RIG-I, MDA5 or MAVS. PCR products were then separated by gel electrophoresis and visualised under UV light. Data shown are representative of $n = 2$ independent experiments.

($2x10^7$ $TCID_{50}$/ml) were prepared as described in Section 2.6.3. At 24 h p.i., cell-free supernatants were collected to determine cytokine release, as measured by ELISA (Section 2.15).

RV-1B elicited CXCL8 release from MRC-5 fibroblasts in a dose-dependent manner (Figure 3.9A), however the levels of CXCL8 released by MRC-5 fibroblasts were approximately 5-fold lower compared to BEAS-2B epithelial cells (Figure 3.9A, D). Interestingly, the UV-deactivated RV-1B was able to induce a noticeable amount of CXCL8 in MRC-5 cells, but not in BEAS-2B cells (Figure 3.9A, D). Importantly, unlike BEAS-2B cells, MRC-5 cells did not produce CCL5 and CXCL10 in response to RV-1B infection (Figure 3.9B, E, C, F). IL-1α and IL-1β release was also undetectable in RV-1B-infected MRC-5 cells (data not shown). Additionally, based on a single experiment, MRC-5 cells could also secrete IL-6 in response to RV-1B, in a pattern similar to the CXCL8 data (Figure 3.9A), furthermore the UV-RV also induced a noticeable level of IL-6 in this cell type (data not shown).

3.6 Higher viral replication occurs in MRC-5 cells compared to BEAS-2B cells

Having found that there was a lack of antiviral CCL5 and CXCL10 cytokine production in RV-infected MRC-5 fibroblasts (Section 3.5) (implicating the lack of IFNs to control viral replication), it was hypothesised that these would result in a high viral replication in this cell type. To test this hypothesis, cells were infected with RV-1B as described in Section 2.6.3. At 24 h p.i., MRC-5 cells (~$5x10^5$) and BEAS-2B cells (~$6.1x10^5$) were lysed, cDNA synthesised and real-time qPCR for RV-1B performed (Section 2.16-2.18). Samples were quantified against a standard curve of plasmids containing RV target sequence.

With the exception of data obtained using $2x10^7$ $TCID_{50}$/ml RV, the amounts of intracellular viral RNA copies were at least 2-log higher in MRC-5 fibroblasts compared to BEAS-2B epithelial cells, at 24 h p.i (Figure 3.10). For example, when cells were infected with $1.0x10^7$ $TCID_{50}$/ml of RV-1B for 24h, ~$6.0x10^9$ RV copies were detected in MRC-5 cells, whilst only ~$3.0x10^8$ RV copies were found in BEAS-2B cells. Furthermore, at $4.0x10^6$ $TCID_{50}$/ml, only ~$2.0x10^8$ RV copies were obtained in RV-1B-infected BEAS-2B epithelial cells, whilst the

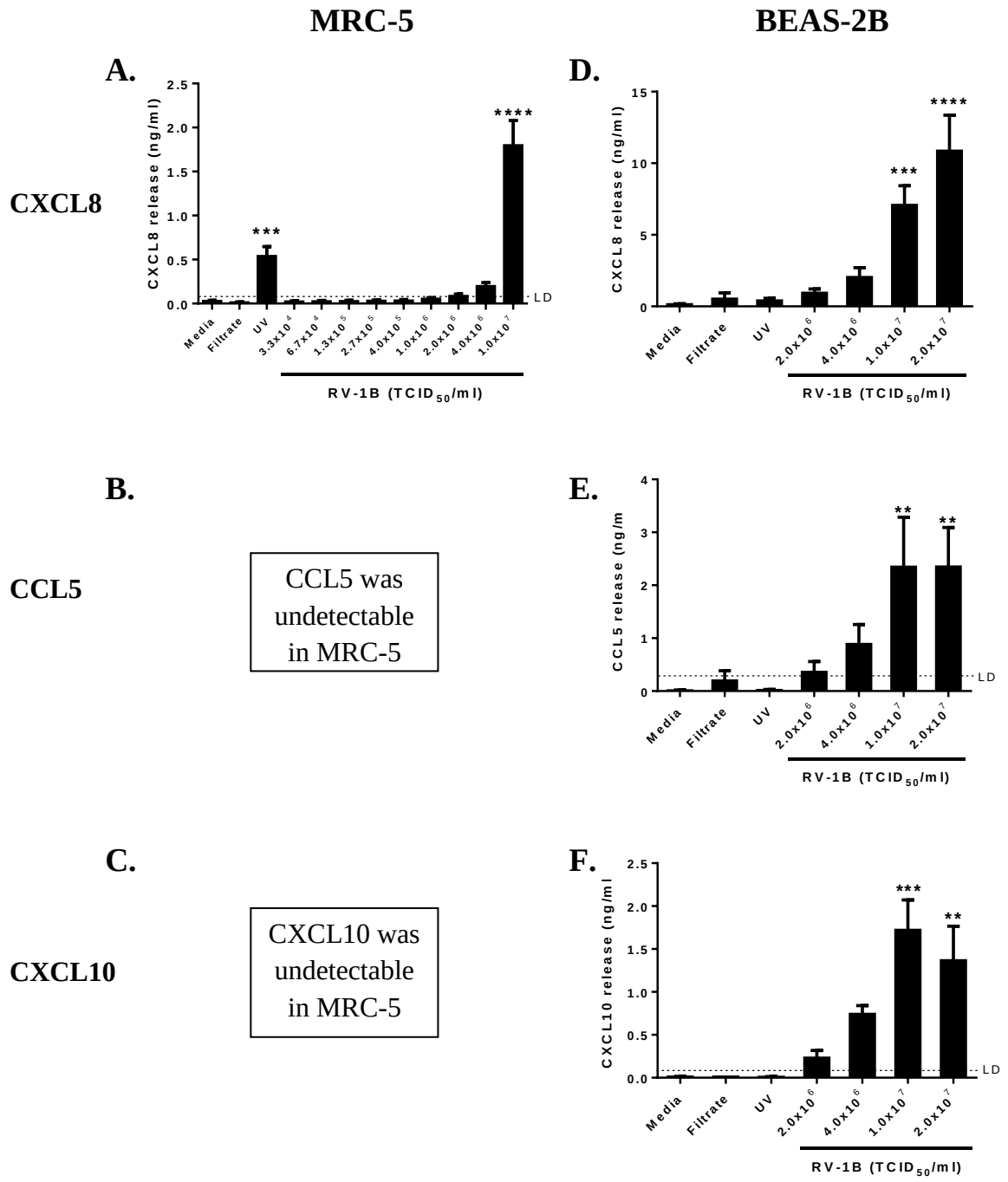

Figure 3. 9 Unlike BEAS-2B cells, MRC-5 cells do not produce CCL5 and CXCL10 in response to RV-1B.

Cells were infected with RV-1B as described in Section 2.6.3 at the indicated $TCID_{50}$/ml. Filtrate and UV-RV control samples ($2x10^7$ $TCID_{50}$/ml) were prepared as described in Section 2.6.3. After 24 h, cell-free supernatants were collected, and CXCL8 (A, D), CCL5 (B, E) and CXCL10 (C, F) release was measured by ELISA. Data shown are mean ± SEM of n = 4 (A, B, D, E) or n = 3 (C, F) independent experiments. Significant differences are indicated by $^{**}p<0.01$, $^{***}p<0.001$ and $^{****}p<0.0001$ (versus media control), as measured by one-way ANOVA with Dunnett's post-test. LD = limit of detection.

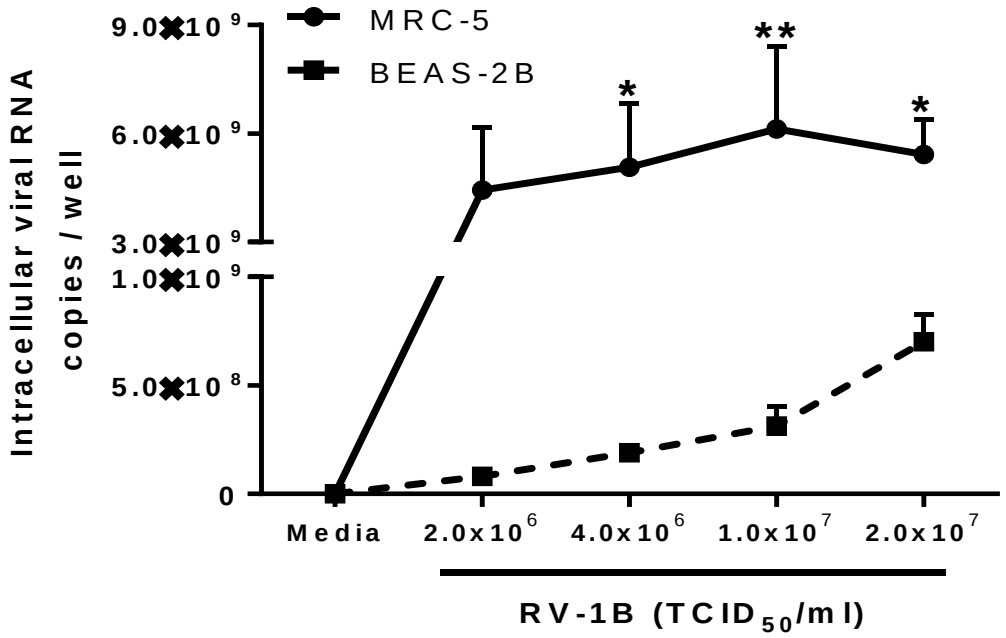

Figure 3. 10 Higher viral replication occurs in MRC-5 cells compared to BEAS-2B cells.

Cells were infected with RV-1B as described in Section 2.6.3 at the indicated $TCID_{50}$/ml. At 24 h p.i., MRC-5 cells (~$5x10^5$) and BEAS-2B cells (~$6.1x10^5$) were lysed, total RNA extracted, cDNA synthesised by RT and real-time PCR for RV-1B performed. Data shown are mean ± SEM of $n = 3$ independent experiments. Significant differences are indicated by *p<0.05 and **p<0.01 (versus BEAS-2B sample at the same $TCID_{50}$/ml), as measured by two-way ANOVA with Bonferroni's post-test.

same concentration of RV-1B resulted in ~$5.0x10^9$ RV copies in MRC-5 fibroblasts, after 24 h infection (Figure 3.10).

3.7 RV infection differentially regulates the expression of TLR3, RIG-I and MDA5 in MRC -5 and BEAS-2B cells

It has been shown that the expression of the viral-detecting PRRs TLR3, RIG-I and MDA5 was upregulated by RV infection in BEAS-2B epithelial cells (Slater et al., 2010, Wang et al., 2009), however the expression of these three PRRs is not yet studied in lung fibroblasts.

Therefore, the ability of RV to regulate the expression of PRRs TLR3, RIG-I and MDA5, as well as the adaptor molecule MAVS was explored in MRC-5 fibroblasts and BEAS-2B epithelial cells. Cells were either left uninfected or infected with RV-1B or RV-16 as described in Section 2.6.3. A $TCID_{50}$/ml of $4.0x10^6$ or $5.0x10^6$ were selected for RV-1B and RV-16 respectively, the concentrations that induced a relatively good level of cytokine production, without causing high cell death in MRC-5 fibroblasts (Figure 3.9A, 3.5A). Cells were lysed at 24 h p.i. and mRNA expression was examined as described in Section 3.4.

Based on two independent experiments, upon RV-1B infection, the mRNA expression of TLR3 was markedly upregulated in BEAS-2B epithelial cells, as determined by the semi-quantitative end-point PCR (Figure 3.11). In contrast, RV-1B did not enhance TLR3 expression in MRC-5 fibroblasts. Expression of RIG-I and MDA5 was augmented in both MRC-5 and BEAS-2B cells in response to RV-1B infection, although the amount of upregulation was much greater in BEAS-2B cells (Figure 3.11). Furthermore, RV-1B did not regulate the expression of TLR7, TLR8 or MAVS in either MRC-5 or BEAS-2B cells (Figure 3.11).

For RV-16, in keeping with the results seen when cells were infected with RV-1B (Figure 3.11), RV-16 infection markedly upregulated the expression of TLR3 in BEAS-2B, but not in MRC-5 cells (Figure 3.12). Again, comparable to the results obtained using RV-1B, RV-16 resulted in a substantial increase of RIG-I and MDA5 expression in BEAS-2B epithelial cells, but only modestly upregulated the expression of the two RLRs in MRC-5 fibroblasts (Figure 3.12). In addition, RV-16 did not alter the expression of TLR7, TLR8 or MAVS in either MRC-5 or BEAS-2B cells (Figure 3.12).

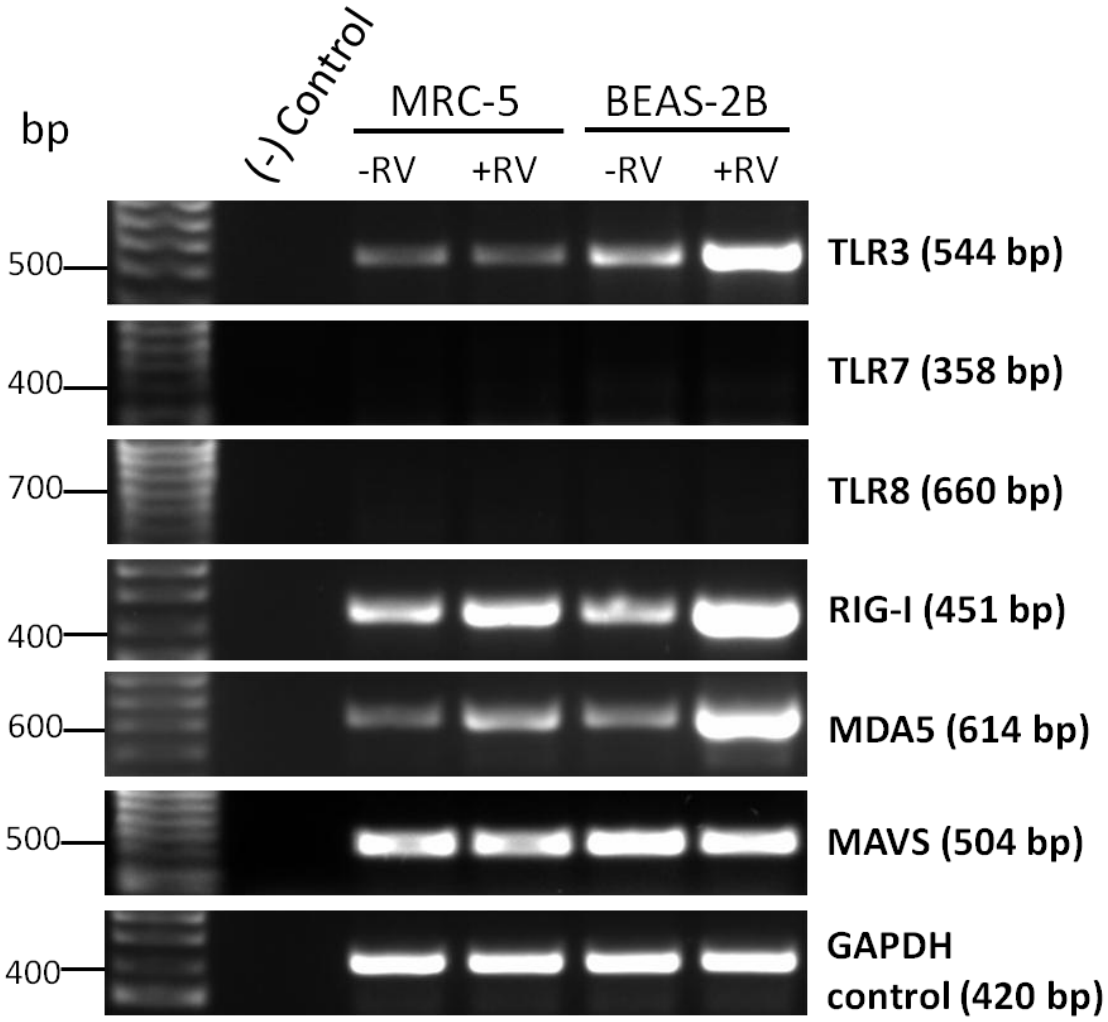

Figure 3. 11 RV-1B infection differentially regulates the expression of TLR3, RIG-I and MDA5 in MRC-5 and BEAS-2B cells.

Cells were left uninfected or infected with RV-1B ($4.0x10^6$ $TCID_{50}$/ml) as described in Section 2.6.3. At 24 h p.i., cells were lysed and total RNA extracted. Synthesised cDNA (from 1 µg RNA) of MRC-5 and BEAS-2B cells were amplified by PCR using primers specific to TLR3, TLR7, TLR8, RIG-I, MDA5, MAVS or GAPDH. PCR products were then separated by gel electrophoresis and visualised under UV light. Data shown are representative of $n = 2$ independent experiments.

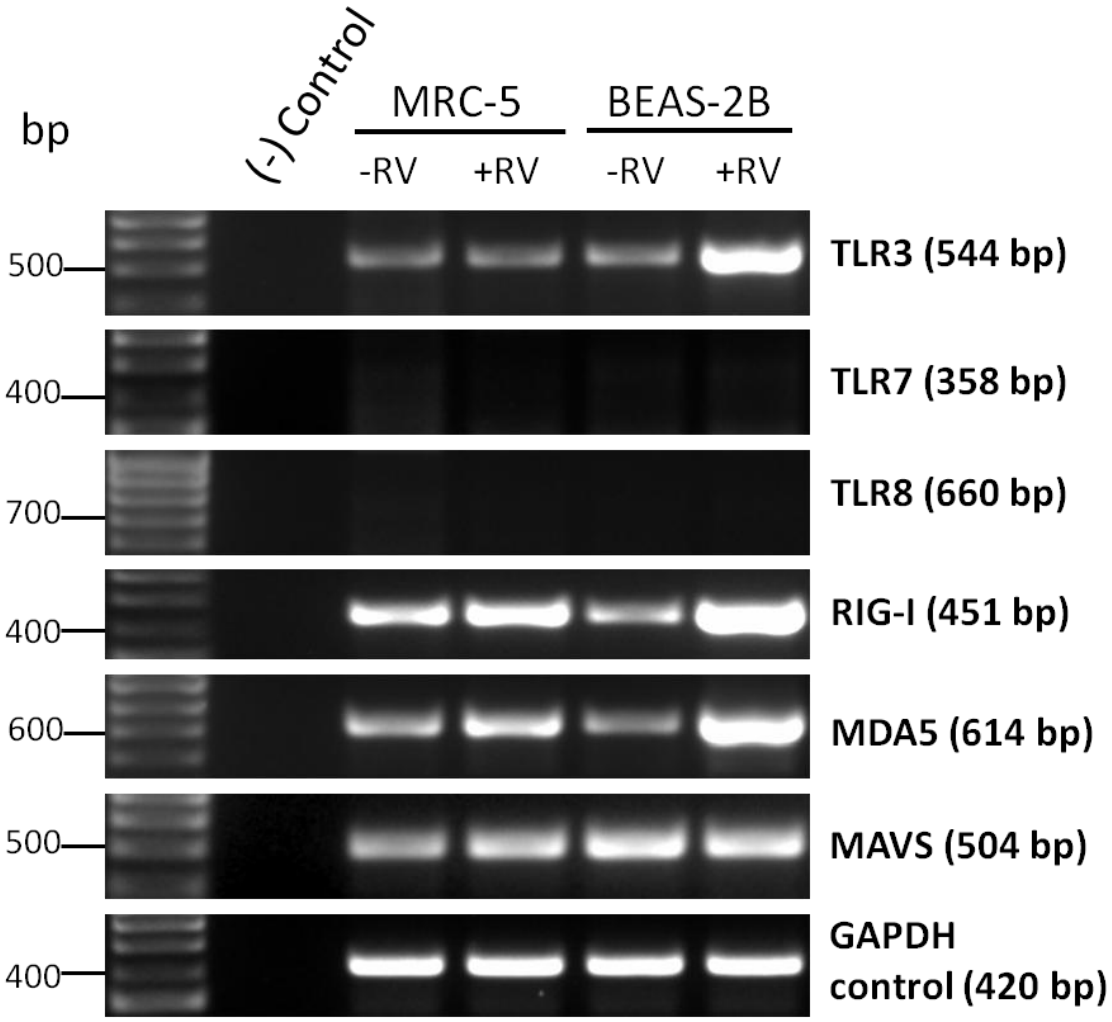

Figure 3. 12 RV-16 infection differentially regulates the expression of TLR3, RIG-I and MDA5 in MRC-5 and BEAS-2B cells.

Cells were left uninfected or infected with RV-16 ($5.0x10^6$ $TCID_{50}$/ml) as described in Section 2.6.3. At 24 h p.i., cells were lysed and total RNA extracted. Synthesised cDNA (from 1 µg RNA) of MRC-5 and BEAS-2B cells were amplified by PCR using primers specific to TLR3, TLR7, TLR8, RIG-I, MDA5, MAVS or GAPDH. PCR products were then separated by gel electrophoresis and visualised under UV light. Data shown are representative of $n = 2$ independent experiments.

3.8 RV infection differentially regulates the expression of IRF1, IRF3 and IRF7 in MRC-5 and BEAS-2B cells

IRFs, particularly IRF1, IRF3 and IRF7, are the crucial transcription factors responsible for type I IFN production (reviewed in Yoneyama and Fujita, 2010, Takeuchi and Akira, 2010). In this study, it was hypothesised that differences in basal expression and regulation of IRFs by RV might be present between airway fibroblasts and epithelial cells. MRC-5 and BEAS-2B cells were either left uninfected, or infected with RV-1B ($TCID_{50}$/ml of $4.0x10^6$) or RV-16 ($TCID_{50}$/ml of $5.0x10^6$) as described in Section 2.6.3. Cells were lysed at 24 h p.i. and mRNA expression was examined as described in Section 3.4.

Based on two independent experiments, MRC-5 fibroblasts and BEAS-2B epithelial cells appeared to constitutively express IRF1 and IRF3, but both cell types had lower IRF7 basal expression, as determined by the semi-quantitative end-point PCR (Figure 3.13, 3.14). RV-1B and RV-16 increased IRF1 expression in BEAS-2B, but not in MRC-5 cells (Figure 3.13, 3.14). Interestingly, upon RV infection expression of IRF7 was dramatically enhanced in BEAS-2B epithelial cells, but not in MRC-5 fibroblasts (Figure 3.13, 3.14). No obvious upregulation of IRF3 was seen in either MRC-5 or BEAS-2B cells in response to RV infection (Figure 3.13, 3.14).

3.9 RV induces substantial cell death in primary human lung fibroblasts (HLFs), but not primary human bronchial epithelial cells (HBECs)

To validate the results obtained using cell lines (Section 3.3-3.8), key experiments were then conducted in primary human lung fibroblasts (HLFs) and human bronchial epithelial cells (HBECs). These primary cells were purchased from PromoCell (Heidelberg, Germany) who isolated the cells from normal human adult tissue (Section 2.3).

3.9.1 RV-induced cytopathic effects in HLFs

HLFs and HBECs were infected with either RV-1B or RV-16 at increasing $TCID_{50}$/ml starting from $3.3x10^4$ $TCID_{50}$/ml (MOI ~0.01) to $1.0x10^7$ (MOI ~3) as described in Section 2.6.3. Filtrate and UV-RV control samples were prepared as described in Section 2.6.3.

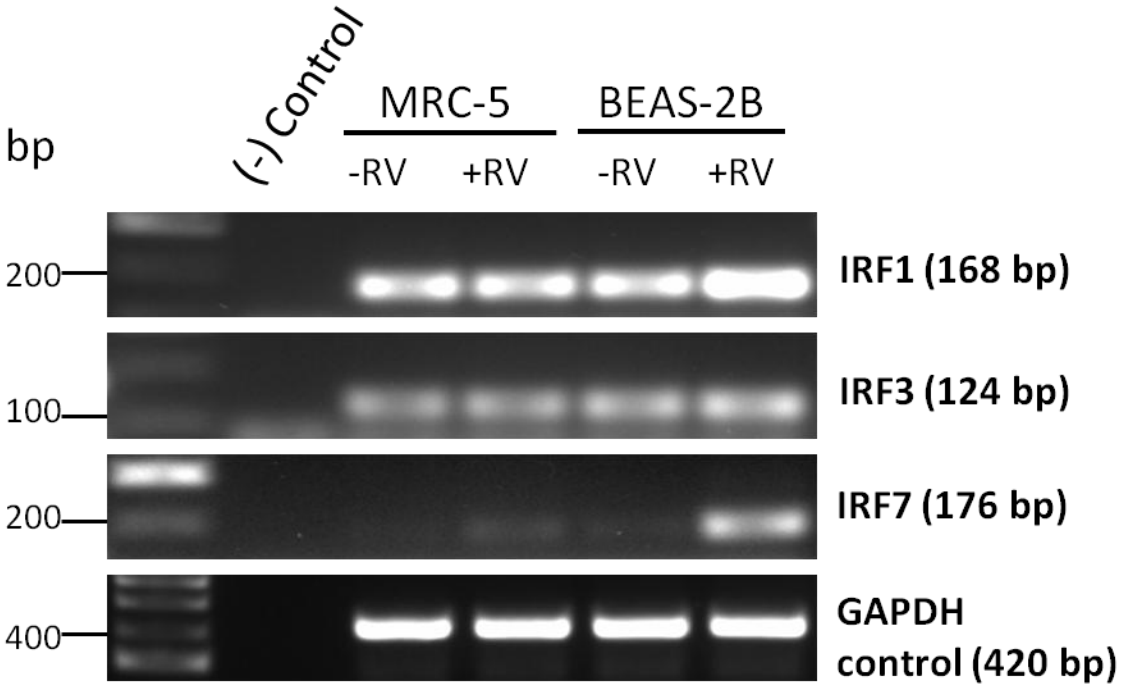

Figure 3. 13 RV-1B infection differentially regulates the expression of IRF1, IRF3 and IRF7 in MRC-5 and BEAS-2B cells.

Cells were left uninfected or infected with RV-1B ($4.0x10^6$ $TCID_{50}$/ml) as described in Section 2.6.3. At 24 h p.i., cells were lysed and total RNA extracted. Synthesised cDNA (from 1 µg RNA) of MRC-5 and BEAS-2B cells were amplified by PCR using primers specific to IRF1, IRF3, IRF7 or GAPDH. PCR products were then separated by gel electrophoresis and visualised under UV light. Data shown are representative of n = 2 independent experiments.

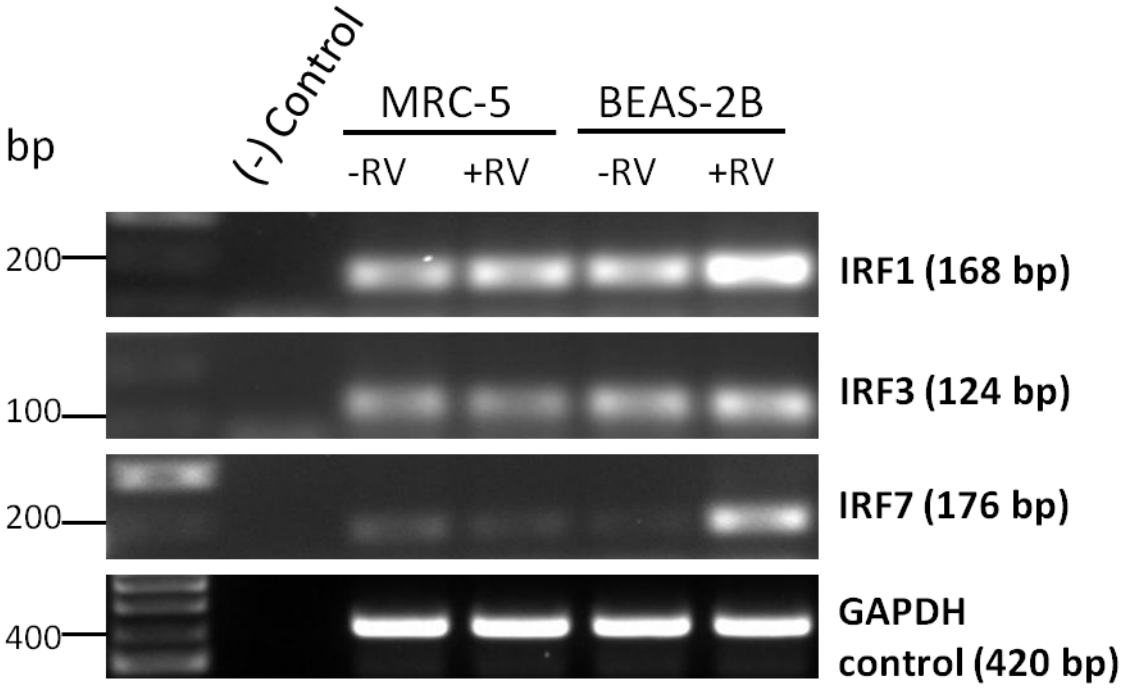

Figure 3. 14 RV-16 infection differentially regulates the expression of IRF1, IRF3 and IRF7 in MRC-5 and BEAS-2B cells.

Cells were left uninfected or infected with RV-16 ($5.0x10^6$ $TCID_{50}$/ml) as described in Section 2.6.3. At 24 h p.i., cells were lysed and total RNA extracted. Synthesised cDNA (from 1 µg RNA) of MRC-5 and BEAS-2B cells were amplified by PCR using primers specific to IRF1, IRF3 or IRF7. PCR products were then separated by gel electrophoresis and visualised under UV light. Data shown are representative of n = 2 independent experiments.

Figure 3.15 shows images of RV-1B-induced cytopathic effects in HLFs infected with $3.3x10^4$ $TCID_{50}$/ml to $1.0x10^7$ of RV-1B. Based on two independent experiments, similar to the results obtained in RV-1B-infected MRC-5 fibroblast cell line (Figure 3.1), RV-1B infection caused major cytopathic effects in HLFs in a dose-dependent manner (Figure 3.15). HLFs started to become rounded and detached from the monolayer when infected with RV-1B at $TCID_{50}$/ml of $4.0x10^5$, $1.0x10^6$, $2.5x10^6$, $5.0x10^6$, and $1.0x10^7$ (Figure 3.15), concentrations of RV-1B that elicited no noticeable cytopathic cell death in HBECs (images not taken). Again, similar to the results seen in MRC-5 cells (Figure 3.1, 3.2), the same concentrations ($TCID_{50}$/ml) of RV-16 elicited lower cytopathic effects in HLFs (Figure 3.16) as compared to RV-1B (Figure 3.15) as determined by visual observation. For example, at $5.0x10^6$ $TCID_{50}$/ml, RV-16 only caused ~20-30% rounded/detaching cells (Figure 3.16), whilst RV-1B induced ~50-60% rounded/detaching cells (Figure 3.15). As expected, no cytopathic effects were observed when HLFs were incubated with filtrate and UV-RV controls (Figure 3.15, 3.16).

3.9.2 RV induces greater cell death in HLFs than in HBECs

To quantify the cytopathic cell death observed in RV-infected HLFs and HBECs, the LDH cytotoxic assay (Section 2.20) was utilised. Consistent with the visual observations described above (Section 3.9.1), RV infection caused greater cytopathic cell death in HLFs than in HBECs (Figure 3.17). For example, the level of cell death seen in HLFs was 2-fold greater than in HBECs following infection with the same dose of RV-1B (i.e. $1x10^7$ $TCID_{50}$/ml) (Figure 3.17A). Similarly, $1x10^7$ $TCID_{50}$/ml of RV-16 caused ~40% higher cell death in HLFs than in HBECs (Figure 3.17B). Interestingly, in keeping with the results attained using cell lines (Section 3.3), primary HLFs and HBECs were more susceptible to RV-1B infection compared to RV-16. Thus, $5x10^6$ $TCID_{50}$/ml RV-1B triggered 53% cell death, whilst RV-16 induced only 23% cell death in HLFs (Figure 3.17). The same patterns were observed in HBECs, emphasising the more virulent characteristic of RV-1B as compared to RV-16 in the two structural airways cells examined in this study.

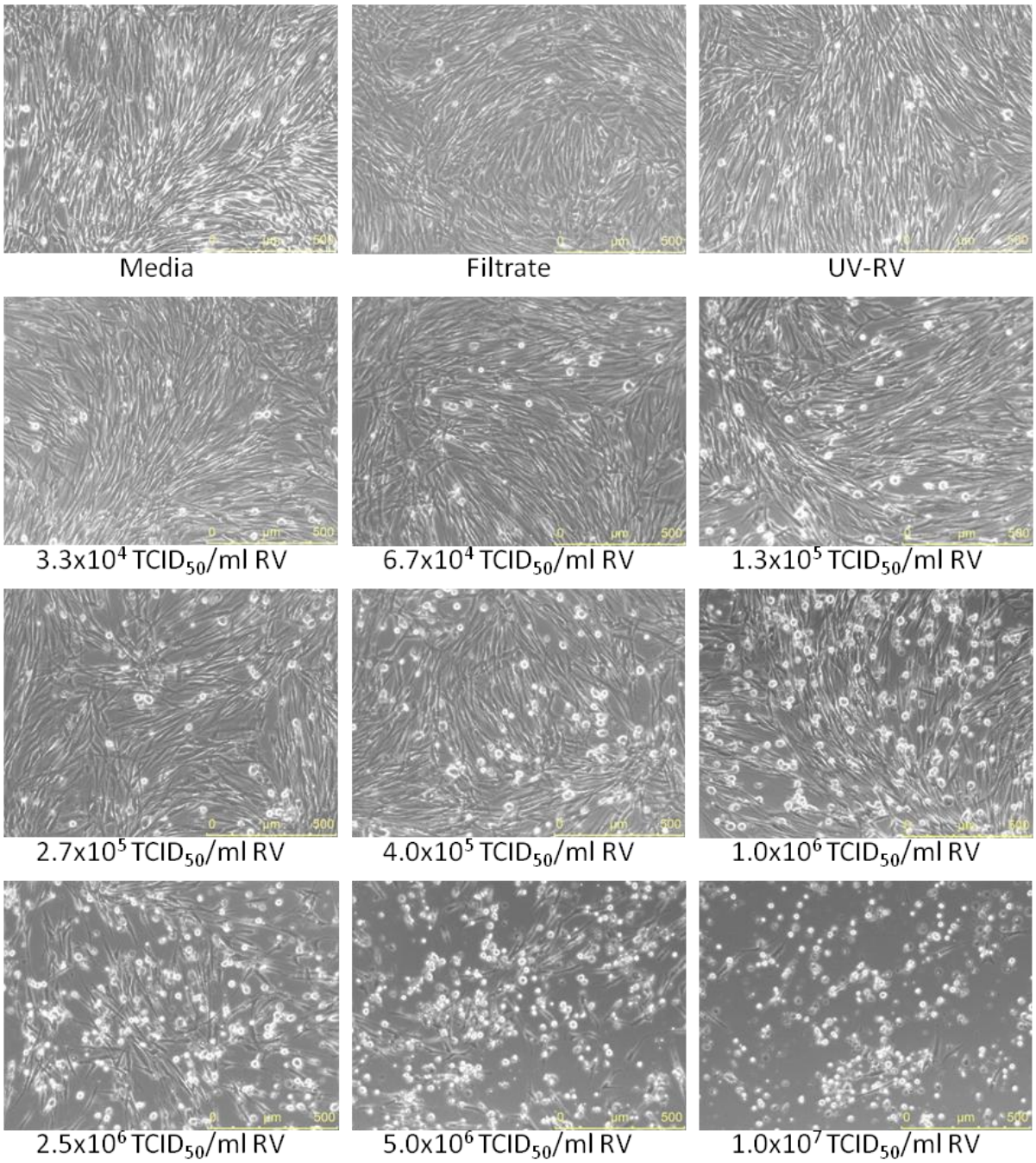

Figure 3. 15 RV-1B-induced cytopathic effects in HLFs.
HLFs were infected with RV-1B as described in Section 2.6.3 at the indicated $TCID_{50}$/ml. Filtrate and UV-RV control samples were prepared as described in Section 2.6.3. After 24 h, cell monolayers were observed using a fluorescence and phase contrast Leica DM14000B inverted microscope at 10x magnification. Data shown are representative of n = 2 independent experiments.

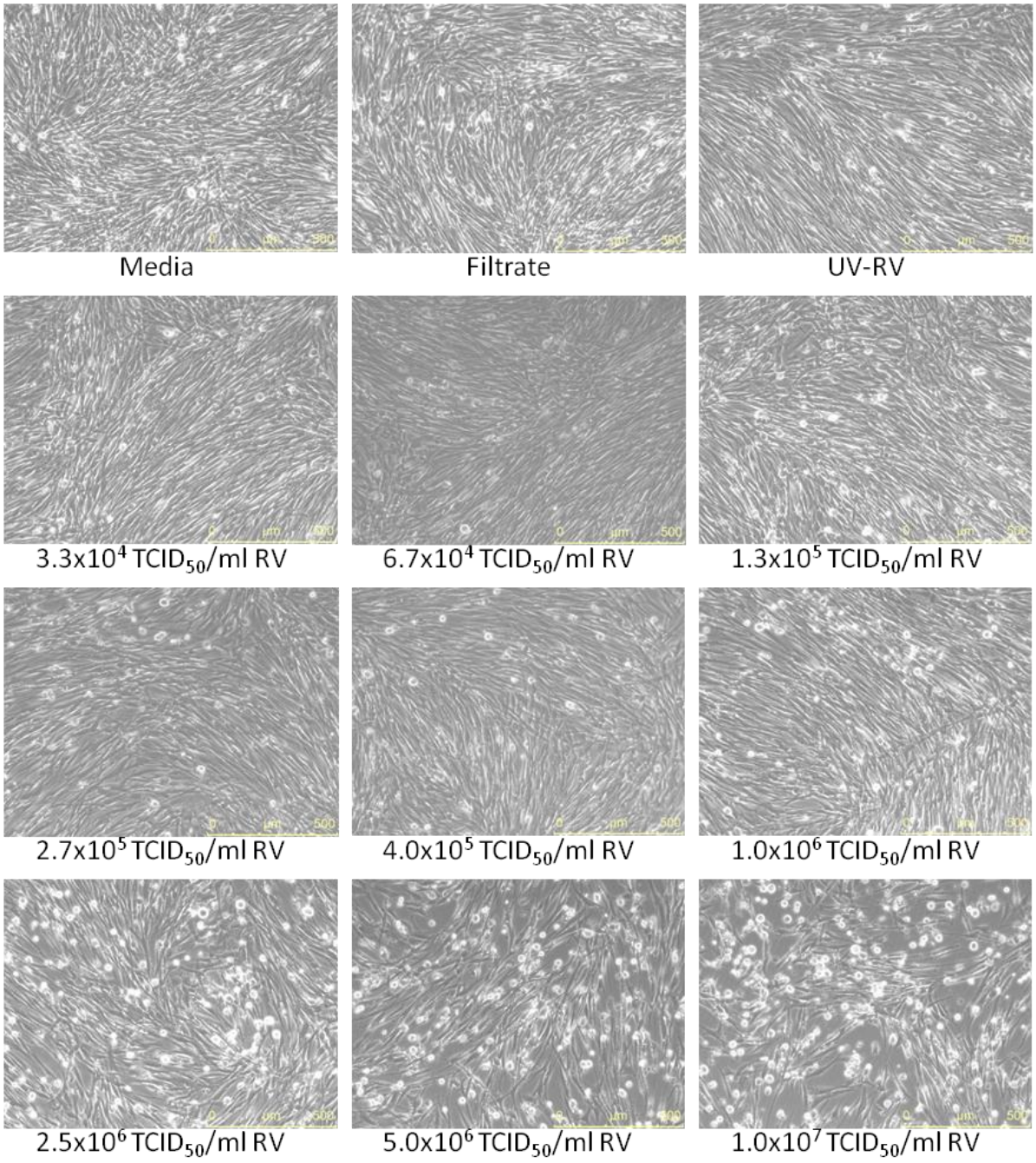

Figure 3. 16 RV-16-induced cytopathic effects in HLFs.
HLFs were infected with RV-16 as described in Section 2.6.3 at the indicated $TCID_{50}$/ml. Filtrate and UV-RV control samples were prepared as described in Section 2.6.3. After 24 h, cell monolayers were observed using a fluorescence and phase contrast Leica DM14000B inverted microscope at 10x magnification. Data shown are representative of n = 2 independent experiments.

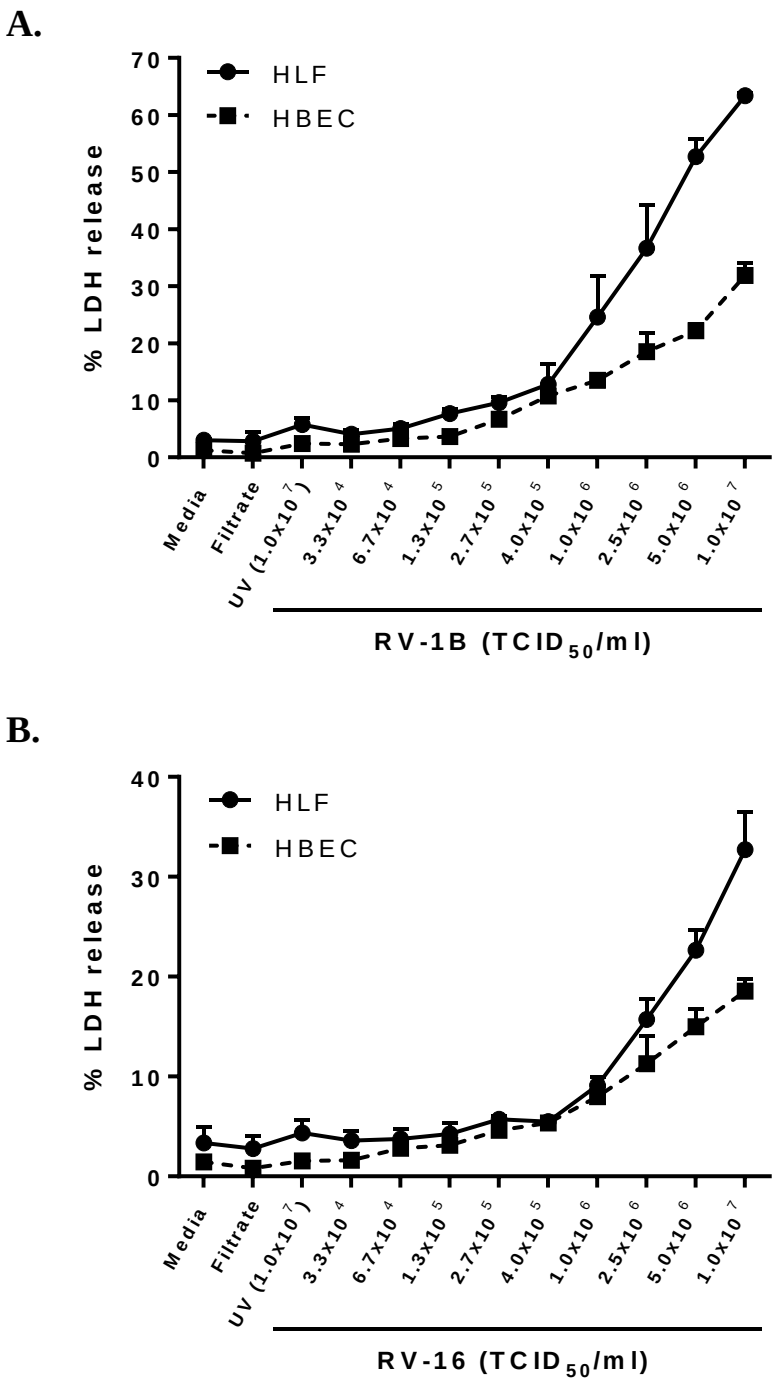

Figure 3. 17 RV infection induces greater cell death in HLFs compared to HBECs.
Cells were infected with RV-1B (A) or RV-16 (B) as described in Section 2.6.3 at the indicated $TCID_{50}$/ml. Filtrate and UV-RV control samples were prepared as described in Section 2.6.3. At 24 h p.i., cell death was measured as described in Section 2.20 and displayed as % LDH release by dead cells. Data shown are mean ± SD of n = 2 independent experiments.

3.10 RV infection triggers distinctive cytokine profiles in HBECs and HLFs

The capability of HLFs and HBECs to produce the proinflammatory cytokine CXCL8 and the antiviral cytokine CCL5 upon RV infection was assessed. Cells were infected with RV using a $TCID_{50}$/ml range of $3.3x10^4$ to $1.0x10^7$ as described in Section 2.6.3. At 24 h p.i., cell-free supernatants were collected to determine cytokine release, as measured by ELISA (Section 2.15).

Based on two independent experiments, in response to RV, HLFs and HBECs secreted comparable amounts of CXCL8 in a dose-dependent manner (Figure 3.18A, C). Importantly, in contrast to HBECs, CCL5 proteins were not detected in HLFs (Figure 3.18B, D), which supports the findings obtained using cell lines (Section 3.5). At high concentrations of RV ($TCID_{50}$/ml of $2.5x10^6$, $5.0x10^6$ and $1.0x10^7$), RV-16 was found to trigger higher levels of CXCL8 release from HLFs compared to RV-1B (Figure 3.18A). On the contrary, HBECs produced greater amounts of CXCL8 proteins when infected with RV-1B compared to RV-16 (Figure 3.18C), although interestingly the amounts of CCL5 release were higher when this cell type was infected with RV-16 compared to RV-1B (Figure 3.18D). Similar to the results seen in RV-infected MRC-5 and BEAS-2B cell lines (Section 3.5), the UV-irradiated RV also induced a noticeable amount of CXCL8 in HLFs, but not in HBECs (Figure 3.18A, C).

3.11 Higher viral replication occurs in HLFs compared to HBECs

Having determined that HLFs were not able to produce the antiviral cytokines CCL5 and CXCL10, again it was hypothesised that this would cause higher viral replication to occur in this cell type. To examine this hypothesis, cells were infected with either RV-1B or RV-16 at the indicated $TCID_{50}$/ml as described in Section 2.6.3. At 24 h p.i., HLFs (~$4x10^5$) and HBECs (~$5.6x10^5$) were lysed, total RNA extracted, cDNA synthesised and real-time PCR for RV performed, samples were then quantified against a standard curve of plasmids containing RV target sequence (Section 2.16-2.18).

Based on two independent experiments, the results recapitulated the phenotype seen in RV-infected MRC-5 and BEAS-2B cell lines (Section 3.6), whereby substantially higher intracellular viral RNA copies were detected in HLFs compared to HBECs, at 24 h p.i.

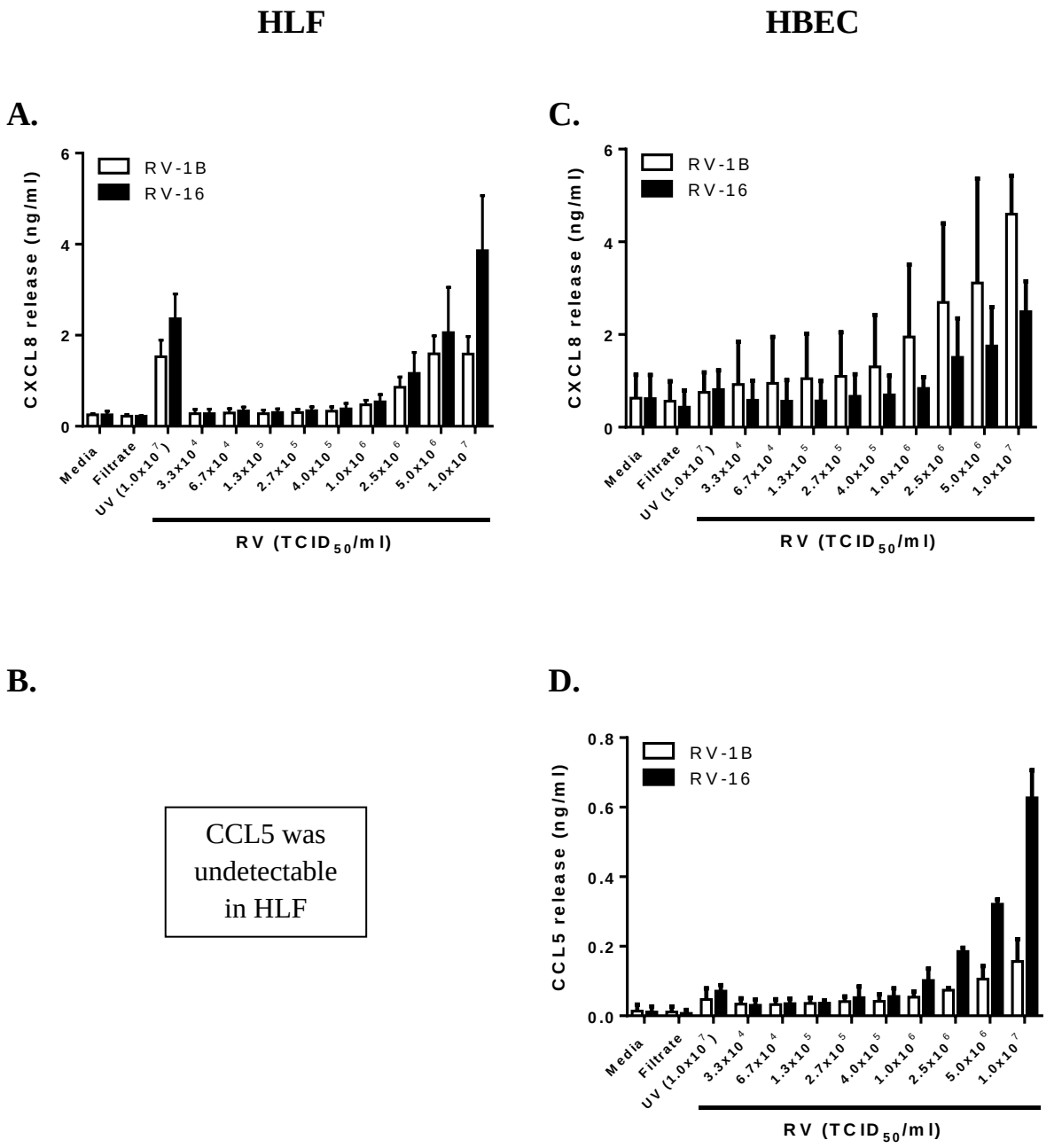

Figure 3. 18 In contrast to HBECs, HLFs only produce CXCL8, but not CCL5 in response to RV infection.

Cells were infected with RV-1B or RV-16 as described in Section 2.6.3 at the indicated $TCID_{50}$/ml. Filtrate and UV-RV control samples were prepared as described in Section 2.6.3. After 24 h, cell-free supernatants were collected, and CXCL8 (A, C) and CCL5 (B, D) release was measured by ELISA. Data shown are mean ± SD of *n* = 2 independent experiments.

(Figure 3.19). For example, when cells were infected with $5.0x10^6$ $TCID_{50}$/ml of RV-1B, ~$1.5x10^{10}$ RV copies were detected in HLFs, whilst only ~$5.0x10^9$ RV copies were detected in BEAS-2B cells, after 24 h infection (Figure 3.19A). Similarly, initial infection with $5.0x10^6$ $TCID_{50}$/ml of RV-16 resulted in ~$4.0x10^9$ RV copies produced in HLFs, whilst HBECs only gave ~$2.0x10^9$ RV copies at 24 h p.i. (Figure 3.19B).

3.12 RV infection of fibroblasts from patients with idiopathic pulmonary fibrosis

IPF is a chronic lung disease of unknown aetiology that often leads to respiratory failure and death within 2-5 years of diagnosis (reviewed in Zolak and de Andrade, 2012). Depending on the rate of disease progression, patients suffering IPF have been divided mainly into two subgroups; the first group is those who remain stable for prolonged periods of time (slow progressors), whilst another group of patients display a rapid, stepwise progression of the disease with accelerated mortality (rapid progressors) (reviewed in Zolak and de Andrade, 2012). There is increasing evidence that viruses such as HSV, EBV and TTV may contribute to the acute IPF exacerbations (Guenther et al., 2010, Lasithiotaki et al., 2011, Wootton et al., 2011). Furthermore, one of the important hallmarks of IPF is the dysregulated, excessive proliferation of fibroblasts (fibrosis) in the lung (reviewed in Hoo and Whyte, 2012). Hence, in the current study the capability of RV to induce inflammatory responses in lung fibroblasts isolated from patients with slowly progressing or rapidly progressing IPF was explored.

Primary Idiopathic Pulmonary Fibrosis patient fibroblasts (IPFFs) used in this study were a kind gift from Prof. C.M. Hogaboam, University of Michigan Medical School, USA. The IPFFs were obtained from surgical lung biopsies of patients exhibiting slow or rapid progression of IPF (see Section 2.6.3). Two samples of slow progressors and three of rapid progressors were utilised in this study, whereby each IPFF sample was isolated from a different donor.

A.

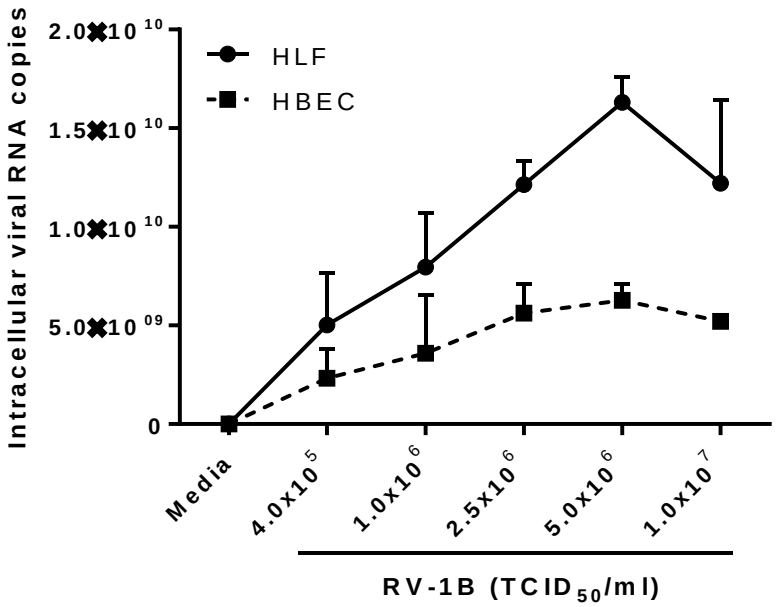

B.

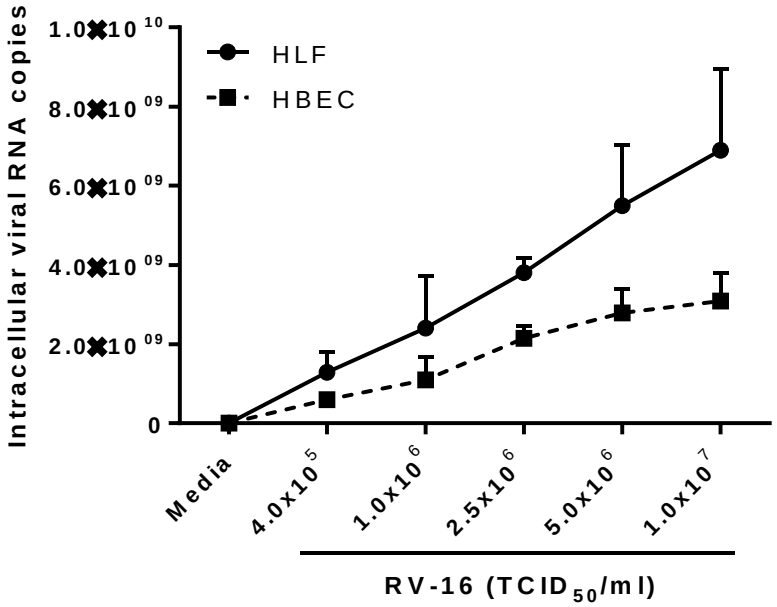

Figure 3. 19 Higher viral replication occurs in HLFs compared to HBECs.
Cells were infected with RV-1B (A) or RV-16 (B) as described in Section 2.6.3 at the indicated $TCID_{50}$/ml. At 24 h p.i., HLFs (~$4x10^5$) and HBECs (~$5.6x10^5$) were lysed, total RNA extracted, cDNA synthesised by RT and real-time PCR for RV performed. Data shown are mean ± SD of $n = 2$ independent experiments.

3.12.1 IPFFs obtained from slow and rapid progressor IPF patients have similar levels of cell death following RV infection

The RV-triggered cytopathic cell death of IPFFs was first determined. IPFFs were infected with either RV-1B or RV-16 at $TCID_{50}$/ml of $1.0x10^6$ (MOI ~0.3), $2.5x10^6$ (MOI ~0.75) or $5.0x10^6$ (MOI ~1.5) as described in Section 2.6.3. Filtrate and UV control samples were prepared as described in Section 2.6.3. At 24 h p.i., samples were collected and cell death was quantified using LDH assay as described in Section 2.20.

In keeping with the microscopic observations (data not shown), RV infection resulted in cell death of IPFFs in a dose-dependent manner (Figure 3.20). No obvious difference in cell death was found between slow and rapid progressors in response to RV-1B (Figure 3.20A) or RV-16 (Figure 3.20B). In keeping with the results obtained using the MRC-5 fibroblast cell line (Section 3.3) and healthy HLFs (Section 3.9), fibroblasts from both slowly and rapidly progressive IPF patients were more susceptible to RV-1B (Figure 3.20A) as compared to RV-16 (Figure 3.20B). For example, at $2.5x10^6$ $TCID_{50}$/ml of RV, the degree of cell death seen in RV-1B-infected stable IPFFs (Figure 3.20A) was 2-fold greater than that detected in RV-16-infected stable IPFFs (Figure 3.20B).

3.12.2 IPFFs obtained from rapid progressor patients release higher levels of CXCL8 compared to IPFFs from slow progressor patients in response to RV infection

The ability of RV to induce proinflammatory cytokine generation in IPFFs was then investigated. Cells were infected with RV as described in Section 3.12.1. After 24 h infection, cell-free supernatants were collected and cytokine release was measured by ELISA as described in Section 2.15. Note that our senior lab technician, Dr Linda Kay, performed ELISA analysis of the IPFF supernatants.

As expected, RV-infected IPFFs produced the proinflammatory cytokine CXCL8 in a $TCID_{50}$-dependent manner (Figure 3.21). Consistent with the results obtained using MRC-5 cells (Section 3.5) and normal HLFs (Section 3.10), release of the antiviral cytokine CCL5 from IPFFs was undetectable (data not shown). Due to the different number of samples available to conduct the experiments (i.e. 2 independent donors for stable IPF versus 3 for rapid IPF), statistics could not be performed on the data obtained. Despite this limitation, it could be observed that in response to RV infection, fibroblasts of rapidly progressing IPF

A. RV-1B

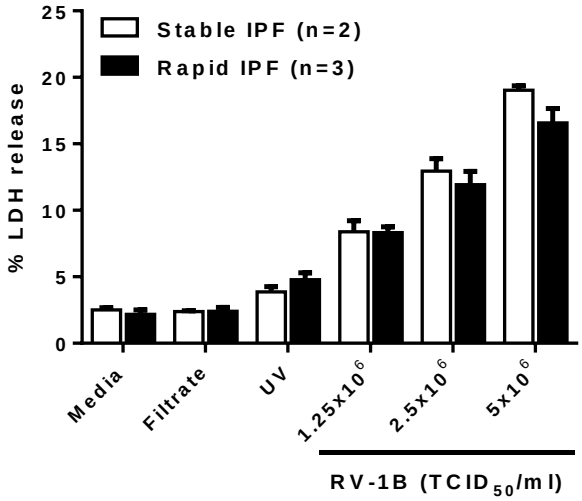

B. RV-16

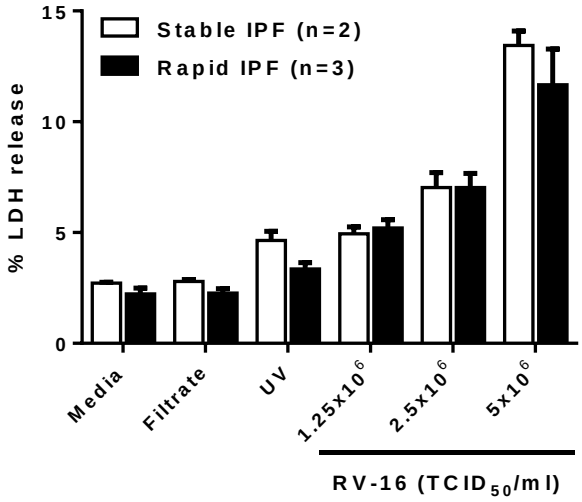

Figure 3. 20 IPFFs of stable and rapid progressors have similar levels of cell death following RV infection.

Cells were infected with RV-1B (A) or RV-16 (B) as described in Section 2.6.3 at the indicated $TCID_{50}$/ml. Filtrate and UV-RV control samples were prepared as described in Section 2.6.3. At 24 h p.i., cell death was measured as described in Section 2.20 and displayed as % LDH release by dead cells. Data shown are mean ± SEM of the results determined with samples collected from 2 (stable IPF) or 3 (rapid IPF) independent patients.

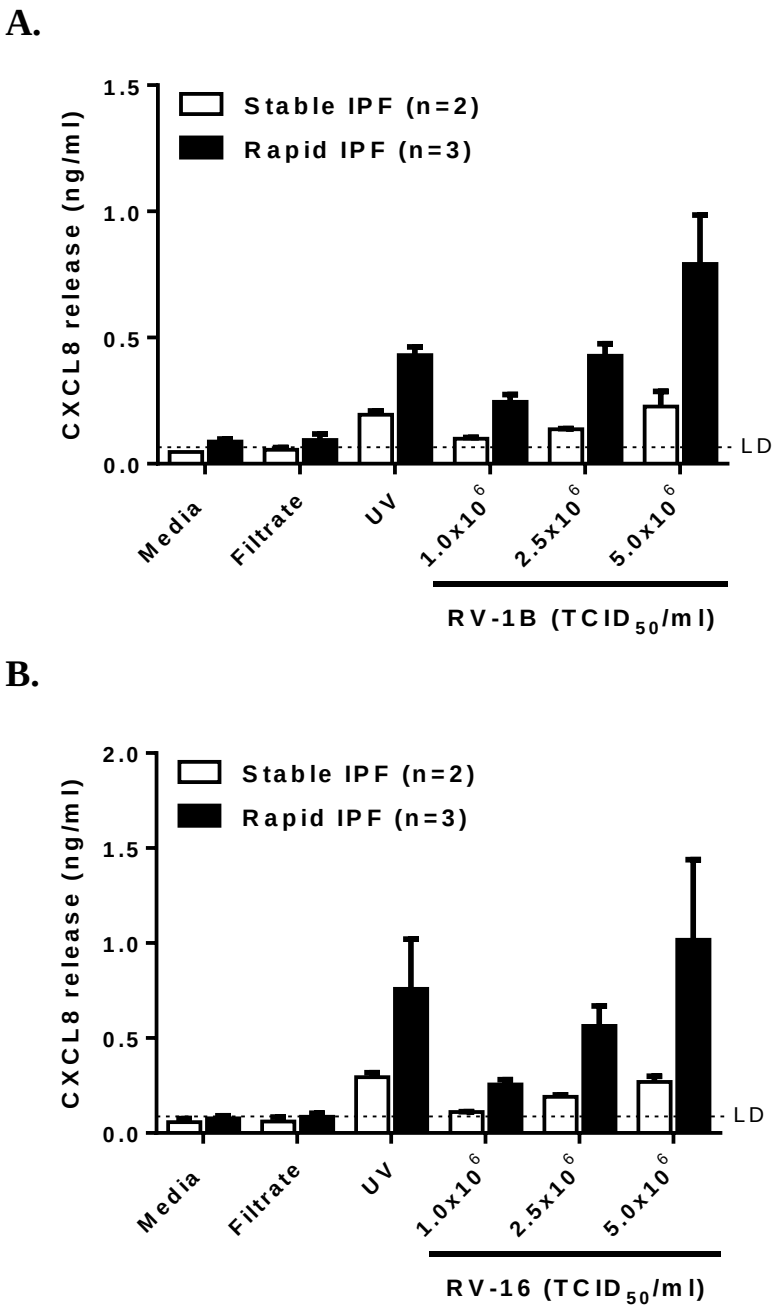

Figure 3. 21 IPFFs of rapid progressors release higher levels of CXCL8 compared to IPFFs of stable progressors in response to RV infection.

Cells were infected with RV-1B (A) or RV-16 (B) as described in Section 2.6.3 at the indicated $TCID_{50}$/ml. Filtrate and UV-RV control samples were prepared as described in Section 2.6.3. After 24 h, cell-free supernatants were collected, and CXCL8 release was measured by ELISA. Data shown are mean ± SEM of the results determined with samples collected from 2 (stable IPF) or 3 (rapid IPF) independent patients. Note that our senior lab technician, Dr Linda Kay, performed ELISA analysis of the IPFF supernatants. LD = Limit of detection.

patients secreted greater amounts of CXCL8 (by ~3-fold) compared to slow progressor patient cells (Figure 3.21). For example, slowly progressor patient IPFFs only released 0.23 ng/ml of CXCL8, whilst the cells from rapid progressor IPF patients produced 0.79 ng/ml of CXCL8, when infected with $5.0x10^6$ $TCID_{50}$/ml of RV-1B (Figure 3.21A). Likewise, $2.5x10^6$ $TCID_{50}$/ml of RV-16 induced 0.56 ng/ml of CXCL8 in rapid IPF patient cells, compared to only 0.19 ng/ml in slowly progressive IPFFs (Figure 3.21B). Additionally, comparable to the results seen in MRC-5 fibroblasts (Section 3.5) and HLFs (Section 3.10), UV-irradiated RV was able to trigger CXCL8 release from both slow and rapid IPFFs (Figure 3.21).

3.12.3 Comparable levels of viral replication occur within IPFFs obtained from slow and rapid progressor IPF patients

The level of viral replication within IPFFs obtained from patients with slow and rapid progressor IPF was also examined. Cells were infected with RV as described in Section 3.12.1. At 24 h p.i., cells were lysed, total RNA extracted, cDNA synthesised and real-time PCR for RV performed, samples were then quantified against a standard curve of plasmid containing RV target sequence (Section 2.16-2.18). Note that the RNA extraction and real-time PCR involving the use of IPFF samples were performed by our senior lab technician, Dr Linda Kay.

Figure 3.22A demonstrates that similar levels of RV-1B replication occurred in IPFFs of slow and rapid progressor. In contrast, replication of RV-16 appeared higher in cells obtained from slow progressor IPF patients compared to those from rapid progressor IPF patients (Figure 3.22B). However, due to the large variation between patients, more samples are required to verify this finding.

3.13 The proinflammatory cytokine IL-1β potentiates CXCL8 production in RV-infected epithelial cells, but not in RV-infected fibroblasts

The proinflammatory cytokine IL-1β has been shown to play a critical role in mediating airway inflammatory diseases such as asthma and COPD (reviewed in Dinarello, 2009). Our group has previously showed that IL-1β could induce CXCL8 release from various airway

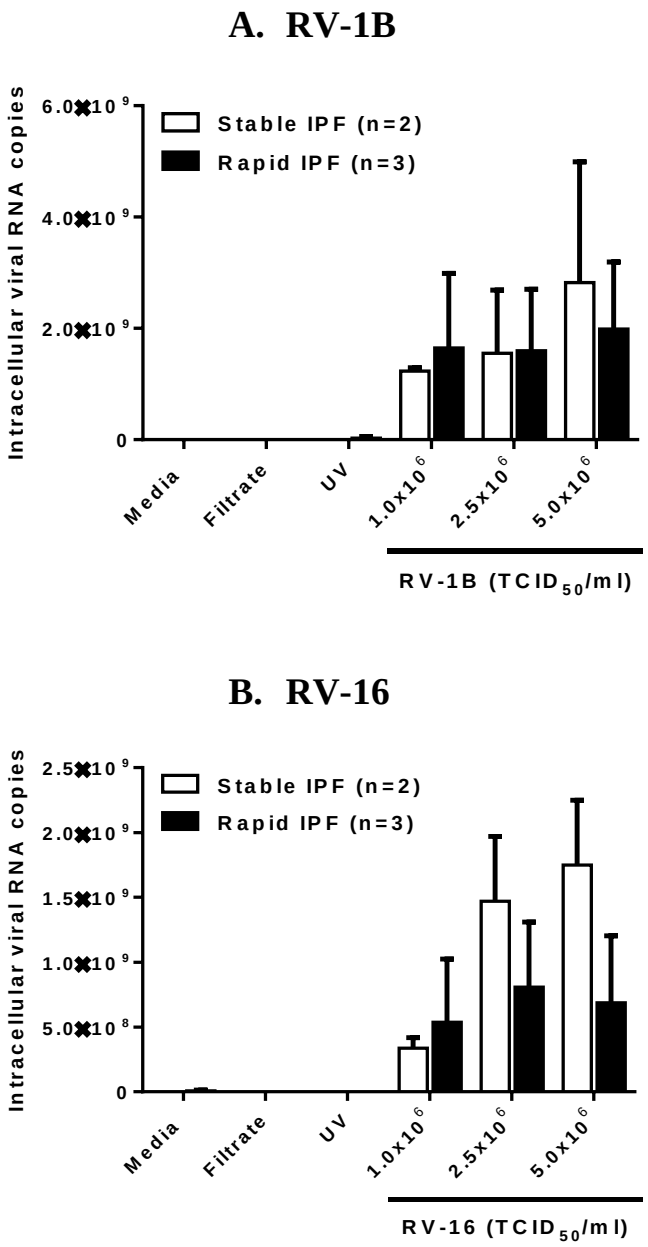

Figure 3. 22 Similar levels of viral replication occur in IPFFs of stable and rapid progressors.

Cells were infected with RV-1B (A) or RV-16 (B) as described in Section 2.6.3 at the indicated $TCID_{50}$/ml. Filtrate and UV-RV control samples were prepared as described in Section 2.6.3. At 24 h p.i., cells were lysed, total RNA extracted, cDNA synthesised by RT and real-time PCR for RV performed. Data shown are mean ± SEM of the results determined with samples collected from 2 (stable IPF) or 3 (rapid IPF) independent patients. Note that the RNA extraction and real-time PCR involving the use of IPFF samples were performed by our senior lab technician, Dr Linda Kay.

tissue cells including epithelial cells and smooth muscle cells (Morris et al., 2006, Morris et al., 2005). Furthermore, our group has demonstrated that IL-1β could synergistically augmented CXCL8 release from poly(I:C)-stimulated cells (Morris et al., 2006). Therefore, in the present study, the potential ability for IL-1β to potentiate the proinflammatory response of structural airway cells infected with RV was explored.

3.13.1 IL-1β potentiates CXCL8, but not CCL5 and CXCL10, release by RV-infected BEAS-2B cells

BEAS-2B cells were infected with RV-1B or RV-16 as described in Section 2.6.3 at $TCID_{50}$/ml ranging from $4.0x10^5$ to $2.0x10^7$. Immediately following the initial infection, IL-1β (0.1 ng/ml) was added to the virally-infected cells.

As demonstrated in Figure 3.23A, RV-1B induced CXCL8 production in a dose-dependent manner. CXCL8 release from the BEAS-2B cells was markedly potentiated when the cells were costimulated with both IL-1β and RV-1B, compared to cells treated with IL-1β alone (by ~4.5-fold) or RV-1B alone (by ~6.5-fold), respectively (at $TCID_{50}$/ml of $2.0x10^7$) (Figure 3.23A). As expected, IL-1β treatment alone did not result in CCL5 and CXCL10 production, whilst all RV-1B-infected cells produced a substantial amount of both chemokines (Figure 3.23B, C). Surprisingly, induction of CCL5 was significantly decreased (by ~46%) in cells dual-stimulated with RV-1B and IL-1β in comparison with RV-1B alone (Figure 3.23B). RV-16-infected BEAS-2B cells elicited similar patterns of cytokine generation to that of RV-1B-infected cells when costimulated with IL-1β (Figure 3.23, 3.24).

3.13.2 IL-1β does not potentiate CXCL8 release by RV-1B infected MRC-5 cells

As IL-1β amplified CXCL8 production in BEAS-2B epithelial cells infected with RV-1B (Section 3.13.1), the effect of IL-1β on CXCL8 release in response to RV-1B infection was determined in MRC-5 cells. Unlike the enhancement observed in BEAS-2B cells, costimulation with RV-1B ($TCID_{50}$/ml of $4.0x10^5$ and $4.0x10^6$) and IL-1β (0.1 and 1 ng/ml) did not result in the potentiation of CXCL8 production in MRC-5 cells (Figure 3.25). CCL5 release was undetectable in RV-infected MRC-5 cells (data not shown).

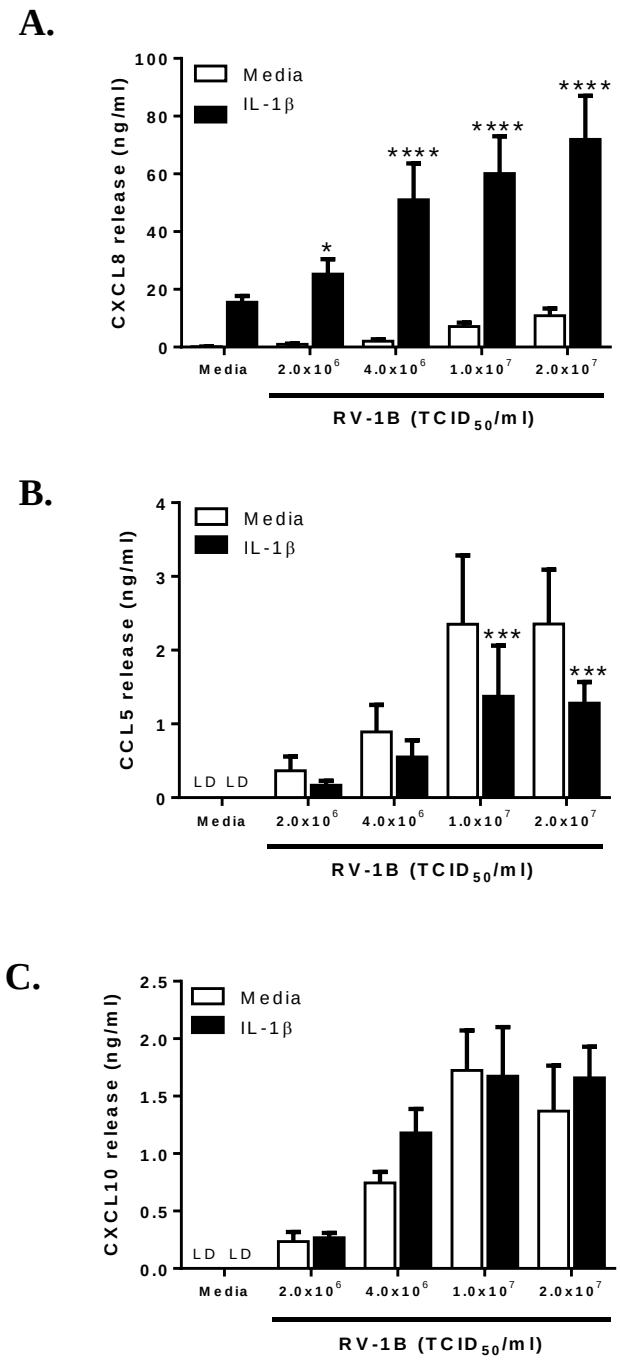

Figure 3. 23 Proinflammatory cytokine IL-1β potentiates CXCL8, but not CCL5 and CXCL10, release by RV-1B-infected BEAS-2B cells.

BEAS-2B cells were infected with RV-1B as described in Section 2.6.3 at the indicated $TCID_{50}$/ml. Following incubation with RV-1B for 1 h, virus was removed, media replaced, and cells were immediately stimulated with IL-1β (0.1 ng/ml). After 24 h, cell-free supernatants were collected and CXCL8 (A), CCL5 (B) and CXCL10 (C) release was measured by ELISA. Data shown are mean ± SEM of $n = 4$ (A, B) or $n = 3$ (C) independent experiments. Significant differences are indicated by *$p<0.05$, ***$p<0.001$ and ****$p<0.0001$ (versus media control at the same $TCID_{50}$/ml), as measured by two-way ANOVA with Bonferroni's post-test. LD = Limit of detection.

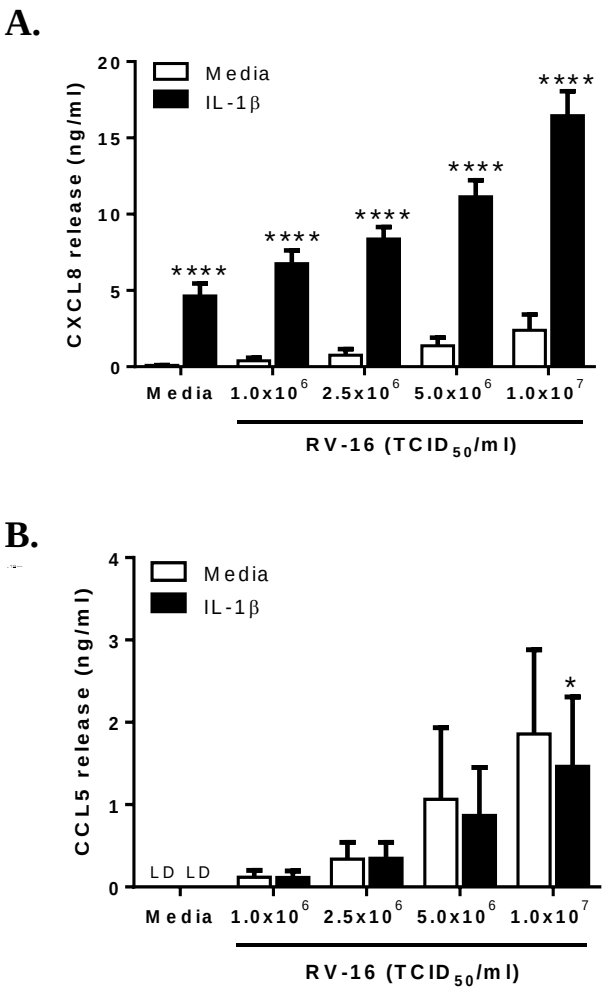

Figure 3. 24 IL-1β potentiates CXCL8, but not CCL5, release by RV-16-infected BEAS-2B cells.

BEAS-2B cells were infected with RV-16 as described in Section 2.6.3 at the indicated $TCID_{50}$/ml. Following incubation with RV-16 for 1 h, virus was removed, media replaced, and cells were immediately stimulated with IL-1β (0.1 ng/ml). After 24 h, cell-free supernatants were collected and CXCL8 (A) and CCL5 (B) release was measured by ELISA. Data shown are mean ± SEM of n = 3 independent experiments. Significant differences are indicated by *p<0.05 and ****p<0.0001 (versus media control at the same $TCID_{50}$/ml), as measured by two-way ANOVA with Bonferroni's post-test. LD = Limit of detection.

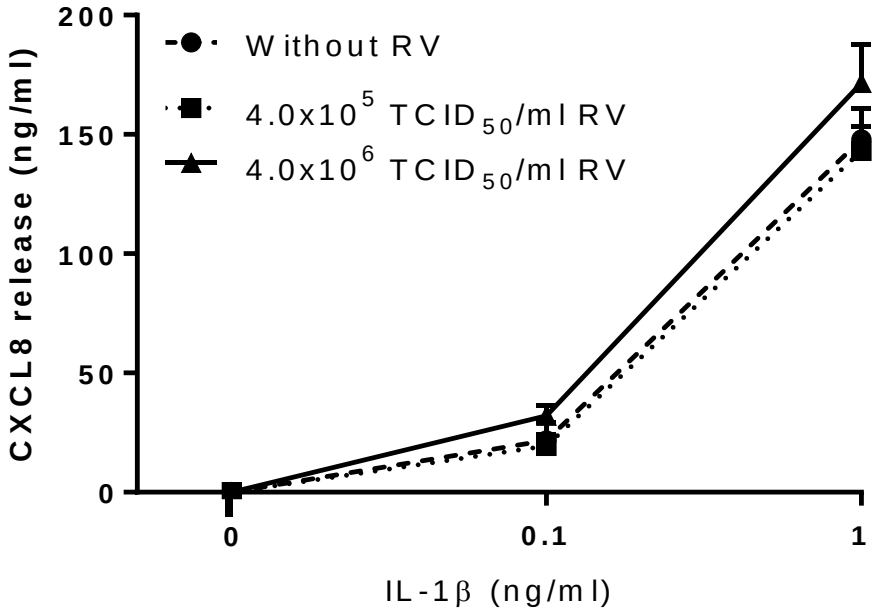

Figure 3. 25 IL-1β does not potentiate RV-1B-induced CXCL8 release by MRC-5 cells. MRC-5 cells were infected with RV-1B as described in Section 2.6.3 at the indicated $TCID_{50}$/ml. Following incubation with RV-1B for 1 h, virus was removed, and cells were immediately stimulated with IL-1β at the indicated concentrations. After 24 h, cell-free supernatants were collected, and CXCL8 release was measured by ELISA. Data shown are mean ± SEM of *n* = 3 independent experiments. No significant differences were obtained (RV-infected versus media control at the same IL-1β concentration), as measured by two-way ANOVA with Bonferroni's post-test.

3.13.3 IL-1β does not potentiate CXCL8 release from RV-infected HLFs, but alone induces high CXCL8 release from HLFs

As shown in the previous sections (3.13.1 and 3.13.2), the proinflammatory cytokine IL-1β can potentiate the release of CXCL8 from the RV-infected BEAS-2B epithelial cell line, but not the MRC-5 fibroblast cell line. Hence, I next wished to determine if similar findings would be obtained in HLFs. HLFs were infected with RV-1B or RV-16 as described in Section 2.6.3 at $TCID_{50}$/ml of $4.0x10^5$, $1.0x10^6$, $2.5x10^6$ and $5.0x10^6$. Immediately following the initial infection, IL-1β (0.1 ng/ml) was added to the RV-infected cells.

Based on two independent experiments, in keeping with the results obtained from RV-infected MRC-5 fibroblasts (Section 3.13.2), costimulation with RV and IL-1β did not result in the amplification of CXCL8 generation in HLFs (Figure 3.26, 3.27). Interestingly, although there was no potentiation of CXCL8 release from the HLFs following costimulation with RV and IL-1β, IL-1β alone induced a very high level of CXCL8 (~270 ng/ml) (Figure 3.26, 3.27). As described in Section 3.10, HLFs produced CXCL8 in response to RV in a dose-dependent manner (Figure 3.26, 3.27) and CCL5 release was not detected following RV-infection of HLFs (data not shown).

3.13.4 IL-1β does not affect cell death of RV-1B-infected MRC-5 and BEAS-2B cells

As IL-1β potentiates CXCL8 release in response to RV-1B infection in BEAS-2B cells (Section 3.13.1), confirmation was sought that this effect was not due to IL-1β protecting cells from virally-induced cell death, allowing more to remain alive to produce cytokines. MRC-5 and BEAS-2B cells were infected with RV-1B at $TCID_{50}$/ml of $4.0x10^6$ and $1.0x10^7$ as described in Section 2.6.3 and then immediately stimulated with IL-1β for 24 h, and cell-free supernatants collected to measure LDH release. IL-1β had no effect on cell death induced by RV-1B infection in MRC-5 (Figure 3.28A) or BEAS-2B cells (Figure 3.28B).

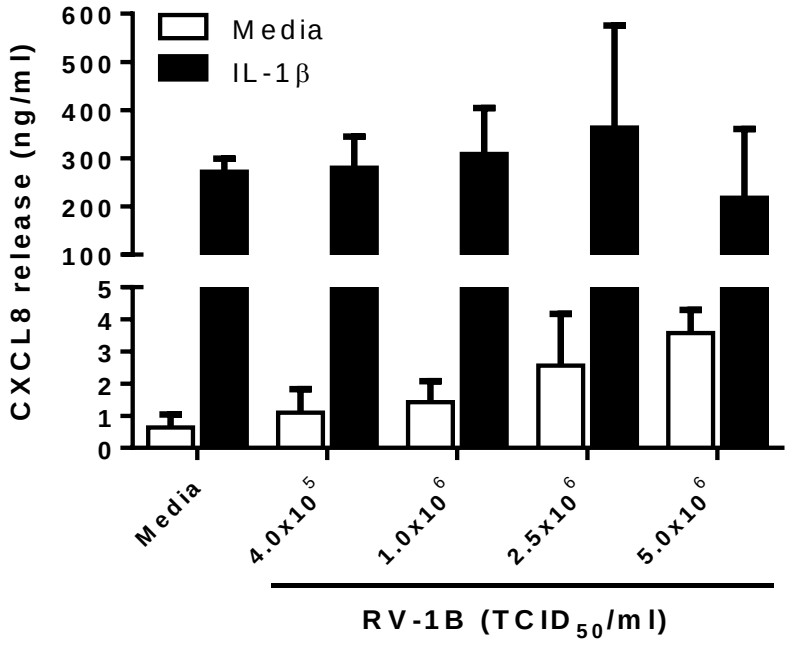

Figure 3. 26 IL-1β does not potentiate CXCL8 release from RV-1B-infected HLFs, but alone induces high CXCL8 release from HLFs.

HLFs were infected with RV-1B as described in Section 2.6.3 at the indicated $TCID_{50}$/ml. Following incubation with RV-1B for 1 h, virus was removed, and cells were immediately stimulated with IL-1β (0.1 ng/ml). After 24 h, cell-free supernatants were collected, and CXCL8 release was measured by ELISA. Data shown are mean ± SD of *n* = 2 independent experiments.

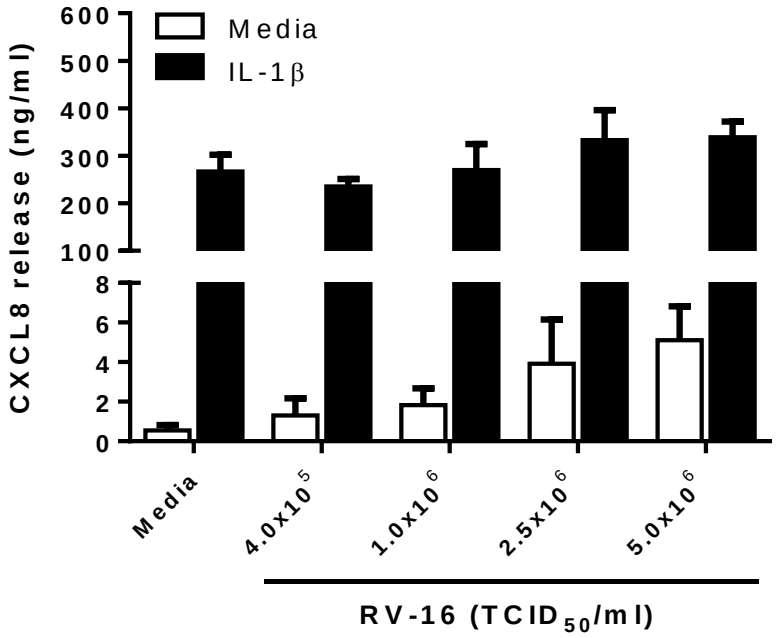

Figure 3. 27 IL-1β does not potentiate CXCL8 release from RV-16-infected HLFs.
HLFs were infected with RV-16 as described in Section 2.6.3 at the indicated $TCID_{50}$/ml. Following incubation with RV-16 for 1 h, virus was removed, and cells were immediately stimulated with IL-1β (0.1 ng/ml). After 24 h, cell-free supernatants were collected, and CXCL8 release was measured by ELISA. Data shown are mean ± SD of n = 2 independent experiments.

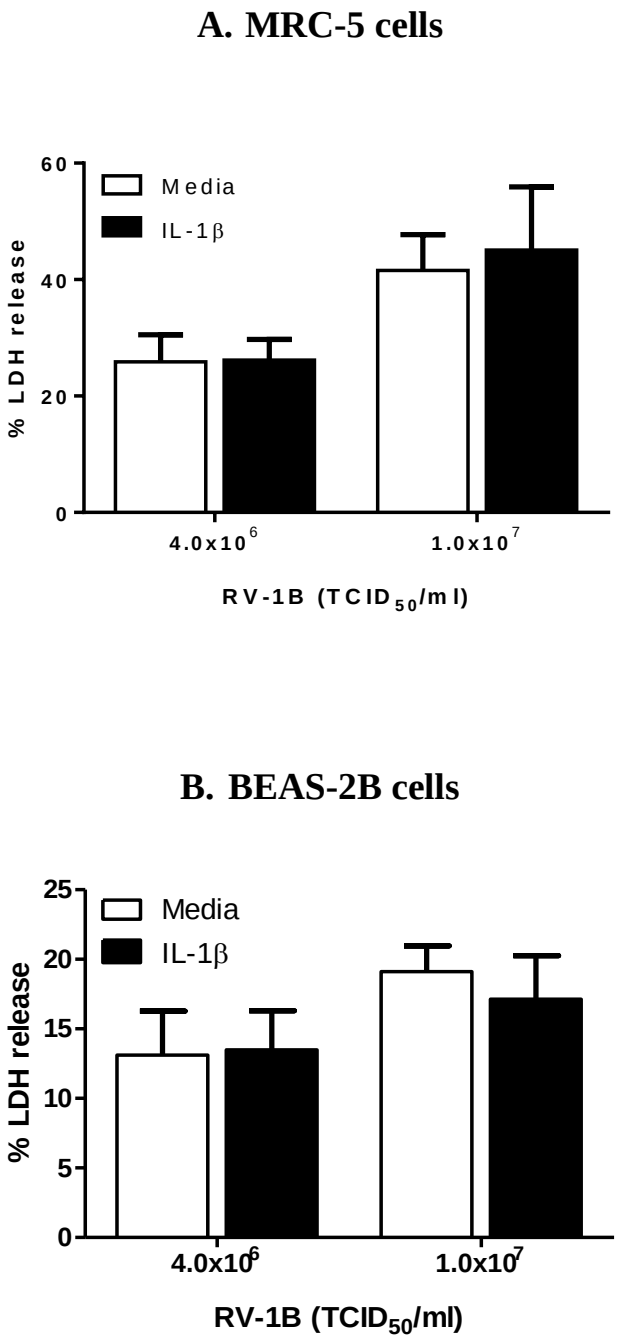

Figure 3. 28 IL-1β does not affect cell death induced by RV-1B infection of MRC-5 or BEAS-2B cells.

Cells were infected with RV-1B as described in Section 2.6.3 at the indicated $TCID_{50}$/ml. Following incubation with RV-1B for 1 h, virus was removed, media replaced, and cells were stimulated with IL-1β (10 ng/ml) (A) or (0.1 ng/ml) (B). After 24 h, cell death was measured as described in Section 2.20 and displayed as % LDH release by dead cells. Data shown are mean ± SD of *n* = 2 (A) or mean ± SEM of *n* = 3 (B) independent experiments.

3.13.5 IL-1β does not regulate viral replication in BEAS-2B epithelial cells

IL-1β potentiates CXCL8, but inhibits release of the IFN-inducible chemokine CCL5, in response to RV-1B infection in BEAS-2B cells (Section 3.13.1). The reduction in CCL5 may indicate that IL-1β could indirectly influence viral replication by down-modulating the cells ability to produce anti-viral cytokines and thus control replication. BEAS-2B cells were infected with RV-1B as described in Section 2.6.3 and then stimulated with IL-1β (0.1 ng/ml) for 24 h. Cells (~$6.1x10^5$) were lysed, cDNA synthesised and real-time PCR for RV-1B performed (Section 2.16-2.18). In contrast to its effects on cytokine release, IL-1β did not regulate viral replication in BEAS-2B cells (Figure 3.29).

3.14 In the presence of monocytes, LPS potentiates cytokine release from BEAS-2B cells infected with RV-1B or stimulated with poly(I:C)

Clinical studies have reported that severe exacerbations of asthma and COPD can be caused by coinfection with bacterial and viral pathogens (Wilkinson et al., 2006, Louie et al., 2009). Our group has previously shown that the bacterial-derived LPS most effectively activated CXCL8 generation from airway epithelial cells and airway smooth muscle cells in the presence of monocytes, but not T cells (Morris et al., 2005, Chaudhuri et al., 2010). Furthermore, our group has demonstrated that costimulation with the viral dsRNA mimic poly(I:C) and LPS enhanced CXCL8 release by BEAS-2B epithelial cells in the presence of PBMCs, by which the activating cell type within the PBMC populations has been previously shown to be the monocyte (Morris et al., 2006, Morris et al., 2005). Therefore, to investigate whether BEAS-2B cell inflammatory responses could be amplified by concurrent stimulations with RV-1B and LPS, experiments were performed by stimulating BEAS-2B cells alone, or BEAS-2B/monocyte cocultures (created with the addition of 9500 highly purified $CD14^+$ monocytes/well following infection with RV-1B ($TCID_{50}$/ml of $2.0x10^6$, $5.0x10^6$ and $1.0x10^7$) and LPS (0.1 ng/ml) (Section 2.7.3).

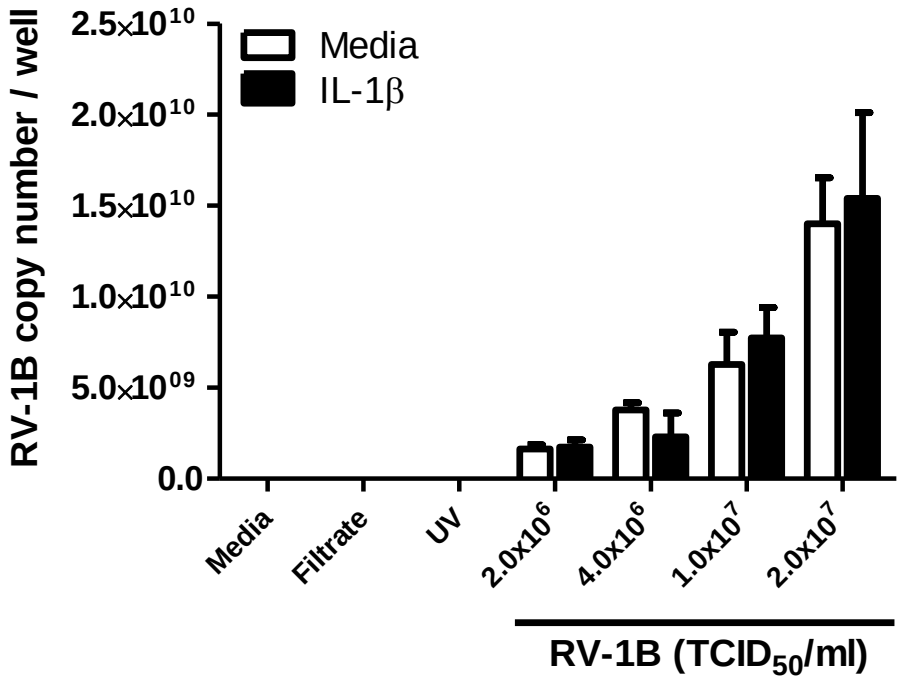

Figure 3. 29 IL-1β does not regulate viral replication in BEAS-2B epithelial cells.
BEAS-2B cells were infected with RV-1B as described in Section 2.6.3 at the indicated $TCID_{50}$/ml. Following incubation with RV-1B for 1 h, virus was removed, media replaced, cells then immediately stimulated with IL-1β (0.1 ng/ml). At 24 h p.i., cells (~6.1 x 10^5) were lysed, total RNA extracted, cDNA synthesised by RT and real-time PCR for RV-1B performed. Data shown are mean ± SEM of n = 3 independent experiments. No significant differences were obtained (IL-1β-treated sample versus media control at the same $TCID_{50}$/ml of RV), as measured by two-way ANOVA with Bonferroni's post-test.

As expected, RV-1B infection triggered the concentration-dependent release of CXCL8 and CCL5 from BEAS-2B cells (Figure 3.30A, B). In the absence of monocytes, LPS did not amplify CXCL8 or CCL5 release from RV-1B infected cells (Figure 3.30A, B). Importantly, in the presence of monocytes LPS drastically enhanced CXCL8 (Figure 3.30C), but not CCL5 (Figure 3.30D), cytokine release from BEAS-2B cells infected with RV-1B. For example, when the BEAS-2B cells were costimulated with $1.0x10^7$ $TCID_{50}$/ml of RV-1B and LPS in the absence of monocytes, only ~6 ng/ml of CXCL8 protein was detected (Figure 3.30A), and when the same concentrations of RV-1B and LPS were used to infect BEAS-2B in the presence of monocytes, ~200 ng/ml of CXCL8 protein was measured (Figure 3.30C). The same potentiation was observed when a higher concentration of LPS (10 ng/ml) was used (data not shown). Note that based on two independent experiments (i.e. the first and second experiments performed for the data shown in Figure 3.30), CXCL8 or CCL5 release was undetectable when the single-culture of monocytes was stimulated with RV-1B or LPS (data not shown).

To determine if poly(I:C)/LPS costimulation elicited the same effect as RV-1B/LPS cotreatment, BEAS-2B cells alone, or BEAS-2B/monocyte cocultures were stimulated with poly(I:C) (1, 10, 100 µg/ml) in the presence or absence of LPS (0.1 ng/ml). Poly(I:C) alone induced higher levels of CXCL8 and CCL5 release from BEAS-2B cells (Figure 3.31A, B) when compared to RV-1B-infected BEAS-2B cells (Figure 3.30A, B). In keeping with the RV-1B data (Figure 3.30), in the absence of monocytes LPS alone had no effect on CXCL8 or CCL5 release and its presence did not amplify the poly(I:C)-induced cytokine production in BEAS-2B cells (Figure 3.31A, B). However, when BEAS-2B/monocyte cocultures were dual-stimulated with LPS and poly(I:C), CXCL8 release was significantly potentiated (Figure 3.31C), compared to the BEAS-2B cells alone (Figure 3.31A), whilst CCL5 release was not modulated (Figure 3.31D). For example, in the absence of monocytes 1 µg/ml poly(I:C) with LPS costimulation only caused ~50 ng/ml of CXCL8 release (Figure 3.31A), whilst in the presence of monocytes, the same concentrations of stimuli resulted in ~180 ng/ml of CXCL8 release (Figure 3.31C). Of note, the effect of poly(I:C) in stimulating CXCL8 production in the BEAS-2B cells was maximal at the concentration of 10 µg/ml.

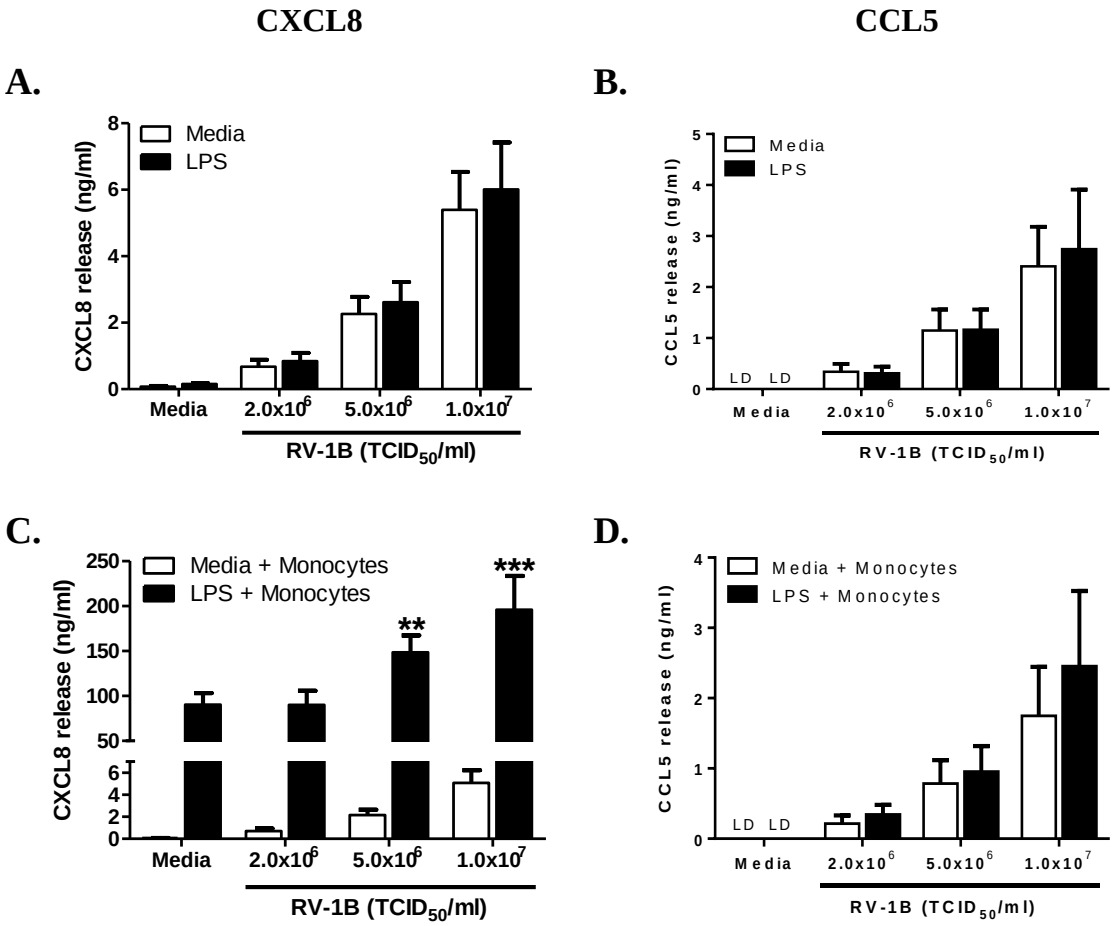

Figure 3. 30 In the presence of monocytes, LPS potentiates cytokine release from BEAS-2B cells infected with RV-1B.

BEAS-2B cells were infected with RV-1B as described in Section 2.6.3 at the indicated $TCID_{50}$/ml, followed by stimulation with media or LPS (0.1 ng/ml). Cocultures were created with the addition of 9500 highly purified $CD14^+$ monocytes. After 24 h, cell-free supernatants were collected and the release of CXCL8 (A, C) and CCL5 (B, D) measured by ELISA. Data shown are mean ± SEM of $n = 4$, with each replicate performed on separate passages of BEAS-2B cells with freshly prepared monocytes from independent donors. Significant differences are indicated by $^{**}p<0.01$ and $^{***}p<0.001$ (versus LPS + Monocytes alone), as measured by two-way ANOVA with Bonferroni's post-test. LD = Limit of detection.

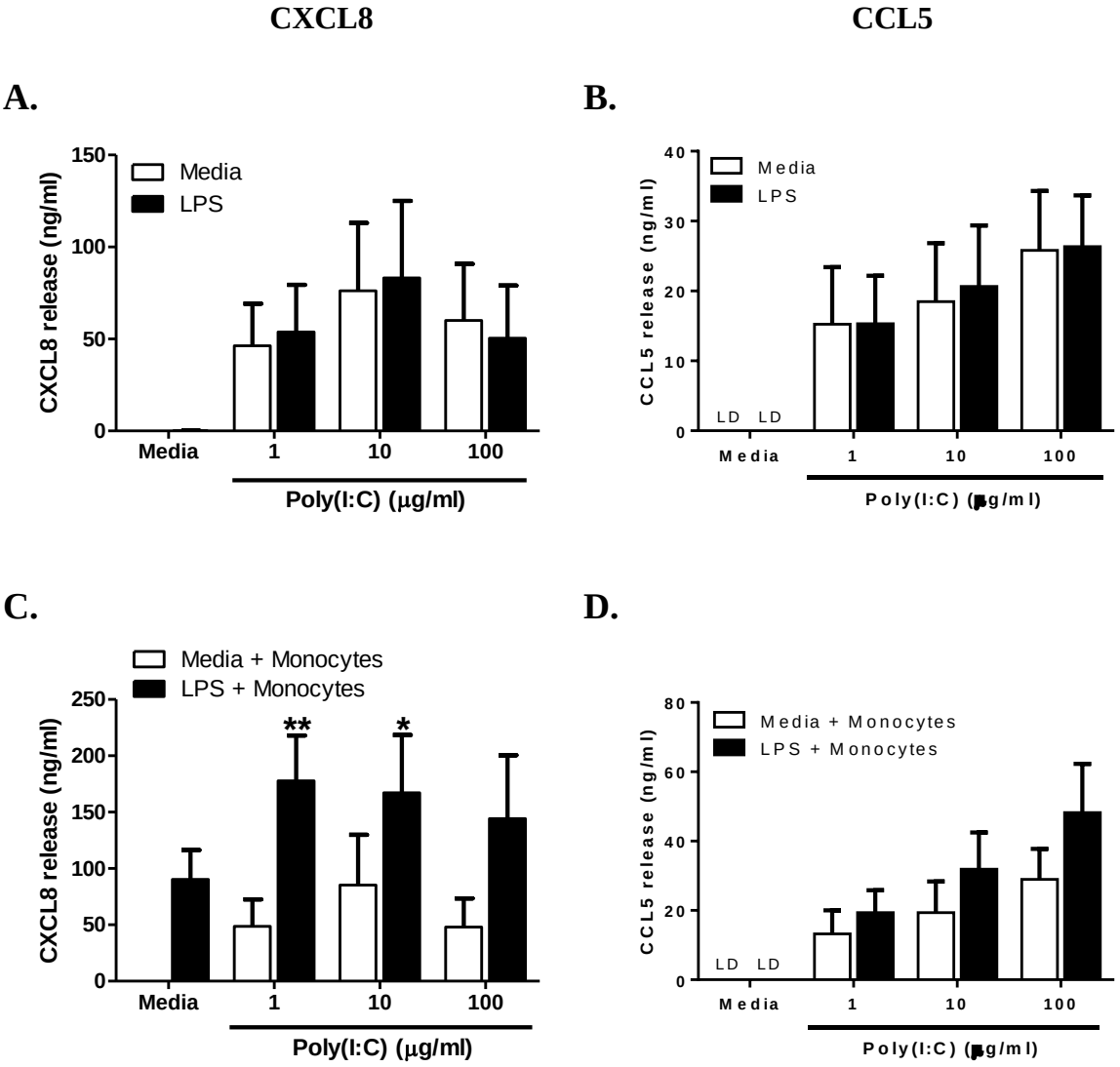

Figure 3. 31 In the presence of monocytes, LPS potentiates cytokine release from BEAS-2B cells stimulated with poly(I:C).

BEAS-2B cells were stimulated with LPS (0.1 ng/ml) alone or dual-stimulated with LPS (0.1 ng/ml) and Poly(I:C) (1, 10, 100 μg/ml). Cocultures were created with the addition of 9500 highly purified $CD14^+$ monocytes. After 24 h, cell-free supernatants were collected and the release of CXCL8 (A, C), and CCL5 (B, D) measured by ELISA. Data shown are mean ± SEM of n = 4, with each replicate performed on separate passages of BEAS-2B cells with freshly prepared monocytes from independent donors. Significant differences are indicated by *p<0.05, **p<0.01 and ***p<0.001 (versus LPS+Monocytes alone), as measured by two-way ANOVA with Bonferroni's post-test. LD = Limit of detection.

3.15 Discussion

3.15.1 Summary

The findings presented in this chapter reveal that normal human airway fibroblasts and epithelial cells express distinct mRNA expression profiles of viral RNA-detecting PRRs and the key signalling molecules involved in viral recognition and type I IFN production. Importantly, RV infection induced differential responses in lung epithelial cells and fibroblasts. Fibroblasts were highly permissive for RV replication which resulted in major cell death, and whilst they were able to secrete proinflammatory cytokines following RV infection, they did not produce antiviral cytokines. The work presented here demonstrated the permissiveness of lung fibroblasts isolated from IPF patients to RV infection. This study also revealed for the first time the ability of IL-1β to enhance proinflammatory responses of RV-1B-infected epithelial cells. Furthermore, this study demonstrated that in the presence of monocytes, RV and bacterial-derived LPS coinfections could act in synergy to augment the proinflammatory responses of airway tissue cells.

3.15.2 A role for fibroblasts in mediating airway inflammation following RV infection

Whilst the inflammatory responses induced by RV infection of airway epithelial cells are well documented, very little is known about the ability of lung fibroblasts to amplify inflammation as a result of RV infection. Therefore, this study aimed to investigate the ability of RV to infect tissues beyond epithelium, particularly fibroblasts, which may contribute to the virally-induced exacerbations of COPD.

This study first utilised the MRC-5 cell line as a model of lung fibroblasts to study the effect of RV infection in this cell type. In fact, MRC-5 cells have been used to propagate and isolate RV from nasopharyngeal and throat swab clinical specimens (Geist and Hayden, 1985). The current study demonstrated that, in response to RV infection, MRC-5 fibroblasts secreted the proinflammatory cytokines CXCL8 and IL-6 in a $TCID_{50}$-dependent manner. To validate the results obtained using a cell line, primary lung fibroblasts were then used. Similar to the results seen in the MRC-5 cell line, primary HLFs also produced CXCL8 upon RV infection. These findings were in agreement with the results attained by other studies which have also

examined the inflammatory responses of primary airway fibroblasts to RV-1B and RV-16 (Van Ly et al., 2011, Bedke et al., 2009, Thomas et al., 2009). Apart from CXCL8, it has been reported that RV-infected primary airway fibroblasts can also release another neutrophil-recruiting chemokine, CXCL5 [previously known as epithelial-derived neutrophil-activating peptide 78 (ENA-78)] (Thomas et al., 2009, Ghildyal et al., 2005). In addition, production of CXCL8 and IL-6 in the MRC-5 fibroblasts in response to RV-39 (major group RV), RV-14 (major group RV) and RV-1A (minor group RV) infection was shown to be elicited by the classic NF-κB-dependent transcriptional activation pathways (Zhu et al., 1997, Zhu et al., 1996).

Intriguingly, in contrast to the results seen when airway epithelial cells were exposed to UV-irradiated-virus, production of CXCL8 and IL-6 was detected in the UV-RV-treated fibroblasts. This is consistent with the findings obtained by Bedke *et al.* by which they found that UV-irradiated RV-1B could trigger CXCL8 and IL-6 generation by primary bronchial fibroblasts (Bedke et al., 2009). Furthermore, using primary human airway smooth muscle cells (ASMCs), a study showed that UV-inactivated RV-16 could also induce CXCL8 and IL-6 release by this cell type (Oliver et al., 2006). This suggests that in mesenchymal cells (i.e. fibroblasts and ASMCs), generation of CXCL8 and IL-6 can occur independently of viral replication. As suggested by several studies (Grunstein et al., 2001, Johnston et al., 1998), one of the potential mechanisms of cytokine induction by UV-RV is via virus-receptor interaction. Johnston *et al.* found that inductions of both CXCL8 mRNA expression and protein release in A549 cells (an alveolar epithelial cell line) were reduced by only ~50% when RV-9 (major group RV) replication was inhibited by UV radiation. However, they demonstrated that prevention of virus-receptor binding (by pre-coating the virus with soluble recombinant ICAM-1, the receptor for major group RV), completely suppressed CXCL8 protein release upon RV-9 infection (Johnston et al., 1998). Similarly, in their studies of primary ASMCs, Grunstein and colleagues showed that whilst RV-16 replication was completely attenuated by UV radiation, UV-irradiated RV-16 remained fully capable of inducing IL-5 and IL-1β production (Grunstein et al., 2001). However, the UV-RV-induced cytokine release was substantially inhibited when the cells were pre-treated with a neutralising antibody against ICAM-1 (Grunstein et al., 2001). Taking this idea into consideration, further work should be done to examine if CXCL8 induction by UV-inactivated RV in fibroblasts could be inhibited by blocking the host cell receptors with the relevant neutralising antibodies. An alternative explanation for the ability of UV-RV to

trigger CXCL8 production in fibroblasts, but not in epithelial cells, could be that fibroblasts are able to respond to cytokines or damage-associated molecular patterns released by the HeLa Ohio cells during propagation of the virus. Again, further study is required to test this hypothesis.

The proinflammatory cytokine IL-1β has been shown to play a vital role in mediating airway inflammatory diseases such as asthma and COPD (reviewed in Dinarello, 2009). Our group has previously demonstrated that exogenous IL-1β could induce CXCL8 release from various airway tissue cells including epithelial cells and smooth muscle cells (Morris et al., 2006, Morris et al., 2005). Furthermore, our group has shown that IL-1β could synergistically amplified CXCL8 production from poly(I:C)-stimulated cells (Morris et al., 2006). Therefore, in the current study, the possible ability of IL-1β to amplify the inflammatory responses induced by RV infection was ascertained. Addition of exogenous IL-1β caused prominent synergistic potentiation of CXCL8 release from the BEAS-2B epithelial cells in response to RV infection, which was in agreement with the data previously obtained in our group using poly(I:C) and IL-1β dual-stimulation (Morris et al., 2006). In contrast, IL-1β did not accentuate CXCL8 production in RV-infected MRC-5 fibroblasts. The potential explanations for these distinct effects of exogenous IL-1β on CXCL8 generation in airway epithelial cells and fibroblasts are discussed in Section 3.15.6. Despite the lack of potentiating effect of IL-1β on CXCL8 release in RV-infected fibroblasts, it is interesting to see that IL-1β alone triggered a high level of CXCL8 release from these structural airway cells. It is known that apart from the ability of the airway epithelial cells to produce CXCL8 in response to IL-1β stimulation, this cell type can itself secrete IL-1β following RV infection (Piper et al., 2013, Shi et al., 2012, Stokes et al., 2011). Therefore, in the context of cellular inflammatory networks, it is highly plausible that the IL-1β derived from the epithelial cells (as a result of viral infection) may then stimulate the neighbouring fibroblasts to further release CXCL8, consequently amplifying the neutrophilic airway inflammation.

This study is the first to demonstrate that, in comparison to bronchial epithelial cells, fibroblasts allow higher viral replication to take place. This might explain why RV induced major cell death of this cell type, as compared to epithelial cells. Viruses replicate within the host cells, produce more virions and the newly synthesised virions are released by lysing the cells. Furthermore, poly(I:C) stimulation did not result in cell death implying that the cell death was not a host-mediated cell death (as a response against PRR activation) but rather

was a virally-induced cell death. The RV-triggered dead fibroblasts may release cell damage products such as high-mobility group box 1 (HMGB1) that could elevate inflammation in the airway (Ferhani et al., 2010). HMGB1 has a distinct structure to chemokines but has all characteristics of a chemokine. It is a nuclear protein that can be released out of the cell during inflammation (reviewed in Degryse and de Virgilio, 2003). Scaffidi and co-workers demonstrated that *HMGB1*$^{-/-}$ mouse embryonic fibroblasts (MEFs) have remarkably reduced capability to promote inflammation as compared to the wild-type MEFs (Scaffidi et al., 2002). Furthermore, a recent study showed that HMGB1 is increased in BALF taken from patients with COPD (Ferhani et al., 2010).

Taken together, the data suggests that fibroblasts may play an important role in virally-induced exacerbations of COPD. The fact that fibroblasts numbers are increased in COPD (reviewed in Araya and Nishimura, 2010) implies that more RV replication can take place, hence worsening the inflammation in this airway disease.

3.15.3 RV infection as a potential cause of exacerbations of IPF

There is a growing body of evidence proposing a role for viruses, such as HSV and EBV, in causing acute exacerbations of IPF (Guenther et al., 2010, Lasithiotaki et al., 2011, Wootton et al., 2011). The course of IPF is variable, some IPF patients remain stable for prolonged periods of time (slow progressors), whilst others experience a rapid, stepwise progression of the disease with accelerated mortality (rapid progressors) (reviewed in Hogaboam et al., 2012). Therefore, this study aimed to explore the ability of RV to induce inflammatory responses in lung fibroblasts isolated from patients with IPF, and to determine whether distinct responses are triggered by RV infection in the IPFFs of rapidly progressing IPF patients and slowly progressing IPF patients. The work presented here demonstrates for the first time the permissiveness of lung fibroblasts isolated from IPF patients to RV infection. Importantly, it was revealed that cells of rapid IPF progressors released higher proinflammatory cytokine CXCL8 compared to that of slow IPF progressors, implicating a possible role for RV infection in triggering IPF exacerbations.

3.15.4 RV infection induces differential responses by airway epithelial cells and fibroblasts

This study aimed to investigate whether differences existed between the responses of airway epithelial cells and fibroblasts to RV infection. The data in this chapter demonstrates that RV induced differential responses in airway epithelial cells and fibroblasts. Of great importance is that RV caused much higher cell death in lung fibroblasts compared to epithelial cells, and this is believed to be due to the greater permissiveness of fibroblasts to viral replication compared to epithelial cells. The levels of cytokine production between bronchial epithelial cells and fibroblasts as a result of RV infection were also found to be dissimilar, with much greater level of CXCL8 release detected from RV-infected epithelial cells compared to RV-infected fibroblasts. Importantly, in contrast to airway epithelial cells, fibroblasts did not produce the antiviral cytokines CCL5 and CXCL10 in response to RV infection. Subsequent experiments indicated that this might be due to the lack of upregulation of viral-detecting PRRs and key signalling molecules (e.g. IRF7) expression that are required for the induction of these proinflammatory and antiviral cytokines in the airway fibroblasts in response to RV infection.

Viral RNA is detected by two-receptor systems: TLRs and RLRs (Section 1.4). TLRs (i.e. TLR3, TLR7 and TLR8) detect viral RNA in the endosomal compartments, whilst RLRs (i.e. RIG-I and MDA5) recognise cytoplasmic viral RNA. This study determined the expression of these viral-detecting PRRs in structural airway lung fibroblasts and epithelial cells at the mRNA level. As a control, expression of viral-detecting PRRs was explored in monocytes, an innate immune cell. This work demonstrated that BEAS-2B epithelial cells and MRC-5 fibroblasts expressed the dsRNA-detecting PRR TLR3, in keeping with previous studies (Matsumoto et al., 2002, Jorgenson et al., 2005, Rudd et al., 2005, Morris et al., 2006). In contrast, the viral ssRNA PRRs TLR7 and TLR8 mRNA were not expressed in BEAS-2B cells, consistent with several studies done using BEAS-2B cells (Homma et al., 2004, Sha et al., 2004) and primary HBECs (Ritter et al., 2005). In agreement with previous reports (Pan et al., 2011, Bekeredjian-Ding et al., 2006), monocytes on the other hand constitutively expressed both TLR7 and TLR8, but not TLR3. These observations partly explain our group's previous findings that BEAS-2B cells did not respond to TLR7/8 agonist gardiquimod; whilst PBMCs (which normally consist of 70-75% lymphocytes, 10-15% monocytes, 5-8% eosinophils, and <5% neutrophils (Harding and Yang, 1984) did respond to

this TLR7/8 agonist (Parker et al., 2008). Slater and co-workers have also shown that TLR7/8 stimulation did not induce cytokine secretion in primary HBECs (Slater et al., 2010), although this is in contrast to the results obtained by other studies (Sykes et al., 2013, Triantafilou et al., 2011). Very recently, Sykes and colleagues reported that TLR7/TLR8 stimulation with resiquimod induced production of several cytokines including CXCL8, IL-6 and IFN-λ in primary HBECs (Sykes et al., 2013). Likewise, Triantafilou *et al.* demonstrated that upon stimulation with RV-6 naked ssRNA, primary HBECs released IL-6 and IFN-β proteins, and this cytokine secretion was reduced when TLR7 or TLR8 expression was knocked down using small-interfering RNA (siRNA) (Triantafilou et al., 2011).

To date, little is known regarding the expression of PRRs in lung fibroblasts. Here it was revealed for the first time that like other structural tissue cells, including airway smooth muscle cells (Morris et al., 2006), lung fibroblasts did not express TLR7 and TLR8. Of relevance, it has been reported that human fibroblasts isolated from other organs (i.e. skin and prostate) also elicited undetectable TLR7 and TLR8 (Agarwal et al., 2011, Kiniwa et al., 2007). Consistent with previous studies (Wang et al., 2009, Le Goffic et al., 2007), BEAS-2B cells constitutively expressed both RLRs RIG-I and MDA5, as determined at the mRNA level. To date, one study has reported expression of both RLRs in mouse lung fibroblasts (Satoh et al., 2010), the work presented here is therefore the first to demonstrate the basal expression of RIG-I and MDA5 in human lung fibroblasts.

In addition to the PRRs, this study has determined the baseline expression of the mitochondrial adaptor molecule MAVS (also known as IPS-1/VISA/Cardif) in structural airway BEAS-2B and MRC-5 cells, as well as in monocytes. MAVS is a CARD domain-containing protein that is involved in RLR signalling pathways (Section 1.5.3), and has been shown to be crucial in antiviral innate immune response (reviewed in Seth et al., 2006). Slater *et al.* demonstrated that knockdown of MAVS reduced the RV-1B-induced production of several proinflammatory and antiviral cytokines including CXCL8, IFN-β, CCL5 and CXCL10 in primary HBECs (Slater et al., 2010). The current work showed that BEAS-2B cells constitutively express MAVS, in accordance with a previous study (Le Goffic et al., 2007), but is the first to report that human lung fibroblasts also constitutively expressed MAVS, whereas monocytes did not, as determined at the level of mRNA.

The work presented here showing that unlike airway epithelial cells, fibroblasts were not able to produce the antiviral CCL5 protein, is consistent with a previous study conducted by

Bedke and colleagues in primary bronchial fibroblasts (Bedke et al., 2009). Furthermore, production of CXCL10 protein by lung fibroblasts following RV infection was also undetectable. This indicates the lack of IFN production in this cell type since both CCL5 and CXCL10 are IFN-stimulated genes (ISGs). Indeed, studies which immediately preceded or were published during the course of this work have also shown that primary airway fibroblasts do not generate IFN-β, IFN-λ1 and IFN-λ2 in response to RV infection (Van Ly et al., 2011, Bedke et al., 2009).

The regulation of viral-detecting PRRs and the adaptor molecule MAVS by RV infection in both MRC-5 and BEAS-2B cells was also investigated, and the results revealed that their modulation is cell-type specific. However, similar patterns of regulation were exhibited by the two RV serotypes RV-1B and RV-16. The finding that mRNA expression of the PRRs TLR3, RIG-I and MDA5 was upregulated by RV infection in BEAS-2B epithelial cells are consistent with previous studies which also detected upregulation of the expression of these three PRRs in BEAS-2B cells and primary HBECs following RV-1B infection (Slater et al., 2010, Wang et al., 2009). Interestingly, TLR3 expression in MRC-5 fibroblasts was not affected by RV infection, whilst the cytosolic PRRs RIG-I and MDA5 expression were upregulated in this cell type, although to a lesser extent than that in BEAS-2B epithelial cells. However, additional experiments using a more sensitive technique such as qPCR are required to confirm these findings. The current data showing upregulation of RIG-I and MDA5, but not MAVS gene expression in BEAS-2B cells by RV is consistent with the results obtained using influenza A virus, which is also a common pathogenic respiratory virus (Le Goffic et al., 2007).

The results presented here show that in MRC-5 fibroblasts, RIG-I and MDA5 mRNA expression could be upregulated without concurrent TLR3 upregulation by RV infection, which are in contrast to the findings obtained by Slater and colleagues using primary HBECs (Slater et al., 2010). Slater and colleagues suggests that innate immune response in primary HBECs involves co-ordinated recognition of RV infection, initially via TLR3 and later via RLRs (Slater et al., 2010). The authors claimed that TLR3 is responsible for the initial recognition of RV dsRNA within primary bronchial epithelium, and that activation of the TLR3-mediated signalling pathway leads to the production of IFN and subsequently triggers RIG-I and MDA5 protein production. They demonstrated that siRNA specific for TLR3 reduced RV-1B-induced RIG-I and MDA5 gene expression. Although the current study

showed that RIG-I and MDA5 mRNA expression in MRC-5 fibroblasts was upregulated independently of TLR3 upregulation, further work is required to explore the expression of these intracellular RNA helicases at the protein level. Of relevance, Slater and co-workers demonstrated that although they detected basal mRNA expression of RIG-I and MDA5 in HBECs, both RIG-I and MDA5 proteins are not constitutively expressed in HBECs, and instead are virally-induced proteins (Slater et al., 2010).

Other distinct responses of MRC-5 fibroblasts and BEAS-2B epithelial cells to RV infection are the different levels of transcription factor IRF expression upon RV infection. IRFs are a family of transcription factors responsible for induction of type I and III IFN production (reviewed in Honda and Taniguchi, 2006). RV infection remarkably enhanced the expression of IRF1 mRNA in BEAS-2B cells, which is consistent with the results acquired by a study using qPCR (Zaheer and Proud, 2010). In keeping with the work conducted by Wang and colleagues using qPCR (Wang et al., 2009), RV also intensified the mRNA expression of IRF7 in BEAS-2B epithelial cells. This work is the first to demonstrate that RV did not modulate the expression of IRF1 and IRF3 mRNA in lung fibroblasts, whilst a very modest increase in IRF7 mRNA expression was observed in lung fibroblasts following RV-1B infection. Again, additional experiments using qPCR are required to validate these findings.

Collectively, the results discussed in this section indicate that in comparison to BEAS-2B bronchial epithelial cells, the lack of viral-detecting PRRs TLR3, RIG-I, MDA5 and virally-induced transcription factors IRF1 and IRF7 in MRC-5 fibroblasts may be a potential explanation as to why the fibroblasts did not secrete the IFN-stimulated cytokines CCL5 and CXCL10 (indicating that the RV-infected fibroblasts did not produce IFNs), therefore providing no antiviral response to limit viral replication, with concomitant cell death. The possible explanations for the lack of antiviral responses of lung fibroblasts to RV infection are discussed in greater details in the following section (Section 3.15.5).

3.15.5 The lack of antiviral responses of lung fibroblasts to RV infection

TLR3, RIG-I and MDA5 have been shown to be crucial in controlling RV replication, which is believed to be due to subsequent production of IFN-β following recognition of the RV by the three PRRs (Slater et al., 2010). Thus, the low expression of TLR3, RIG-I and MDA5 in MRC-5 fibroblasts may leave them highly susceptible to RV infection through their inability

to produce IFN-β. Indeed, pre-treatment with exogenous IFN-β protected primary fibroblasts from RV-induced cell death with concomitant reduction of viral replication (Bedke et al., 2009, Thomas et al., 2009).

IFNs play crucial roles in the antiviral innate immune response. There are three different types of IFNs: type I, II and III. Type I IFNs include IFN-α and IFN-β, type II IFN is represented by a single gene product, IFN-γ and type III IFNs include IFN-λ1, - λ2 and λ3 (reviewed in Trinchieri, 2010). Among all types of IFNs, type I IFNs are the best characterised. Upon viral infection, type I IFNs such as IFN-β and IFN-α are produced by the virally-infected cells. The newly secreted IFN-β and IFN-α then trigger expression of over 300 ISGs in neighbouring cells via binding to the cell surface receptors (IFNAR1/2) that eventually activates the Janus kinase (Jak)/signal transducer and activator of transcription (STAT) signalling pathways (Reviwed in Samuel, 2001, Grandvaux et al., 2002). The newly produced ISGs that have antiviral actions include protein kinase R (PKR) (inhibits mRNA translation and cell growth), the 2'-5'-oligoadenylate synthetase (OAS) (induces RNA degradation) and Mx protein GTPase (inhibits viral nucleocapsid transport and viral RNA synthesis) (reviewed in Grandvaux et al., 2002, Trinchieri, 2010).

Production of type I IFNs is mainly controlled at the gene transcriptional level where members of the IRF family of transcription factors act as major regulators of the type I IFN gene expression (reviewed in Honda and Taniguchi, 2006). Among nine members of IRF family, IRF3 and IRF7 are believed to be the key regulators of virally-induced type I IFN production. IRF3, which is constitutively expressed in most cells, is responsible for the initial induction of IFN-β and IFN-α production by the virally-infected cells. The newly produced IFN-β and IFN-α then exert a positive feedback loop by inducing the transcription of IRF7 (therefore IRF7 itself is an ISG) via Jak/STAT signalling pathways, in which activated IRF7 is responsible for further amplification of type I IFN production (reviewed in Grandvaux et al., 2002, Erickson and Gale, 2008). IRF7 has been shown to be important for the transcription of IFN-α and IFN-β, which then induce production of IFN-stimulated genes including CCL5 and CXCL10 (Wang et al., 2009, Honda et al., 2005). CCL5 is a chemoattractant of eosinophils and T cells whilst CXCL10 is a chemokine responsible for recruitment of monocytes and T cells (reviewed in Smith et al., 1997).

In addition to IRF3 and IRF7, IRF1 is another important transcription factor for IFN generation (reviewed in Ozato et al., 2007). Of relevance to the current study, RV-induced

production of CXCL10 in primary HBECs has been shown to be dependent upon IRF1 (Zaheer and Proud, 2010). Furthermore, Matsuzaki *et al.* demonstrated that IRF1 was required for the IFN-γ- and TNFα-induced CCL5 release from primary HBECs (Matsuzaki et al., 2010). The current work revealed that whilst IRF1 and IRF7 mRNA expression was dramatically enhanced in BEAS-2B epithelial cells by RV infection, no change of IRF1 and IRF7 expression was seen in RV-infected MRC-5 fibroblasts. Therefore, it is likely that the inability of lung fibroblasts to produce IFNs in response to RV infection is due to the low basal and RV-induced expression of IRF1 and IRF7 in this cell type.

The mechanisms underlying the low expression of IRF1 and IRF7 mRNA in fibroblasts warrant further investigations. One potential explanation is the fact that IRF genes are acetylated, resulting in an alteration in DNA binding and transcriptional activities (reviewed in Ozato et al., 2007). Furthermore, Cho *et al.* has demonstrated that the differential permissivity to viral replication between two subtypes of neurons (i.e. granule cell neurons and cortical neurons) was due to the distinct innate immune programs elicited by the two cell types (Cho et al., 2013). They proposed that the differential antiviral programs observed between granule cell neurons and cortical neurons might be due to the differences in the epigenetic state of key antiviral genes, which are influenced by the expression of specific microRNA (miRNAs). Specifically, they discovered that in comparison to granule cell neurons, cortical neurons (which were more permissive to viral replication) expressed higher level of miR-132 (an miRNA that targets the p300 coactivator of Stat1, a vital transcription factor of IFN) (Cho et al., 2013). Taking this idea into consideration, further work should be done to determine whether lung fibroblasts and airway epithelial cells express different levels of specific miRNAs that control expression of ISGs including IRF7.

3.15.6 IL-1β potentiates epithelial cell responses to RV infection

Our group has previously reported that the direct addition of IL-1β amplifies cytokine responses to poly(I:C) in airway epithelial cells (Morris et al., 2006). As discussed in Section 3.15.2, one of the aims of this study was to determine if IL-1β could enhance proinflammatory responses of RV-infected structural airway cells. It was discovered that exogenous IL-1β could synergistically augment the RV-induced CXCL8 production in airway epithelial cells, but not in lung fibroblasts. This might be due to the fact that IL-1β

alone induced a high level of CXCL8 production in fibroblasts, and if the CXCL8 release had reach its maximal level, the potentiating actions of IL-1β on CXCL8 generation may be compromised. Additional experiments using lower concentrations of IL-1β are required to test this speculation, and if negative results are obtained, this would imply that the ability of IL-1β to augment the inflammatory responses of RV-infected cells is cell type-dependent. It is important to note that the presence of IL-1β did not affect viral replication and cell death of virally-infected cells. This therefore excludes the possibility that perhaps the higher CXCL8 release observed was due to the 'protective' effect of IL-1β on the RV-infected cells, hence providing more viable cells to secrete cytokines. The mechanisms underlying the synergistic intensifying effect of IL-1β on the RV-induced CXCL8 production in BEAS-2B epithelial cells remain to be examined.

Intriguingly, in contrast to its effect on CXCL8 generation, IL-1β modestly inhibited CCL5 release from the RV-infected BEAS-2B cells. To partly explain this current finding, a previous study done by Siednienko and colleagues revealed that MyD88, an important signalling adaptor for IL-1β (Section 1.5.1), negatively regulates TLR3-induced IRF3 activation, subsequently limiting IFN-β and CCL5 production (Siednienko et al., 2011). They demonstrated that inhibition of MyD88 using either MyD88 inhibitory peptides or MyD88 endoribonuclease-prepared siRNAs (esiRNAs) substantially increased RV-1B- and RV-16-induced IFN-β and CCL5 gene induction, without affecting virally-induced TNF-α expression, in BEAS-2B cells. Subsequently, using HEK293 cells (a human embryonic kidney cell line), they showed that the mechanism by which MyD88 downregulates type I IFN production is by specifically inhibiting IKKε-, but not TBK1-, mediated phosphorylation of IRF3 (Siednienko et al., 2011).

3.15.7 Coinfection with RV and bacterial LPS potentiates epithelial cell proinflammatory responses

Coinfections with viral and bacterial pathogens are common within the airways of asthmatic and COPD patients (Wilkinson et al., 2006, Louie et al., 2009). Using *in vitro* models of tissue inflammation, this study aimed to explore the cellular and cytokine networks that underpin these exacerbations of airways diseases caused by multiple pathogenic infections. Our group has previously shown that costimulation with poly(I:C) and LPS enhanced CXCL8

release by BEAS-2B cells in the presence of PBMCs (Morris et al., 2006). Consistent with this, the present study demonstrates for the first time that RV-1B and bacterial-derived LPS could synergistically accentuate CXCL8 production in BEAS-2B cells, with this synergistic effect again hypothesised to be due to IL-1β generation by LPS-activated monocytes (Morris et al., 2005, Chaudhuri et al., 2010). It is important to note that CXCL8 protein was undetectable when the single-culture of monocytes was stimulated with LPS (data not shown). Interestingly, monocytes alone did not modulate cytokine release by the RV-1B-infected BEAS-2B cells. One possible explanation is that although RV could enter monocytes which express RV receptors, viral replication did not take place (Gern et al., 1996). In relevance to asthma and COPD, the dramatic increase of proinflammatory cytokine CXCL8 by coinfection with viral and bacterial pathogens may explain the acute exacerbations of asthma and COPD patients when coinfected with viral and bacterial pathogens. The current results provides further evidence of our group's previous findings (Chaudhuri et al., 2010, Morris et al., 2006, Morris et al., 2005) that cooperative signalling between airway tissue cells and infiltrating leukocytes is crucial for the effective CXCL8 release, subsequently leading to neutrophilic inflammation in the airways.

3.15.8 Conclusions and future work

The results presented in this chapter demonstrate that RV infection induces differential responses in normal human airway fibroblasts and epithelial cells. In comparison to airway epithelial cells, the lack of viral-detecting PRRs TLR3, RIG-I, MDA5 and virally-induced transcription factors IRF1 and IRF7 in fibroblasts may be a potential explanation as to why the fibroblasts do not secrete the IFN-stimulated cytokines CCL5 and CXCL10 (indicating that the RV-infected fibroblasts do not produce IFNs), therefore providing no antiviral response to limit viral replication, with concomitant cell death. The data shown in this chapter also show the permissiveness of lung fibroblasts isolated from IPF patients to RV infection. This study also reveals for the first time the ability of IL-1β to enhance proinflammatory responses of RV-1B-infected epithelial cells. Furthermore, the work presented in this chapter demonstrate that in the presence of monocytes, RV and bacterial-derived LPS coinfections can act in synergy to amplify the proinflammatory responses of airway tissue cells.

As discussed in Section 3.15.2, HMGB1 has been shown to be amplified in the BALF of COPD patients and this cell damage product has the capacity to potentiate inflammation. Therefore, it would be interesting to determine the potential release of HMGB1 by RV-infected fibroblasts by ELISA. If positive results are obtained, this will further support the ability of RV-infected fibroblasts to amplify airway inflammation, independent of cytokine-mediated inflammation.

In this chapter, using semi-quantitative end-point PCR it has been demonstrated that the mRNA expression profiles of viral RNA detecting-PRRs and key signalling molecules involved in viral recognition and the downstream production of IFNs can be regulated by RV infection (Section 3.7, 3.8). However, these findings need to be confirmed using a more sensitive technique such as real-time qPCR. Moreover, it would be necessary to quantify protein expression of the relevant molecules by western blotting.

The mechanisms leaving fibroblasts more susceptible to RV infection, as compared to epithelial cells, require further study. As discussed in Section 3.15.5, IRF7 is a key regulator of type I IFN production and its role in controlling viral replication and modulating cytokine release in BEAS-2B and MRC-5 cells could be explored further using siRNA to reduce IRF7 levels in epithelial cells or overexpression techniques to increase IRF7 levels in fibroblasts. Furthermore, further study should be done to determine whether specific miRNAs that control ISG expression are differentially expressed in airway fibroblasts and epithelial cells. Another work that should be done to further explain the greater permissiveness of lung fibroblasts to RV replication compared to airway epithelial cells (apart from the inability of fibroblasts to produce antiviral cytokines to control viral replication), is to simply determine whether fibroblasts express higher levels of RV cellular receptors than epithelial cells that may result in higher infectivity rates in this cell type.

To explore the cellular networking and cellular responses of epithelial cells and fibroblasts in close contact, as would occur in lung, BEAS-2B/MRC-5 coculture model could be developed to investigate the cooperative responses of both airway epithelial cells and fibroblasts to RV infection. It is plausible that RV-infected BEAS-2B cells would signal the neighbouring fibroblasts to generate more cytokine responses thus aggravating the RV-triggered inflammation. Or perhaps if RVs pass through the epithelial cell layer to infect the adjacent fibroblasts, more viral replication would occur within fibroblasts, hence producing more viruses to further infect the epithelial cells. It is also feasible that the pathogenic effects of

RV on fibroblasts would release cell damage product such as HMGB1 that could elevate inflammatory responses of epithelial cells. Additionally, potential modification of the tissue cell responses to RV infection by innate immune cells (e.g. monocytes and macrophages) remains to be investigated. For this purpose, innate immune cells such as macrophages should be added to the BEAS-2B/MRC-5 cocultures.

Chapter 4: Results. Phosphoinositide 3-kinase, but not autophagy, inhibition modulates responses of human bronchial epithelial cells to RV infection

4.1 Introduction

As discussed in Chapter 3 (Section 3.15), the first line of immune defence against RV infection is the recognition of RV by the endosomal pattern recognition receptor TLR3, consequently inducing the generation of type I IFNs and proinflammatory cytokines. Activation of the TLR3 signaling pathway also triggers production of cytoplasmic pattern recognition receptors RIG-I and MDA5, which are responsible for recognising RV in the cytosol (Slater et al., 2010), subsequently amplifying the cellular responses to control viral replication. RV infection has also been shown to activate phosphoinositide 3-kinase (PI3K) signalling (Lau et al., 2008, Newcomb et al., 2005) (Section 1.9), although the relative role of each class of PI3K in modulating responses to RV remains to be clarified.

After entering the host cells via endocytosis, RVs then release their ssRNA genomes into the cytoplasm where viral protein synthesis and RNA replication occur (Section 1.3.2). TLR3 detects dsRNA, generated during RV replication (Wang et al., 2009, Slater et al., 2010). However, the mechanisms by which cytoplasmic dsRNA reaches the endosome are poorly understood. Macroautophagy (referred to herein as autophagy) is a PI3K-dependent pathway that involves sequestration of cytosolic damaged organelles and unused proteins in double-membrane vesicles termed autophagosomes, and the autophagic cargo is later delivered to lysosomes for degradation and recycling of amino acid pools (reviewed in Codogno et al., 2012) (Section 1.8). Autophagy is principally used as cellular adaptation to a variety of stress conditions, such as nutrient starvation, thus contributing to cell survival; although it may also be involved in the cell death pathway (reviewed in Richetta and Faure, 2013, Patel et al., 2013). Beyond its role in cellular homeostasis, autophagy has also been proposed as one of the mechanisms by which the host cells defend against microbial infections including viruses (reviewed in Yordy et al., 2012) (Section 1.8.2). Autophagy participates in antiviral innate immunity via multiple mechanisms such as by directly entrapping and degrading virions and virion components (a process termed xenophagy), and by mediating the detection of cytosolic

viral RNAs by endosomal TLRs (reviewed in Deretic et al., 2013, Jordan and Randall, 2011). In VSV infection, the production of antiviral IFN-α by murine plasmacytoid DCs was found to be dependent upon the autophagic delivery of viral replication intermediates to endosomal TLR7 (Lee et al., 2007). Similarly, Manuse and colleagues demonstrated that TLR7-dependent secretion of IFN-α by simian virus 5 (SV5) in human plasmacytoid DCs was dependent on autophagy (Manuse et al., 2010). More recently, Zhou *et al.* have shown that TLR7-dependent IFN-α production requires autophagy in human plasmacytoid DCs following infection with HIV-1 (Zhou et al., 2012). However, whether autophagy is necessary for the delivery of cytoplasmic dsRNA intermediates to TLR3-containing endosomes remains unknown.

Whilst there are no studies to date specifically exploring the roles of autophagy in the induction of inflammatory responses to RV infection, several studies have reported the requirement for autophagy in RV replication, although this remains controversial. In their studies of RV-2 (a minor group RV serotype), Brabec-Zaruba *et al.* showed that this particular serotype of RV does not induce autophagy and that modulation of autophagy does not affect viral replication (Brabec-Zaruba et al., 2007). In contrast, another group has demonstrated that RV-2 and RV-14 (a major group RV serotype) induce autophagosome formation and that both RV serotypes exploit the autophagy machinery to promote their replication (Klein and Jackson, 2011, Jackson et al., 2005). However, all these published studies were performed using HeLa cells, a human cervical epithelial cell line, and since RV is a natural respiratory tract pathogen, it would be of greater relevance to explore the roles of autophagy in RV infection of airway cells. Furthermore, autophagy has recently been shown to participate in the regulation of the proinflammatory cytokine IL-1β processing and secretion (Dupont et al., 2011, Harris et al., 2011) and our group has recently demonstrated that IL-1β signalling plays a pivotal role in modulating inflammatory responses of airway epithelial cells to RV infection (Stokes et al., 2011).

4.2 Hypothesis and Aims

It was hypothesised that autophagy is required for the presentation of cytoplasmic RV dsRNA to the TLR3-containing endosomes, and therefore plays a role in RV-induced innate

immune responses (See Figure 4.0 for the proposed model of autophagy-mediated RV recognition by endosomal TLR3).

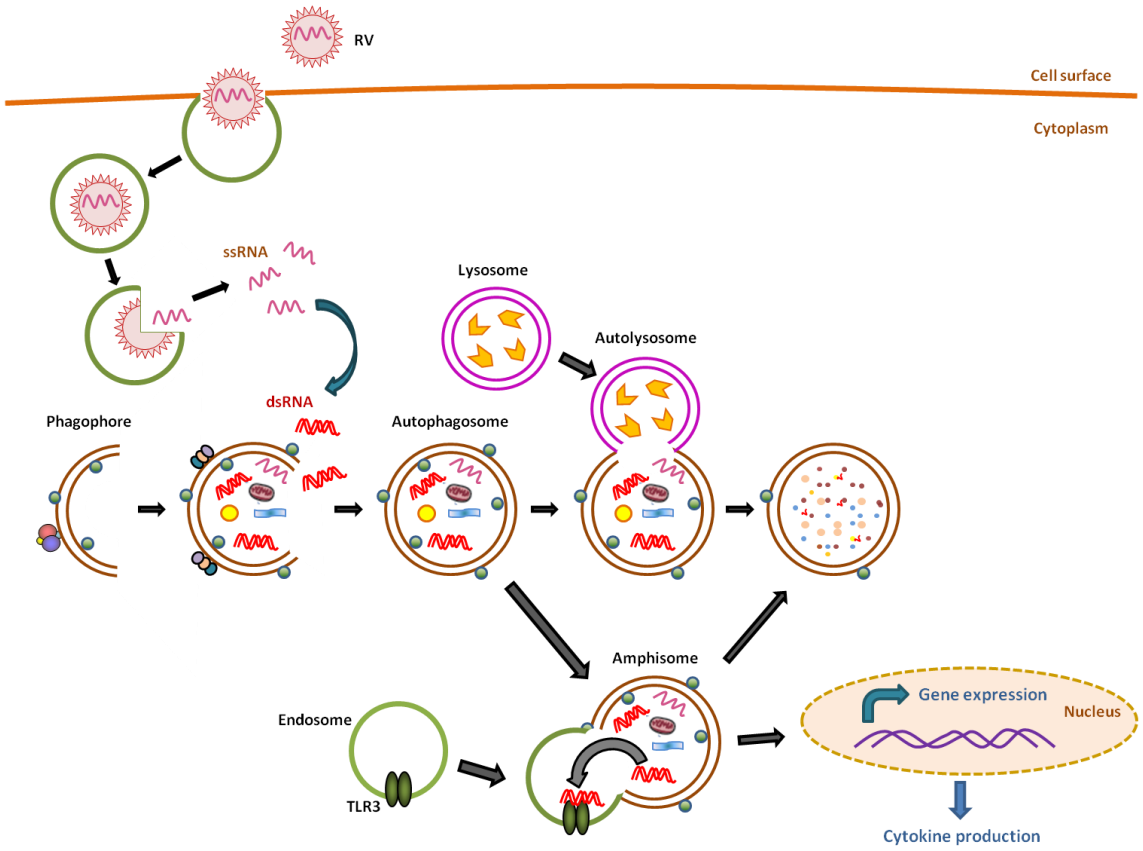

Figure 4.0 Proposed model of autophagy-mediated RV recognition by endosomal TLR3.
RVs enter host cells via endocytosis, and ssRNA genome is then released into the cytoplasm where viral replication occurs. The newly formed replication intermediate dsRNA located in the cytosol can be engulfed by phagophore and captured in autophagosome. Apart from lysosome, autophagosome can also fuse with TLR-containing endosome, forming an amphisome. Autophagosome presents the RV dsRNA to the endosomal TLR3, and thus initiating the downstream signalling of cytokine production. The viral products are subsequently delivered to the autolysosome for degradation. (See List of Abbreviations for the abbreviations used in this figure legend.)

The specific aims of this chapter were to investigate:

1. The potential role of autophagy in mediating the innate immune responses of structural airway cells to RV infection.
2. The extent to which the innate immune responses to RV were dependent upon PI3K signalling.
3. Whether autophagy and PI3K pathways are involved in the control of RV replication.

4.3 Effect of 3-MA (commonly used to inhibit autophagy) on responses of airway epithelial (BEAS-2B) cells or airway fibroblast (MRC-5) cells to RV infection or poly(I:C) stimulation

4.3.1 3-MA inhibits proinflammatory cytokine production induced by RV infection or poly(I:C) stimulation

To explore the potential role of autophagy in regulating the inflammatory responses of structural airway cells to RV infection, 3-methyladenine (3-MA), a pharmacological class III PI3K inhibitor commonly used to inhibit autophagy (Wong et al., 2008, Brabec-Zaruba et al., 2007, Jackson et al., 2005), was utilised. Whether 3-MA could inhibit cytokine production in response to the viral dsRNA mimic poly(I:C) and to the proinflammatory cytokine IL-1β was also examined. Bronchial epithelial (BEAS-2B) cells or lung fibroblast (MRC-5) cells were left uninfected (media control), infected with RV-1B or RV-16 at $1x10^7$ $TCID_{50}$/ml (MOI ~3) for 1 h as described in Section 2.6.3; or stimulated with poly(I:C) (1 μg/ml) or IL-1β (1 ng/ml). Cells were then immediately treated with 3-MA (1 or 10 mM) and cultured for 24 h. Cell-free supernatants were collected to determine cytokine release, as measured by ELISA (Section 2.15). Cells were also lysed, total RNA extracted, cDNA synthesised and real-time qPCR for IFN-β performed (Section 2.16-2.18). Samples were quantified against a standard curve of plasmids containing IFN-β target sequence.

3-MA treatment at both lower (1 mM) and higher (10 mM) tested concentrations significantly inhibited the generation of antiviral cytokines IFN-β and CCL5 in BEAS-2B epithelial cells, in response to RV-1B, RV-16 or poly(I:C) (Figure 4.1B, C, E, F). For example, induction of CCL5 or IFN-β was substantially decreased (by ~75% or 55%, respectively) in cells cotreated with RV-1B and 3-MA (1 mM), in comparison with RV-1B alone (Figure 4.1B). The inhibitory effect of 3-MA was less potent on CXCL8 production, as only the higher dose of 3-MA resulted in a significant reduction of this cytokine, following RV infection or poly(I:C) stimulation (Figure 4.1A, D). However, the higher concentration of 3-MA also reduced IL-1β-induced CXCL8 production in BEAS-2B cells, suggesting that 3-MA may exhibit off-target actions at the frequently exploited concentration of 10 mM (Figure 4.1D).

In contrast to the results obtained using BEAS-2B cells, 1 mM of 3-MA treatment did not inhibit CXCL8 release from MRC-5 fibroblasts, in response to RV infection or poly(I:C) stimulation (Figure 4.2). 1 mM of 3-MA caused an increase of CXCL8 production in RV-

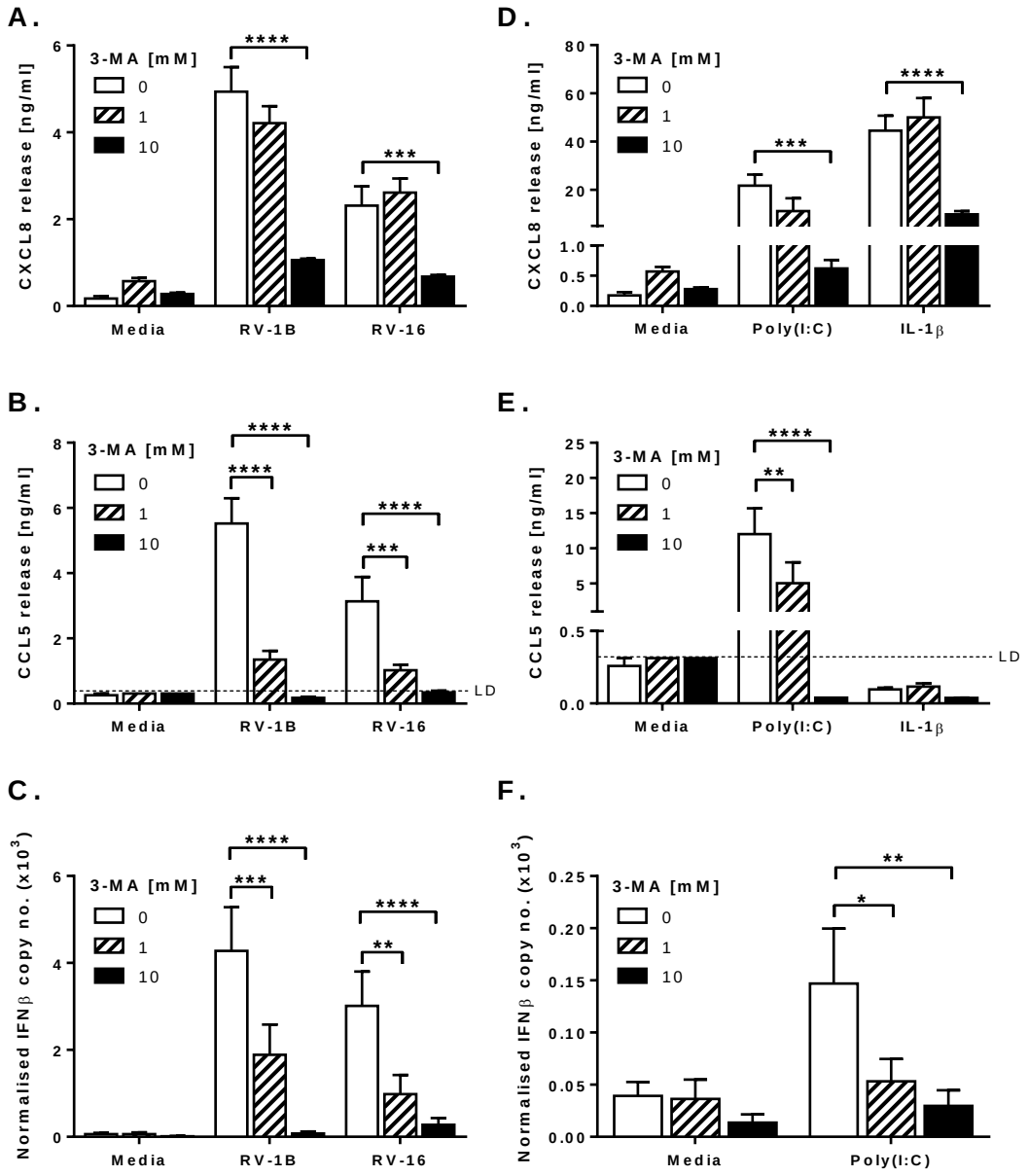

Figure 4. 1 3-MA inhibits RV- or poly(I:C)-induced proinflammatory cytokine production in BEAS-2B cells.

BEAS-2B cells were infected with RV-1B or RV-16 at $1x10^7$ $TCID_{50}$/ml for 1 h (following which supernatants were replaced with media) (A, B, C); or stimulated with poly(I:C) (1 µg/ml) or IL-1β (1 ng/ml) (D, E, F). Cells were then immediately treated with 3-MA at the indicated concentrations and cultured for 24 h. Cell-free supernatants were collected, and CXCL8 (A, D) and CCL5 (B, E) release was measured by ELISA. RNA was extracted and reverse transcribed for qPCR analysis of IFN-β mRNA expression (C, F), with IFNβ copy number normalized to the GAPDH copy number as a loading control. Data shown are mean ± SEM of $n = 5$ independent experiments. Significant differences are indicated by *, $p < 0.05$; **, $p < 0.01$; ***, $p < 0.001$ and ****, $p < 0.0001$, analysed by two-way ANOVA with Bonferroni's post-test. Media controls shown on the left and right panel sets are the same. LD = limit of detection.

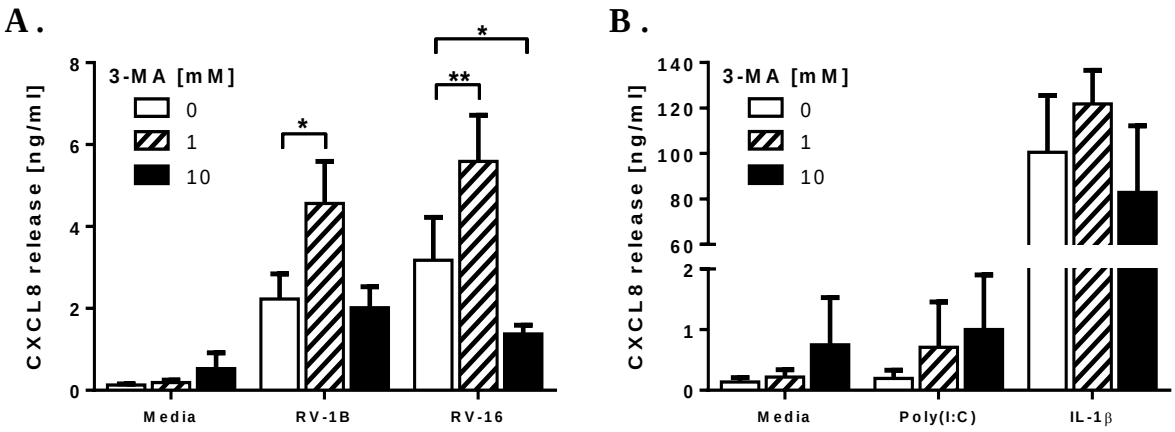

Figure 4. 2 3-MA does not show inhibition of RV-induced proinflammatory cytokine production in MRC-5 cells, which may be associated with cell viability.

MRC-5 cells were infected with RV-1B or RV-16 at $1x10^7$ $TCID_{50}$/ml for 1 h (following which supernatants were replaced with media) (A); or stimulated with poly(I:C) (1 μg/ml) or IL-1β (1 ng/ml) (B). Cells were then immediately treated with 3-MA at the indicated concentrations and cultured for 24 h. Cell-free supernatants were collected, and CXCL8 release was measured by ELISA. Data shown are mean ± SEM of $n = 3$ (A) or mean ± SD of $n = 2$ (B) independent experiments. Significant differences are indicated by *, $p < 0.05$ and **, $p < 0.01$, analysed by two-way ANOVA with Bonferroni's post-test. Media controls shown on the left and right panel sets are the same.

infected MRC-5 cells (Figure 4.2A), although this might be associated with the viability of the cells (described further in Section 4.3.2). As described in Chapter 3, IFN-β or CCL5 generation was undetectable in MRC-5 cells, following RV infection or poly(I:C) stimulation (data not shown).

4.3.2 3-MA does not increase the cell death of RV-infected cells

As 3-MA inhibits cytokine production in response to RV and poly(I:C) (Section 4.3.1), confirmation was sought that this effect was not due to 3-MA causing cell death, hence reducing the number of cells that remained alive to produce cytokines. Levels of cell death were initially determined by microscopic observation. BEAS-2B epithelial cells or MRC-5 fibroblasts were left uninfected or infected with RV-1B or RV-16 at $1x10^7$ $TCID_{50}$/ml as described in Section 2.6.3. Cells were then immediately treated with 3-MA (1 or 10 mM) and cultured for 24 h.

The higher tested concentration of 3-MA (10 mM) alone induced a slight toxicity to both MRC-5 cells (Figure 4.3) and BEAS-2B cells (images not taken), as the cells appeared smaller in size. Interestingly, 3-MA reduced the RV-induced cytopathic cell death in MRC-5 cells, in a dose-dependent manner (Figure 4.3). For example, at $1.0x10^7$ $TCID_{50}$/ml, RV-1B alone resulted in ~50% rounded/detaching cells. However, in the presence of 1 mM or 10 mM of 3-MA, RV-1B-induced cell death was decreased to only ~30% or 15%, respectively (Figure 4.3). The same reductions were observed when RV-16-infected cells were cotreated with 3-MA (Figure 4.3).

To quantify the cell death observed in 3-MA-treated cells, the LDH cytotoxic assay (Section 2.20) was utilised. The higher tested concentration of 3-MA induced significant (~8%) cell death in BEAS-2B epithelial cells when added alone, but did not measurably increase epithelial cell death beyond that caused by RV infection alone (Figure 4.4A). In keeping with the microscopic observations (Figure 4.3), 10 mM of 3-MA alone caused an increased level of cell death (~10%) in MRC-5 fibroblasts compared to control cells (Figure 4.4B) and reduced the percentage of RV-induced cell death in MRC-5 cells in a dose-dependent pattern (Figure 4.4B) as determined by LDH cytotoxic assay, although to a lesser extent than what was observed microscopically (Figure 4.3).

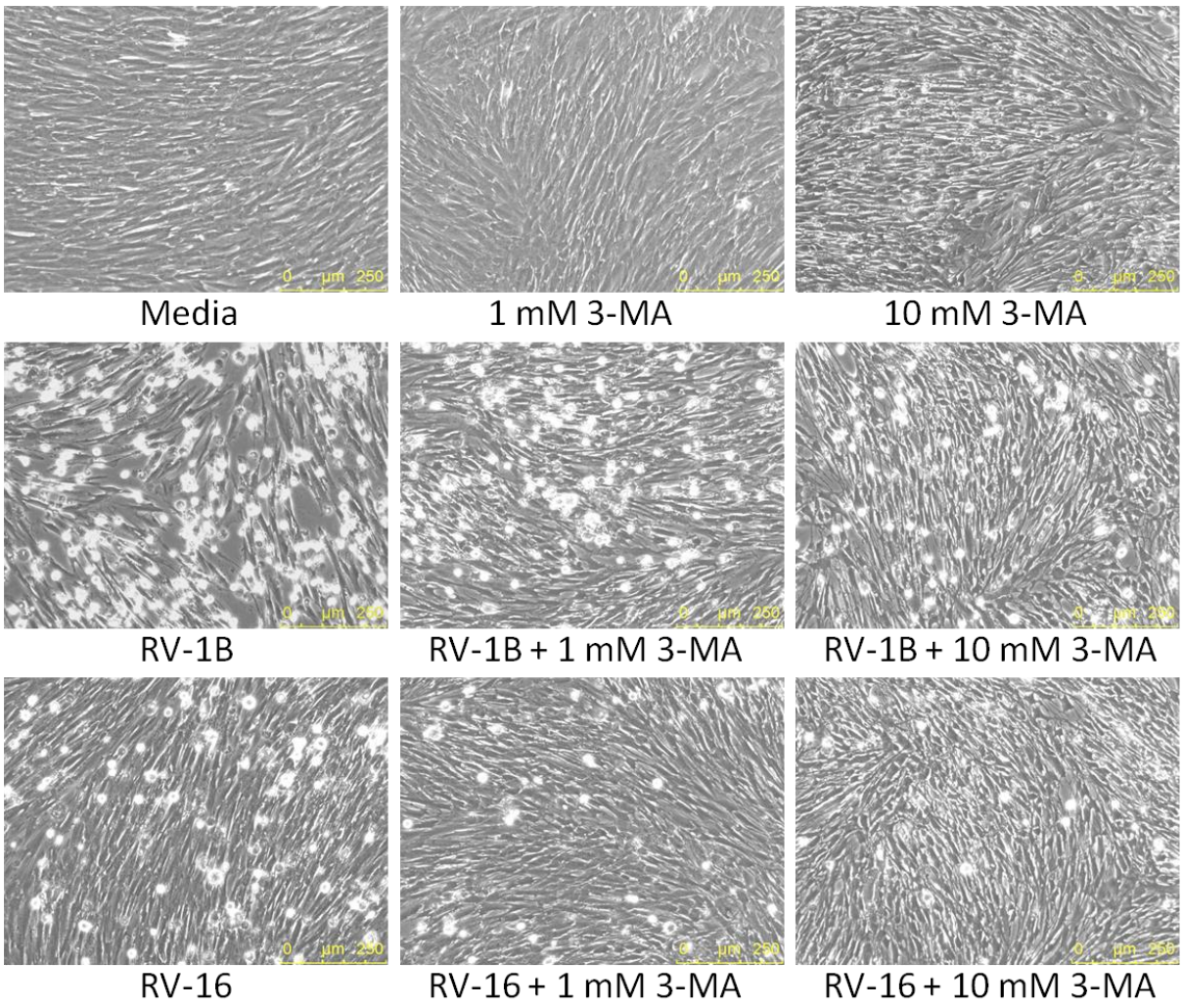

Figure 4. 3 3-MA reduces RV-induced cell death in MRC-5 cells.

MRC-5 cells were infected with RV-1B or RV-16 at $1x10^7$ $TCID_{50}$/ml for 1 h (following which supernatants were replaced with media). Cells were then immediately treated with 3-MA at the indicated concentrations. After 24 h, cell monolayers were observed using a fluorescence and phase contrast Leica DM14000B inverted microscope at 10x magnification. Data shown are representative images of $n = 3$ independent experiments.

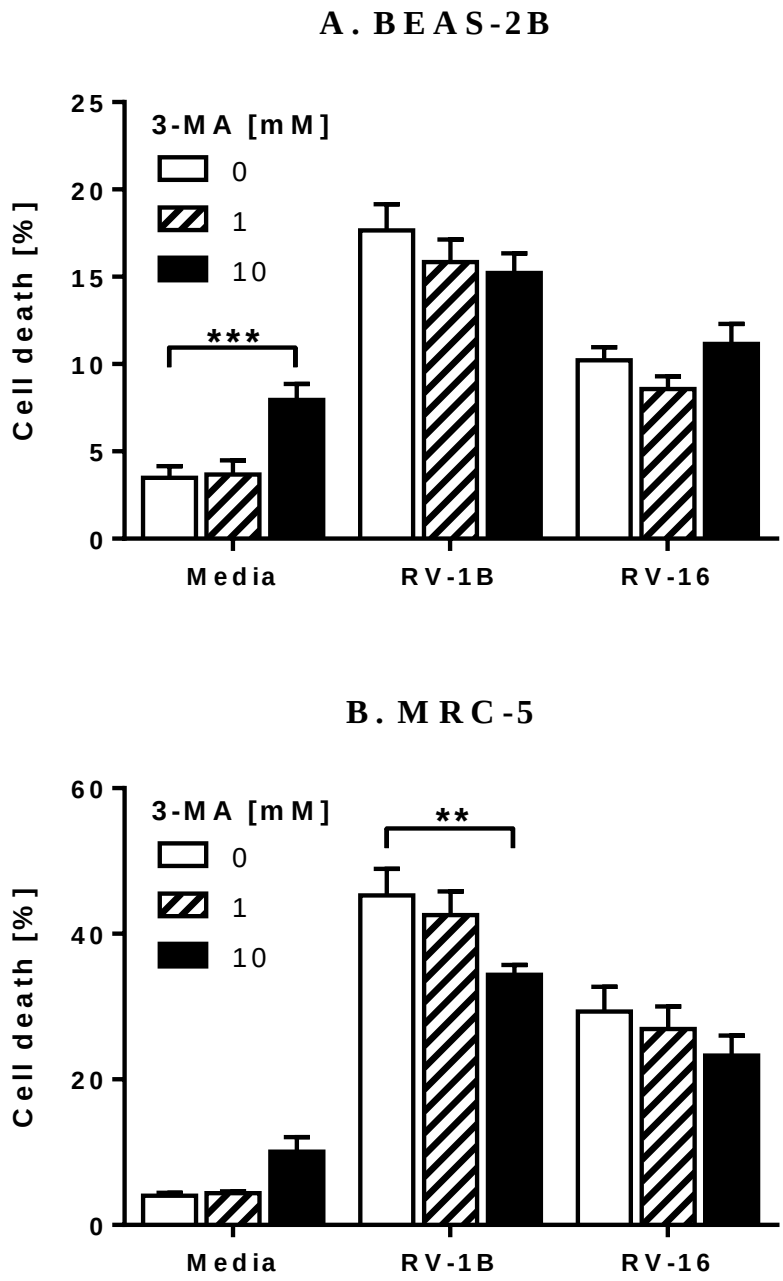

Figure 4. 4 3-MA does not increase the cell death of RV-infected cells.
BEAS-2B (A) or MRC-5 (B) cells were infected with RV-1B or RV-16 at $1x10^7$ $TCID_{50}$/ml for 1 h (following which supernatants were replaced with media). Cells were then immediately treated with 3-MA at the indicated concentrations and cultured for 24 h. Percentage of cell death was measured by LDH assay. Data shown are mean ± SEM of $n = 4$ (A) or $n = 3$ (B) independent experiments. Significant differences are indicated by **, $p < 0.01$ and ***, $p < 0.001$, analysed by two-way ANOVA with Bonferroni's post-test.

4.3.3 3-MA inhibits viral replication

Viruses replicate within the host cells, producing newly synthesised virions that are released through host cell lysis. Having found that 3-MA could reduce RV-induced cytopathic cell death, particularly in MRC-5 fibroblasts (Figure 4.3), it was hypothesised that this may be due to the potential capability of 3-MA to inhibit viral replication. To test this hypothesis, cells were infected with RV and then treated with 3-MA as described in Section 4.3.2. At 24 h p.i., BEAS-2B cells (~$6.1x10^5$) and MRC-5 cells (~$5x10^5$) were lysed, cDNA synthesised and real-time qPCR for RV performed (Section 2.16-2.18). Samples were quantified against a standard curve of plasmids containing RV target sequence.

3-MA significantly inhibited the production of RV-1B in both BEAS-2B epithelial cells and MRC-5 fibroblasts, in a concentration-dependent manner (Figure 4.5). For example, the lower concentration of 3-MA (1 mM) caused a marked reduction of the intracellular RV-1B copies by ~40% in BEAS-2B cells (Figure 4.5A) and~65% in MRC-5 cells (Figure 4.5B). Interestingly, the inhibitory actions of 3-MA was less potent on RV-16 replication, as the 1 mM of 3-MA had no or very modest effects on the production of RV-16 (Figure 4.5).

4.3.4 Low doses of 3-MA inhibit cytokine production induced by poly(I:C)

Having observed that 3-MA could impede viral replication (Section 4.3.3), it was possible that the inhibitory effect of 3-MA on RV-induced cytokine production in BEAS-2B cells (Figure 4.1A-C) was due to a reduction in the viral dsRNA replicates responsible for triggering this response. However, the ability of 3-MA (at 1 mM, a concentration that did not cause toxicity to the cells) to inhibit cytokine generation induced by the synthetic dsRNA mimic poly(I:C) (Figure 4.1D-F) suggests that the mechanisms of action of 3-MA on cytokine generation were independent of viral replication. However, this conclusion was only drawn based on a single concentration of poly(I:C) (1 μg/ml). A pilot experiment was then performed to see if the inhibitory actions of 3-MA on poly(I:C)-induced cytokine production could still be seen when lower concentrations of 3-MA are used. Cells were stimulated with poly(I:C) at 1, 10 or 100 μg/ml, and were then immediately treated with a range of concentrations of 3-MA starting from 0.25 mM to 2. After 24 h, cell-free supernatants were collected to determine cytokine release, as measured by ELISA (Section 2.15).

Based on a single experiment, the low concentrations of 3-MA (0.25 to 2 mM) inhibited poly(I:C)-induced CCL5 (Figure 4.6B), but not CXCL8 (Figure 4.6A), release from BEAS-

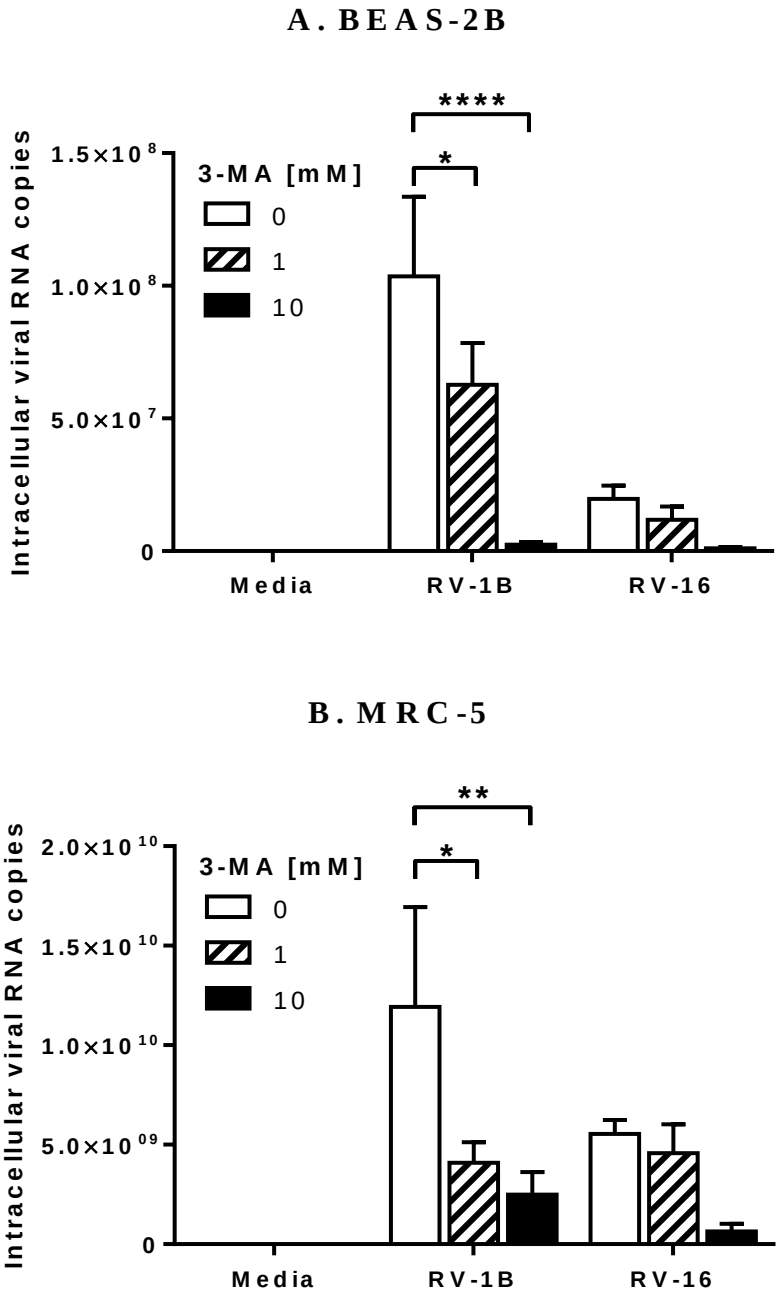

Figure 4. 5 3-MA inhibits viral replication.

BEAS-2B (A) or MRC-5 (B) cells were infected with RV-1B or RV-16 at $1x10^7$ $TCID_{50}$/ml for 1 h (following which supernatants were replaced with media), and were then immediately treated with 3-MA at the indicated concentrations and cultured for 24 h. RNA was extracted and reverse transcribed for qPCR analysis of RV RNA expression, with data presented as the total intracellular viral RNA copies per well. Data shown are mean ± SEM of $n = 4$ (A) or $n = 3$ (B) independent experiments. Significant differences are indicated by *, $p < 0.05$; **, $p < 0.01$ and ****, $p < 0.0001$, analysed by two-way ANOVA with Bonferroni's post-test.

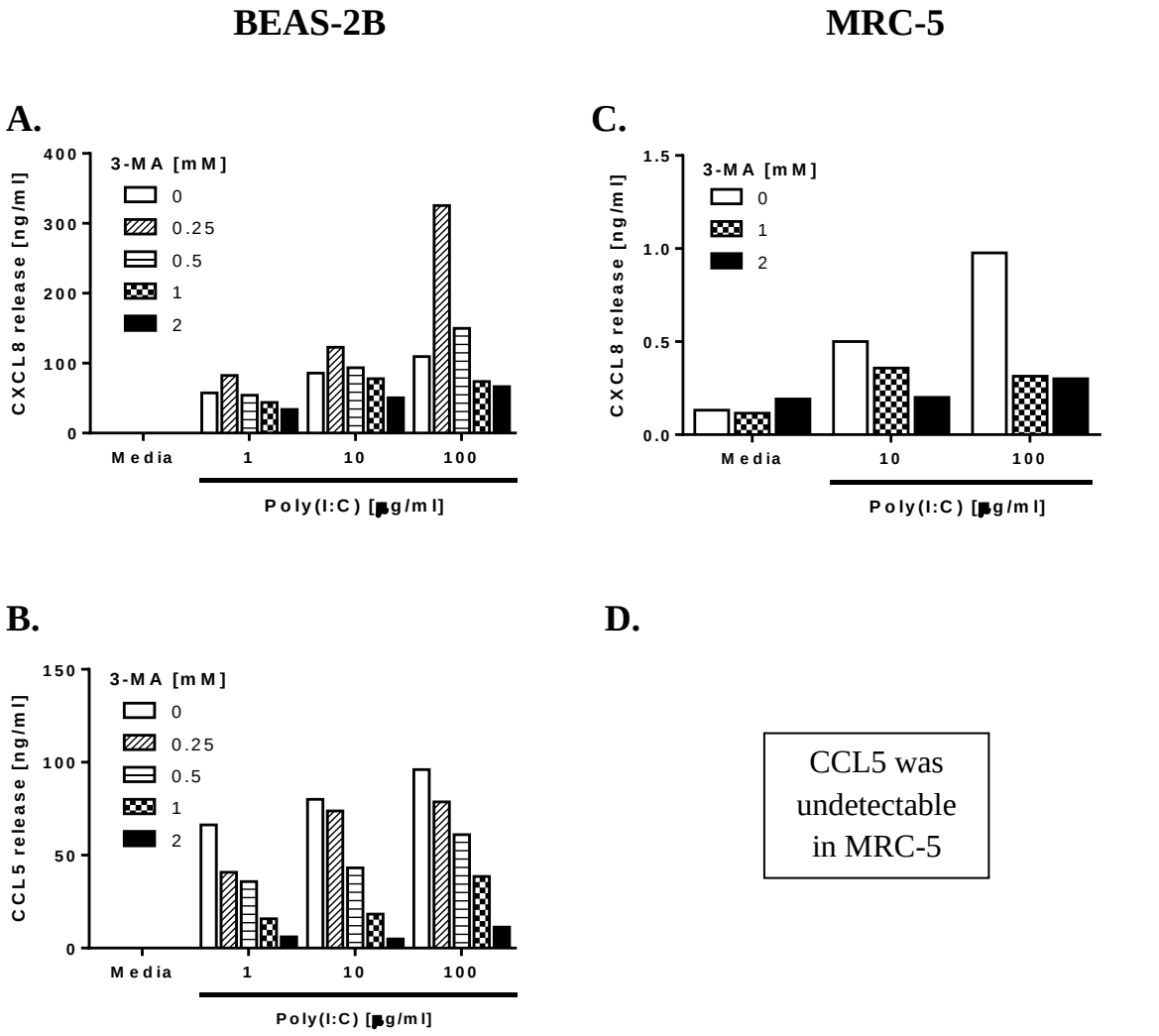

Figure 4. 6 Low doses of 3-MA inhibit cytokine production induced by poly(I:C). BEAS-2B (A, B) or MRC-5 (C, D) cells were stimulated with poly(I:C) at the indicated concentrations, and were then immediately treated with 3-MA at the indicated concentrations and cultured for 24 h. Cell-free supernatants were collected, and CXCL8 (A, C) and CCL5 (B, D) release was measured by ELISA. Data shown are $n = 1$.

2B cells in a concentration-dependent manner. Importantly, the 2 mM of 3-MA (a concentration of 3-MA that did not cause toxicity to the cells, as observed microscopically; images not taken) markedly decreased CCL5 production in BEAS-2B cells by at least 90%, in response to all three concentrations of poly(I:C) used (Figure 4.6B). Interestingly, the lowest concentration of 3-MA utilised (0.25 mM) resulted in an increase of CXLC8 generation in poly(I:C)-stimulated BEAS-2B cells (Figure 4.6A). Both 1 and 2 mM of 3-MA measurably reduced CXCL8 generation in poly(I:C)-stimulated MRC-5 fibroblasts (Figure 4.6C), although the amounts of CXCL8 release by MRC-5 cells (Figure 4.6C) were much lower compared to BEAS-2B epithelial cells (Figure 4.6A).

4.3.5 3-MA does not inhibit cytokine production induced by TNFα, IL-6 or IFN-β

Since 1 mM of 3-MA inhibited cytokine generation induced by RV infection or poly(I:C), but not IL-1β (Section 4.3.1, 4.3.2, 4.3.4), the inhibitory effect of 3-MA on cytokine production may be specific to pathways that require TLR3 signalling. To test this hypothesis, further experiments were performed using TNFα, IL-6 and IFN-β, all of which do not require TLR3 activation to signal.

BEAS-2B or MRC-5 cells were stimulated with IL-6 (50 ng/ml), TNFα (20 ng/ml), IFN-β (20 ng/ml) or TNFα/IFN-β in combination (concentrations of these stimuli were chosen based on concentration-response data previously obtained by our senior lab technician, Dr. Linda Kay). Cells were then immediately treated with 3-MA at 1 mM and cultured for 24 h. Cell-free supernatants were collected to determine cytokine release, as measured by ELISA (Section 2.15).

In contrast to the results obtained when cells were stimulated with TLR3 ligands (i.e. RV and poly(I:C) (Section 4.3.1, 4.3.4)), 3-MA treatment did not inhibit cytokine generation induced by TNFα, IL-6 or IFN-β in both BEAS-2B and MRC-5 cells (Figure 4.7).

4.4 Measuring autophagic activity in BEAS-2B cells

Subsequent experiments utilised only BEAS-2B epithelial cells to explore further the role of autophagy in regulating cellular responses to RV infection for two main reasons. Firstly,

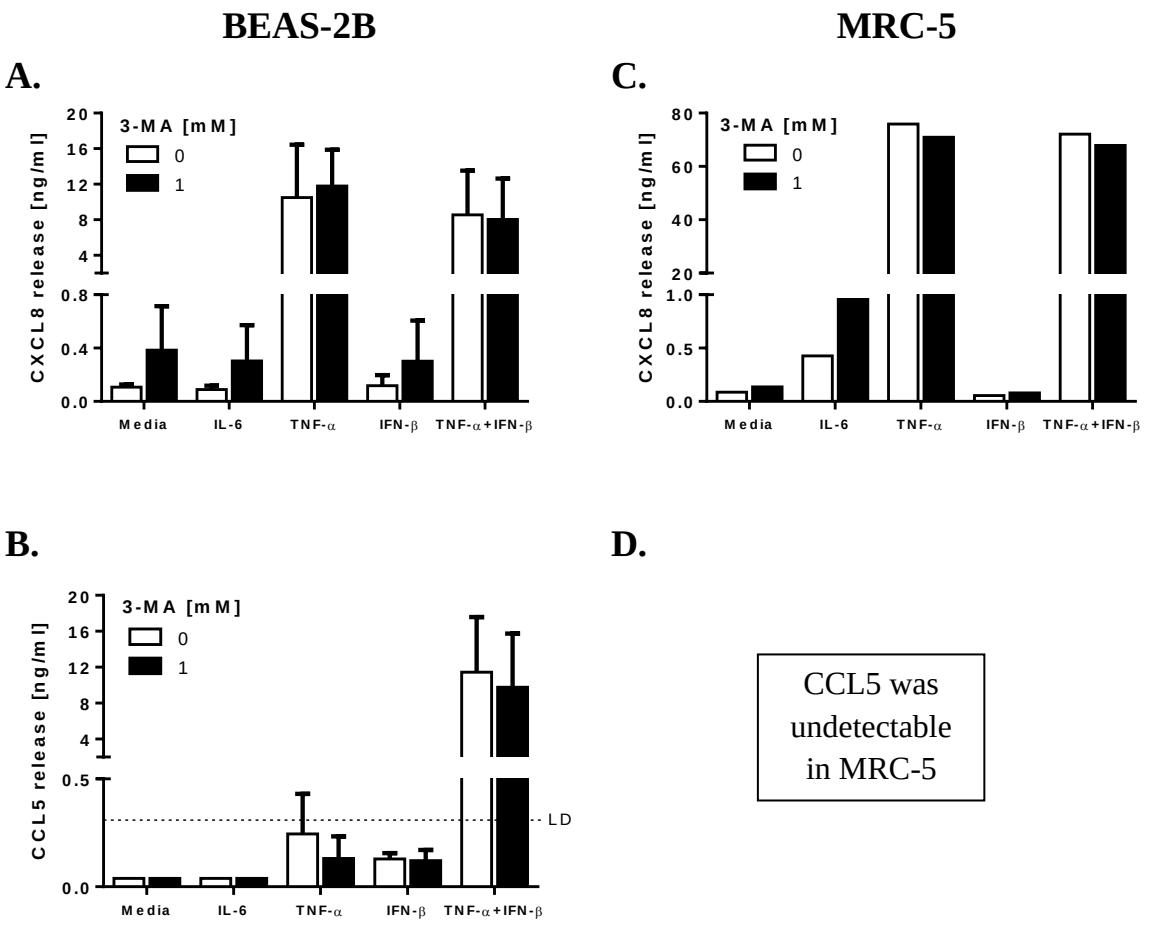

Figure 4. 7 3-MA does not inhibit cytokine production induced by TNFα, IL-6 or IFN-β.

BEAS-2B (A, B) or MRC-5 (C, D) cells were stimulated with IL-6 (50 ng/ml), TNF-α (20 ng/ml), IFN-β (20 ng/ml) or TNF-α/IFN-β in combination. Cells were then immediately treated with 3-MA at 1 mM and cultured for 24 h. Cell-free supernatants were collected, and CXCL8 (A, C) and CCL5 (B, D) release was measured by ELISA. Data shown are mean ± SEM of *n* = 3 independent experiments (A, B) or values from *n* = 1 (C, D). No significant differences were obtained (3-MA treated samples versus non-treated), as measured by two-way ANOVA with Bonferroni's post-test (A, B). LD = limit of detection.

epithelial cells are the primary target of RV within the airway, and secondly, the inhibitory effects of 3-MA were more marked on production of IFN-β and CCL5 than CXCL8, and MRC-5 fibroblasts did not secrete IFN-β and CCL5 (Section 4.3).

4.4.1 RV infection induces a subtle increase of LC3-II expression in BEAS-2B cells, as measured by LC3 western blotting

Upon activation of autophagy, LC3-I, the cytosolic form of microtubule-associated protein 1 light chain 3 (LC3) is conjugated to phosphatidylethanolamine (PE) to become LC3-II, the autophagosome-membrane bound form (reviewed in Tanida et al., 2004). Therefore, levels of LC3-II are routinely used as an indication of autophagic flux, with bafilomycin A1, an inhibitor of autophagosomal degradation, utilised to confirm basal autophagosomal activity (reviewed in Mizushima et al., 2010).

Having found that 3-MA suppressed viral-induced cytokine production in BEAS-2B epithelial cells (Figure 4.1), presumably by inhibiting autophagy, I next wished to investigate if RV infection could induce autophagy in this cell type. Poly(I:C) has been associated with autophagy activation in macrophages (Shi and Kehrl, 2008, Harris et al., 2011), hence it would be interesting to explore if poly(I:C) could also induce autophagy in BEAS-2B cells. Cells were left uninfected, infected with RV-1B or RV-16 at $1x10^7$ $TCID_{50}$/ml as described in Section 2.6.3; or stimulated with poly(I:C) (1 μg/ml). Cells were then immediately treated with bafilomycin A1 (baf, 100 nM) or 3-MA (1 mM) and cultured for 6 or 24 h. The incubation times were chosen based on previous studies (Klein and Jackson, 2011, Jackson et al., 2005) that examined the effects of RV infection and bafilomycin A1/3-MA treatment on autophagy activation in the human cervical epithelial HeLa cell line. Cells were lysed, total protein extracted, and western blotting for LC3-II and actin performed (Section 2.14). Using NIH ImageJ software, LC3-II expression was densitometrically analysed and normalised to the actin expression as a loading control. Note that the reason LC3-II/LC3-I ratios were not calculated (as another way of presenting autophagy induction data) is because LC3-II proteins tend to be much more sensitive to be detected by immunoblotting than LC3-I proteins, thus comparing the amount of LC3-II alone between samples is probably a more accurate method (Mizushima and Yoshimori, 2007).

Levels of LC3-II were significantly increased upon inhibition of autophagosomal degradation by bafilomycin A1, indicating that autophagy was basally active in BEAS-2B cells (Figure

4.8A, C, F). However, RV infection only resulted in a very subtle increase of autophagic flux in BEAS-2B cells, as observed at 6 or 24 h p.i. (Figure 4.8A, B, E). Increased levels of LC3-II were seen in poly(I:C)-treated BEAS-2B cells at 6 h, but not at 24h (Figure 4.8A, B, E). Furthermore, 3-MA treatment did not result in any changes of LC3-II expression in cells infected with RV or stimulated with poly(I:C) (Figure 4.8A, D, G).

4.4.2 LC3-II expression is not increased when BEAS-2B cells are nutrient-starved or treated with rapamycin, as measured by LC3 western blotting

Having observed that RV only caused a modest increase of autophagic flux in BEAS-2B airway epithelial cells, I next wished to demonstrate if a significant increase of autophagic activity in this cell type could be achieved using other known autophagy stimuli. Mammalian target of rapamycin (mTOR), a serine/threonine protein kinase, is a negative regulator of the autophagic pathway (reviewed in Meijer and Codogno, 2004). Studies have shown that rapamycin (an mTOR inhibitor), and nutrient starvation, can activate autophagy in BEAS-2B cells (Zhang et al., 2012, Persson et al., 2001). Therefore, these two autophagy inducers were utilised in pilot experiments. Cells were cultured in nutrient-rich media (Complete media) or starvation media [Hank's Balanced Salt Solution (HBSS) buffer], in the absence or presence of rapamycin (200 nM), with or without bafilomycin A1 (100 nM) for 2, 4 or 8 h. Cells were lysed, total protein extracted, and western blotting for LC3-II and actin performed (Section 2.14).

Based on a single experiment, in contrast to the results obtained in previous studies (Zhang et al., 2012, Persson et al., 2001), no obvious upregulation of LC3-II levels was seen in our BEAS-2B cells, following starvation or rapamycin treatment (Figure 4.9A). Cells that were nutrient-starved and cotreated with rapamycin also did not show an increase of LC3-II expression at any of the studied time-points (Figure 4.9A). As expected, blocking autophagosomal degradation using bafilomycin A1 resulted in an accumulation of LC3-II proteins in a time-dependent manner (Figure 4.9B), although the effects are less obvious in nutrient-starved cells, which may be due to the small variability in protein levels observed.

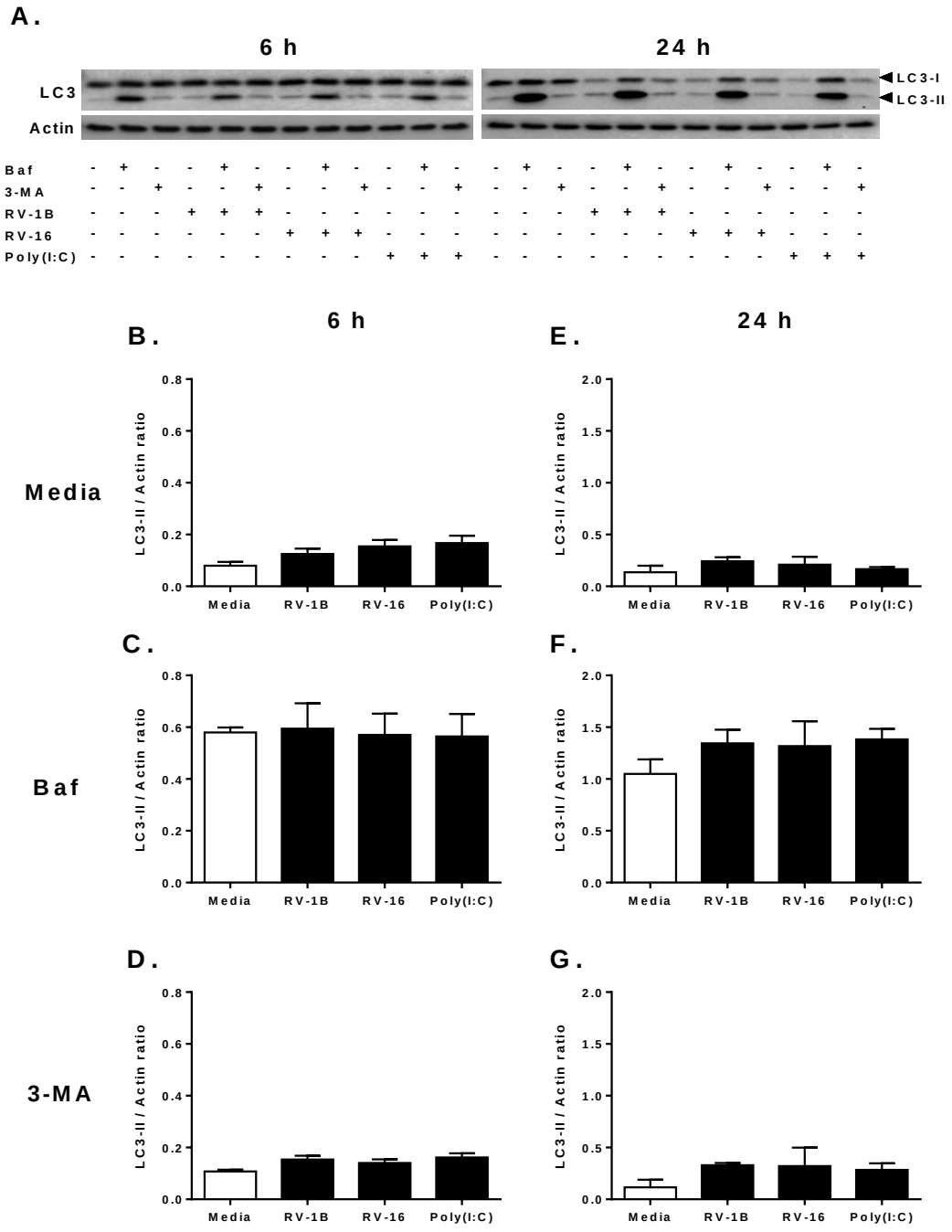

Figure 4. 8 RV infection induces a subtle increase of LC3-II expression in BEAS-2B cells, as measured by LC3 western blotting.

BEAS-2B cells were infected with RV-1B or RV-16 at $1x10^7$ $TCID_{50}$/ml for 1 h (following which supernatants were replaced with media), or stimulated with poly(I:C) (1 µg/ml). Cells were then immediately treated with bafilomycin A1 (Baf, 100 nM) or 3-MA (1 mM) and cultured for 6 h (B, C, D) or 24 h (E, F, G). (A) Whole-cell lysates were analysed by Western blot using Abs specific to LC3 or actin. A blot representative of 3 independent experiments is shown. (B, C, D, E, F, G) LC3-II expression was densitometrically analysed and normalized to the actin expression as a loading control. Data shown are mean ± SEM of *n* = 3 independent experiments.

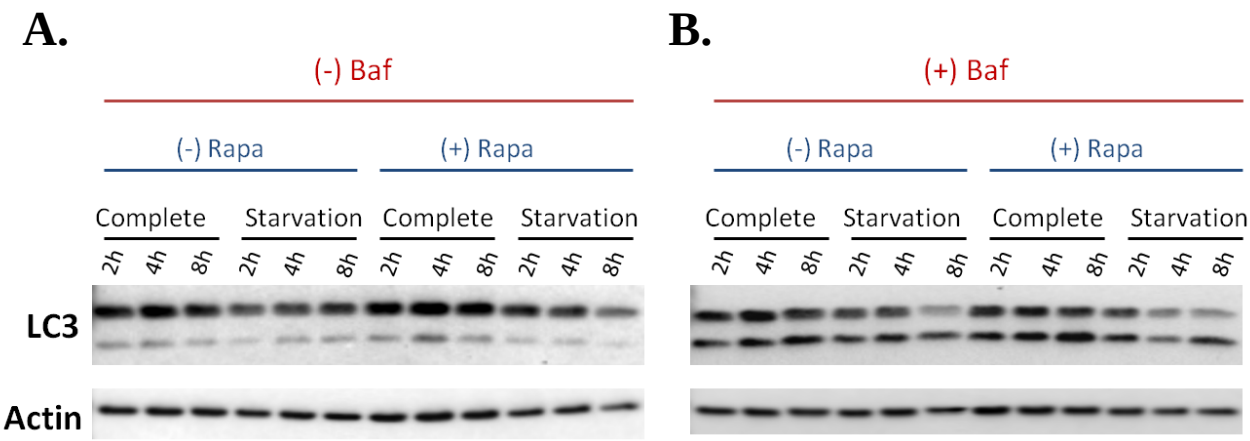

Figure 4. 9 Increased of LC3-II expression is not detected when BEAS-2B cells were nutrient-starved or treated with rapamycin, as measured by LC3 western blotting. BEAS-2B cells were cultured in nutrient-rich media (Complete) or starvation media (HBSS buffer), in the absence or presence of rapamycin (Rapa; 200 nM), with (A) or without (B) bafilomycin A1 (Baf; 100 nM) for 2, 4 or 8 h. Whole-cell lysates were analysed by Western blot using Abs specific to LC3 or actin. Data shown are $n = 1$.

4.4.3 Cigarette smoke extract, rapamycin or starvation treatment in BEAS-2B cells is not associated with increased GFP-LC3 puncta

As nutrient starvation and rapamycin failed to induce autophagy as assessed by LC3 western blotting, another technique commonly used to monitor autophagic activity (i.e. fluorescence microscopy) was employed. Accumulation of green fluorescent protein (GFP)-tagged-LC3 puncta in cells transfected with GFP-LC3-expressing plasmids is a widely accepted marker of autophagosome formation (reviewed in Mizushima et al., 2010). The exogenous GFP-LC3 fusion protein is a cytosolic protein; however during autophagy, it is lipidated and incorporated into autophagosomal membranes, and therefore scored as cytoplasmic puncta by fluorescence microscopy (reviewed in Mizushima et al., 2010).

Cigarette smoke extract (CSE) has also been shown to activate autophagy in BEAS-2B cells (Hwang et al., 2010, Chen et al., 2008); thus it was used in the current study in addition to nutrient starvation and rapamycin treatment. BEAS-2B cells were grown on glass cover slips and transfected with GFP-LC3-expressing plasmids as described in Section 2.11. After 48 h transfection, cells were either left untreated, or treated with 20% CSE (See section 2.9.3 for description of the CSE preparation) or rapamycin (500 nM) for 6 h. Cells were fixed, nuclei were stained with DAPI (blue), and GFP-LC3 (green) was visualised by fluorescence microscopy at x40 objective lens magnification (Sections 2.12 and 2.13). At least 4 fields (containing approximately 20-30 cells) were viewed for each sample.

Based on two independent experiments, the transfection efficiencies (indicated by the percentage of GFP-expressing cells) were relatively low, and varied between samples, ranging from ~ 15% to 40% (Figure 4.10A-C). CSE or rapamycin treatment failed to increase formation of exogenous GFP-LC3 puncta, compared to untreated control (Figure 4.10).

In the previous experiments cells were fixed prior to visualisation by fluorescence microscopy (Figure 4.10). It was of concern that the fixation steps might affect autophagic activity in the cells, therefore influencing the results obtained under this experimental condition. I therefore sought to conduct similar experiments but with no fixation step and immediate visualisation. BEAS-2B cells were grown in glass bottom dishes and transfected with GFP-LC3-expressing plasmids as described in Section 2.11. After 48 h transfection, cells were either left untreated, or treated with 20% CSE (Section 2.9.3) or rapamycin (500 nM); or nutrient-starved (immersed in HBSS buffer), for 6 h. Live-cell imaging was

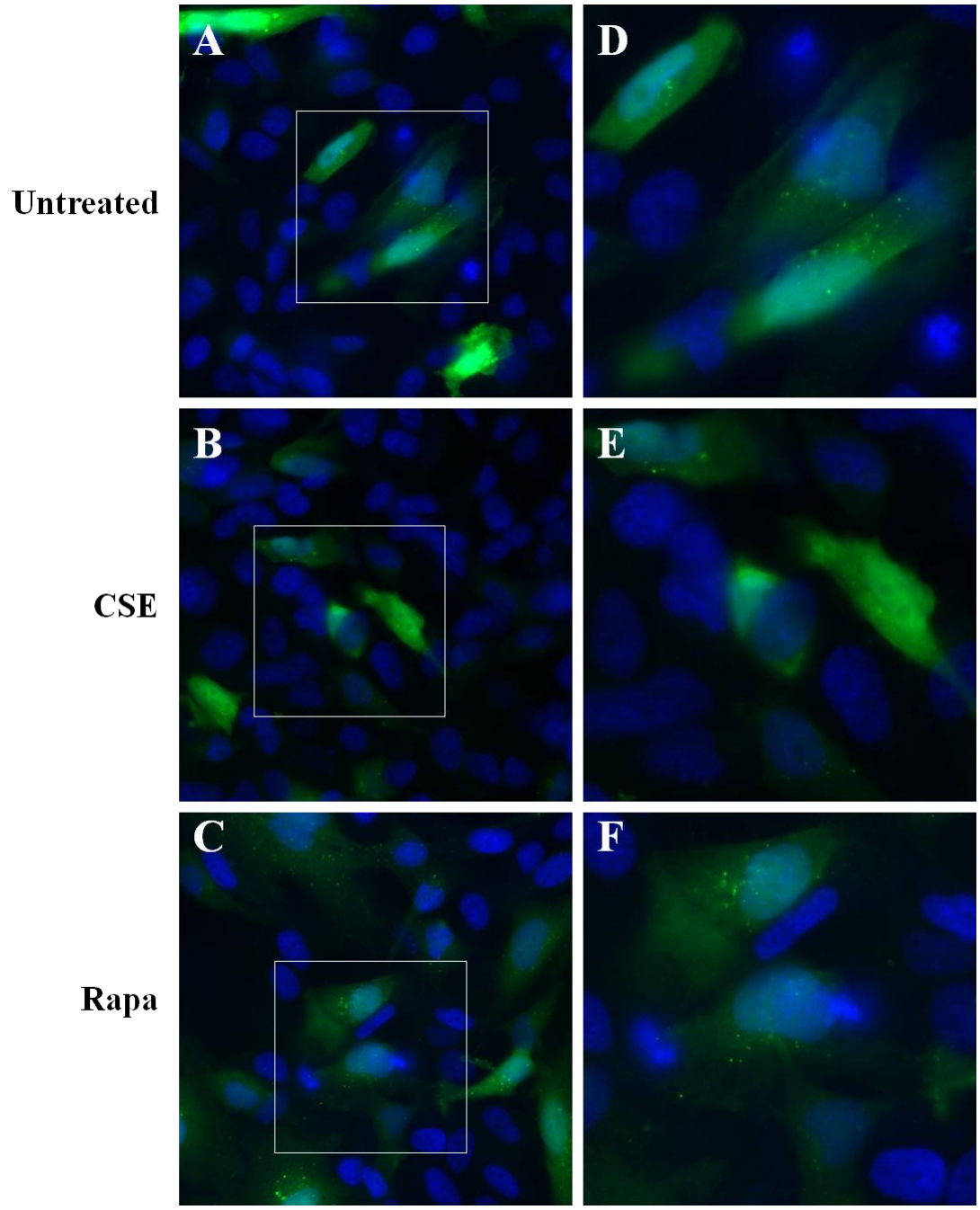

Figure 4. 10 CSE or rapamycin treatment in BEAS-2B cells is not associated with increased GFP-LC3 puncta, as analysed following fixation of the cells.

BEAS-2B cells were grown on glass cover slips and transfected with GFP-LC3-expressing plasmids. After 48 h transfection, cells were either left untreated (A, D), or treated with 20% CSE (B, E) or rapamycin (Rapa; 500 nM) (C, F) for 6 h. Cells were then fixed and stained for nucleus (blue). Images were captured using fluorescence microscopy at x40 objective lens magnification. The green GFP-LC3 puncta represent autophagosomes. Images shown on the right panel set are the magnified versions of the boxed regions of interest of the images shown on the left panel set. Data shown are representative images of n = 2 independent experiments.

performed using fluorescence microscopy at x60 objective lens magnification, with the microscope enclosed in an environmental chamber equilibrated to 37°C. At least 4 fields (containing approximately 5-10 cells) were viewed for each sample.

Based on a single experiment, no enhancement of GFP-LC3 puncta formation was observed upon CSE, rapamycin or starvation treatment, compared to untreated control, as analysed by live-cell imaging (Figure 4.11).

4.4.4 Increased of autophagy by starvation or torin2 treatment in BEAS-2B cells is detected using endogenous LC3 immunostaining assay

As discussed in an extensive review article detailing the use and interpretation of assays for monitoring autophagy (Klionsky et al., 2012), the main reason exogenous GFP-LC3 transfection assay is utilised by many studies to monitor autophagic activity (and therefore used in the present work) is because endogenous LC3 protein is not always detectable by fluorescence microscopy, due to its very low expression in certain cell types. However, as induction of autophagy using the GFP-LC3 transfection assay was unsuccessful, autophagic flux was subsequently explored by detecting endogenous LC3 protein using an anti-LC3 antibody.

BEAS-2B cells were grown on glass cover slips, and either left untreated, nutrient-starved (immersed in HBSS buffer), or treated with torin2 (a newly characterised mTOR inhibitor that can induce autophagy) (reviewed in Klionsky et al., 2012) for 2 h. Cells were fixed and stained for endogenous LC3 and nuclei using anti-LC3 antibody and DAPI, respectively (Section 2.12) and staining was visualised by fluorescence microscopy (Section 2.13). At least 4 fields (containing approximately 7-20 cells) were viewed for each sample.

Based on a single experiment, the number of endogenous LC3 puncta was markedly increased in cells exposed to starvation or torin2 treatment (Figure 4.12). These data indicate that autophagy occurs and can be upregulated in BEAS-2B cells.

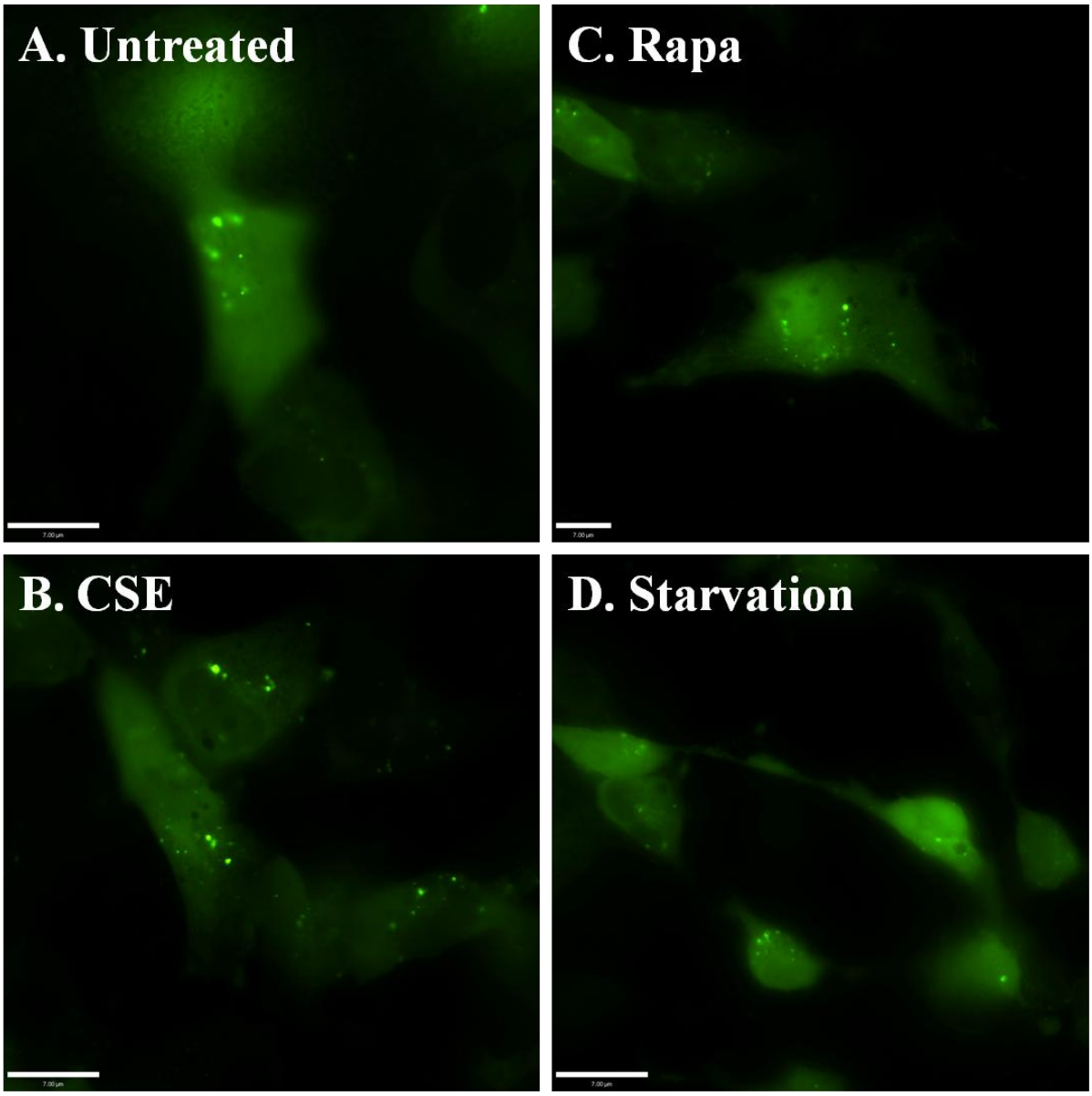

Figure 4. 11 CSE, rapamycin or starvation treatment in BEAS-2B cells is not associated with increased GFP-LC3 puncta, as analysed by live-cell imaging.
BEAS-2B cells were grown in glass bottom dishes and transfected with GFP-LC3-expressing plasmids. After 48 h transfection, cells were either left untreated (A), or treated with 20% CSE (B) or rapamycin (Rapa; 500 nM) (C); or nutrient-starved (Starvation; immersed in HBSS buffer) (D) for 6 h. Images of live cells were captured using fluorescence microscopy at x60 objective lens magnification, with the microscope enclosed in an environmental chamber equilibrated to 37°C. The green GFP-LC3 puncta represent autophagosomes. Data shown are $n = 1$.

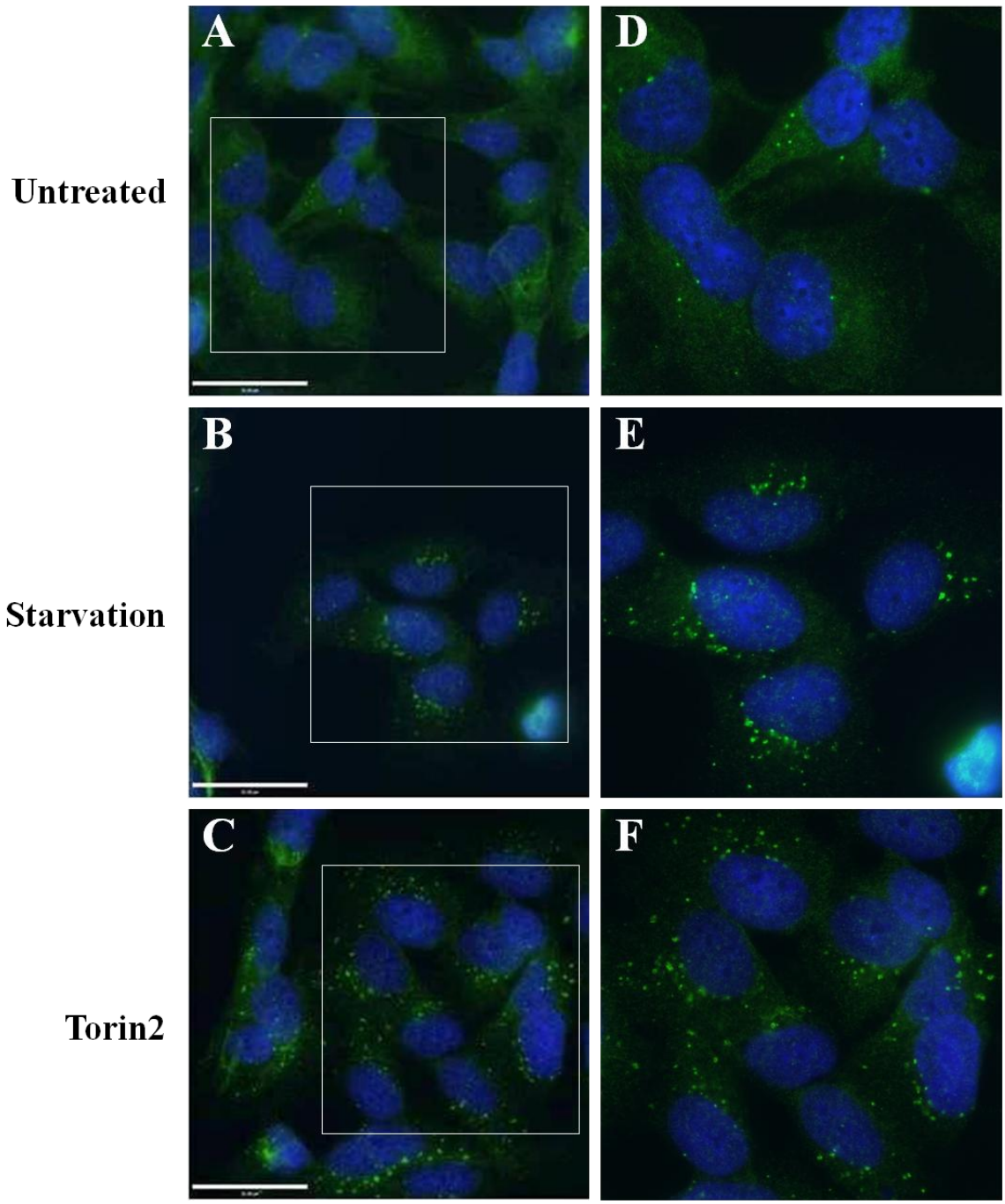

Figure 4. 12 Increased of autophagy by starvation or torin2 treatment in BEAS-2B cells is detected using endogenous LC3 immunostaining assay.

BEAS-2B cells were grown on glass cover slips, and were either left untreated (A, D), nutrient-starved (Starvation; immersed in HBSS buffer) (B, E) or treated with torin2 (10 nM (C, F) for 2 h. Cells were then fixed and immunostained for endogenous LC3 (green) and nucleus (blue). Images were captured using fluorescence microscopy at x60 objective lens magnification. The green LC3 puncta represent autophagosomes. Images shown on the right panel set are the magnified versions of the boxed regions of interest of the images shown on the left panel set. Data shown are $n = 1$.

4.5 Knockdown of autophagy regulators has minimal effects on responses of BEAS-2B cells to RV infection

To confirm the results obtained using the pharmacological inhibitor 3-MA (Section 4.3), inhibition of autophagy was next performed using a more specific approach, small interfering RNA (siRNA). Briefly, artificially synthesised siRNAs are designed to target their specific mRNAs for destruction via RNA interference pathway, subsequently silencing expression of the relevant proteins (Elbashir et al., 2001). The siRNAs targeting several autophagy proteins utilised in this study were purchased from Thermo Scientific, Lafayette, Colorado (Section 2.10).

4.5.1 Knockdown of Beclin-1 or Atg7 inhibits basal autophagy and nutrient-starvation-induced autophagy in BEAS-2B cells

The canonical pathway of macroautophagy requires the class III PI3K, Vps34, regulated by its binding partner Beclin-1 (Bec1) and dependent upon autophagy-related protein 7 (Atg7) for LC3-II lipidation (reviewed in Codogno et al., 2012) (See Figure 1.8 for the schematic diagram of the autophagy pathway). To investigate the roles of autophagy, BEAS-2B cells were transfected with siRNAs targeting the autophagy proteins Bec1 and Atg7.

Prior to conducting the functional assays, pilot experiments were conducted to determine the optimal concentrations for Bec1- and Atg7-targeting siRNAs to be used, and to assess at which time-point the target proteins showed the greatest knockdown. BEAS-2B cells were left untransfected, transfected with the transfection reagent alone (mock), or transfected with a non-targeting scrambled control siRNA or siRNA targeting Bec1 or Atg7 at 100 or 200 nM. After 24, 48 or 72 h transfection, cells were lysed, total protein extracted, and western blotting for Bec1, Atg7 and actin performed (Section 2.14).

Based on a single experiment, similar levels of knockdown were observed in cells treated with 100 and 200 nM of Bec1-targeting siRNA, at all studied time points (Figure 4.13). Expression of Bec1 protein was most markedly decreased after 48 h transfection, and remained low at 72 h post-transfection (Figure 4.13). Similar to the observations of Bec1 knockdown (Figure 4.13), expression of Atg7 protein was substantially suppressed only after 48 h transfection, and was found to be further reduced at 72 h post-transfection (Figure 4.14).

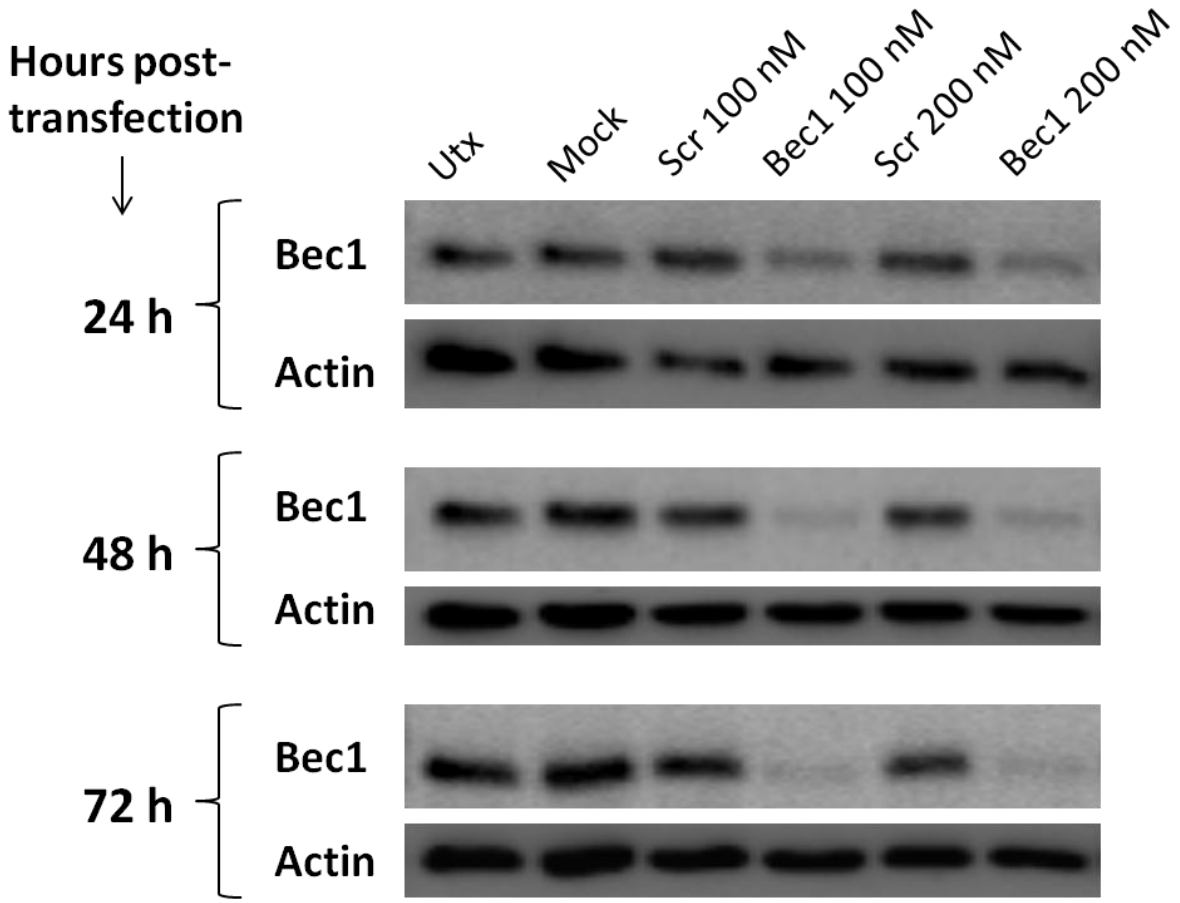

Figure 4. 13 Time- and dose-response of siRNA-mediated knockdown of Beclin-1. BEAS-2B cells were either left untransfected (Utx), transfected with the transfection reagent alone (Mock); or transfected with a non-targeting scrambled control siRNA (Scr) or siRNA targeting Beclin-1 (Bec1) at 100 or 200 nM. After 24, 48 or 72 h transfection, whole-cell lysates were prepared and analysed by Western blot using Abs specific to Bec1 or actin. Data shown are $n = 1$.

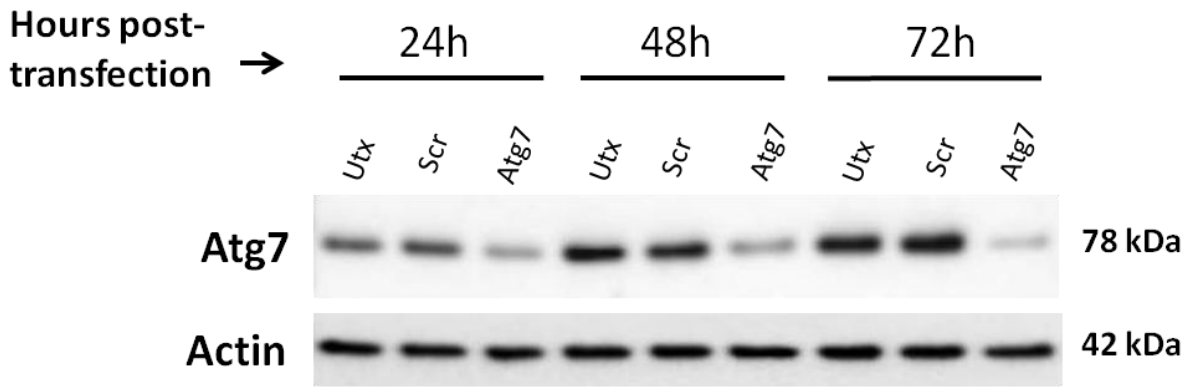

Figure 4. 14 Time-response of siRNA-mediated knockdown of Atg7.
BEAS-2B cells were either left untransfected (Utx), or transfected with a non-targeting scrambled control siRNA (Scr) or siRNA targeting Atg7 at 100 nM. After 24, 48 or 72 h transfection, whole-cell lysates were prepared and analysed by Western blot using Abs specific to Atg7 or actin. Data shown are $n = 1$.

To verify the requirement for Bec1 and Atg7 in canonical autophagy induction in BEAS-2B cells, cells were transfected with a non-targeting scrambled control siRNA, or siRNA targeting Bec1 or Atg7 at 100 nM. After 48 h transfection, cells were either left untreated, or nutrient-starved (immersed in HBSS buffer) for 2 h. Cells were then fixed and immunostained for endogenous LC3 (green) and nuclei (blue) (Section 2.12). Images were captured using fluorescence microscopy at x60 objective lens magnification (Section 2.13). At least 4 fields (containing approximately 7-15 cells) were viewed for each sample. As shown in Figure 4.15, knockdown of Bec1 or Atg7 notably diminished basal autophagy and starvation-induced autophagy in BEAS-2B airway epithelial cells.

4.5.2 Knockdown of Beclin-1 or Atg7 modestly inhibits RV-induced CXCL8, but not CCL5, production in BEAS-2B cells

After confirming that knockdown of autophagy regulators Bec1 and Atg7 inhibited autophagic activity in BEAS-2B cells, the effect of the knockdown on RV-induced inflammatory responses was next investigated. Viral infection was conducted after 48 h siRNA-transfection, the time-point at which the autophagy proteins were shown to be effectively knocked down (Figure 4.13, 4.14).

BEAS-2B cells were left untransfected, transfected with a non-targeting scrambled control siRNA, or transfected with siRNA targeting Bec1 or Atg7, at 100 nM. After 48 h transfection, cells were infected with RV at a $TCID_{50}$/ml of $0.5x10^7$ or $1.0x10^7$ as described in Section 2.6.3, or stimulated with poly(I:C) at 1 or 10 µg/ml. After 24 h (i.e. 72 h post-transfection), cell-free supernatants were collected to determine cytokine release, as measured by ELISA (Section 2.15). Cells were also lysed, total protein extracted, and western blotting for Bec1, Atg7 and actin performed (Section 2.14).

Figure 4.16A shows that Bec1 knockdown remained evident, although incomplete, at 24 h p.i. (i.e. 72 h after siRNA transfection). However, knockdown of Bec1 protein only resulted in a moderate reduction of CXCL8 production in response to RV-1B only, with no effects on generation of CXCL8 or CCL5 induced by RV-16 or poly(I:C) (Figure 4.16).

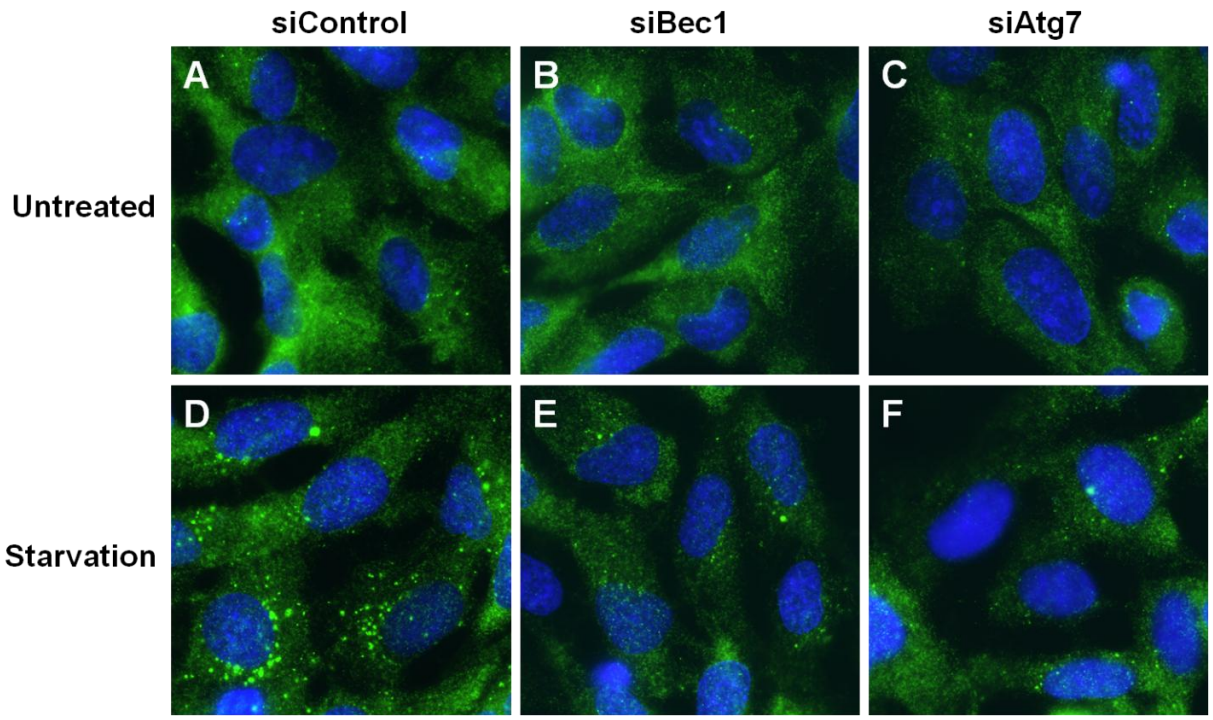

Figure 4. 15 Knockdown of Beclin-1 or Atg7 inhibits basal autophagy and nutrient-starvation-induced autophagy in BEAS-2B cells.

BEAS-2B cells were grown on glass cover slips and transfected with a non-targeting scrambled control siRNA (siControl) (A, D), or siRNA targeting Beclin-1 (siBec1) (B, E) or Atg7 (siAtg7) (C, F) at 100 nM. After 48 h transfection, cells were either left untreated (A-C), or nutrient-starved (Starvation; immersed in HBSS buffer) for 2 h (D-F). Cells were then fixed and immunostained for endogenous LC3 (green) and nucleus (blue). Images were captured using fluorescence microscopy at x60 objective lens magnification. The green LC3 puncta represent autophagosomes. Data shown are representative images of n = 3 independent experiments.

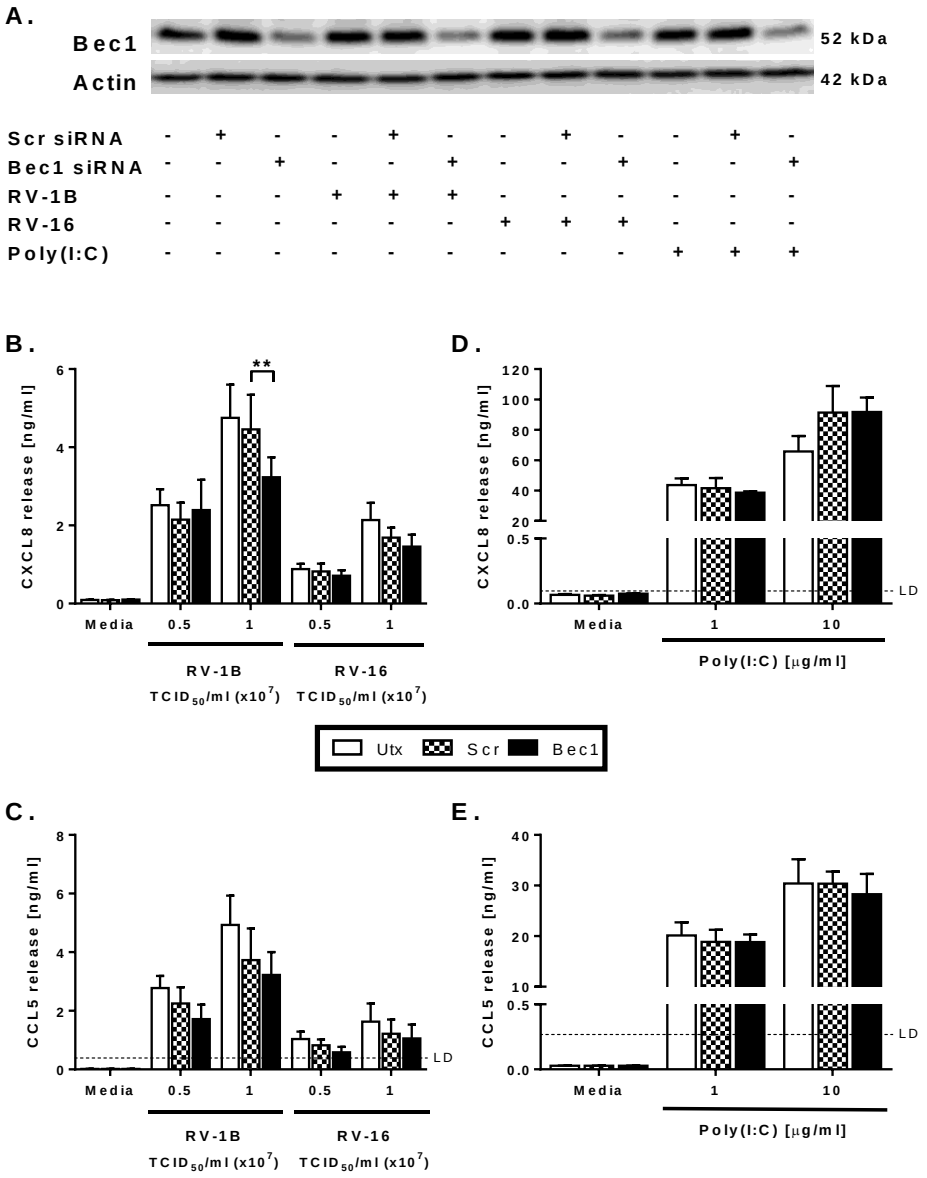

Figure 4. 16 Knockdown of Beclin-1 modestly inhibits RV-induced CXCL8, but not CCL5, production in BEAS-2B cells.

BEAS-2B cells were either left untransfected (Utx), or transfected with a non-targeting scrambled control siRNA (Scr) or siRNA targeting Beclin-1 (Bec1) at 100 nM. After 48 h transfection, cells were infected with RV-1B or RV-16 at the indicated $TCID_{50}$/ml for 1 h (following which supernatants were replaced with media) (B, C), or stimulated with poly(I:C) at the indicated concentrations (D, E); and cells were then cultured for 24 h. (A) Whole-cell lysates were analysed by Western blot using Abs specific to Bec1 or actin. A blot representative of 3 independent experiments is shown. Data shown for RV-1B and RV-16 are using a $TCID_{50}$/ml of $0.5x10^7$, and for poly(I:C) is using a concentration of 1 μg/ml. Cell-free supernatants were also collected, and CXCL8 (B, D) and CCL5 (C, E) release was measured by ELISA. Data shown are mean ± SEM of n = 3 independent experiments. The only significant difference on chosen statistical testing is indicated by **, $p < 0.01$, analysed by two-way ANOVA with Bonferroni's post-test. LD = limit of detection.

Despite the strong knockdown observed (Figure 4.17A), silencing of Atg7 expression only modestly attenuated CXCL8 generation caused by RV-16 infection or poly(I:C) (Figure 4.17B, D). Similar to the Bec1 knockdown data (Figure 4.16C, E), CCL5 production in response to both RV infection or poly(I:C) was preserved in Atg7-knockdown-BEAS-2B cells (Figure 4.17C, E).

4.5.3 Knockdown of LC3 does not inhibit RV-induced cytokine production in BEAS-2B cells

SiRNA-mediated knockdown of Bec1 or Atg7 had only moderate effects on CXCL8 generation, with no effects on CCL5 production (Section 4.5.2). In contrast, 3-MA suppressed IFN/CCL5 production more potently than CXCL8 generation (Section 4.3.1). Recently, studies have shown that non-canonical forms of macroautophagy can bypass Bec1 and Atg7, but LC3 remains crucial to autophagy (reviewed in Codogno et al., 2012). To assess whether RV and poly(I:C) could induce non-canonical autophagy susceptible to 3-MA but not Bec1 or Atg7 knockdown, siRNA-mediated knockdown of LC3 was performed.

Again, a pilot experiment was first carried out to determine the optimal concentration of LC3-targeting siRNA to be used, and to assess at which time-point LC3 protein knockdown is most efficient. BEAS-2B cells were left untransfected, incubated with the transfection reagent alone (mock), or transfected with a non-targeting scrambled control siRNA or siRNA targeting LC3 at 100 or 200 nM. After 48 or 72 h transfection, cells were lysed, total protein extracted, and western blotting for LC3 and actin performed (Section 2.14). Based on a single experiment, comparable levels of knockdown were seen in cells treated with 100 and 200 nM of LC3-targeting siRNA (Figure 4.18). Expression of LC3 protein was substantially knocked down at 48 h post-transfection, and remained low after 72 h transfection (Figure 4.18).

Having established the optimal conditions for LC3 knockdown assays, the effect of LC3 knockdown on RV-induced cytokine responses was then examined. BEAS-2B cells were left untransfected, transfected with a non-targeting scrambled control siRNA, or transfected with siRNA targeting LC3 at 100 nM. After 48 h transfection, cells were infected with RV at a $TCID_{50}$/ml of $0.5x10^7$ or $1.0x10^7$ as described in Section 2.6.3, or stimulated with poly(I:C) at 1 or 10 µg/ml. After 24 h (i.e. 72 h post-transfection), cell-free supernatants were collected to determine cytokine release, as measured by ELISA (Section 2.15). Cells were also lysed, total protein extracted, and western blotting for LC3 and actin performed (Section 2.14).

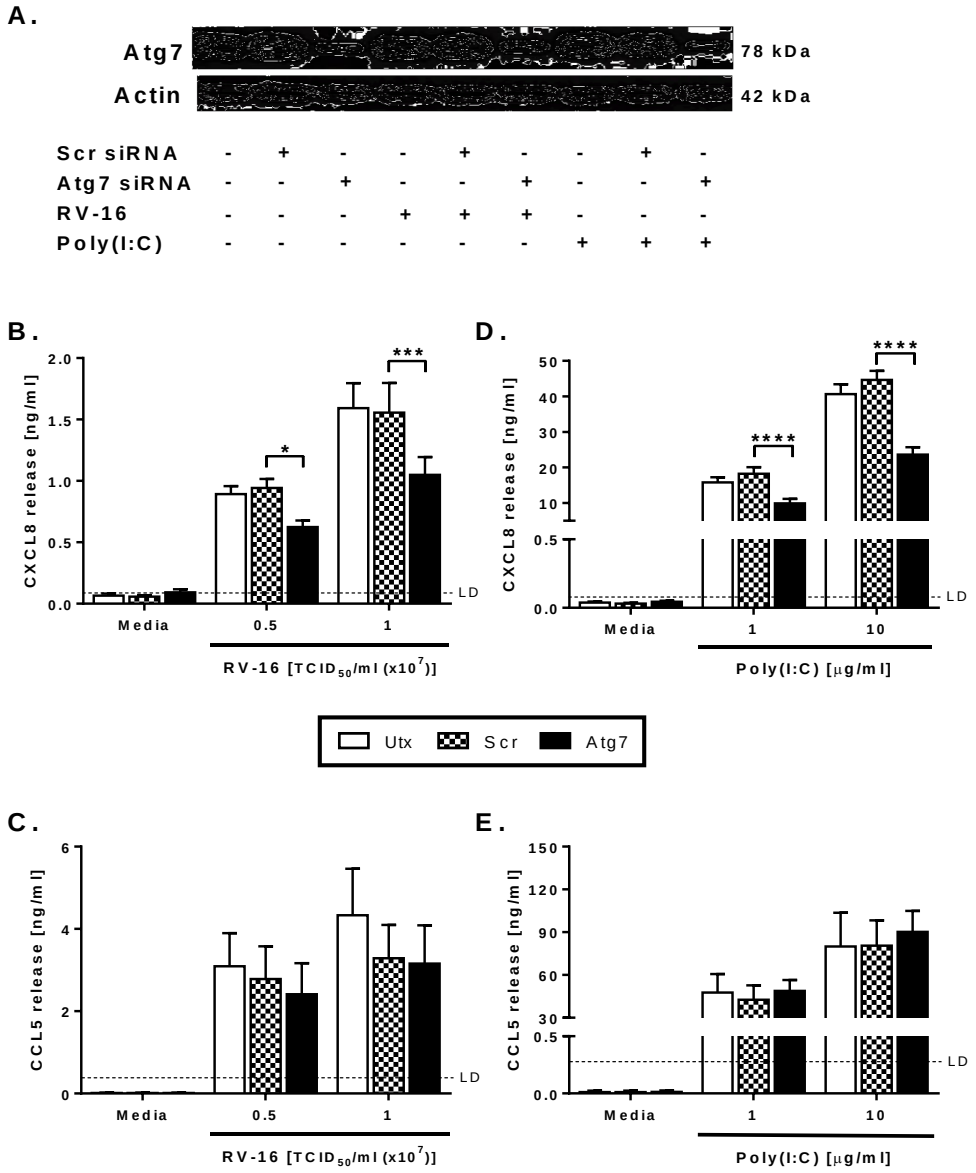

Figure 4. 17 Knockdown of Atg7 modestly inhibits RV-induced CXCL8, but not CCL5, production in BEAS-2B cells.

BEAS-2B cells were either left untransfected (Utx), or transfected with a non-targeting scrambled control siRNA (Scr) or siRNA targeting Atg7 at 100 nM. After 48 h transfection, cells were infected with RV-16 at the indicated $TCID_{50}$/ml for 1 h (following which supernatants were replaced with media) (B, C), or stimulated with poly(I:C) at the indicated concentrations (D, E); and cells were then cultured for 24 h. (A) Whole-cell lysates were analysed by Western blot using Abs specific to Atg7 or actin. A blot representative of 4 independent experiments is shown. Data shown for RV-16 are using a $TCID_{50}$/ml of $0.5x10^7$, and for poly(I:C) is using a concentration of 1 μg/ml. Cell-free supernatants were also collected, and CXCL8 (B, D) and CCL5 (C, E) release was measured by ELISA. Data shown are mean ± SEM of $n = 4$ independent experiments. Significant differences are indicated by *, $p < 0.05$; ***, $p < 0.001$ and ****, $p < 0.0001$, analysed by two-way ANOVA with Bonferroni's post-test. LD = limit of detection.

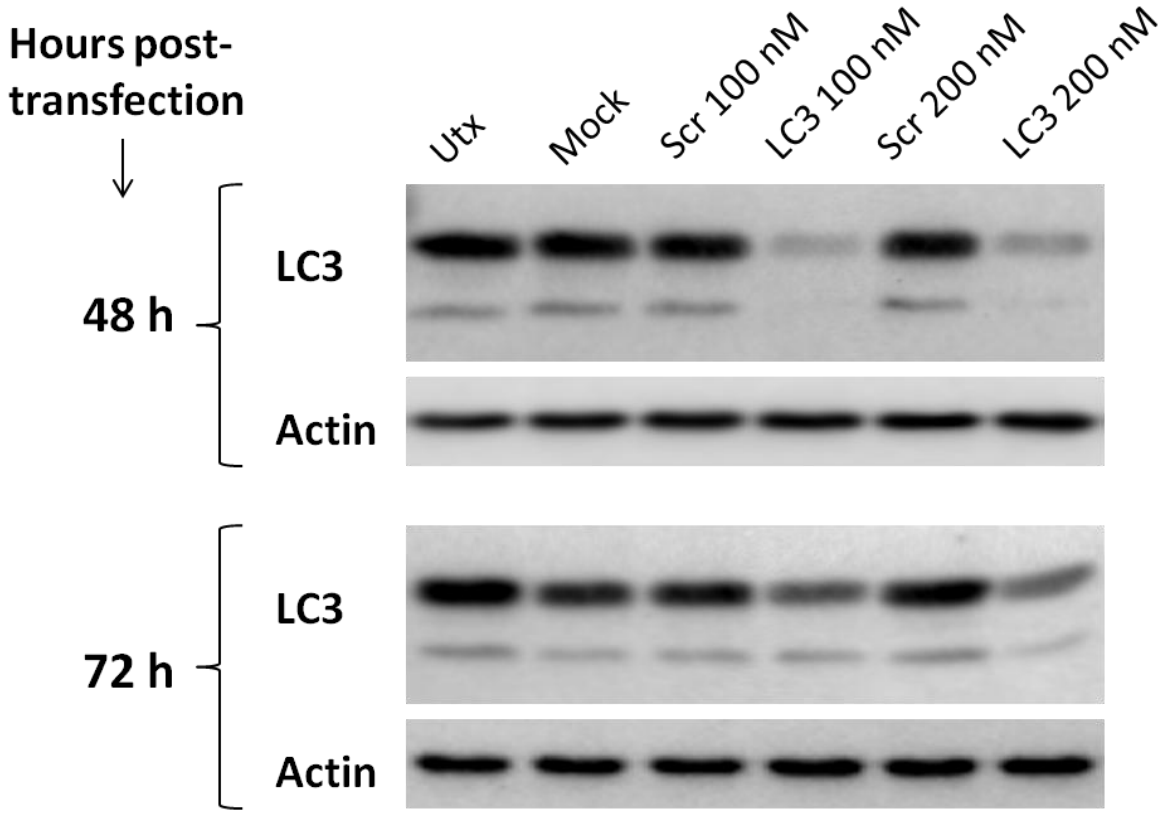

Figure 4. 18 Time- and dose-response of siRNA-mediated knockdown of LC3.
BEAS-2B cells were either left untransfected (Utx), transfected with the transfection reagent alone (Mock); or transfected with a non-targeting scrambled control siRNA (Scr) or siRNAs targeting LC3 at 100 or 200 nM. After 48 or 72 h transfection, whole-cell lysates were prepared and analysed by Western blot using Abs specific to LC3 or actin. Data shown are *n* = 1.

siRNA targeting of LC3 did not cause a reduction of CXCL8 or CCL5 release from BEAS-2B cells, in response to RV infection (Figure 4.19B, C). Interestingly, LC3 knockdown modestly suppressed CXCL8 production induced by the higher concentration of poly(I:C) only (Figure 4.19D). However, LC3-II expression was significantly increased upon RV infection (Figure 4.19A), whilst in the previous set of experiments (Figure 4.8A, E), only a subtle increase of LC3-II expression was seen in RV-infected cells; as measured at 24 h p.i. Figure 4.20A shows all blots obtained from the three independent experiments originally performed for Figure 4.19. As shown in Figure 4.20B, densitometric analysis shows that RV-1B and RV-16 significantly increased LC3-II expression (by ~65% and ~55%, respectively). Note that different concentrations of RV were used in the two sets of experiments of Figures 4.8 and 4.19, which might explain the different results obtained (discussed in Section 4.8.2.3).

4.5.4 Knockdown of autophagy pathway proteins has minimal consequences for viral replication

There have been conflicting reports in the literature on the requirement for autophagy in RV replication (Klein and Jackson, 2011, Brabec-Zaruba et al., 2007, Jackson et al., 2005), and to date, no studies have reported the roles of autophagy in RV replication of airway epithelial cells. To study if changes were occurring in viral replication in the absence of modulation of cytokine generation, the ability of Bec1 or LC3 knockdown to affect RV replication was investigated. BEAS-2B cells were either transfected with a non-targeting scrambled control siRNA, or transfected with siRNA targeting Bec1 or LC3 at 100 nM. After 48 h transfection, cells were infected with RV at a $TCID_{50}$/ml of $0.5x10^7$ or $1.0x10^7$ as described in Section 2.6.3. After 24 h infection (i.e. 72 h post-transfection), cells (~$6.1x10^5$) were lysed, cDNA synthesised and real-time qPCR for RV performed (Section 2.16-2.18). Samples were quantified against a standard curve of plasmids containing RV target sequence.

In contrast to the effects of 3-MA (Section 4.3.3), knockdown of autophagy protein Bec1 or LC3 did not impede viral replication, with an exception of the data obtained in Bec1 knockdown cells infected with $1x10^7$ $TCID_{50}$/ml of RV-1B which was modestly reduced, and did achieve statistical significance (Figure 4.21).

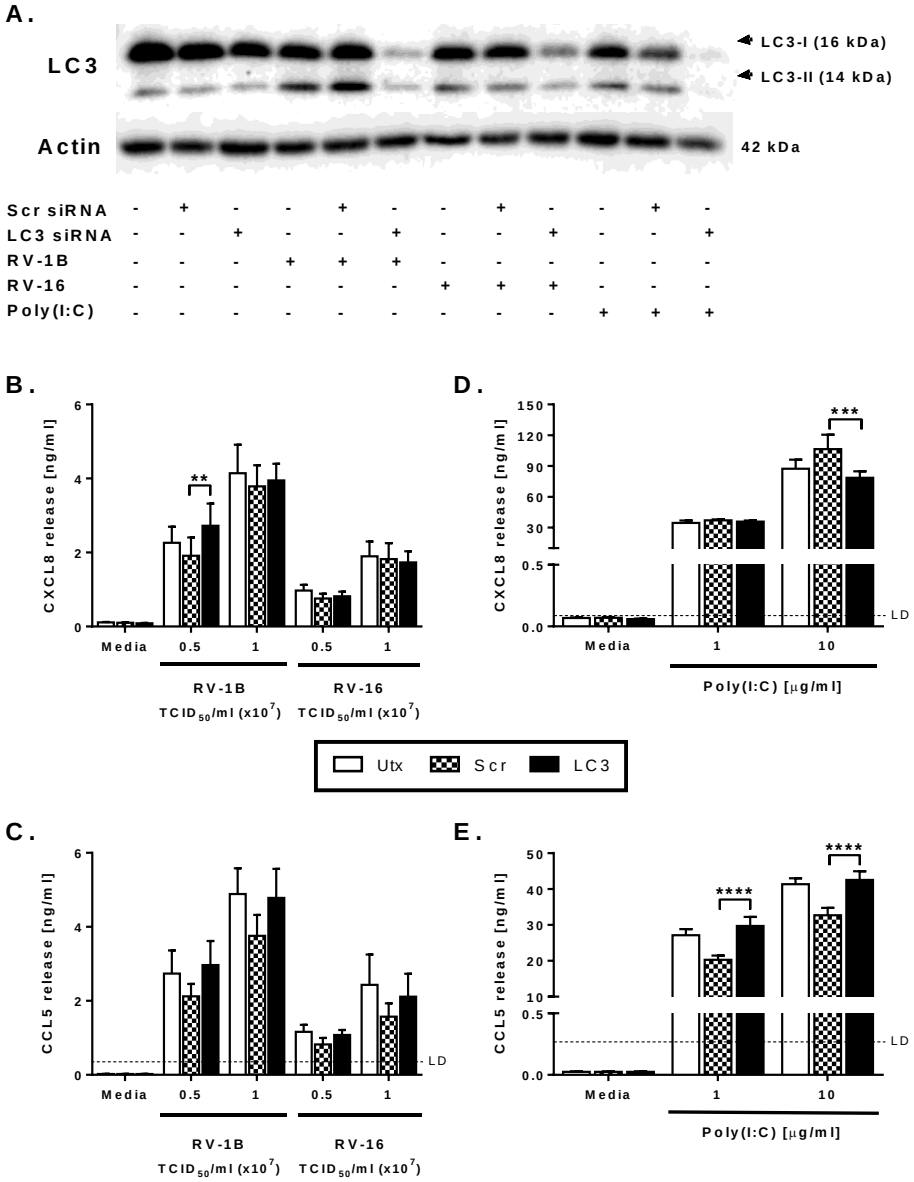

Figure 4. 19 Knockdown of LC3 does not inhibit RV-induced cytokine production in BEAS-2B cells.

BEAS-2B cells were either left untransfected (Utx), or transfected with a non-targeting scrambled control siRNA (Scr) or siRNAs targeting LC3 at 100 nM. After 48 h transfection, cells were infected with RV-1B or RV-16 at the indicated $TCID_{50}$/ml for 1 h (following which supernatants were replaced with media) (B, C), or stimulated with poly(I:C) at the indicated concentrations (D, E); and cells were then cultured for 24 h. (A) Whole-cell lysates were analysed by Western blot using Abs specific to LC3 or actin. A blot representative of 3 independent experiments is shown. Data shown for RV-1B and RV-16 are using a $TCID_{50}$/ml of $0.5x10^7$, and for poly(I:C) is using a concentration of 1 μg/ml. Cell-free supernatants were also collected, and CXCL8 (B, D) and CCL5 (C, E) release was measured by ELISA. Data shown are mean ± SEM of n = 3 independent experiments. Significant differences are indicated by **, $p < 0.01$; ***, $p < 0.001$ and ****, $p < 0.0001$, analysed by two-way ANOVA with Bonferroni's post-test. LD = limit of detection.

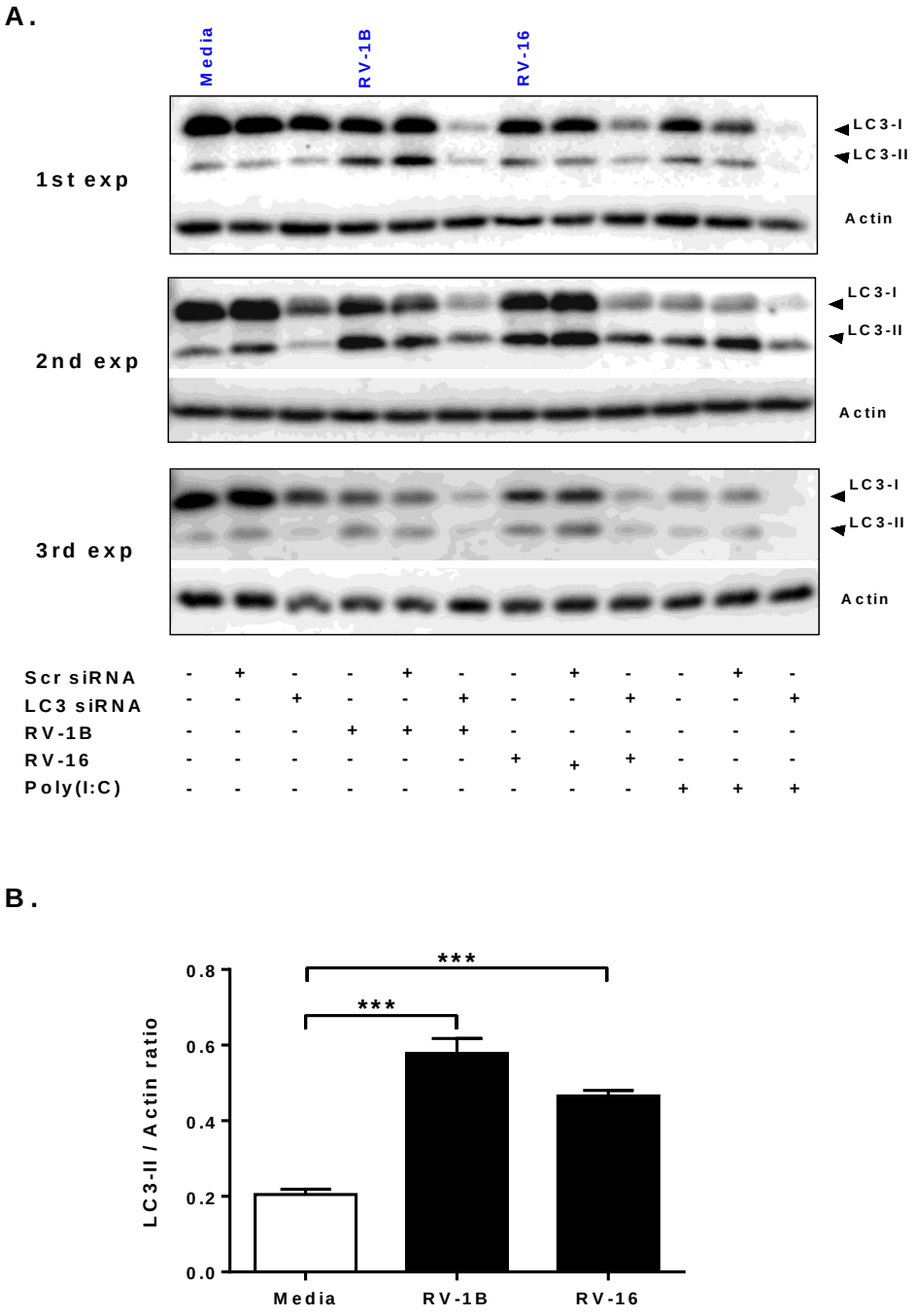

Figure 4. 20 RV infection significantly increases levels of LC3-II expression in BEAS-2B cells, as measured by LC3 western blotting.

Experiments were performed as described in the figure legend of Figure 4.19. Whole-cell lysates were analysed by Western blot using Abs specific to LC3 or actin. (A) Blots from 3 independent experiments are shown. Samples that were densitometrically analysed for LC3-II expression (as shown in B) are labelled in blue-font. (B) LC3-II expression was densitometrically analysed and normalised to the actin expression as a loading control. Data shown are mean ± SEM of n = 3 independent experiments. Significant differences are indicated by ***, $p < 0.001$, analysed by one-way ANOVA with Dunnett's post-test.

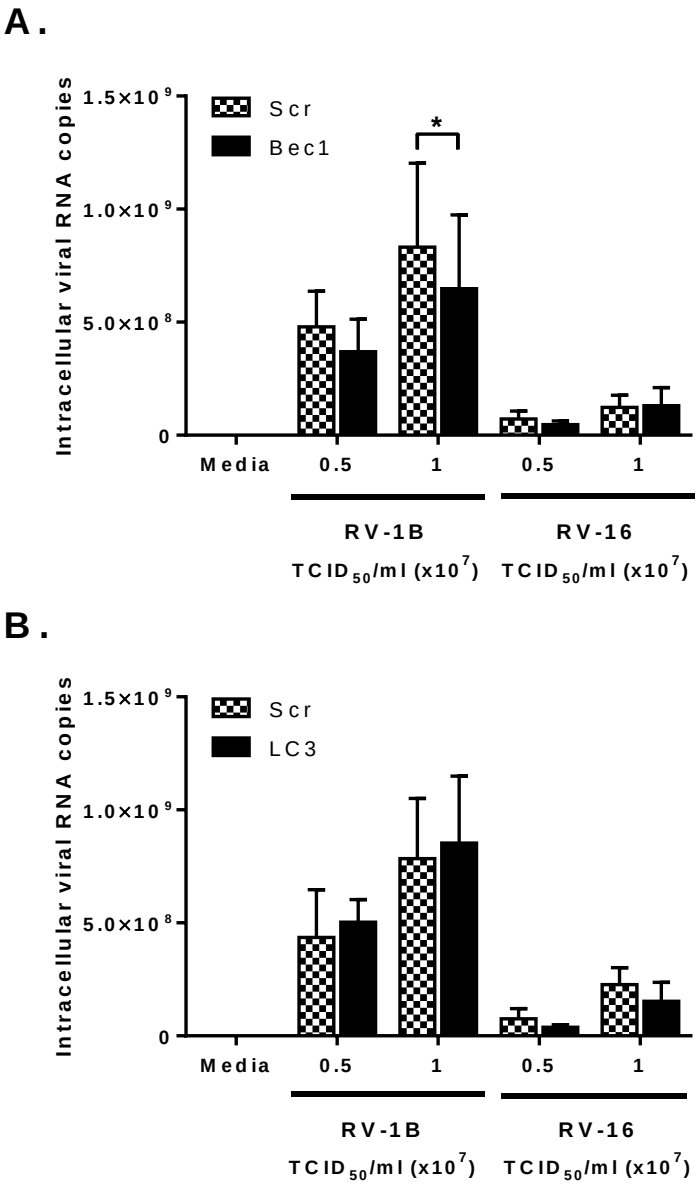

Figure 4. 21 Knockdown of autophagy pathway proteins has minimal consequences for viral replication.

BEAS-2B cells were transfected with a non-targeting scrambled control siRNA (Scr), or siRNA targeting Bec1 (A) or LC3 (B) at 100 nM. After 48 h transfection, cells were infected with RV-1B or RV-16 at the indicated $TCID_{50}$/ml for 1 h (following which supernatants were replaced with media), and cultured for 24 h. RNA was extracted and reverse transcribed for qPCR analysis of HRV RNA expression, with data presented as the total intracellular viral RNA copies per well. Data shown are mean ± SEM of $n = 3$ independent experiments. The only significant difference on chosen statistical testing is indicated by *, $p < 0.05$, analysed by two-way ANOVA with Bonferroni's post-test.

4.6 Involvement of PI3Ks in responses to RV infection

4.6.1 Effects of isoform-selective class I PI3K inhibitors on RV-induced cytokine production in BEAS-2B cells

The class III PI3K chemical inhibitor 3-MA, traditionally used to inhibit autophagy, suppressed CXCL8, IFN-β and CCL5 generation induced by RV and poly(I:C) (Section 4.3.1). However, using a more definitive approach (i.e. siRNA-mediated gene knockdown) to inhibit autophagy, it was found that autophagy had no or minimal effects on cytokine production (Section 4.5). It was therefore postulated that the inhibitory actions of 3-MA might be independent of autophagy. Furthermore, recent studies reported that 3-MA can also inhibit class I PI3Ks (Lin et al., 2012, Wu et al., 2010). Accordingly, I next wished to compare the actions of 3-MA with the effects of a general PI3K inhibitor, LY294002, and a panel of selective class I PI3K inhibitors, on RV-induced inflammatory responses.

Class I PI3Ks have four isoforms, divided based on their structural features and modes of regulation: p110α, p110β, p110δ and p110γ (reviewed in Vanhaesebroeck et al., 2010) (Section 1.9.1). In this study, concentrations of selective class I PI3K inhibitors were chosen as being approximately 10-fold above the published IC_{50} values (the concentration of an inhibitor where the response is reduced by half), and were without noticeable cell toxicity, as determined in preliminary concentration-response experiments (data not shown). The PI3K inhibitors used were as follows: LY294002 at 10 μM, a general PI3K inhibitor (Vlahos et al., 1994); PIK-75 at 0.1 μM, predominantly inhibiting class I p110α (IC_{50} 0.006 μM) and to a lesser degree p110γ (IC_{50} 0.08 μM) (Knight et al., 2006); TGX-221 at 0.1 μM, predominantly inhibiting class I p110β (IC_{50} 0.007 μM) and to a lesser degree p110δ (IC_{50} 0.1 μM) (Poon et al., 2012); IC87114 at 5 μM, inhibiting class I p110δ (IC_{50} 0.5 μM) (Patel et al., 2012); AS605240 at 0.1 μM, predominantly inhibiting class I p110γ (IC_{50} 0.008 μM) and to a lesser degree p110α (IC_{50} 0.06 μM) (Juss et al., 2012); PI-103 at 0.5 μM, a pan class I inhibitor (Knight et al., 2006).

BEAS-2B cells were left uninfected or infected with RV-1B or RV-16 at $1x10^7$ $TCID_{50}$/ml as described in Section 2.6.3. Cells were then immediately treated with DMSO control, or with the following PI3K inhibitor: LY294002 (10 μM), PIK-75 (0.1 μM), TGX-221 (0.1 μM), IC87114 (5 μM), AS605240 (0.1 μM) or PI-103 (0.5 μM), individually or in combination; and cultured for 24 h. Cell-free supernatants were collected to determine cytokine release, as

measured by ELISA (Section 2.15). Experiments in Figures 4.22 and Figure 4.23 were conducted simultaneously, but results were divided over separate figures for clarity, resulting in duplication of the DMSO control bars and PI-103-alone bars in both figures.

As shown in Figure 4.22, the broad PI3K inhibitor, LY294002, markedly inhibited CXCL8 (by ~80%) and CCL5 (by ~90%) generation in response to RV-1B or RV-16 infection in BEAS-2B epithelial cells. PI-103, a pan class I PI3K inhibitor, also showed a substantial reduction of RV-induced CXCL8 and CCL5 production (by ~50% and 70%, respectively) (Figure 4.22). However, inhibition of any individual class I PI3K isoform failed to significantly reduce RV-induced cytokine production, with the exception of inhibition of p110β or p110δ, which significantly suppressed CCL5 generation induced by RV-1B by ~30% (Figure 4.22E).

A recently published article revealed that pharmacological inhibition of at least three class I PI3K isoforms is required to effectively regulate human neutrophil apoptosis (Juss et al., 2012). In view of this finding, the effects of combinations of multiple isoform-selective class I PI3K inhibitors on RV-induced inflammatory responses were then examined. In agreement with the results obtained when the inhibitors were used individually (Figure 4.22), RV-triggered cytokine responses were least inhibited by p110α and p110γ combinations (Figure 4.23). Similar to the actions of 3-MA (Figure 4.1), inhibition of any two class I PI3K isoforms attenuated CCL5 generation more effectively than CXCL8 production (Figure 4.23). For example, inhibition of p110β and p110δ isoforms resulted in ~40% reduction of CCL5, but only ~25% reduction of CXCL8 production, in response to RV-1B infection (Figure 4.23B, E). Interestingly, the pan class I PI3K inhibitor PI-103, suppressed CXCL8 (by ~50%) and CCL5 (by ~70%) production more potently than combination of inhibitors targeting all four class I PI3K isoforms which only caused ~20% and ~35% reduction of CXCL8 and CCL5, respectively (Figure 4.23).

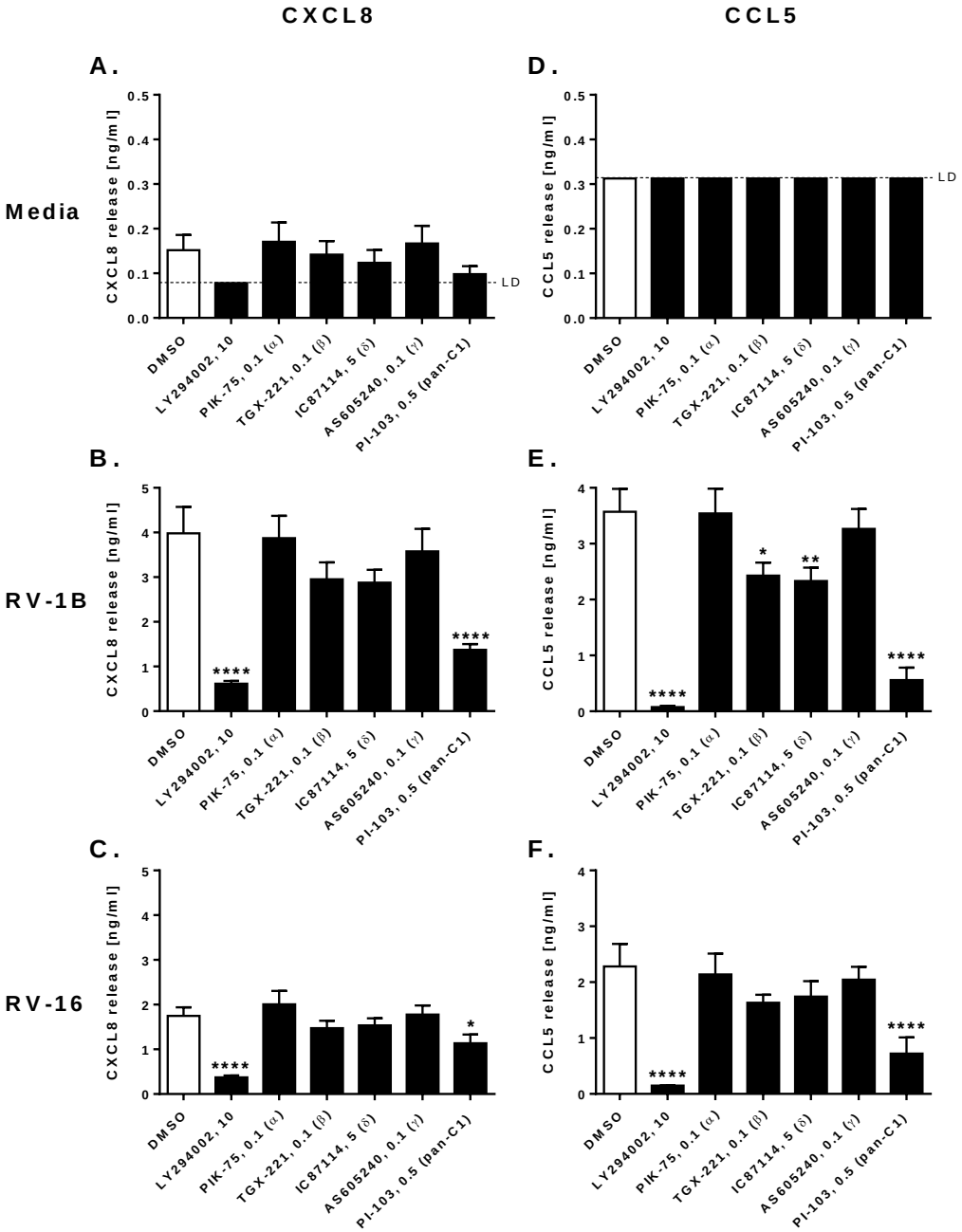

Figure 4. 22 Effects of isoform-selective class I PI3K inhibitors on RV-induced cytokine production in BEAS-2B cells.

BEAS-2B cells were left uninfected (A, D); or infected with RV-1B (B, E) or RV-16 (C, F) at $1x10^7$ $TCID_{50}$/ml for 1 h (following which supernatants were replaced with media). Cells were then immediately treated with DMSO control, or with the indicated PI3K inhibitors (the numbers shown after inhibitor names indicate the concentrations used in μM); and cultured for 24 h. Cell-free supernatants were collected, and CXCL8 (A, B, C) and CCL5 (D, E, F) release was measured by ELISA. Data shown are mean ± SEM of n = 4 independent experiments. Significant differences are indicated by *, $p < 0.05$; **, $p < 0.01$; and ****, $p < 0.0001$ (versus DMSO control), analysed by one-way ANOVA with Tukey's post-test [Abbreviation: C1 = class I inhibitor]. LD = limit of detection.

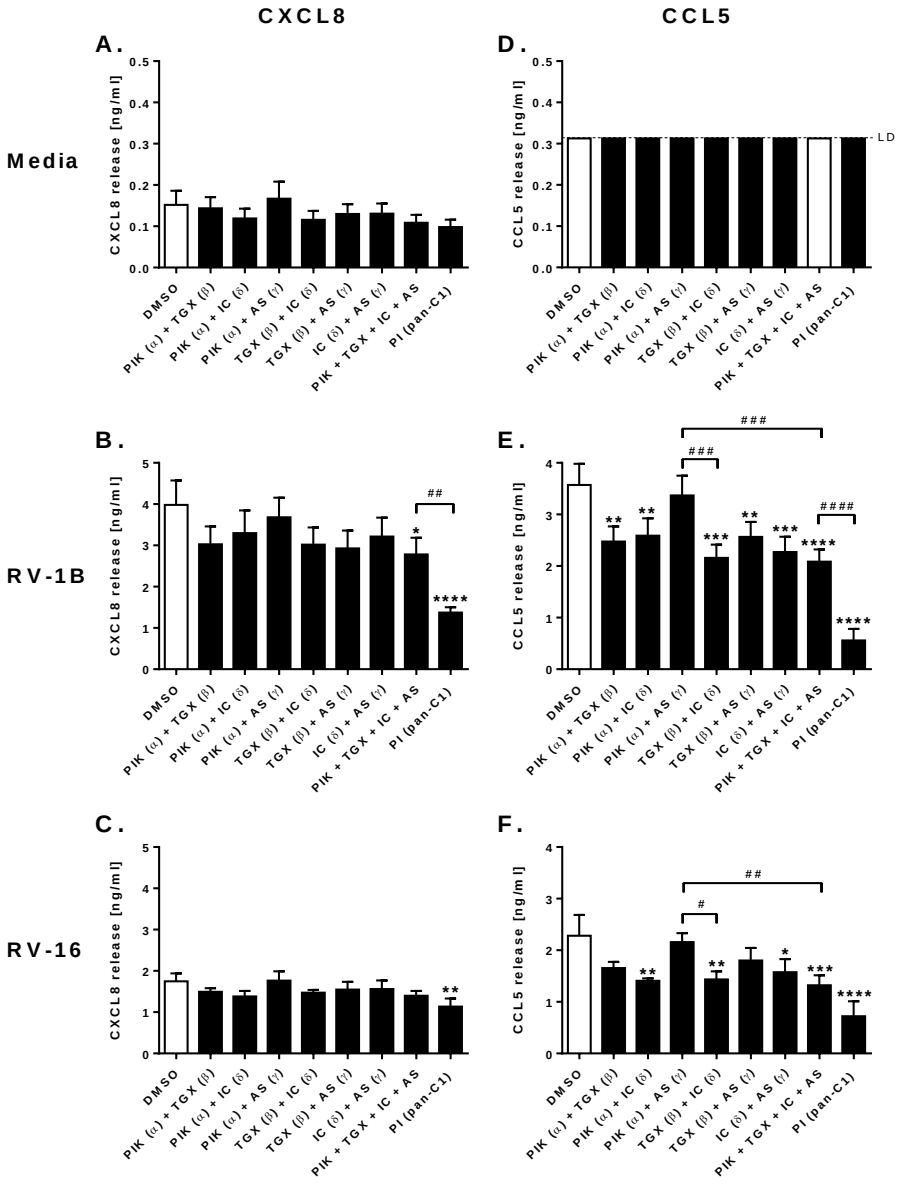

Figure 4. 23 Effects of combinations of multiple isoform-selective class I PI3K inhibitors on RV-induced cytokine production in BEAS-2B cells.

BEAS-2B cells were left uninfected (A, D); or infected with RV-1B (B, E) or RV-16 (C, F) at $1x10^7$ $TCID_{50}$/ml for 1 h (following which supernatants were replaced with media). Cells were then immediately treated with DMSO control, or with PIK-75 (PIK, 0.1 μM), TGX-221 (TGX, 0.1 μM), IC87114 (IC, 5 μM), AS605240 (AS, 0.1 μM) or PI-103 (PI, 0.5 μM), individually or in combination; and cells were then cultured for 24 h. Cell-free supernatants were collected, and CXCL8 (A, B, C) and CCL5 (D, E, F) release was measured by ELISA. Note that the data for DMSO controls and for the PI-103 alone are the same experimental data that are also displayed in Figure 4.21. Data shown are mean ± SEM of $n = 4$ independent experiments. Significant differences are indicated by *, $p < 0.05$; **, $p < 0.01$; ***, $p < 0.001$ and ****, $p < 0.0001$ (versus DMSO control); or #, $p < 0.05$; ##, $p < 0.01$; ###, $p < 0.001$ and ####, $p < 0.0001$; analysed by one-way ANOVA with Tukey's post-test [Abbreviation: C1 = class I inhibitor]. LD = limit of detection.

4.6.2 Knockdown of the sole class III PI3K, Vps34 does not inhibit RV-induced cytokine release, and does not increase the inhibition of cytokine production achieved by a combination of isoform-selective class I PI3K inhibitors in BEAS-2B cells

LY294002 is believed to target all three classes of PI3K: class I, II and III (Vlahos et al., 1994); whilst 3-MA has recently been shown to inhibit both class I and III PI3Ks (Lin et al., 2012, Wu et al., 2010). Having found that LY294002 and 3-MA could inhibit RV-induced cytokine production (Sections 4.3.1 and 4.6.1), I sought to combine the isoform-selective class I PI3K inhibitors tested above with knockdown of the class III PI3K enzyme, Vps34, as another strategy to elucidate the effect of simultaneous inhibition of class I and class III PI3Ks on cytokine responses.

Initially, a pilot experiment was conducted to assess at which time-point Vps34 protein knockdown is most efficient. BEAS-2B cells were left untransfected, incubated with the transfection reagent alone (mock), or transfected with a non-targeting scrambled control siRNA or siRNA targeting Vps34 at 100 nM. After 24, 48 or 72 h transfection, cells were lysed, total protein extracted, and western blotting for Vps34 and actin performed (Section 2.14). Based on a single experiment, expression of Vps34 protein was substantially suppressed after 48 h transfection, and was found to be further reduced at 72 h post-transfection (Figure 4.24).

Having determined the time-point at which Vps34 is effectively suppressed, the effects of Vps34 knockdown alone, or in combination with isoform-selective class I PI3K inhibitors, on RV-induced cytokine production were next examined. BEAS-2B cells were left untransfected, transfected with a non-targeting scrambled control siRNA, or transfected with siRNA targeting Vps34 at 100 nM. After 48 h transfection, cells were infected with RV at $1.0x10^7$ $TCID_{50}$/ml as described in Section 2.6.3. Cells were then either left untreated or treated with a combination of four isoform-selective class I PI3K inhibitors: PIK-75 (α) (0.1 μM), TGX-221 (β) (0.1 μM), IC87114 (δ) (5 μM) and AS605240 (γ) (0.1 μM), and cultured for 24 h. Cell-free supernatants were collected to determine cytokine release, as measured by ELISA (Section 2.15). Cells were also lysed, total protein extracted, and western blotting for Vps34 and actin performed (Section 2.14).

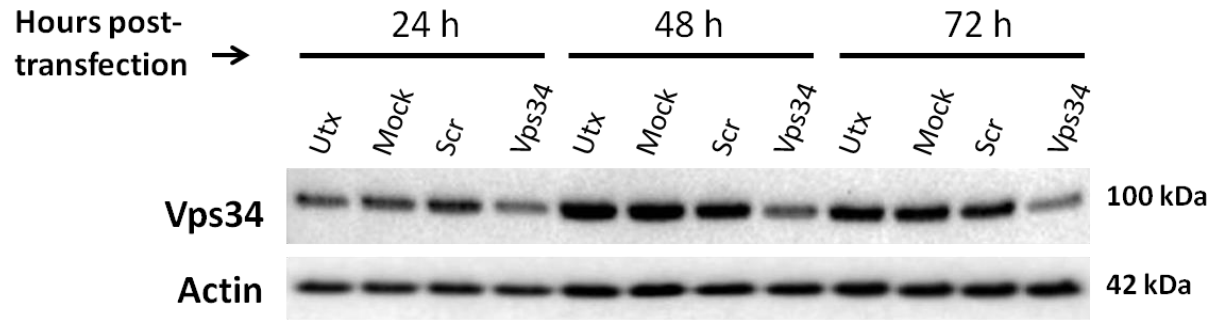

Figure 4. 24 Time-response of siRNA-mediated knockdown of the sole class III PI3K, Vps34.

BEAS-2B cells were either left untransfected (Utx), transfected with the transfection reagent alone (Mock); or transfected with a non-targeting scrambled control siRNA (Scr) or siRNA targeting Vps34 at 100 nM. After 24, 48 or 72 h transfection, whole-cell lysates were prepared and analysed by Western blot using Abs specific to Vps34 or actin. Data shown are $n = 1$.

Similar to the results obtained previously (Figure 4.23), a combination of all four isoform-selective class I PI3K inhibitors significantly reduced cytokine production induced by RV-1B or RV-16 infection (Figure 4.25). However, siRNA targeting of Vps34 did not affect cytokine generation, and did not intensify the inhibition of cytokine production achieved by a combination of class I PI3K inhibitors (Figure 4.25).

4.6.3 Simultaneous knockdown of class I PI3Ks p110β and p110δ does not inhibit RV-induced cytokine production in BEAS-2B cells

As described in Section 4.6.1, pharmacological inhibition of p110β or p110δ, but not p110α or p110γ, isoform of class I PI3K significantly suppressed CCL5 production, whilst inhibition of all four isoforms was required to significantly reduce both CXCL8 and CCL5 release. To try to definitively demonstrate the involvement of p110β and p110δ in modulating RV-induced cytokine responses, inhibition of both p110β and p110δ was next carried out using siRNA knockdown.

BEAS-2B cells were left untransfected, or transfected with a non-targeting scrambled control siRNA or siRNAs targeting both p110β and p110δ at 200 nM. After 48 h transfection, cells were infected with RV-16 at $1x10^7$ $TCID_{50}$/ml as described in Section 2.6.3. A parallel set of siRNA-transfected cells was lysed to verify protein knockdown at this time-point. After 24 h infection (i.e. 72 h post-transfection), cell-free supernatants were collected to determine cytokine release, as measured by ELISA (Section 2.15). Cells were also lysed, total protein extracted, and western blotting for p110β, p110δ and actin performed (Section 2.14).

As shown in Figure 4.26A, effective, although incomplete, knockdown of class I PI3K p110β was achieved after cells were transfected for 48 h (i.e. the time-point by which cells were infected with RV) and 72 h (i.e. 24 h post-infection). However, knockdown of p110δ could not be confirmed as the commercially available anti-p110δ antibodies tested did not generate clean westerns that would allow valid interpretation of levels of knockdown. With an assumption that p110δ was successfully knocked down (similar to that of p110β), simultaneous knockdown of both beta and delta isoforms of class I PI3K failed to inhibit cytokine production in response to RV-16 infection (Figure 4.26).

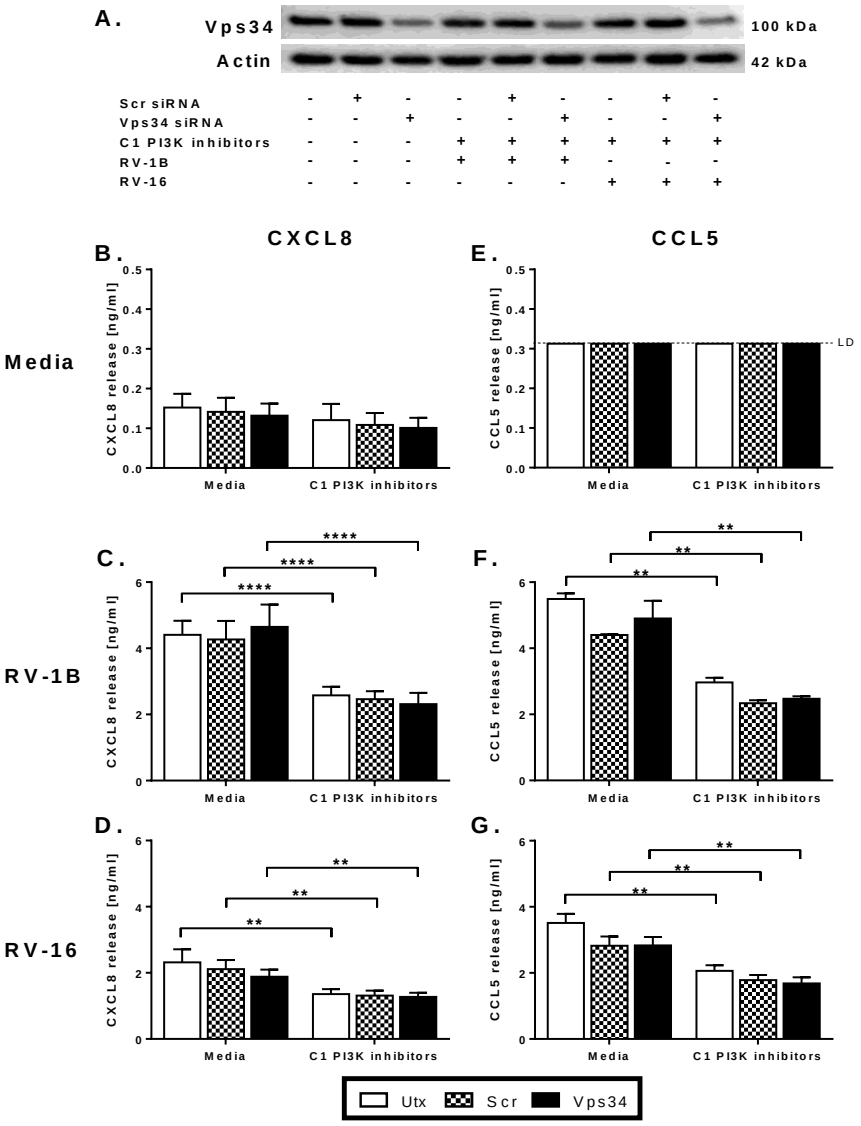

Figure 4. 25 Knockdown of the sole class III PI3K, Vps34 does not inhibit RV-induced cytokine release, and does not increase the inhibition of cytokine production achieved by a combination of isoform-selective class I PI3K inhibitors in BEAS-2B cells.

BEAS-2B cells were either left untransfected (Utx), or transfected with a non-targeting scrambled control siRNA (Scr) or siRNA targeting Vps34 at 100 nM. After 48 h transfection, cells were infected with RV-1B (C, F) or RV-16 (D, G) at $1x10^7$ $TCID_{50}$/ml for 1 h (following which supernatants were replaced with media). Cells were then either left untreated or treated with a combination of four isoform-selective class I (C1) PI3K inhibitors [PIK-75 (α) (0.1 μM), TGX-221 (β) (0.1 μM), IC87114 (δ) (5 μM) and AS605240 (γ) (0.1 μM)]; and cultured for 24 h. (A) Whole-cell lysates were analysed by Western blot using Abs specific to Vps34 or actin. Image shown is a representative blot of levels of Vps34 knockdown. Cell-free supernatants were collected, and CXCL8 (B, C, D) and CCL5 (E, F, G) release was measured by ELISA. Data shown are mean ± SEM of n = 3 independent experiments. Significant differences are indicated by **, $p < 0.01$ and ****, analysed by two-way ANOVA with Bonferroni's post-test. LD = limit of detection.

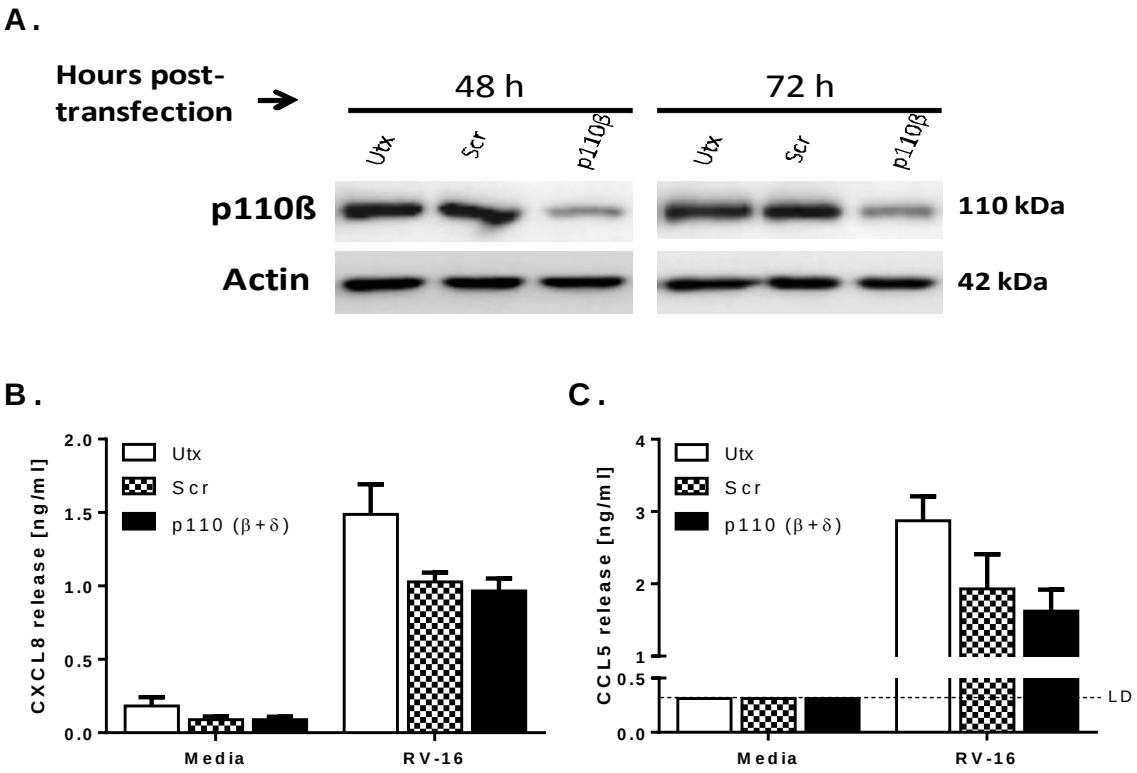

Figure 4. 26 Simultaneous knockdown of class I PI3Ks p110β and p110δ does not inhibit RV-induced cytokine production in BEAS-2B cells.

BEAS-2B cells were either left untransfected (Utx), or transfected with a non-targeting scrambled control siRNA (Scr) or siRNAs targeting p110β and p110δ at 200 nM. After 48 h transfection, cells were infected with RV-16 at $1x10^7$ $TCID_{50}$/ml for 1 h (following which supernatants were replaced with media); and cultured for 24 h. (A) Whole-cell lysates were analysed by Western blot using Abs specific to p110β or actin. A blot representative of 3 independent experiments is shown. Cell-free supernatants were also collected, and CXCL8 (B) and CCL5 (C) release was measured by ELISA. Data shown are mean ± SEM of n = 3 independent experiments. Knockdown of p110δ could not be confirmed by Western blot as there was no good p110δ antibody available. LD = limit of detection.

4.6.4 PI3K inhibitors LY294002 and PI-103 reduce viral replication

As the PI3K inhibitor 3-MA can inhibit viral replication (Section 4.3.3), the ability of LY294002, PI-103 and a cocktail of isoform-selective class I PI3K inhibitors to modulate viral replication was then studied. BEAS-2B cells were infected with RV-1B or RV-16 at $1x10^7$ $TCID_{50}$/ml as described in Section 2.6.3. Cells were then immediately treated with DMSO control, or with LY294002 (10 μM), PI-103 (0.5 μM) or a combination of four isoform-selective class I PI3K inhibitors [PIK-75 (α) (0.1 μM), TGX-221 (β) (0.1 μM), IC87114 (δ) (5 μM) and AS605240 (γ) (0.1 μM)]; and cultured for 24 h. Cells (~$6.1x10^5$) were lysed, cDNA synthesised and real-time qPCR for RV performed (Section 2.16-2.18). Samples were quantified against a standard curve of plasmids containing RV target sequence.

Similar to the effects of 3-MA (Section 4.3.3), both LY294002 and PI-103 markedly suppressed viral replication (by ~70% and ~40%, respectively), although statistical significance was only achieved for LY294002 (Figure 4.27). The combination of class I PI3K inhibitors only modestly reduced RV-1B replication by ~20% (Figure 4.27A), but did not affect RV-16 replication (Figure 4.27B).

4.6.5 LY294002 and PI-103 inhibit poly(I:C)-induced cytokine production in BEAS-2B cells

To ascertain if PI3K inhibition could regulate TLR3-dependent cytokine induction, independently of its ability to impede viral replication that could also result in reduced cytokine production, the effects of LY294002 and PI-103 on poly(I:C)-induced cytokine generation were investigated. BEAS-2B cells were stimulated with poly(I:C) at 1 or 10 μg/ml, and treated with DMSO control, or with LY294002 (10 μM) or PI-103 (0.5 μM); and cultured for 24 h. Cell-free supernatants were collected to determine cytokine release, as measured by ELISA (Section 2.15).

The PI3K inhibitor LY294002 significantly inhibited CXCL8 and CCL5 production induced by poly(I:C) (Figure 4.28). Comparable to the actions of 3-MA, PI-103 suppressed CCL5 production (Figure 4.28B) more potently than CXCL8 generation (Figure 4.28A).

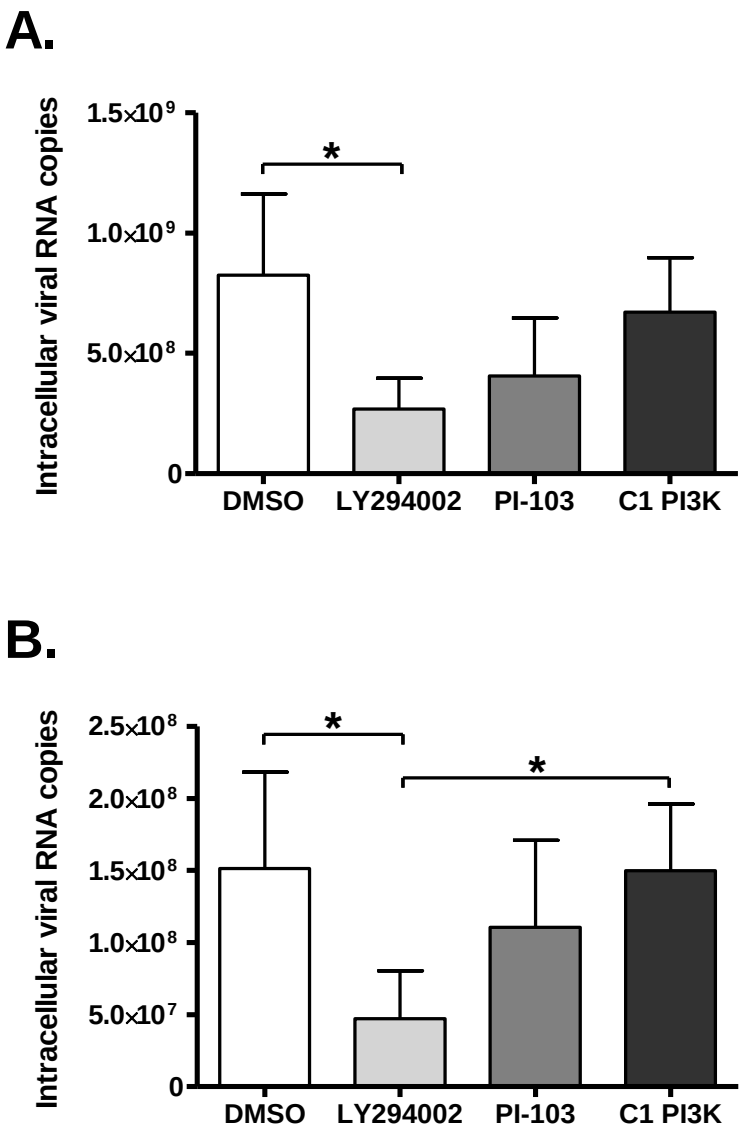

Figure 4. 27 PI3K inhibitors LY294002 and PI-103 reduce viral replication in BEAS-2B cells.

BEAS-2B cells were infected with RV-1B (A) or RV-16 (B) at $1x10^7$ $TCID_{50}$/ml for 1 h (following which supernatants were replaced with media). Cells were then immediately treated with DMSO control, or with LY294002 (10 μM), PI-103 (0.5 μM) or a combination of four isoform-selective class I (C1) PI3K inhibitors [PIK-75 (α) (0.1 μM), TGX-221 (β) (0.1 μM), IC87114 (δ) (5 μM) and AS605240 (γ) (0.1 μM)]; and cultured for 24 h. RNA was extracted and reverse transcribed for qPCR analysis of HRV RNA expression, with data presented as the total intracellular viral RNA copies per well. Data shown are mean ± SEM of $n = 4$ independent experiments. Significant differences are indicated by *, $p < 0.05$, analysed by one-way ANOVA with Tukey's post-test.

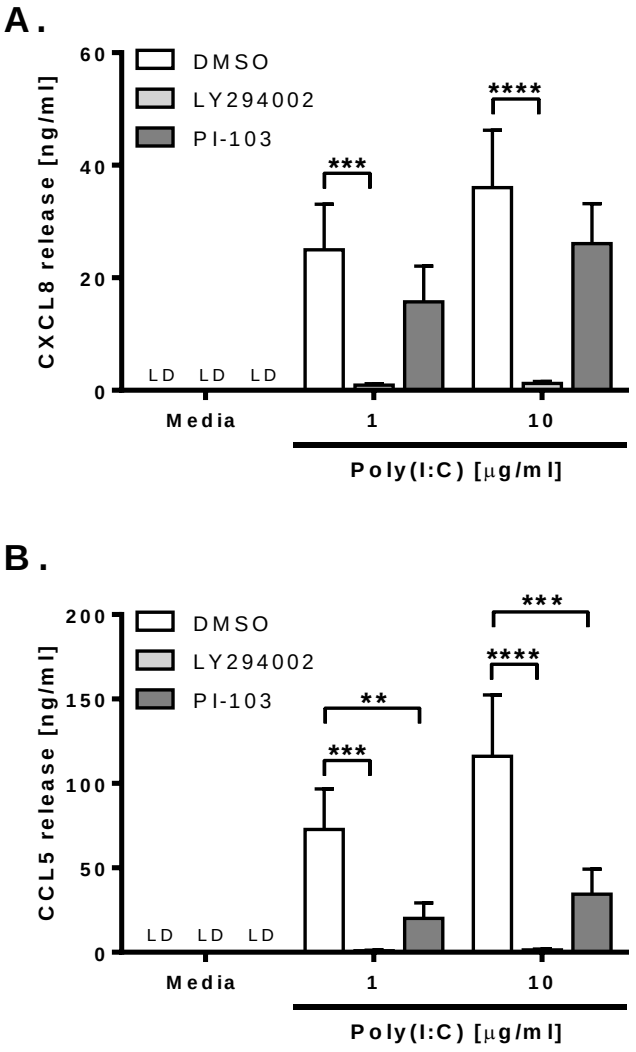

Figure 4. 28 LY294002 and PI-103 inhibit poly(I:C)-induced cytokine production in BEAS-2B cells.

BEAS-2B cells were stimulated with poly(I:C) at the indicated concentrations and treated with DMSO control, or with LY294002 (10 µM) or PI-103 (0.5 µM). After 24 h, cell-free supernatants were collected, and release of CXCL8 (A) and CCL5 (B) were measured by ELISA. Data shown are mean ± SEM of n = 4 independent experiments. Significant differences are indicated by **, $p < 0.01$; ***, $p < 0.001$ and ****, $p < 0.0001$, analysed by two-way ANOVA with Bonferroni's post-test. LD = limit of detection.

4.6.6 3-MA also targets IFN signalling pathways

Having found that PI3K inhibition, rather than effects on autophagy, appeared to account for the results obtained using 3-MA, I then returned to study 3-MA and examine its ability to regulate other pathways that are involved in antiviral immunity. A serine/threonine protein kinase, Akt, is the best studied downstream effector of PI3K (reviewed in Manning and Cantley, 2007). PI3K and Akt pathways have been shown to modulate the cellular responses to IFNs (Kaur et al., 2008a). I therefore wished to explore if the inhibitory actions of 3-MA is due to its direct effects on TLR3 signalling, or through additional inhibition of the resulting autocrine IFN signalling. Thus, I sought to examine whether exogenous IFN could rescue the poly(I:C)-induced cytokine generation, in the presence of 3-MA. BEAS-2B cells were stimulated with poly(I:C) at 1 or 10 μg/ml, and treated with IFN-β (100 ng/ml), 3-MA (3 mM) or IFN-β/3-MA in combination; and cultured for 24 h. Cell-free supernatants were collected to determine cytokine release, as measured by ELISA (Section 2.15).

No production of CXCL8 or CCL5 was observed upon treatment with exogenous IFN-β alone (Figure 4.29). However, IFN-β augmented the production of CCL5 induced by poly(I:C) (Figure 4.29B). Interestingly, IFN-β treatment was able to rescue the production of CXCL8 induced by poly(I:C) that had been impaired by 3-MA (Figure 4.29A), and partially rescue the actions of 3-MA on the generation of CCL5 (Figure 4.29B). These data imply that the effects of 3-MA may be mediated at least in part through targeting of IFN signalling.

4.7 Rapamycin, an mTOR inhibitor, reduces RV- or poly(I:C)-induced cytokine production in BEAS-2B cells

The serine/threonine protein kinase, mTOR, is one of the downstream targets of the class I PI3Ks, and is involved in many cellular processes including protein synthesis and cell proliferation (reviewed in Sarbassov et al., 2005). As mentioned in Section 4.4.2, mTOR also serves as an autophagy suppressor (reviewed in Meijer and Codogno, 2004) (See Section 1.9.2.2 for the role of mTOR signalling in autophagy modulation). I noted that both LY294002 and PI-103 can also directly inhibit mTOR at the concentrations used in this study (Brunn et al., 1996, Knight et al., 2006), and 3-MA can inhibit mTOR via inhibition of PI3K function (Wu et al., 2010). It was therefore hypothesised that the inhibitory effect of

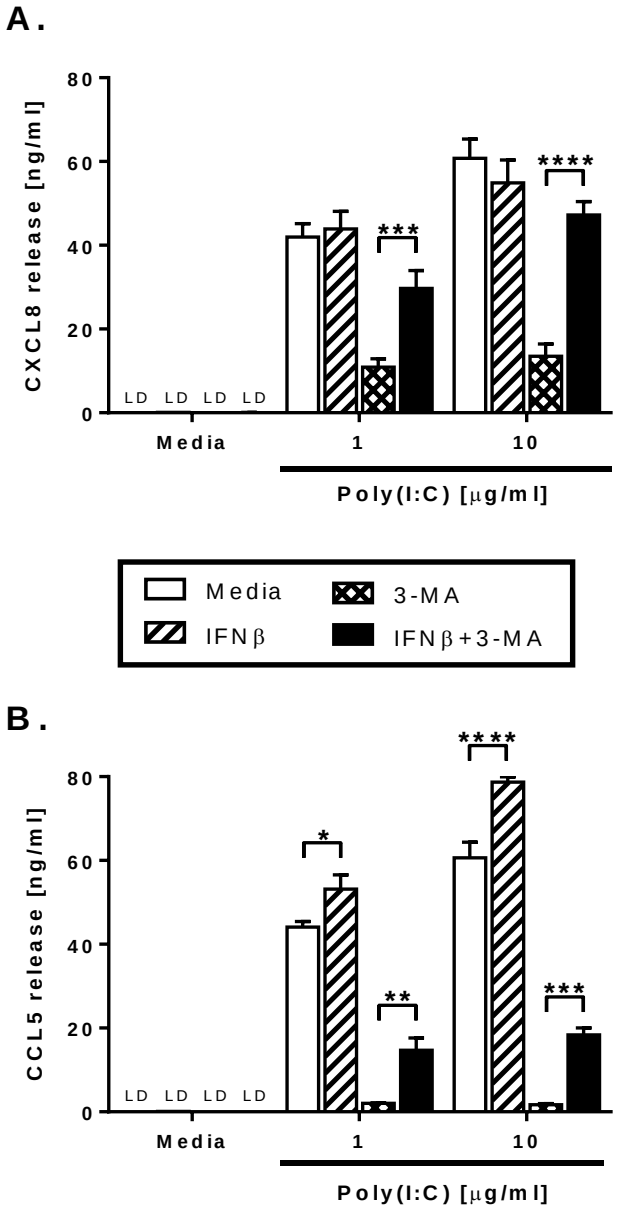

Figure 4. 29 3-MA in part targets IFN signalling pathways in BEAS-2B cells.
BEAS-2B cells were stimulated with poly(I:C) at the indicated concentrations and treated with IFN-β (100 ng/ml), 3-MA (3 mM) or IFN-β/3-MA in combination. After 24 h, cell-free supernatants were collected, and release of CXCL8 (A) and CCL5 (B) were measured by ELISA. Data shown are mean ± SEM of n = 4 independent experiments. Significant differences are indicated by *, $p < 0.05$; **, $p < 0.01$; ***, $p < 0.001$ and ****, $p < 0.0001$, analysed by two-way ANOVA with Bonferroni's post-test. LD = limit of detection.

LY294002, PI-103 and 3-MA on cytokine responses might be partly due to mTOR inhibition. To test this hypothesis, rapamycin, an mTOR inhibitor, was utilised.

BEAS-2B cells were infected with RV-16 at $1x10^7$ $TCID_{50}$/ml as described in Section 2.6.3, or stimulated with poly(I:C) at 10 μg/ml. Cells were then immediately treated with rapamycin at 100 or 200 nM, and cultured for 24 h. Cell-free supernatants were collected to determine cytokine release, as measured by ELISA (Section 2.15). As shown in Figure 4.30, rapamycin suppressed CCL5 generation, and to a lower degree CXCL8 generation, induced by RV-16 infection or poly(I:C) stimulation.

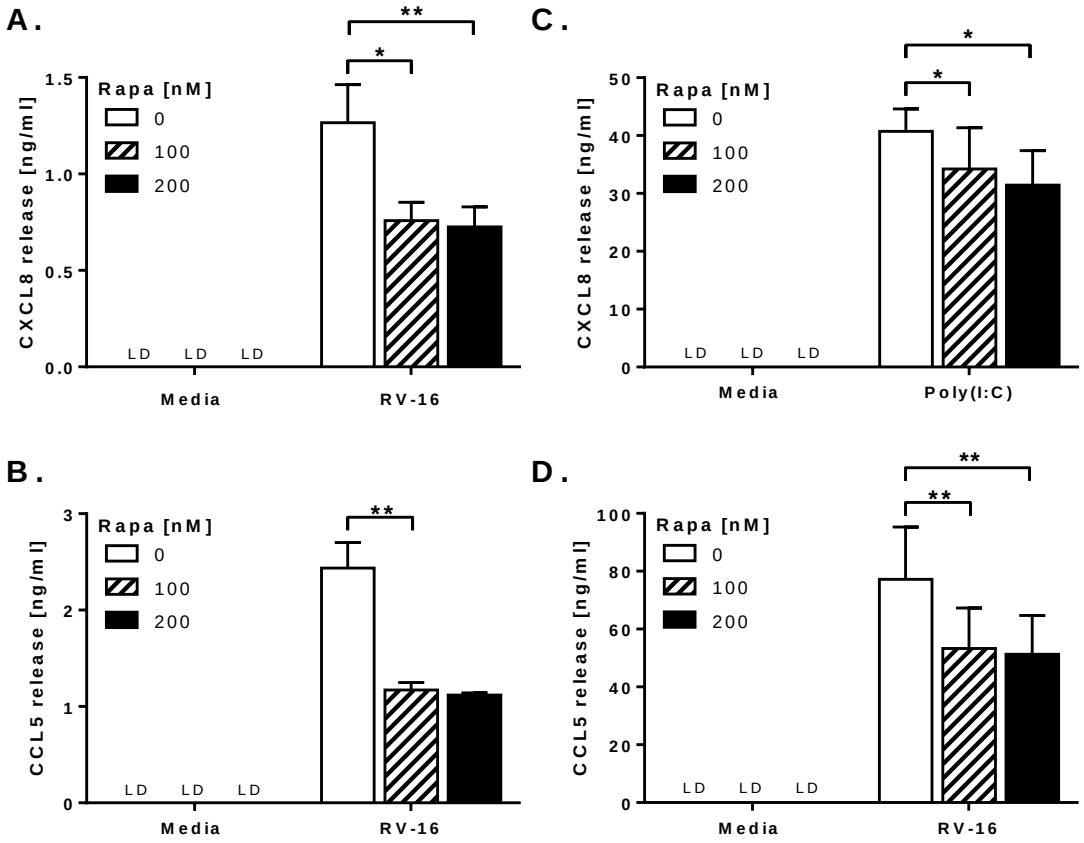

Figure 4. 30 Rapamycin reduces RV- or poly(I:C)-induced cytokine production in BEAS-2B cells.

BEAS-2B cells were infected with RV-16 at $1x10^7$ $TCID_{50}$/ml for 1 h (following which supernatants were replaced with media) (A, B), or stimulated with poly(I:C) at 10 µg/ml (C, D). Cells were then immediately treated with rapamycin at the indicated concentrations and cultured for 24 h. Cell-free supernatants were collected, and release of CXCL8 (A, C) and CCL5 (B, D) were measured by ELISA. Data shown are mean ± SEM of $n = 3$ independent experiments. Significant differences are indicated by *, $p < 0.05$ and **, $p < 0.01$, analysed by two-way ANOVA with Bonferroni's post-test. LD = limit of detection.

4.8 Discussion

4.8.1 Summary

The results presented in this chapter show for the first time that the PI3K pharmacological inhibitor 3-MA, typically used to inhibit autophagy, suppressed RV-induced cytokine production in airway epithelial cells. In contrast to the actions of 3-MA, specific targeting of the autophagy proteins Bec1, LC3, Atg7, or the autophagy-specific class III PI3K Vps34 by siRNA had very modest effects on RV-induced cytokine responses. Knockdown of autophagy proteins by siRNA also had minimal effects on RV replication. However, it was found that RV infection induced autophagy in the airway epithelial cells, although additional work is required to confirm this finding. Subsequent experiments performed using a panel of broad and class I-selective PI3K small-molecule inhibitors demonstrated functional redundancy of class I PI3K isoforms in modulating the RV-induced inflammation. The PI3K inhibitors 3-MA and LY294002 also remarkably reduced viral replication, suggesting that PI3Ks exert their roles in controlling RV infection via multiple mechanisms. Moreover, preliminary data suggests a potential role for mTOR in regulating the proinflammatory responses to RV infection.

4.8.2 The role of autophagy in responses to RV infection

TLR3 recognises RV dsRNA, formed during viral replication (Wang et al., 2009, Slater et al., 2010). However, how the cytosolic dsRNA gains access to the endosome where TLR3 resides remains unclear. Autophagy is a PI3K-dependent pathway that involves sequestration of cytosolic damaged organelles and unused proteins in double-membrane vesicles termed autophagosomes, and the autophagic cargo is later delivered to lysosomes for degradation and recycling of amino acid pools (reviewed in Codogno et al., 2012) (Section 1.8). Beyond its key function in cellular homeostasis, autophagy has recently been shown to participate in antiviral innate immunity via multiple mechanisms, such as by directly entrapping and degrading virions and virion components (a process termed xenophagy), and by mediating the detection of cytosolic viral RNAs by endosomal TLRs (reviewed in Deretic et al., 2013, Jordan and Randall, 2011). In VSV infection, the production of antiviral IFN-α by murine plasmacytoid DCs was found to be dependent upon the autophagic delivery of viral

replication intermediates to endosomal TLR7 (Lee et al., 2007). However, whether autophagy is required for the presentation of cytoplasmic dsRNA to the TLR3-containing endosomes remains unknown. Therefore, the present study aimed to examine if the TLR3-mediated inflammatory responses to RV infection are dependent upon the autophagy pathway, and to investigate whether autophagy is involved in the control of RV replication.

In the context of COPD, increasing evidence suggests that autophagy may play a complex role in this lung disease, by which autophagy may cause either a favourable or deleterious phenotype depending on the disease process (reviewed in Mizumura et al., 2012, Haspel and Choi, 2011). Chen and colleagues demonstrated that autophagy was augmented in lung tissue samples derived from patients with COPD at all stages of disease severity (GOLD stage 0 to 4) (Chen et al., 2008). The authors also showed that autophagy was increased *in vitro* in normal primary HBECs exposed to CSE, and *in vivo* in the lungs of mice that were chronically exposed to cigarette smoke (Chen et al., 2008). The same group also found that autophagy and apoptosis were concomitantly activated in the BEAS-2B lung epithelial cell line in response to CSE treatment (Kim et al., 2008). Taken together, these studies provide evidence of the adverse effects of autophagy on COPD, by triggering lung epithelial cell death commonly associated with the development of emphysema, a key condition seen in COPD (See Section 1.1.1). In contrast to the previous results obtained in CSE-treated-lung epithelial cells (Chen et al., 2008, Kim et al., 2008), a recent study by Monick *et al.* demonstrated that autophagic activity was impaired in alveolar macrophages isolated from either patients with COPD, actively smoking patients without COPD (with a greater than 10 pack-year smoking history) or non-smokers; following CSE treatment (Monick et al., 2010). It is possible that the pathophysiological roles of autophagy are cell-type specific.

Since airway epithelial cells are known to be the primary site of RV infection and replication (Papadopoulos et al., 2000, reviewed in Jackson and Johnston, 2010), this study utilised this cell type to investigate the potential role for autophagy in mediating RV-induced inflammatory responses. Furthermore, RV-induced acute exacerbations of COPD are initially mediated by the proinflammatory cytokines produced by airway epithelial cells (reviewed in Papi et al., 2007, Mallia and Johnston, 2006) (Section 1.3.3).

4.8.2.1 Autophagy has little role in the cytokine response to RV or control of RV replication in airway epithelial cells

Whilst studies exploring the involvement of autophagy in RV replication have been reported (Klein and Jackson, 2011, Brabec-Zaruba et al., 2007, Jackson et al., 2005), there are no studies to date specifically investigating the roles of autophagy in the induction of cytokine responses to RV infection. Meanwhile, autophagy has been shown to play a role in regulating the production of proinflammatory cytokines and type I IFNs in response to other viral infections including RSV (Morris et al., 2011), VSV (Lee et al., 2007), coxsackie virus (Gorbea et al., 2010), simian virus 5 (Manuse et al., 2010), avian influenza virus H5N1 (Pan et al., 2013), and HIV-1 (Zhou et al., 2012).

To begin exploring the effects of inhibition of autophagy on RV-induced innate cytokine production, I initially utilised 3-MA, which whilst originally thought of as a specific inhibitor of class III PI3K (and thus autophagy), is now known to be able to inhibit class I PI3K (Lin et al., 2012, Wu et al., 2010). However, 3-MA is still a commonly used approach to inhibit autophagy. In fact, it was utilised by the two studies investigating the requirement for autophagy in RV replication (Klein and Jackson, 2011, Brabec-Zaruba et al., 2007), and by several studies investigating the role of autophagy in the responses to other viral infections such as RSV (Morris et al., 2011), VSV (Lee et al., 2007) and coxsackie virus (Gorbea et al., 2010, Wong et al., 2008). In this thesis, it was found that 3-MA suppressed production of CXCL8, IFN-β and the IFN-stimulated gene CCL5 in the BEAS-2B airway epithelial cells, in response to RV infection (discussed further in Section 4.8.3).

Inhibition of autophagy was then performed using a more specific approach, siRNA, by which proteins crucial to this pathway (i.e. Bec1, Atg7 and LC3) were knocked down using this technique. The autophagy-related proteins were chosen for their vital roles during the nucleation, elongation and closure of autophagosomes (reviewed in Codogno et al., 2012) (See Figure 1.8 for the schematic diagram of the autophagy pathway). Initially, confirmation was sought that targeting of these proteins could indeed inhibit autophagy. Although total knockdown of the autophagy-related proteins Bec1 and Atg7 was not achieved, suppression of these proteins by siRNAs resulted in the reduction of basal autophagy and nutrient starvation-induced autophagy.

In contrast to the actions of 3-MA, knockdown of Bec1 or Atg7 had only modest effects on RV-induced CXCL8 production, with no effects on CCL5 generation; whilst knockdown of LC3 failed to inhibit both CXCL8 and CCL5 release from the BEAS-2B airway epithelial cells. This led to the hypothesis that the inhibitory actions of the pharmacological inhibitor 3-

MA on RV-induced cytokine production might not be due to autophagy inhibition, and in fact the subsequent experiments suggested that 3-MA might exert its inhibitory effects on RV-induced cytokine responses via class I PI3K inhibition (discussed further in Section 4.8.3). Furthermore, to improve the targeting of the autophagy pathway, another member of our research group has conducted experiments with dual siRNA-mediated knockdown of Bec1 and Atg7; and the results showed no additional effects on RV-induced cytokine generation when both siRNAs were combined (Ismail et al., 2014). This is the first study to demonstrate that autophagy is not involved in the cytokine responses to RV infection, whilst previous studies have reported that autophagy is required for the cytokine induction upon other viral infections. Morris *et al*. showed that in Bec1-deficient mice, or murine DCs deficient in LC3 following siRNA-mediated knockdown, the production of several innate cytokines was reduced, including IL-6, TNF-α, IFN-β and CCL5, in response to infection with RSV, which is also a respiratory virus (Morris et al., 2011). Furthermore, a study by Lee and colleagues demonstrated that DCs isolated from Atg5-deficient mice secreted less IFN-α following VSV infection, as compared to the control mice (Lee et al., 2007).

Our group has recently shown that autocrine release of the proinflammatory cytokine IL-1β by RV-infected airway epithelial cells can amplify CXCL8 production (Stokes et al., 2011, Piper et al., 2013). Therefore, one potential explanation for the current finding that inhibition of autophagy only modestly affected RV-induced CXCL8 generation, without impairing production of CCL5, is due to the direct roles of autophagy in mediating IL-1β processing and secretion (Dupont et al., 2011, Harris et al., 2011) (discussed further in Section 4.8.2.2). Autophagy inhibition would result in lower release of RV-induced IL-1β from epithelial cells consequently suppressing production of CXCL8 by these cells.

There have been conflicting reports in the literature on the requirement for autophagy in RV replication. In their studies of RV-2 (a minor group of RV), Brabec-Zaruba *et al.* showed that this particular serotype of RV does not induce autophagy and that modulation of autophagy does not affect viral replication (Brabec-Zaruba et al., 2007). In contrast, another group has demonstrated that RV-2 and RV-14 (a major group of RV) induce autophagosome formation and that both RV serotypes exploit the autophagy machinery to favour their replications (Klein and Jackson, 2011, Jackson et al., 2005). The two separate groups suggested that the potential reasons for the conflicting data could be due to the different assays used to monitor autophagy induction, and the different concentrations of viruses and pharmacological

autophagy inhibitors used (Brabec et al., 2006, Klein and Jackson, 2011, Jackson et al., 2005). However, these three previously published studies were performed using HeLa cells, a human cervical epithelial cell line, and since RV is a natural respiratory tract pathogen, it would be of greater relevance to explore the roles of autophagy in RV infection of airway cells. This study aimed to investigate if autophagy could still regulate viral replication in the absence of modulation of cytokine generation in BEAS-2B airway epithelial cells. For the first time, the current study showed that knockdown of autophagy protein Bec1 or Atg7 did not impede RV replication in airway epithelial cells, consistent with the data obtained by Brabec-Zaruba and colleagues using HeLa cells (Brabec-Zaruba et al., 2007).

Taken together, this study is the first to show that autophagy is not important in the control of inflammatory responses to RV or control of RV replication in the airway epithelial cells. Although one may argue that a role for autophagy in regulating RV-induced responses was not seen due to the incomplete knockdown of Bec1, Atg7 or LC3, the finding that siRNA-mediated suppression of Bec1 or Atg7 protein resulted in the reduction of basal autophagy and nutrient starvation-induced autophagy suggests otherwise. Furthermore, subsequent experiments suggested that the inhibitory effects of 3-MA (traditionally used to inhibit autophagy) on RV-induced cytokine production was due to its effects beyond the class III PI3K enzyme, potentially via targeting of the class I PI3K family (discussed further in Section 4.8.3).

4.8.2.2 The modest decrease of RV-induced CXCL8 production upon autophagy inhibition may be due to the roles of autophagy in regulating IL-1β production and secretion

As discussed in Section 4.8.2.1, siRNA-mediated knockdown of autophagy proteins Bec1 and Atg7 only modestly reduced CXCL8, and did not affect CCL5, production in RV-infected airway epithelial cells. One potential explanation may be the direct roles of autophagy in regulating IL-1β processing and secretion (Dupont et al., 2011), and indeed our group has demonstrated that autocrine release of IL-1β by RV-infected airway epithelial cells can augment CXCL8 expression (Stokes et al., 2011, Piper et al., 2013). Our group also revealed that addition of IL-1ra, the specific antagonist of IL-1R1 (the receptor for IL-1β; see Section 1.5), reduced RV-1B-induced CXCL8 generation in BEAS-2B airway epithelial cells (Stokes et al., 2011). Furthermore, similar results were obtained in MyD88-deficient cells (MyD88 is an important adaptor protein involved in IL-1β signalling; see Section 1.5.1)

(Stokes et al., 2011). A related study performed by our collaborators using primary HBECs demonstrated that addition of IL-1ra completely inhibited the production of CXCL8 and IL-6, without affecting CXCL10 generation (Piper et al., 2013). Meanwhile, Dupont and coworkers showed that autophagy was involved in the unconventional secretion of IL-1β in murine bone marrow-derived macrophages (Dupont et al., 2011). The group found that starvation-induced autophagy enhanced IL-1β secretion and that blocking autophagosome maturation using bafilomycin A1 reduced the IL-1β release from the starvation-treated cells. Using immunofluorescence confocal microscopy, they discovered that IL-1β and the key marker of autophagosomes, LC3, colocalised. The authors also discovered that autophagy can capture cytosolic IL-1β and mediates its release via an unconventional secretory pathway that is dependent on the Golgi reassembly stacking protein (GRASP) and post-Golgi membrane trafficking and exocytosis regulator, Rab8a (Dupont et al., 2011).

Collectively, although autophagy is not directly involved in the cytokine induction in response to RV infection (particularly for antiviral cytokines) (Section 4.8.2.1), the current data in conjunction with previous studies suggest that autophagy inhibition could modestly reduce RV-induced CXCL8 generation by inhibiting autocrine IL-1β production and secretion. Further investigation is needed to verify this proposed mechanism and if positive results were obtained, this would then imply that therapeutic targeting of autophagic pathway may reduce the virally induced, CXCL8-mediated, neutrophilic inflammation caused by the proinflammatory cytokine IL-1β, without affecting the antiviral arm of the innate immune response.

4.8.2.3 RV infection induces autophagy in airway epithelial cells

There have been conflicting data in the literature on the ability of RV to promote autophagy. In their studies of RV-2 (a minor group RV serotype), Brabec-Zaruba *et al.* showed that this particular serotype of RV did not induce autophagy (Brabec-Zaruba et al., 2007). In contrast, another group demonstrated that RV-2 and RV-14 (a major group RV serotype) induced autophagosome formation (Klein and Jackson, 2011, Jackson et al., 2005); although the groups more recent publication also showed that RV-1A, another minor group RV serotype, did not promote autophagy (Klein and Jackson, 2011). However, again these published studies were performed using HeLa cells, a human cervical epithelial cell line. It would be of greater relevance to perform the experiments using the natural host cell of RV, the airway

epithelium. Therefore, this study aimed to investigate if RV could promote autophagy in the airway epithelial cells.

The most widely used indication of autophagic activation is the modification of the cellular protein LC3 from a cytosolic form (LC3-I) to a membrane-bound form (LC3-II) (reviewed in Klionsky et al., 2012). LC3-II protein levels can be detected by several techniques, however the easiest and cheapest approach is by western blotting. Hence this assay was first utilised in this study. BEAS-2B airway epithelial cells were infected with RV, and autophagy induction was assessed at 6 h and 24 h p.i. as previous studies have shown that RV significantly induced autophagy in cervical epithelial HeLa cells at these two time-points (Klein and Jackson, 2011, Brabec-Zaruba et al., 2007). Initially, it was found that RV infection only caused a subtle increase of LC3-II protein in the airway epithelial cells, as analysed by western blotting (Section 4.4.1). Meanwhile, levels of LC3-II were significantly increased by bafilomycin A1 (an inhibitor of autophagosomal degradation), indicating that autophagy was basally active in BEAS-2B cells. Having found that RV only caused a very modest increase of autophagic activity (as determined by western blotting), further experiments were then carried out to examine if significant increases in LC3-II expression could be detected in BEAS-2B cells using other known autophagy stimuli (i.e. rapamycin, nutrient starvation and CSE) (Sections 4.4.2-4.4.4). Furthermore, it was crucial to find a reliable and reproducible technique to measure autophagy and an effective autophagy stimulus prior to performing the subsequent autophagy protein knockdown experiments (Section 4.5) (these optimisation experiments are discussed further in the following paragraph). Of note, in the subsequent LC3-II knockdown experiments (Section 4.5.3) a lower concentration of RV significantly upregulated LC3-II expression, although further work using a range of viral concentrations is required to confirm this finding. Moreover, a report was published during the course of this work showing that RV-16 infection induced autophagy in NCI-H292 cells, which is also a human lung epithelial cell line (Wu et al., 2013); hence supporting the data obtained in the present study.

As mentioned earlier, several optimisation experiments were performed to find a good assay to monitor autophagic activity and an effective autophagy stimulus, prior to conducting autophagy protein knockdown experiments. However, methods for assessing autophagy are not straight-forward (reviewed in Klionsky et al., 2012, Mizushima et al., 2010). In contrast to previous studies (Zhu et al., 2013a, Zhang et al., 2012), increased levels of LC3-II were not

seen when the BEAS-2B cells were treated with the autophagy stimuli rapamycin and nutrient starvation; as detected by western blotting. The reasons for not seeing increased LC3-II levels remain unknown. As nutrient starvation and rapamycin failed to induce autophagy when assessed by LC3 western blotting another technique commonly used to monitor autophagic activity (i.e. fluorescence microscopy) was then utilised. Accumulation of GFP-tagged-LC3 puncta in cells transfected with GFP-LC3-expressing plasmids is a widely accepted marker of autophagosome formation (reviewed in Mizushima et al., 2010) and was therefore used in the present study. This study also utilised CSE as another autophagy stimulus as it has been shown to activate autophagy in BEAS-2B cells (Hwang et al., 2010, Chen et al., 2008). It was found that the transfection efficiencies (indicated by the percentage of GFP-expressing cells) were relatively low, and varied between samples. CSE, rapamycin or nutrient starvation treatment failed to induce formation of exogenous GFP-LC3 puncta; regardless of whether the cells were fixed prior to visualisation, or visualised live. The explanations for not observing increased levels of LC3 puncta as analysed by fluorescence microscopy are unclear, although it could be merely because the experimental protocol was not optimised. As discussed in a recent extensive review article detailing the use and interpretation of assays for measuring autophagy (Klionsky et al., 2012), the main reason exogenous GFP-LC3 transfection assay is used by many studies to monitor autophagy induction (and therefore used in the present work) is because endogenous LC3 protein is not always detectable by fluorescence microscopy, due to its very low expression in certain cell types. However, the initial attempt to monitor autophagy induction using GFP-LC3 transfection assay was unsuccessful, thus autophagic activity was subsequently determined by detecting endogenous LC3 protein using fluorescence microscopy. Using the endogenous LC3-II staining assay, a markedly increased number of endogenous LC3 puncta were observed in cells exposed to nutrient starvation or torin2 (a newly characterised mTOR inhibitor that can induce autophagy). Accordingly, this approach was next utilised in the subsequent experiments to confirm the siRNA-mediated knockdown of autophagy proteins (Section 4.5.1). Due to time constraints, experiments using this technique to validate if RV infection could indeed promote autophagy in the lung epithelial cells have not been performed in this study. Other methods that can be used to assess autophagy are discussed in Section 4.8.5 (Limitations and future work).

Overall, this study shows that RV infection can induce autophagy in the airway epithelial cells; although further experiments using a different approach to measure autophagy (i.e.

endogenous LC3 staining) and a range of viral doses are required to validate this finding. The data also highlight the limitations associated with the methods used for measuring autophagic activity. In fact, in the extensive review on guidelines for monitoring autophagy (Klionsky et al., 2012), the authors pointed out that the success of assays used in autophagy research is highly dependent on the organisms, cell types, and experimental conditions.

4.8.2.4 Regulation of autophagy by type I IFNs

As discussed in Section 4.8.2.1, inhibition of the autophagic pathway by siRNA targeting autophagy specific proteins did not affect RV-induced type I IFN production, as judged by the induction of the ISG CCL5. However, whether virally-induced type I IFNs could regulate autophagy has not been explored in this study. To understand the interplay between autophagy and antiviral IFNs during viral infections, this section summarised some of the publications which have investigated this subject area.

Recent studies suggest a new role for the type I IFNs, IFN-α and IFN-β, in regulating autophagy (reviewed in Faure and Lafont, 2013, Deretic et al., 2013). As discussed in Section 4.8.2.3, consistent with the data obtained in this thesis, Wu and colleagues showed that RV-16 induced autophagy in the human airway epithelial cell line NCI-H292 cells (Wu et al., 2013). Importantly, the authors also demonstrated that exogenous IFN-β and IFN-λ1 (type III IFN) inhibited RV-16-induced autophagy in these airway epithelial cells, although the mechanism of action was not explored. For future work, it would be interesting to examine whether similar results would be obtained when exogenous IFNs are added to our RV-infected BEAS-2B airway epithelial cells. Another recent study by Buchser *et al.* also showed a negative regulation of autophagy by type I IFNs, with the authors demonstrating that IFN-α inhibited autophagy in several human cancer cell lines (Buchser et al., 2012).

In contrast, other studies have proposed type I IFNs as positive regulators of autophagy (reviewed in Faure and Lafont, 2013). Very recently, Zhu and colleagues showed that exogenous IFN-α induced autophagic flux in primary bone marrow mononuclear cells (BMMCs) obtained from patients with chronic myeloid leukaemia, via a pathway involving STAT1 and NF-κB, whereby both transcription factors could contribute to upregulation of Bec1 (Zhu et al., 2013b). A similar study done by Ambjorn *et al.* demonstrated that IFN-β induced autophagic flux in several human breast cancer cell lines, believed to be through inhibition of mTOR and activation of STAT1 signalling (Ambjorn et al., 2013). Additionally,

Schmeisser and coworkers showed that exogenous IFN-α could induce autophagy in various human cancer cell lines including lymphoma Daudi cells, brain cancer T98G cells, cervical epithelial HeLa cells and lung epithelial A549 cells; and further experiments performed using lymphoma Daudi cells suggested that the upregulation of autophagy by IFN-α was due to mTOR inhibition (Schmeisser et al., 2013).

In summary, the crosstalk between autophagy and type I IFN signalling appears to be complex, given that the type I IFNs can act as both positive and negative regulators of autophagic pathway. This complexity may relate to the important function of autophagy in cellular homeostasis, explaining why its activation is tightly regulated by many different factors and signalling systems.

4.8.3 The role of PI3Ks in responses to RV infection

As previously discussed in Section 4.8.2.1, I initially utilised 3-MA to inhibit autophagy, as it is commonly used in studies examining the roles of autophagy in various viral infections including RV (Klein and Jackson, 2011, Brabec-Zaruba et al., 2007), RSV (Morris et al., 2011), VSV (Lee et al., 2007) and coxsackie virus (Gorbea et al., 2010, Wong et al., 2008). Whilst formerly thought of as a specific inhibitor of class III PI3K (and thus autophagy), 3-MA is now known to be capable of inhibiting class I PI3K (Lin et al., 2012, Wu et al., 2010). The findings that 3-MA significantly reduced cytokine production in response to RV infection (Section 4.3.1), whilst specific knockdown of autophagy proteins by siRNAs did not affect RV-induced cytokine responses (Section 4.8.2.1) indicated that the inhibitory effects of 3-MA were not due to autophagy inhibition, but perhaps class I PI3Ks.

PI3Ks are lipid kinases that phosphorylate the 3-hydroxyl group of the inositol ring of three species of phosphatidylinositol (PtdIns) lipid substrates; namely, PtdIns, PtdIns4phosphate (PtdIns4P) and PtdIns4,5bisphosphate (PtdIns(4,5)P_2) (reviewed in Vanhaesebroeck et al., 2010, Okkenhaug, 2013). The newly formed 3-phosphorylated phosphoinositides act as second messenger molecules, which modulate the intracellular localisation and activity of various effector proteins. The most essential downstream effector of PI3K is the serine/threonine kinase Akt. The PI3K/Akt signalling pathway regulates many crucial cellular

responses including cell growth, proliferation, intracellular vesicle trafficking, autophagy and immunity (reviewed in McNamara and Degterev, 2011, Vanhaesebroeck et al., 2010).

There are eight mammalian PI3Ks which have been divided into three classes: class I, II and III; based upon structural characteristics and lipid substrate specificities (reviewed in Vanhaesebroeck et al., 2010, Okkenhaug, 2013) (See Figure 1.9). Members of the class I PI3K family are composed of a catalytic subunit (termed p110) and a regulatory subunit (p85-type, p101 or p87) (reviewed in Vanhaesebroeck et al., 2010, Okkenhaug, 2013). Class I PI3K isoforms are subdivided into class IA and class IB depending upon which regulatory subunit they employ. The class IA PI3Ks (p110α, p110β and p110δ) bind the p85 type of regulatory subunit, whilst the class IB PI3K (p110γ) binds one of two related regulatory subunits, p101 and p87 (See Figure 1.9). There are three isoforms of class II PI3Ks in mammals: C2α, C2β, andC2γ (See Figure 1.9). Class III PI3K has only one member, namely, Vps34. The protein kinase Vps15, which forms a complex with Vps34, has been identified as a regulatory protein, however its specific role in Vps34 regulation remains poorly understood (reviewed in Vanhaesebroeck et al., 2010, Okkenhaug, 2013) (See Figure 1.9) (See Section 1.9.1 for more description of PI3K classes).

4.8.3.1 Inhibition of class I, but not class III, PI3Ks reduces the cytokine response to RV infection

It was hypothesised that the discrepancies of the results obtained using the pharmacological inhibitor 3-MA and siRNAs to inhibit autophagy (Section 4.8.2.1) were due to the extended inhibitory effect of 3-MA on class I PI3K, as recently reported by two separate studies (Lin et al., 2012, Wu et al., 2010). Therefore, this study aimed to further explore the potential role for class I PI3Ks in regulating the inflammatory responses to RV by comparing the actions of 3-MA with those of a broad PI3K inhibitor, LY294002, a pan class I inhibitor, PI-103, and a panel of isoform-selective class I inhibitors.

Whilst the general PI3K inhibitor LY294002 and the pan class I inhibitor PI-103 markedly suppressed CXCL8 and CCL5 generation in response to RV-1B and RV-16 infection, inhibition of any individual class I PI3K isoform did not, with the exception of inhibition of p110β or 110δ, which significantly suppressed CCL5 generation induced by RV-1B (Section 4.6.1). Of note, all the PI3K inhibitors did not affect the cell death in untreated cells or in RV-infected cells. The results obtained using LY294002 are consistent with published studies

demonstrating that inhibition of PI3K using LY294002 decreased the CXCL8 production in response to RV-39 (a major group of RV), in 16HBE140 cells (also a human bronchial epithelial cell line) (Newcomb et al., 2005), although the group subsequently reported that this was due to the ability of LY294002 to block the internalisation of RV into the host cells (Newcomb et al., 2005, Bentley et al., 2007) (The potential involvement of PI3Ks in RV cellular entry is discussed further in Section 4.8.3.2). The same group also demonstrated that pretreatment of RV-infected mice with LY294002 reduced the percentage of neutrophils in BALF and several cytokines including murine CXCL8 homolog KC, macrophage-inflammatory protein (MIP)-2 and IFN-γ (Newcomb et al., 2008). The inhibitory effect of LY294002 on the ISG CCL5 observed in the current study is similar with a very recent publication which showed that LY294002 inhibited RV-16-induced CXCL10 generation in primary HBECs obtained from pediatric subjects (Cakebread et al., 2014). This present study is the first to show that PI-103 inhibited RV-cytokine productions, which is comparable with several previous reports showing the inhibitory effects of this PI3K inhibitor on cytokine generation in response to other microbial stimuli (Sly et al., 2009, Ivison et al., 2010, Wong et al., 2010). In their studies of human colorectal epithelial carcinoma cells, Ivison and colleagues reported that PI-103 inhibited CXCL8 production induced by bacterial flagellin (Ivison et al., 2010). Furthermore, a study done by Sly *et al.* showed that PI-103 suppressed the production of LPS-induced TNF-α in murine bone marrow-derived macrophages (Sly et al., 2009). Of note, similar to the effects of 3-MA, LY294002 and PI-103 inhibited CCL5 production more potently than CXCL8 generation (discussed further in Section 4.8.3.3).

A recently published article revealed that pharmacological inhibition of at least three class I PI3K isoforms is required to effectively regulate human neutrophil apoptosis (Juss et al., 2012). In view of this finding, the effects of combinations of multiple isoform-selective class I PI3K inhibitors on RV-induced inflammatory responses were then examined. In agreement with the results obtained when the inhibitors were used individually, RV-triggered cytokine responses were least inhibited by p110α and p110γ combinations. Again, inhibition of any two class I PI3K isoforms attenuated CCL5 generation more effectively than CXCL8 production; suggesting that PI3Ks play a more important role on the type I IFN signalling, as compared to the NF-κB-dependent signalling (discussed further in Section 4.8.3.3). Furthermore, the only combination of isoform-selective class I inhibitors which significantly suppressed RV-induced CXCL8 production, was that which targeted all of α, β, δ and γ isoforms, indicating functional redundancy amongst these isoforms; similar to the results

obtained in a recent publication showing their roles in the regulation of neutrophil apoptosis (Juss et al., 2012). Interestingly, the pan-class I PI3K inhibitor, PI-103, acted differently than the combination of all four isoform-selective class I inhibitors, but very similar to that of LY294002 and 3-MA. Studies have shown that LY294002, PI-103, and 3-MA can all inhibit class I and class III PI3Ks (Wu et al., 2010, Knight et al., 2006, Kong et al., 2010, Raynaud et al., 2007), implying that the actions of these chemical inhibitors on the RV-induced cytokine responses could be mediated upon both PI3K classes. However, in this study, PI-103 was used at 0.5 μM, and its IC_{50} for class III PI3K is 2.3-4 μM (Knight et al., 2006, Raynaud et al., 2007), indicating that PI-103 was unlikely to be affecting class III PI3K in the current experiments.

To further examine the hypothesis that class III PI3K was not engaged in cytokine responses to RV, which would also provide further evidence that autophagy is not involved in responses to RV (Section 4.8.2); the sole class III PI3K catalytic subunit, Vps34, was knocked down by siRNA, and cells were treated with a cocktail of isoform-selective class I PI3K inhibitors. For the first time, it was shown that knockdown of Vps34 did not increase the inhibition of cytokine production achieved by the class I PI3K inhibitors alone. This further highlights the lack of a role for class III PI3K, and by extension autophagy, in regulating the innate immune response to RV.

Although the most well-characterised and specific, isoform-selective class I PI3K inhibitors currently available were utilised, the present data could still be subject to unforeseen off-target effects (reviewed in Crabbe et al., 2007). siRNAs were then used to target the β or δ isoforms, the class I PI3K isoforms which are believed to have crucial roles in cytokine induction based on the previous data generated using pharmacological inhibitors. Unfortunately, effective knockdown of one of the key isoforms, p110δ, could not be confirmed due to problems finding reliable commercially available antibodies to check protein knockdown in western blotting. With an assumption that p110δ was successfully knocked down (similar to that of p110β), simultaneous knockdown of both beta and delta isoforms of class I PI3K failed to inhibit cytokine production in response to RV-16 infection. Another member of our research group has also carried out experiments with dual siRNA-mediated knockdown of the class I PI3K regulatory subunit proteins, p85α and p85β (See Section 1.9.1 for the brief overview of the class I PI3Ks and their regulatory subunits). Using western blotting, it was confirmed that both p85α and p85β protein levels were successfully

knocked down, although neither protein could be suppressed to undetectable levels (Ismail et al., 2014). The knockdown of both regulatory proteins had only modest effects on RV-induced CXCL8 production, with no effects on CCL5 generation (Ismail et al., 2014). The discrepancies of the results obtained using PI3K small molecule inhibitors and siRNAs are not known, although it is possible that effective doses of small molecule inhibitors attained a greater relative inhibition of PI3K than incomplete protein knockdown by siRNAs (Ismail et al., 2014).

Having found that the general PI3K inhibitors LY294002, PI-103 and 3-MA; and a cocktail of all four isoform-selective class I PI3K inhibitors reduced RV-induced cytokine production, this study aimed to explore if these observations were due to the separate effects of PI3K inhibition on viral replication and infection (that could also suppress cytokine generation). It was found that the broad, non-class I PI3K-selective inhibitors LY294002, PI-103 and 3-MA, suppressed viral replication; whilst the cocktail of class I PI3K isoform inhibitors did not. This could partly explain the significant reduction of RV-induced cytokine production, following treatment with the general PI3K inhibitors LY294002, PI-103 and 3-MA. The potential mechanism by which PI3K inhibition reduced viral replication is discussed further in the following section (Section 4.8.3.2).

The serine/threonine protein kinase mTOR is one of the downstream targets of the class I PI3Ks, and is involved in many cellular processes including protein synthesis and cell proliferation (reviewed in Sarbassov et al., 2005) (See Section 1.9.2.2). mTOR also serves as a negative regulator of autophagic pathway (reviewed in Meijer and Codogno, 2004). Importantly, mTOR has been shown to play roles in IFN production following activation of TLR3 in keratinocytes (Zhao et al., 2010) and TLR9 in dendritic cells (Cao et al., 2008). Furthermore, LY294002 has recently been shown to inhibit TLR3/4-mediated IFN-β production via a PI3K-independent mechanism (Zhao et al., 2012). It was noted that both LY294002 and PI-103 can also directly inhibit mTOR at the concentrations used in this study (Brunn et al., 1996, Knight et al., 2006), and 3-MA can inhibit mTOR via inhibition of PI3K function (Wu et al., 2010). Thus it was hypothesised that the inhibitory effects of LY294002, PI-103 and 3-MA on cytokine responses might be partly due to mTOR inhibition. Preliminary data showed that rapamycin, a widely known mTOR pharmacological inhibitor, suppressed CCL5 production, and to a less extent CXCL8 generation, induced by RV and

poly(I:C). The potential role for mTOR in mediating the cytokine response to RV infection is discussed further in Section 4.8.4.

4.8.3.2 The involvement of PI3Ks in RV cellular entry

Having determined that the broad PI3K inhibitors LY294002, PI-103 and 3-MA; and a cocktail of all four isoform-selective class I PI3K inhibitors suppressed RV-induced cytokine production (Section 4.8.3.2), this study aimed to determine if these observations were due to the separate effects of PI3K inhibition on viral replication and infection (that could also reduce cytokine production). It was found that the general, non-class I PI3K-selective inhibitors, LY294002, PI-103 and 3-MA, inhibited viral replication; whilst the cocktail of class I PI3K isoform inhibitors did not. The results obtained using LY294002 are consistent with the previous studies specifically investigating the involvement of PI3Ks in the RV-induced CXCL8 production (Newcomb et al., 2005, Bentley et al., 2007). Newcomb and colleagues showed that inhibition of PI3K using LY294002 blocked the internalisation of fluorescent-labeled RV-39 into the human bronchial epithelial 16HBE140 cells, which partly explains the concomitant reduction of RV-39-induced CXCL8 expression, following treatment with LY294002 (Newcomb et al., 2005). Further work performed by the same group showed the requirement for the tyrosine kinase Src/p110β PI3K/Akt-dependent pathway in RV internalisation to 16HBE140 cells (Bentley et al., 2007). In view of these previous publications (Newcomb et al., 2005, Bentley et al., 2007), further experiments should be carried out to confirm if LY294002, PI-103 and 3-MA could indeed block RV internalisation into our BEAS-2B airway epithelial cells.

To try to examine the roles of PI3K in TLR3 signalling, without being perplexed by a separate reduction of viral replication, the effects of LY294002, PI-103 and 3-MA on cytokine production induced by the synthetic agonist poly(I:C) were also investigated. It was found that these PI3K inhibitors also inhibited cytokine responses to poly(I:C), with LY294002 attaining complete inhibition of cytokine generation. These data are consistent with the work done by Sun *et al.* showing that LY294002 potently inhibited poly(I:C)-induced production of IL-6 and IFN-β in murine BMDCs. However, a very recent study demonstrated that wortmannin, which is also a general PI3K inhibitor, could inhibit the uptake of fluorescent-labelled poly(I:C) into the endosome (where TLR3 is located) in murine peritoneal macrophages (Zhou et al., 2013). Again, further work should be performed using fluorescent-tagged poly(I:C) to investigate if PI3K inhibition could affect the uptake of

poly(I:C) into our BEAS-2B airway epithelial cells. Furthermore, in this thesis it was found that 3-MA treatment did not affect the cytokine production induced by IL-1β, TNF-α, IL-6 and IFN-β, all of which do not require TLR3 activation to signal (reviewed in Dinarello, 2009, Wajant et al., 2003, Heinrich et al., 2003, Takaoka and Yanai, 2006). These data suggest that PI3K inhibition reduced the poly(I:C)-induced cytokine production potentially by suppressing the uptake of poly(I:C) to endosome where TLR3 resides, although it remains possible that the PI3K inhibition can exhibit its action at any other point in TLR3 signalling pathway.

Taken together, the results discussed in this section in conjunction with previous studies (Newcomb et al., 2005, Bentley et al., 2007) indicate that inhibition of PI3Ks may also block internalisation of RV; implying that the requirement of PI3Ks for RV-induced cytokine production (Section 4.8.3.1), at least in part, could be due to its role in RV cellular entry.

4.8.3.3 The regulation of type I IFN signalling by PI3Ks

Despite the potential explanation that the PI3K inhibitors 3-MA, LY294002 and PI-103 suppressed RV- or poly(I:C)-induced cytokine production, in part, by blocking the internalisation of RV or the uptake of poly(I:C) to endosome (Section 4.8.3.2), these PI3K inhibitors attenuated CCL5 production more potently than CXCL8 generation. Furthermore, a cocktail of isoform-selective class I PI3K inhibitors also inhibited CCL5 generation more effectively than CXCL8 production. These current data could be partly explained by the results obtained by Guiducci and colleagues which showed that inhibition of PI3K by LY294002 selectively blocked the nuclear translocation of IRF-7, but not NF-κB, in CpG DNA-stimulated human plasmacytoid DCs (Guiducci et al., 2008).

PI3Ks have been shown to regulate the induction of type I IFN-mediated ISGs (reviewed in Joshi et al., 2010, Bonjardim et al., 2009). This study aimed to investigate if the inhibitory actions of 3-MA on the ISG CCL5 production is due to its effects on TLR3 signalling, or through additional inhibition of the resulting autocrine IFN signalling mediated by IFNAR (Section 1.7.2). Thus, whether exogenous IFN could rescue poly(I:C)-induced cytokine production, in the presence of 3-MA, was determined. This is the first study to show that IFN-β treatment rescued the generation of CXCL8 induced by poly(I:C) that had been impaired by 3-MA, and partially rescued the inhibitory actions of 3-MA on the production of

CCL5. These data suggest that the effects of 3-MA may be mediated through targeting of TLR3-mediated IFN production, but not the resulting autocrine IFN signalling.

Previous studies have demonstrated positive roles for PI3Ks in the production of type I IFNs or ISGs (reviewed in Joshi et al., 2010, Bonjardim et al., 2009). Using human embryonic kidney 293 (HEK293) cells, Sarkar and colleagues showed that poly(I:C)-induced phosphorylation and activation of IRF3 was inhibited by LY294002 (Sarkar et al., 2004). Similarly, a study done by Kaur *et al*. observed lower transcription levels of IRF7, ISG15 and CXCL10 genes in double p85α/p85β knockout mouse embryonic fibroblasts (MEFs), in response to IFN-α treatment (Kaur et al., 2008b). Moreover, Zheng and co-workers showed that LY294002 or wortmannin inhibited IFN-β production induced by LPS or poly(I:C), in murine peritoneal macrophages (Zheng et al., 2010). A similar study performed by Peltier *et al*. also reported that poly(I:C)-induced IFN-β mRNA levels were reduced by LY294002 in a neuronal cell line (Peltier et al., 2010). Furthermore, Guiducci and colleagues demonstrated that LY294002 inhibited the transcription of IFN-α induced by CpG DNA in human plasmacytoid DCs (Guiducci et al., 2008). More recently, LY294002 has also been shown to inhibit the production of IFN-α induced by myxoma virus in human plasmacytoid DCs (Cao et al., 2012).

Collectively, the data discussed in this section in conjunction with previous studies described above suggest that PI3Ks play important roles in the regulation of type I IFN-mediated ISG induction, following TLR3 activation.

4.8.4 A potential role for mTOR in regulating the cytokine response to RV infection

The serine/threonine protein kinase mTOR is one of the downstream targets of the class I PI3Ks, and is involved in many cellular processes including protein synthesis and cell proliferation (reviewed in Sarbassov et al., 2005) (See Section 1.9.2.2). LY294002 has recently been demonstrated to inhibit TLR3/4-mediated IFN-β production via a PI3K-independent mechanism (Zhao et al., 2012). As briefly discussed in Section 4.8.3.1, it was noted that both LY294002 and PI-103 can also directly inhibit mTOR at the concentrations used in this current study (Brunn et al., 1996, Knight et al., 2006), and 3-MA can inhibit mTOR via inhibition of PI3K function (Wu et al., 2010). Thus it was hypothesised that the

inhibitory actions of LY294002, PI-103 and 3-MA on cytokine responses could be partly mediated by mTOR inhibition. Indeed, recent data obtained by another member of our group revealed that the PI3K inhibitors LY294002 and PI-103 could inhibit phosphorylation of the mTOR target p70S6K (Ismail et al., 2014). This thesis is the first to demonstrate that rapamycin, a widely used mTOR pharmacological inhibitor, suppressed cytokine production induced by RV and poly(I:C) in airway epithelial cells.

Several studies have shown the involvement of mTOR in mediating cytokine induction (reviewed in Powell et al., 2012, Weichhart and Saemann, 2009). Cao and colleagues demonstrated that rapamycin inhibited CpG DNA-induced IFN-α and IFN-β secretion by human plasmacytoid DCs (Cao et al., 2008). They also reported that *in vivo* administration of rapamycin suppressed IFN-α and IFN-β production by mouse plasmacytoid DCs, in response to CpG DNA or yellow fever virus infection. Further work performed by the authors revealed that inhibition of mTOR by rapamycin blocked the interaction of TLR9 with the adaptor molecule MyD88, which in turn inhibited the phosphorylation and nuclear translocation of IRF-7 (Cao et al., 2008). Similarly, in their studies of human oral keratinocytes, Zhao *et al.* showed that poly(I:C)-induced production of IL-1β, TNF-α and IFN-β was inhibited by rapamycin, which was thought to be due to the ability of rapamycin to regulate the activation of NF-κB and IRF-3 (Zhao et al., 2012). Furthermore, a very recent study also demonstrated that AZD8055, a newly characterised mTOR inhibitor, suppressed LPS-induced generation of CXCL8, IL-6, IL-1β and TNF-α in human THP-1 derived macrophages (Xie et al., 2014).

Taken together, the data suggest that the inhibitory effects of the PI3K inhibitors used in this study may be due to mTOR inhibition. The results obtained using the mTOR inhibitor rapamycin suggest a potential role for mTOR in the inflammatory responses to RV infection, although validation of these data using a more specific technique (i.e. siRNA) is necessary. Furthermore, it has not been determined whether rapamycin could inhibit viral internalisation (which may also result in reduced cytokine production) which requires further investigation. However, since mTOR also serves as a negative regulator of autophagic pathway (reviewed in Meijer and Codogno, 2004) (See Section 1.9.2.2 for the role of mTOR signalling in autophagy modulation), the preliminary data obtained using rapamycin provides further evidence that autophagy is not required for the cytokine response to RV infection.

4.8.5 Limitations and future work

4.8.5.1 Methods for measuring autophagy induction

As discussed in Section 4.8.2.3, methods for assessing autophagy are not straight-forward. In this study, several assays were tested in an attempt to find a good approach to monitor autophagic activity including LC3-II western blotting, GFP-LC3 fluorescence microscopy and endogenous LC3-II immunohistochemistry (Section 4.8.2.3). However, only endogenous LC3-II immunohistochemistry staining revealed a markedly increased autophagic activity in cells exposed to known autophagy inducers (Section 4.8.2.3). Due to time constraints, the ability of RV infection to induce autophagy in airway epithelial cells remains to be determined using this technique.

Recently, Klionsky *et al.* have published an extensive review article discussing various other methods that can be used to monitor autophagy (Klionsky et al., 2012), which could be used to further explore the role of autophagy in responses to RV infection. One of the most informative methods for measuring autophagy is using transmission electron microscopy (TEM), as this technique can be used for qualitative and quantitative analysis of changes in various autophagic structures that are normally very small in size (reviewed in Klionsky et al., 2012). Another method that can be used to monitor autophagy is using the fluorescence-activated cell sorter (FACS), however this flow cytometry technique is particularly useful for cells that grow in suspension, and using this method it is feasible to capture images of up to 1000 cells per second (reviewed in Klionsky et al., 2012).

As pointed out by Klionsky *et al.*, autophagy is a highly dynamic process and there is no individual assay that is guaranteed to be applicable in every biological and experimental context (reviewed in Klionsky et al., 2012). Therefore, it is strongly recommended that multiple assays are used to monitor autophagy to confirm the validity of the data obtained.

4.8.5.2 Validation of results using primary airway epithelial cells

The data presented in this chapter exploring the roles of autophagy and PI3Ks in the responses to RV infection were obtained using BEAS-2B epithelial cell line, and due to time constraints, repetition of several key experiments using primary airway epithelial cells could not be performed. Given that autophagy research is highly dependent on the cell types and experimental conditions (reviewed in Klionsky et al., 2012), it is particularly important to

validate the results obtained with regards to the role of autophagy in RV-induced responses using primary cells, and thus this work is currently being carried out by another member of our research group.

4.8.6 Conclusions

Determining the possible roles of autophagy and PI3K in the control of RV infection is crucial to direct anti-inflammatory strategies in RV-induced exacerbations of airway diseases. My hypothesis that autophagosomes are required to deliver replication intermediates of RV RNA to TLR3 in endosomes appears incorrect. The results presented in this chapter reveal for the first time that autophagy plays a limited role in the responses to RV infection in airway epithelial cells. Specifically, siRNA-mediated knockdown of the autophagy protein Bec-1, Atg7 or LC3 had only modest effects on CXCL8 production, with no effect on CCL5 generation. This study also shows the roles for, and redundancy amongst, class I PI3Ks in controlling the inflammatory responses to RV infection. However, this conclusion was drawn based on the results obtained using pharmacological inhibitors, thus further work using a more specific approach (e.g. siRNA) is required to confirm this finding. Meanwhile, targeting the class III PI3K Vps34 by siRNA did not affect RV-induced cytokine production, implying the lack of a role for class III PI3K, and by extension autophagy, in the regulation of innate immune response to RV. Furthermore, the data in this chapter also suggest a role for mTOR in the regulation of RV-induced inflammation. The signalling molecules determined in this chapter to be involved in the RV-induced cytokine responses are summarised in Figure 4.31.

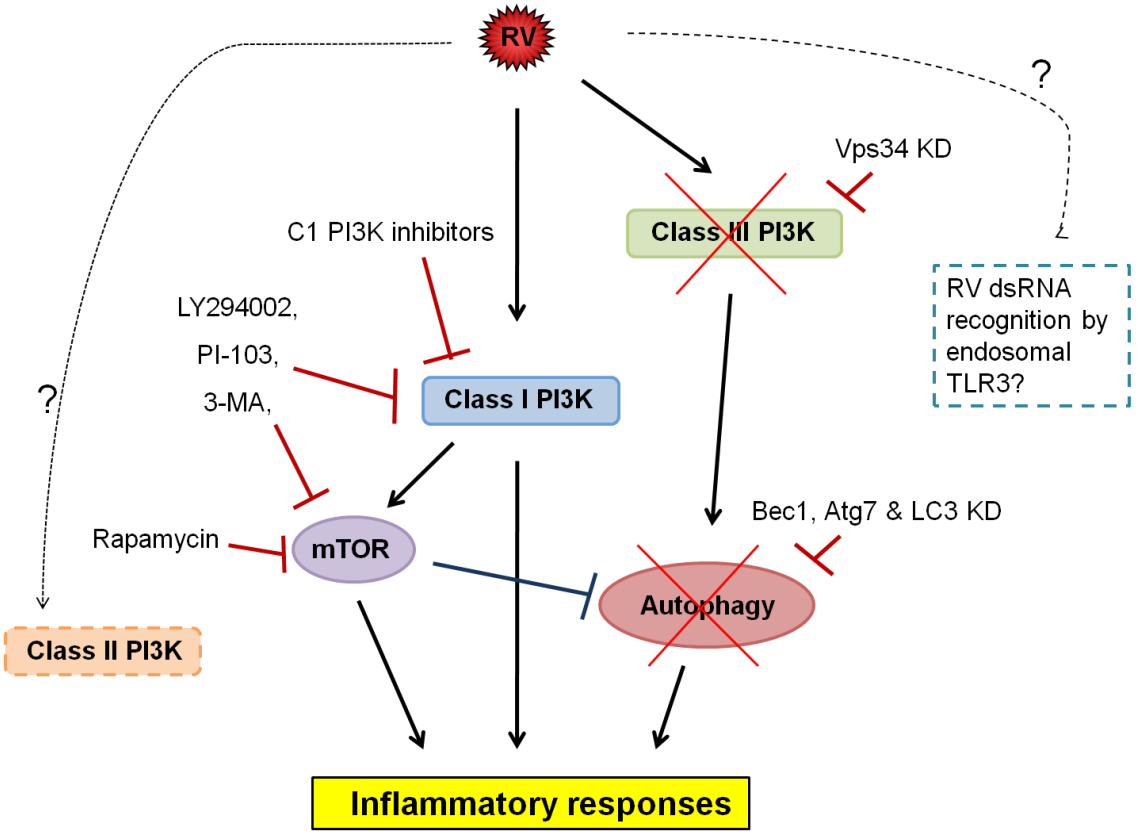

Figure 4. 31 A schematic diagram summarising the signalling molecules determined in this chapter (using pharmacological inhibitors and siRNAs) to be involved in the inflammatory responses to RV infection.

Pharmacological inhibitors LY294002, PI-103, 3-MA, a cocktail of isoform-selective class I PI3K inhibitors, and rapamycin can all inhibit cytokine production in response to RV infection, suggesting the important roles for class I PI3Ks and mTOR in the inflammatory responses to RV infection. Meanwhile, siRNA-mediated knockdown of the sole class III PI3K Vps34 does not affect RV-induced cytokine generation, implying the lack of a role for class III PI3K in mediating the inflammatory responses to RV (marked by the red cross in the diagram). However, whether class II PI3K is involved in the regulation of RV-induced responses remains to be determined. Additionally, siRNA-mediated knockdown of the autophagy protein Bec-1, Atg7 or LC3 has only modest effect on CXCL8 production, with no effect on CCL5, suggesting that autophagy plays a little if any role in the RV-induced responses. The fact that mTOR is a negative regulator of autophagy, and that the mTOR inhibitor rapamycin inhibited cytokine generation, provides further evidence that autophagy is not important in the inflammatory responses to RV infection. The initial hypothesis that autophagy may be required for the presentation of RV dsRNA replication intermediate from the cytoplasm to the endosomal TLR3 (which may therefore affect TLR-mediated cytokine production) appears incorrect, and thus how cytosolic RV dsRNA gains access to the endosome remains to be elucidated.

Chapter 5: General discussion and conclusions

Whilst discussion of individual experimental results has been provided within the relevant results chapters (Chapters 3 and 4), this chapter will highlight the key findings of this thesis and their implications.

5.1 How does this thesis add to our current knowledge of the regulation of inflammatory responses of airway epithelial cells and fibroblasts to RV infection?

Airway epithelial cells are important tissue cells involved in the development of COPD as they are able to secrete various mediators of COPD including proinflammatory cytokines and reactive oxygen species. Lung fibroblasts have been documented to play central roles in the fibrotic component of COPD, where their excessive proliferation results in fibrosis in the small airways (reviewed in Araya and Nishimura, 2010). However, limited studies have shown the potential role of fibroblasts in mediating RV-induced inflammation in COPD. The primary objective of this thesis was to increase our understanding of the signalling pathways involved in the inflammatory responses of structural airway cells to RV infection, which may provide potential novel targets for the treatment of virally-induced exacerbations of airway diseases such as asthma and COPD. The first aim of this thesis was to examine the inflammatory responses of human airway fibroblasts to RV infection, and to compare those responses with those of airway epithelial cells (Chapter 3); and the second aim of this thesis was to investigate whether autophagy is involved in the TLR3-mediated detection of RV infection, and therefore regulates the RV-induced responses of airway epithelial cells.

This is the first study to directly compare the responses of lung fibroblasts to RV infection with those of lung epithelial cells. As discussed in detail in Chapter 3, this thesis is the first to demonstrate that:

- RV infection induced differential responses by airway epithelial cells and fibroblasts. Importantly, it was found that RV caused much higher cell death in airway fibroblasts compared to epithelial cells, and this is thought to be due to the greater permissiveness of fibroblasts to viral replication compared to epithelial cells.

- The lack of antiviral responses of lung fibroblasts to RV infection. In comparison to airway epithelial cells, the lack of viral-detecting PRRs TLR3, RIG-I, MDA5 and virally-induced transcription factors IRF1 and IRF7 in fibroblasts may be a potential explanation as to why the fibroblasts do not secrete the IFN-stimulated antiviral cytokines CCL5 and CXCL10.
- The permissiveness of lung fibroblasts isolated from IPF patients to RV infection. It was revealed that cells of rapid IPF progressors released higher proinflammatory cytokine CXCL8 compared to that of slow IPF progressors.
- Exogenous IL-1β could synergistically augment the RV-induced CXCL8 production in airway epithelial cells, but not in lung fibroblasts.
- RV-1B and bacterial-derived LPS could synergistically accentuate CXCL8 production in BEAS-2B cells, with this synergistic effect is thought to be due to IL-1β generation by LPS-activated monocytes.

This study is also the first to explore whether autophagy is involved in the cytokine responses to RV infection. As discussed in detail in Chapter 4, this thesis is the first to show that:

- Autophagy is not important in the control of inflammatory responses to RV or control of RV replication in the airway epithelial cells.
- The roles for, and redundancy amongst, class I PI3Ks in regulating the inflammatory responses to RV infection, which at least in part, could be due to its role in RV cellular entry.
- The lack of a role for class III PI3K, and by extension autophagy, in regulating the innate immune response to RV.
- Rapamycin, a widely used mTOR pharmacological inhibitor, suppressed cytokine production induced by RV and poly(I:C) in airway epithelial cells.

5.2 What implications does this have for airway diseases?

The results presented in Chapter 3 showed that in comparison to airway epithelial cells, lung fibroblasts allow higher viral replication to take place. Importantly, it was found that RV-infected airway fibroblasts could secret proinflammatory cytokines such as CXCL8 and IL-6,

but were not able to produce antiviral cytokines such as IFNs. The fact that fibroblasts numbers are increased in COPD (reviewed in Araya and Nishimura, 2010) implies that more RV replication can take place, hence worsening the inflammation in this airway disease. Furthermore, it has been shown that in asthmatic airways, the bronchial epithelium is damaged (Puddicombe et al., 2000). This may give greater probability for RV to infect the adjacent fibroblasts, which in turn may elevate the inflammation during asthma exacerbation. This study also revealed that cells of rapid IPF progressors released higher proinflammatory cytokine CXCL8 compared to that of slow IPF progressors, implicating a possible role for RV infection in triggering IPF exacerbations.

The results in Chapter 4 demonstrated that pharmacological inhibition of PI3Ks suppressed RV-induced cytokine production in airway epithelial cells, which in part could be through inhibition of RV cellular entry. Thus PI3K seemed to be a potential therapeutic intervention for the treatment of RV-induced exacerbations of airway diseases such as asthma and COPD.

5.3 Future studies

Whilst future studies have been discussed within the relevant results chapters of this thesis, this section will only highlight several important areas that require further investigation.

As discussed in Chapter 4, using known PI3K pharmacological inhibitors this study showed that PI3Ks are involved in the cytokine response of airway epithelial cells to RV infection. However, this finding needs to be confirmed using a more specific technique such as siRNA or knockout cells. Additionally, further work should be done investigating if the pharmacological inhibitors used in this study could indeed block RV internalisation into our BEAS-2B airway epithelial cells.

The data presented in Chapter 4 has also demonstrated the potential role of mTOR in regulating RV-induced cytokine production, as evidenced by the use of the mTOR inhibitor rapamycin. Again, validation of these data using a more specific technique such as siRNA or knockout cells is required. Furthermore, whether mTOR inhibition could inhibit viral internalisation (which may also result in reduced cytokine production) demands further investigation.

The results presented in Chapter 4 were obtained using BEAS-2B airway epithelial cell line, and due to time constraints, repetition of several key experiments using primary airway epithelial cells could not be performed. Given that autophagy research is highly dependent on the cell types and experimental conditions (reviewed in Klionsky et al., 2012), it is particularly important to validate the results obtained with regards to the role of autophagy in RV-induced responses using primary cells.

5.4 Conclusions

Understanding the complex innate immune responses of structural airway cells to RV infection is crucial for the better treatment of RV-induced exacerbations of airway diseases such as asthma and COPD. The data obtained in this study suggest a role for airway fibroblasts in mediating virally-induced inflammation. This study also reveals for the first time the ability of IL-1β to enhance proinflammatory responses of RV-1B-infected epithelial cells. Furthermore, the work presented in this thesis demonstrate that in the presence of monocytes, RV and bacterial-derived LPS coinfections can act in synergy to amplify the proinflammatory responses of airway tissue cells. Importantly, this study is the first to show that autophagy plays a limited role in the responses to RV infection in airway epithelial cells. Furthermore, this study shows the roles for, and redundancy amongst, class I PI3Ks in controlling the inflammatory responses to RV infection. Meanwhile, class III PI3K was not involved in RV-induced responses. Furthermore, data from this thesis also suggest a role for mTOR in the regulation of RV-induced inflammation. A better understanding of the mechanisms underlying PI3K- or mTOR-mediated inflammatory responses may provide potentially novel therapeutic targets to treat RV-induced exacerbations of asthma and COPD.

References

AGARWAL, S. K., WU, M., LIVINGSTON, C. K., PARKS, D. H., MAYES, M. D., ARNETT, F. C. & TAN, F. K. 2011. Toll-like receptor 3 upregulation by type I interferon in healthy and scleroderma dermal fibroblasts. *Arthritis Res Ther,* 13**,** R3.

AKSOY, E., VANDEN BERGHE, W., DETIENNE, S., AMRAOUI, Z., FITZGERALD, K. A., HAEGEMAN, G., GOLDMAN, M. & WILLEMS, F. 2005. Inhibition of phosphoinositide 3-kinase enhances TRIF-dependent NF-kappa B activation and IFN-beta synthesis downstream of Toll-like receptor 3 and 4. *Eur J Immunol,* 35**,** 2200-9.

ALDONYTE, R., JANSSON, L., PIITULAINEN, E. & JANCIAUSKIENE, S. 2003. Circulating monocytes from healthy individuals and COPD patients. *Respir Res,* 4**,** 11.

ALEXOPOULOU, L., HOLT, A. C., MEDZHITOV, R. & FLAVELL, R. A. 2001. Recognition of double-stranded RNA and activation of NF-kappaB by Toll-like receptor 3. *Nature,* 413**,** 732-8.

AMBJORN, M., EJLERSKOV, P., LIU, Y., LEES, M., JAATTELA, M. & ISSAZADEH-NAVIKAS, S. 2013. IFNB1/interferon-beta-induced autophagy in MCF-7 breast cancer cells counteracts its proapoptotic function. *Autophagy,* 9**,** 287-302.

ANDINO, R., BODDEKER, N., SILVERA, D. & GAMARNIK, A. V. 1999. Intracellular determinants of picornavirus replication. *Trends Microbiol,* 7**,** 76-82.

ANDROULIDAKI, A., ILIOPOULOS, D., ARRANZ, A., DOXAKI, C., SCHWORER, S., ZACHARIOUDAKI, V., MARGIORIS, A. N., TSICHLIS, P. N. & TSATSANIS, C. 2009. The kinase Akt1 controls macrophage response to lipopolysaccharide by regulating microRNAs. *Immunity,* 31**,** 220-31.

ARAYA, J. & NISHIMURA, S. L. 2010. Fibrogenic reactions in lung disease. *Annu Rev Pathol,* 5**,** 77-98.

ARDEN, K. E., FAUX, C. E., O'NEILL, N. T., MCERLEAN, P., NITSCHE, A., LAMBERT, S. B., NISSEN, M. D., SLOOTS, T. P. & MACKAY, I. M. 2010. Molecular characterization and distinguishing features of a novel human rhinovirus (HRV) C, HRVC-QCE, detected in children with fever, cough and wheeze during 2003. *J Clin Virol,* 47**,** 219-23.

ARNOLD, E. & ROSSMANN, M. G. 1990. Analysis of the structure of a common cold virus, human rhinovirus 14, refined at a resolution of 3.0 A. *J Mol Biol,* 211**,** 763-801.

BAINES, K. J., HSU, A. C., TOOZE, M., GUNAWARDHANA, L. P., GIBSON, P. G. & WARK, P. A. 2013. Novel immune genes associated with excessive inflammatory and antiviral responses to rhinovirus in COPD. *Respir Res,* 14**,** 15.

BARALDO, S., TURATO, G., BADIN, C., BAZZAN, E., BEGHE, B., ZUIN, R., CALABRESE, F., CASONI, G., MAESTRELLI, P., PAPI, A., FABBRI, L. M. & SAETTA, M. 2004. Neutrophilic infiltration within the airway smooth muscle in patients with COPD. *Thorax,* 59**,** 308-12.

BARNES, P. J. 2004a. Alveolar macrophages as orchestrators of COPD. *COPD,* 1**,** 59-70.

BARNES, P. J. 2004b. Mediators of chronic obstructive pulmonary disease. *Pharmacol Rev,* 56**,** 515-48.

BARNES, P. J. 2008. Immunology of asthma and chronic obstructive pulmonary disease. *Nat Rev Immunol,* 8**,** 183-92.

BARNES, P. J. 2009. The cytokine network in chronic obstructive pulmonary disease. *Am J Respir Cell Mol Biol,* 41**,** 631-8.

BATEMAN, E. D., HURD, S. S., BARNES, P. J., BOUSQUET, J., DRAZEN, J. M., FITZGERALD, M., GIBSON, P., OHTA, K., O'BYRNE, P., PEDERSEN, S. E., PIZZICHINI, E., SULLIVAN, S. D., WENZEL, S. E. & ZAR, H. J. 2008. Global strategy for asthma management and prevention: GINA executive summary. *Eur Respir J,* 31**,** 143-78.

BEDARD, K. M. & SEMLER, B. L. 2004. Regulation of picornavirus gene expression. *Microbes Infect,* 6**,** 702-13.

BEDKE, N., HAITCHI, H. M., XATZIPSALTI, M., HOLGATE, S. T. & DAVIES, D. E. 2009. Contribution of bronchial fibroblasts to the antiviral response in asthma. *J Immunol,* 182**,** 3660-7.

BEKEREDJIAN-DING, I., ROTH, S. I., GILLES, S., GIESE, T., ABLASSER, A., HORNUNG, V., ENDRES, S. & HARTMANN, G. 2006. T cell-independent, TLR-induced IL-12p70 production in primary human monocytes. *J Immunol,* 176**,** 7438-46.

BENTLEY, J. K., NEWCOMB, D. C., GOLDSMITH, A. M., JIA, Y., SAJJAN, U. S. & HERSHENSON, M. B. 2007. Rhinovirus activates interleukin-8 expression via a Src/p110beta phosphatidylinositol 3-kinase/Akt pathway in human airway epithelial cells. *J Virol,* 81**,** 1186-94.

BHAT, N. & FITZGERALD, K. A. 2014. Recognition of cytosolic DNA by cGAS and other STING-dependent sensors. *Eur J Immunol,* 44**,** 634-40.

BHOWMIK, A., SEEMUNGAL, T. A., SAPSFORD, R. J. & WEDZICHA, J. A. 2000. Relation of sputum inflammatory markers to symptoms and lung function changes in COPD exacerbations. *Thorax,* 55**,** 114-20.

BOCHKOV, Y. A., PALMENBERG, A. C., LEE, W. M., RATHE, J. A., AMINEVA, S. P., SUN, X., PASIC, T. R., JARJOUR, N. N., LIGGETT, S. B. & GERN, J. E. 2011. Molecular modeling, organ culture and reverse genetics for a newly identified human rhinovirus C. *Nat Med,* 17**,** 627-32.

BONJARDIM, C. A., FERREIRA, P. C. & KROON, E. G. 2009. Interferons: signaling, antiviral and viral evasion. *Immunol Lett,* 122**,** 1-11.

BRABEC-ZARUBA, M., BERKA, U., BLAAS, D. & FUCHS, R. 2007. Induction of autophagy does not affect human rhinovirus type 2 production. *J Virol,* 81**,** 10815-7.

BRABEC, M., BLAAS, D. & FUCHS, R. 2006. Wortmannin delays transfer of human rhinovirus serotype 2 to late endocytic compartments. *Biochem Biophys Res Commun,* 348**,** 741-9.

BRUNN, G. J., WILLIAMS, J., SABERS, C., WIEDERRECHT, G., LAWRENCE, J. C., JR. & ABRAHAM, R. T. 1996. Direct inhibition of the signaling functions of the mammalian target of rapamycin by the phosphoinositide 3-kinase inhibitors, wortmannin and LY294002. *EMBO J,* 15**,** 5256-67.

BUCCHIONI, E., KHARITONOV, S. A., ALLEGRA, L. & BARNES, P. J. 2003. High levels of interleukin-6 in the exhaled breath condensate of patients with COPD. *Respir Med,* 97**,** 1299-302.

BUCHSER, W. J., LASKOW, T. C., PAVLIK, P. J., LIN, H. M. & LOTZE, M. T. 2012. Cell-mediated autophagy promotes cancer cell survival. *Cancer Res,* 72**,** 2970-9.

BUCKLEY, C. D., PILLING, D., LORD, J. M., AKBAR, A. N., SCHEEL-TOELLNER, D. & SALMON, M. 2001. Fibroblasts regulate the switch from acute resolving to chronic persistent inflammation. *Trends Immunol,* 22**,** 199-204.

BURGE, P. S., CALVERLEY, P. M., JONES, P. W., SPENCER, S., ANDERSON, J. A. & MASLEN, T. K. 2000. Randomised, double blind, placebo controlled study of fluticasone propionate in patients with moderate to severe chronic obstructive pulmonary disease: the ISOLDE trial. *BMJ,* 320**,** 1297-303.

CAKEBREAD, J. A., HAITCHI, H. M., XU, Y., HOLGATE, S. T., ROBERTS, G. & DAVIES, D. E. 2014. Rhinovirus-16 induced release of IP-10 and IL-8 is augmented by Th2 cytokines in a pediatric bronchial epithelial cell model. *PLoS One,* 9**,** e94010.

CAO, H., DAI, P., WANG, W., LI, H., YUAN, J., WANG, F., FANG, C. M., PITHA, P. M., LIU, J., CONDIT, R. C., MCFADDEN, G., MERGHOUB, T., HOUGHTON, A. N., YOUNG, J. W., SHUMAN, S. & DENG, L. 2012. Innate immune response of human plasmacytoid dendritic cells to poxvirus infection is subverted by vaccinia E3 via its Z-DNA/RNA binding domain. *PLoS One,* 7**,** e36823.

CAO, W., MANICASSAMY, S., TANG, H., KASTURI, S. P., PIRANI, A., MURTHY, N. & PULENDRAN, B. 2008. Toll-like receptor-mediated induction of type I interferon in plasmacytoid dendritic cells requires the rapamycin-sensitive PI(3)K-mTOR-p70S6K pathway. *Nat Immunol,* 9**,** 1157-64.

CARTY, M. & BOWIE, A. G. 2010. Recent insights into the role of Toll-like receptors in viral infection. *Clin Exp Immunol*.

CASASNOVAS, J. M. & SPRINGER, T. A. 1994. Pathway of rhinovirus disruption by soluble intercellular adhesion molecule 1 (ICAM-1): an intermediate in which ICAM-1 is bound and RNA is released. *J Virol,* 68**,** 5882-9.

CHAUDHURI, N., DOWER, S. K., WHYTE, M. K. & SABROE, I. 2005. Toll-like receptors and chronic lung disease. *Clin Sci (Lond),* 109**,** 125-33.

CHAUDHURI, N., PAIVA, C., DONALDSON, K., DUFFIN, R., PARKER, L. C. & SABROE, I. 2010. Diesel exhaust particles override natural injury-limiting pathways in the lung. *Am J Physiol Lung Cell Mol Physiol,* 299**,** L263-71.

CHEN, Z. H., KIM, H. P., SCIURBA, F. C., LEE, S. J., FEGHALI-BOSTWICK, C., STOLZ, D. B., DHIR, R., LANDRENEAU, R. J., SCHUCHERT, M. J., YOUSEM, S. A., NAKAHIRA, K., PILEWSKI, J. M., LEE, J. S., ZHANG, Y., RYTER, S. W. & CHOI, A. M. 2008. Egr-1 regulates autophagy in cigarette smoke-induced chronic obstructive pulmonary disease. *PLoS One,* 3**,** e3316.

CHO, H., PROLL, S. C., SZRETTER, K. J., KATZE, M. G., GALE, M., JR. & DIAMOND, M. S. 2013. Differential innate immune response programs in neuronal subtypes determine susceptibility to infection in the brain by positive-stranded RNA viruses. *Nat Med,* 19**,** 458-64.

CHOI, A. M., RYTER, S. W. & LEVINE, B. 2013. Autophagy in human health and disease. *N Engl J Med,* 368**,** 1845-6.

CHOW, J., FRANZ, K. M. & KAGAN, J. C. 2015. PRRs are watching you: Localization of innate sensing and signaling regulators. *Virology,* 479-480**,** 104-9.

CHURCH, L. D. & MCDERMOTT, M. F. 2009. Canakinumab, a fully-human mAb against IL-1beta for the potential treatment of inflammatory disorders. *Curr Opin Mol Ther,* 11**,** 81-9.

CODOGNO, P., MEHRPOUR, M. & PROIKAS-CEZANNE, T. 2012. Canonical and non-canonical autophagy: variations on a common theme of self-eating? *Nat Rev Mol Cell Biol,* 13**,** 7-12.

COMBADIERE, C., AHUJA, S. K., TIFFANY, H. L. & MURPHY, P. M. 1996. Cloning and functional expression of CC CKR5, a human monocyte CC chemokine receptor selective for MIP-1(alpha), MIP-1(beta), and RANTES. *J Leukoc Biol,* 60**,** 147-52.

COURTNEY, K. D., CORCORAN, R. B. & ENGELMAN, J. A. 2010. The PI3K pathway as drug target in human cancer. *J Clin Oncol,* 28**,** 1075-83.

CRABBE, T., WELHAM, M. J. & WARD, S. G. 2007. The PI3K inhibitor arsenal: choose your weapon! *Trends Biochem Sci,* 32**,** 450-6.

CULPITT, S. V., ROGERS, D. F., P., S., C., D. M., R.E., R., L.E., D. & P.J., B. 2003. Impaired inhibition by dexamethasone of cytokine release by alveolar macrophages from patients with chronic obstructive pulmonary disease. *Am J Respir Crit Care Med,* 167**,** 24-31.

CURTIS, J. L., FREEMAN, C. M. & HOGG, J. C. 2007. The immunopathogenesis of chronic obstructive pulmonary disease: insights from recent research. *Proc Am Thorac Soc,* 4**,** 512-21.

DALTON, D. K., PITTS-MEEK, S., KESHAV, S., FIGARI, I. S., BRADLEY, A. & STEWART, T. A. 1993. Multiple defects of immune cell function in mice with disrupted interferon-gamma genes. *Science,* 259**,** 1739-42.

DAUGHERTY, B. L., SICILIANO, S. J., DEMARTINO, J. A., MALKOWITZ, L., SIROTINA, A. & SPRINGER, M. S. 1996. Cloning, expression, and characterization of the human eosinophil eotaxin receptor. *J Exp Med,* 183**,** 2349-54.

DAVIS, M. E. & GACK, M. U. 2015. Ubiquitination in the antiviral immune response. *Virology,* 479-480**,** 52-65.

DE PALMA, A. M., VLIEGEN, I., DE CLERCQ, E. & NEYTS, J. 2008. Selective inhibitors of picornavirus replication. *Med Res Rev,* 28**,** 823-84.

DEGRYSE, B. & DE VIRGILIO, M. 2003. The nuclear protein HMGB1, a new kind of chemokine? *FEBS Lett,* 553**,** 11-7.

DERETIC, V. 2008. Autophagosome and phagosome. *Methods in molecular biology,* 445**,** 1-10.

DERETIC, V., SAITOH, T. & AKIRA, S. 2013. Autophagy in infection, inflammation and immunity. *Nat Rev Immunol,* 13**,** 722-37.

DEWALD, B., MOSER, B., BARELLA, L., SCHUMACHER, C., BAGGIOLINI, M. & CLARK-LEWIS, I. 1992. IP-10, a gamma-interferon-inducible protein related to interleukin-8, lacks neutrophil activating properties. *Immunol Lett,* 32**,** 81-4.

DHIMOLEA, E. 2010. Canakinumab. *MAbs,* 2**,** 3-13.

DINARELLO, C. A. 2009. Immunological and inflammatory functions of the interleukin-1 family. *Annu Rev Immunol,* 27**,** 519-50.

DONNELLY, R. P. & KOTENKO, S. V. 2010. Interferon-lambda: a new addition to an old family. *J Interferon Cytokine Res,* 30**,** 555-64.

DORMAN, S. E., PICARD, C., LAMMAS, D., HEYNE, K., VAN DISSEL, J. T., BARETTO, R., ROSENZWEIG, S. D., NEWPORT, M., LEVIN, M., ROESLER, J., KUMARARATNE, D., CASANOVA, J. L. & HOLLAND, S. M. 2004. Clinical features of dominant and recessive interferon gamma receptor 1 deficiencies. *Lancet,* 364**,** 2113-21.

DUNSMORE, S. E. & RANNELS, D. E. 1996. Extracellular matrix biology in the lung. *Am J Physiol,* 270**,** L3-27.

DUPONT, N., JIANG, S., PILLI, M., ORNATOWSKI, W., BHATTACHARYA, D. & DERETIC, V. 2011. Autophagy-based unconventional secretory pathway for extracellular delivery of IL-1beta. *EMBO J,* 30**,** 4701-11.

ELBASHIR, S. M., HARBORTH, J., LENDECKEL, W., YALCIN, A., WEBER, K. & TUSCHL, T. 2001. Duplexes of 21-nucleotide RNAs mediate RNA interference in cultured mammalian cells. *Nature,* 411**,** 494-8.

ERICKSON, A. K. & GALE, M., JR. 2008. Regulation of interferon production and innate antiviral immunity through translational control of IRF-7. *Cell Res,* 18**,** 433-5.

FALASCA, M. & MAFFUCCI, T. 2012. Regulation and cellular functions of class II phosphoinositide 3-kinases. *Biochem J,* 443**,** 587-601.

FAURE, M. & LAFONT, F. 2013. Pathogen-induced autophagy signaling in innate immunity. *J Innate Immun,* 5**,** 456-70.

FERHANI, N., LETUVE, S., KOZHICH, A., THIBAUDEAU, O., GRANDSAIGNE, M., MARET, M., DOMBRET, M. C., SIMS, G. P., KOLBECK, R., COYLE, A. J., AUBIER, M. & PRETOLANI, M. 2010. Expression of high-mobility group box 1 and of receptor for advanced glycation end products in chronic obstructive pulmonary disease. *Am J Respir Crit Care Med,* 181**,** 917-27.

FLOREANI, A. A., WYATT, T. A., STONER, J., SANDERSON, S. D., THOMPSON, E. G., ALLEN-GIPSON, D. & HEIRES, A. J. 2003. Smoke and C5a induce airway epithelial intercellular adhesion molecule-1 and cell adhesion. *Am J Respir Cell Mol Biol,* 29**,** 472-82.

FUKAO, T., TANABE, M., TERAUCHI, Y., OTA, T., MATSUDA, S., ASANO, T., KADOWAKI, T., TAKEUCHI, T. & KOYASU, S. 2002. PI3K-mediated negative feedback regulation of IL-12 production in DCs. *Nat Immunol,* 3**,** 875-81.

GAIDAROV, I., SMITH, M. E., DOMIN, J. & KEEN, J. H. 2001. The class II phosphoinositide 3-kinase C2alpha is activated by clathrin and regulates clathrin-mediated membrane trafficking. *Mol Cell,* 7**,** 443-9.

GANLEY, I. G., LAM DU, H., WANG, J., DING, X., CHEN, S. & JIANG, X. 2009. ULK1.ATG13.FIP200 complex mediates mTOR signaling and is essential for autophagy. *J Biol Chem,* 284**,** 12297-305.

GAO, J. L., KUHNS, D. B., TIFFANY, H. L., MCDERMOTT, D., LI, X., FRANCKE, U. & MURPHY, P. M. 1993. Structure and functional expression of the human macrophage inflammatory protein 1 alpha/RANTES receptor. *J Exp Med,* 177**,** 1421-7.

GEIST, F. C. & HAYDEN, F. G. 1985. Comparative susceptibilities of strain MRC-5 human embryonic lung fibroblast cells and the Cooney strain of human fetal tonsil cells for isolation of rhinoviruses from clinical specimens. *J Clin Microbiol,* 22**,** 455-6.

GERN, J. E., DICK, E. C., LEE, W. M., MURRAY, S., MEYER, K., HANDZEL, Z. T. & BUSSE, W. W. 1996. Rhinovirus enters but does not replicate inside monocytes and airway macrophages. *J Immunol,* 156**,** 621-7.

GHILDYAL, R., DAGHER, H., DONNINGER, H., DE SILVA, D., LI, X., FREEZER, N. J., WILSON, J. W. & BARDIN, P. G. 2005. Rhinovirus infects primary human airway fibroblasts and induces a neutrophil chemokine and a permeability factor. *J Med Virol,* 75**,** 608-15.

GIBSON, P. G., POWELL, H. & DUCHARME, F. M. 2007. Differential effects of maintenance long-acting beta-agonist and inhaled corticosteroid on asthma control and asthma exacerbations. *J Allergy Clin Immunol,* 119**,** 344-50.

GITLIN, L., BARCHET, W., GILFILLAN, S., CELLA, M., BEUTLER, B., FLAVELL, R. A., DIAMOND, M. S. & COLONNA, M. 2006. Essential role of mda-5 in type I IFN responses to polyriboinosinic:polyribocytidylic acid and encephalomyocarditis picornavirus. *Proc Natl Acad Sci U S A,* 103**,** 8459-64.

GONZALEZ-NAVAJAS, J. M., LEE, J., DAVID, M. & RAZ, E. 2012. Immunomodulatory functions of type I interferons. *Nat Rev Immunol,* 12**,** 125-35.

GORBEA, C., MAKAR, K. A., PAUSCHINGER, M., PRATT, G., BERSOLA, J. L., VARELA, J., DAVID, R. M., BANKS, L., HUANG, C. H., LI, H., SCHULTHEISS, H. P., TOWBIN, J. A., VALLEJO, J. G. & BOWLES, N. E. 2010. A role for Toll-like receptor 3 variants in host susceptibility to enteroviral myocarditis and dilated cardiomyopathy. *J Biol Chem,* 285**,** 23208-23.

GOTTLIEB, D. J., STONE, P. J., SPARROW, D., GALE, M. E., WEISS, S. T., SNIDER, G. L. & O'CONNOR, G. T. 1996. Urinary desmosine excretion in smokers with and without rapid decline of lung function: the Normative Aging Study. *Am J Respir Crit Care Med,* 154**,** 1290-5.

GRANDVAUX, N., TENOEVER, B. R., SERVANT, M. J. & HISCOTT, J. 2002. The interferon antiviral response: from viral invasion to evasion. *Curr Opin Infect Dis,* 15**,** 259-67.

GREENBERG, S. B., ALLEN, M., WILSON, J. & ATMAR, R. L. 2000. Respiratory viral infections in adults with and without chronic obstructive pulmonary disease. *Am J Respir Crit Care Med,* 162**,** 167-73.

GREVE, J. M., DAVIS, G., MEYER, A. M., FORTE, C. P., YOST, S. C., MARLOR, C. W., KAMARCK, M. E. & MCCLELLAND, A. 1989. The major human rhinovirus receptor is ICAM-1. *Cell,* 56**,** 839-47.

GRUENBERGER, M., WANDL, R., NIMPF, J., HIESBERGER, T., SCHNEIDER, W. J., KUECHLER, E. & BLAAS, D. 1995. Avian homologs of the mammalian low-density lipoprotein receptor family bind minor receptor group human rhinovirus. *J Virol,* 69**,** 7244-7.

GRUNSTEIN, M. M., HAKONARSON, H., WHELAN, R., YU, Z., GRUNSTEIN, J. S. & CHUANG, S. 2001. Rhinovirus elicits proasthmatic changes in airway responsiveness independently of viral infection. *J Allergy Clin Immunol,* 108**,** 997-1004.

GUENTHER, J. F., CAMERON, J. E., NGUYEN, H. T., WANG, Y., SULLIVAN, D. E., SHAN, B., LASKY, J. A., FLEMINGTON, E. K. & MORRIS, G. F. 2010.

Modulation of lung inflammation by the Epstein-Barr virus protein Zta. *American journal of physiology. Lung cellular and molecular physiology,* 299**,** L771-84.

GUIDUCCI, C., GHIRELLI, C., MARLOIE-PROVOST, M. A., MATRAY, T., COFFMAN, R. L., LIU, Y. J., BARRAT, F. J. & SOUMELIS, V. 2008. PI3K is critical for the nuclear translocation of IRF-7 and type I IFN production by human plasmacytoid predendritic cells in response to TLR activation. *J Exp Med,* 205**,** 315-22.

GUTTERIDGE, J. M. & HALLIWELL, B. 2000. Free radicals and antioxidants in the year 2000. A historical look to the future. *Ann N Y Acad Sci,* 899**,** 136-47.

HABJAN, M., ANDERSSON, I., KLINGSTROM, J., SCHUMANN, M., MARTIN, A., ZIMMERMANN, P., WAGNER, V., PICHLMAIR, A., SCHNEIDER, U., MUHLBERGER, E., MIRAZIMI, A. & WEBER, F. 2008. Processing of genome 5' termini as a strategy of negative-strand RNA viruses to avoid RIG-I-dependent interferon induction. *PLoS One,* 3**,** e2032.

HALLGREN, O., NIHLBERG, K., DAHLBACK, M., BJERMER, L., ERIKSSON, L. T., ERJEFALT, J. S., LOFDAHL, C. G. & WESTERGREN-THORSSON, G. 2010. Altered fibroblast proteoglycan production in COPD. *Respir Res,* 11**,** 55.

HARDING, M. W. & YANG, T. J. 1984. Amplification of lymph node cell tube leukocyte adherence inhibition (LAI) reactivity by leukocyte adherence inhibition factor (LAIF). *Cell Immunol,* 87**,** 206-16.

HARRIS, J., HARTMAN, M., ROCHE, C., ZENG, S. G., O'SHEA, A., SHARP, F. A., LAMBE, E. M., CREAGH, E. M., GOLENBOCK, D. T., TSCHOPP, J., KORNFELD, H., FITZGERALD, K. A. & LAVELLE, E. C. 2011. Autophagy controls IL-1beta secretion by targeting pro-IL-1beta for degradation. *J Biol Chem,* 286**,** 9587-97.

HARVALA, H., MCINTYRE, C. L., MCLEISH, N. J., KONDRACKA, J., PALMER, J., MOLYNEAUX, P., GUNSON, R., BENNETT, S., TEMPLETON, K. & SIMMONDS, P. 2012. High detection frequency and viral loads of human rhinovirus species A to C in fecal samples; diagnostic and clinical implications. *J Med Virol,* 84**,** 536-42.

HASPEL, J. A. & CHOI, A. M. 2011. Autophagy: A Core Cellular Process with Emerging Links to Pulmonary Disease. *Am J Respir Crit Care Med*.

HAUTAMAKI, R. D., KOBAYASHI, D. K., SENIOR, R. M. & SHAPIRO, S. D. 1997. Requirement for macrophage elastase for cigarette smoke-induced emphysema in mice. *Science,* 277**,** 2002-4.

HAZEKI, K., NIGORIKAWA, K. & HAZEKI, O. 2007. Role of phosphoinositide 3-kinase in innate immunity. *Biol Pharm Bull,* 30**,** 1617-23.

HE, X., JIA, H., JING, Z. & LIU, D. 2013. Recognition of pathogen-associated nucleic acids by endosomal nucleic acid-sensing toll-like receptors. *Acta Biochim Biophys Sin (Shanghai),* 45**,** 241-58.

HEFFNER, J. E. 2011. Advance care planning in chronic obstructive pulmonary disease: barriers and opportunities. *Curr Opin Pulm Med,* 17**,** 103-9.

HEINRICH, P. C., BEHRMANN, I., HAAN, S., HERMANNS, H. M., MULLER-NEWEN, G. & SCHAPER, F. 2003. Principles of interleukin (IL)-6-type cytokine signalling and its regulation. *Biochem J,* 374**,** 1-20.

HELLERMANN, G. R., NAGY, S. B., KONG, X., LOCKEY, R. F. & MOHAPATRA, S. S. 2002. Mechanism of cigarette smoke condensate-induced acute inflammatory response in human bronchial epithelial cells. *Respir Res,* 3**,** 22.

HENRICKS, P. A. & NIJKAMP, F. P. 2001. Reactive oxygen species as mediators in asthma. *Pulm Pharmacol Ther,* 14**,** 409-20.

HERAS-SANDOVAL, D., PEREZ-ROJAS, J. M., HERNANDEZ-DAMIAN, J. & PEDRAZA-CHAVERRI, J. 2014. The role of PI3K/AKT/mTOR pathway in the modulation of autophagy and the clearance of protein aggregates in neurodegeneration. *Cell Signal,* 26**,** 2694-2701.

HEWSON, C. A., JARDINE, A., EDWARDS, M. R., LAZA-STANCA, V. & JOHNSTON, S. L. 2005. Toll-like receptor 3 is induced by and mediates antiviral activity against rhinovirus infection of human bronchial epithelial cells. *J Virol,* 79**,** 12273-9.

HIGASHIMOTO, Y., ELLIOTT, W. M., BEHZAD, A. R., SEDGWICK, E. G., TAKEI, T., HOGG, J. C. & HAYASHI, S. 2002. Inflammatory mediator mRNA expression by adenovirus E1A-transfected bronchial epithelial cells. *Am J Respir Crit Care Med,* 166**,** 200-7.

HOFER, F., GRUENBERGER, M., KOWALSKI, H., MACHAT, H., HUETTINGER, M., KUECHLER, E. & BLAAS, D. 1994. Members of the low density lipoprotein receptor family mediate cell entry of a minor-group common cold virus. *Proc Natl Acad Sci U S A,* 91**,** 1839-42.

HOGABOAM, C. M., TRUJILLO, G. & MARTINEZ, F. J. 2012. Aberrant innate immune sensing leads to the rapid progression of idiopathic pulmonary fibrosis. *Fibrogenesis & tissue repair,* 5 Suppl 1**,** S3.

HOGG, J. C. 2008. Lung structure and function in COPD. *Int J Tuberc Lung Dis,* 12**,** 467-79.

HOGG, J. C., CHU, F., UTOKAPARCH, S., WOODS, R., ELLIOTT, W. M., BUZATU, L., CHERNIACK, R. M., ROGERS, R. M., SCIURBA, F. C., COXSON, H. O. & PARE, P. D. 2004. The nature of small-airway obstruction in chronic obstructive pulmonary disease. *N Engl J Med,* 350**,** 2645-53.

HOLT 2012. Viral infections and atopy in asthma pathogenesis: new rationales for asthma prevention and treatment.

HOLT, P. G. & SLY, P. D. 2012. Viral infections and atopy in asthma pathogenesis: new rationales for asthma prevention and treatment. *Nat Med,* 18**,** 726-35.

HOMMA, T., KATO, A., HASHIMOTO, N., BATCHELOR, J., YOSHIKAWA, M., IMAI, S., WAKIGUCHI, H., SAITO, H. & MATSUMOTO, K. 2004. Corticosteroid and cytokines synergistically enhance toll-like receptor 2 expression in respiratory epithelial cells. *Am J Respir Cell Mol Biol,* 31**,** 463-9.

HONDA, K., TAKAOKA, A. & TANIGUCHI, T. 2006. Type I interferon [corrected] gene induction by the interferon regulatory factor family of transcription factors. *Immunity,* 25**,** 349-60.

HONDA, K. & TANIGUCHI, T. 2006. IRFs: master regulators of signalling by Toll-like receptors and cytosolic pattern-recognition receptors. *Nat Rev Immunol,* 6**,** 644-58.

HONDA, K., YANAI, H., NEGISHI, H., ASAGIRI, M., SATO, M., MIZUTANI, T., SHIMADA, N., OHBA, Y., TAKAOKA, A., YOSHIDA, N. & TANIGUCHI, T.

2005. IRF-7 is the master regulator of type-I interferon-dependent immune responses. *Nature,* 434**,** 772-7.

HONG, M., YOON, S. I. & WILSON, I. A. 2012. Structure and functional characterization of the RNA-binding element of the NLRX1 innate immune modulator. *Immunity,* 36**,** 337-47.

HOO, Z. H. & WHYTE, M. K. 2012. Idiopathic pulmonary fibrosis. *Thorax,* 67**,** 742-6.

HORNUNG, V., ELLEGAST, J., KIM, S., BRZOZKA, K., JUNG, A., KATO, H., POECK, H., AKIRA, S., CONZELMANN, K. K., SCHLEE, M., ENDRES, S. & HARTMANN, G. 2006. 5'-Triphosphate RNA is the ligand for RIG-I. *Science,* 314**,** 994-7.

HOSOKAWA, N., HARA, T., KAIZUKA, T., KISHI, C., TAKAMURA, A., MIURA, Y., IEMURA, S., NATSUME, T., TAKEHANA, K., YAMADA, N., GUAN, J. L., OSHIRO, N. & MIZUSHIMA, N. 2009. Nutrient-dependent mTORC1 association with the ULK1-Atg13-FIP200 complex required for autophagy. *Mol Biol Cell,* 20**,** 1981-91.

HUGHES, A. L. 2004. Phylogeny of the Picornaviridae and differential evolutionary divergence of picornavirus proteins. *Infect Genet Evol,* 4**,** 143-52.

HWANG, J. W., CHUNG, S., SUNDAR, I. K., YAO, H., ARUNACHALAM, G., MCBURNEY, M. W. & RAHMAN, I. 2010. Cigarette smoke-induced autophagy is regulated by SIRT1-PARP-1-dependent mechanism: implication in pathogenesis of COPD. *Arch Biochem Biophys,* 500**,** 203-9.

ICHINOHE, T., LEE, H. K., OGURA, Y., FLAVELL, R. & IWASAKI, A. 2009. Inflammasome recognition of influenza virus is essential for adaptive immune responses. *J Exp Med,* 206**,** 79-87.

ISHII, K. J., TAKESHITA, F., GURSEL, I., GURSEL, M., CONOVER, J., NUSSENZWEIG, A. & KLINMAN, D. M. 2002. Potential role of phosphatidylinositol 3 kinase, rather than DNA-dependent protein kinase, in CpG DNA-induced immune activation. *J Exp Med,* 196**,** 269-74.

ISHIKAWA, H. & BARBER, G. N. 2008. STING is an endoplasmic reticulum adaptor that facilitates innate immune signalling. *Nature,* 455**,** 674-8.

ISHIKAWA, H., MA, Z. & BARBER, G. N. 2009. STING regulates intracellular DNA-mediated, type I interferon-dependent innate immunity. *Nature,* 461**,** 788-92.

ISMAIL, S., STOKES, C. A., PRESTWICH, E. C., ROBERTS, R. L., JUSS, J. K., SABROE, I. & PARKER, L. C. 2014. Phosphoinositide-3 Kinase Inhibition Modulates Responses to Rhinovirus by Mechanisms that Are Predominantly Independent of Autophagy. *PLoS One,* 9**,** e116055.

IVISON, S. M., KHAN, M. A., GRAHAM, N. R., SHOBAB, L. A., YAO, Y., KIFAYET, A., SLY, L. M. & STEINER, T. S. 2010. The p110alpha and p110beta isoforms of class I phosphatidylinositol 3-kinase are involved in toll-like receptor 5 signaling in epithelial cells. *Mediators Inflamm,* 2010.

JACKSON, D. J., EVANS, M. D., GANGNON, R. E., TISLER, C. J., PAPPAS, T. E., LEE, W. M., GERN, J. E. & LEMANSKE, R. F., JR. 2012. Evidence for a causal relationship between allergic sensitization and rhinovirus wheezing in early life. *Am J Respir Crit Care Med,* 185**,** 281-5.

JACKSON, D. J., GANGNON, R. E., EVANS, M. D., ROBERG, K. A., ANDERSON, E. L., PAPPAS, T. E., PRINTZ, M. C., LEE, W. M., SHULT, P. A., REISDORF, E., CARLSON-DAKES, K. T., SALAZAR, L. P., DASILVA, D. F., TISLER, C. J., GERN, J. E. & LEMANSKE, R. F., JR. 2008. Wheezing rhinovirus illnesses in early life predict asthma development in high-risk children. *Am J Respir Crit Care Med,* 178**,** 667-72.

JACKSON, D. J. & JOHNSTON, S. L. 2010. The role of viruses in acute exacerbations of asthma. *J Allergy Clin Immunol,* 125**,** 1178-87; quiz 1188-9.

JACKSON, R. J. & KAMINSKI, A. 1995. Internal initiation of translation in eukaryotes: the picornavirus paradigm and beyond. *RNA,* 1**,** 985-1000.

JACKSON, W. T., GIDDINGS, T. H., JR., TAYLOR, M. P., MULINYAWE, S., RABINOVITCH, M., KOPITO, R. R. & KIRKEGAARD, K. 2005. Subversion of cellular autophagosomal machinery by RNA viruses. *PLoS Biol,* 3**,** e156.

JACOBS, S. R. & DAMANIA, B. 2012. NLRs, inflammasomes, and viral infection. *J Leukoc Biol,* 92**,** 469-77.

JEFFERY, P. K. 2001. Lymphocytes, chronic bronchitis and chronic obstructive pulmonary disease. *Novartis Found Symp,* 234**,** 149-61; discussion 161-8.

JOHNSTON, S. L., PAPI, A., BATES, P. J., MASTRONARDE, J. G., MONICK, M. M. & HUNNINGHAKE, G. W. 1998. Low grade rhinovirus infection induces a prolonged release of IL-8 in pulmonary epithelium. *J Immunol,* 160**,** 6172-81.

JORDAN, T. X. & RANDALL, G. 2011. Manipulation or capitulation: Virus interactions with autophagy. *Microbes Infect*.

JORGENSON, R. L., YOUNG, S. L., LESMEISTER, M. J., LYDDON, T. D. & MISFELDT, M. L. 2005. Human endometrial epithelial cells cyclically express Toll-like receptor 3 (TLR3) and exhibit TLR3-dependent responses to dsRNA. *Hum Immunol,* 66**,** 469-82.

JOSHI, S., KAUR, S., KROCZYNSKA, B. & PLATANIAS, L. C. 2010. Mechanisms of mRNA translation of interferon stimulated genes. *Cytokine,* 52**,** 123-7.

JUNG, C. H., JUN, C. B., RO, S. H., KIM, Y. M., OTTO, N. M., CAO, J., KUNDU, M. & KIM, D. H. 2009. ULK-Atg13-FIP200 complexes mediate mTOR signaling to the autophagy machinery. *Mol Biol Cell,* 20**,** 1992-2003.

JUSS, J. K., HAYHOE, R. P., OWEN, C. E., BRUCE, I., WALMSLEY, S. R., COWBURN, A. S., KULKARNI, S., BOYLE, K. B., STEPHENS, L., HAWKINS, P. T., CHILVERS, E. R. & CONDLIFFE, A. M. 2012. Functional Redundancy of Class I Phosphoinositide 3-Kinase (PI3K) Isoforms in Signaling Growth Factor-Mediated Human Neutrophil Survival. *PLoS One,* 7**,** e45933.

KANNEGANTI, T. D., BODY-MALAPEL, M., AMER, A., PARK, J. H., WHITFIELD, J., FRANCHI, L., TARAPOREWALA, Z. F., MILLER, D., PATTON, J. T., INOHARA, N. & NUNEZ, G. 2006. Critical role for Cryopyrin/Nalp3 in activation of caspase-1 in response to viral infection and double-stranded RNA. *J Biol Chem,* 281**,** 36560-8.

KATO, H., SATO, S., YONEYAMA, M., YAMAMOTO, M., UEMATSU, S., MATSUI, K., TSUJIMURA, T., TAKEDA, K., FUJITA, T., TAKEUCHI, O. & AKIRA, S. 2005. Cell type-specific involvement of RIG-I in antiviral response. *Immunity,* 23**,** 19-28.

KATO, H., TAKEUCHI, O., MIKAMO-SATOH, E., HIRAI, R., KAWAI, T., MATSUSHITA, K., HIIRAGI, A., DERMODY, T. S., FUJITA, T. & AKIRA, S. 2008. Length-dependent recognition of double-stranded ribonucleic acids by retinoic acid-inducible gene-I and melanoma differentiation-associated gene 5. *J Exp Med,* 205**,** 1601-10.

KATO, H., TAKEUCHI, O., SATO, S., YONEYAMA, M., YAMAMOTO, M., MATSUI, K., UEMATSU, S., JUNG, A., KAWAI, T., ISHII, K. J., YAMAGUCHI, O., OTSU, K., TSUJIMURA, T., KOH, C. S., REIS E SOUSA, C., MATSUURA, Y., FUJITA, T. & AKIRA, S. 2006. Differential roles of MDA5 and RIG-I helicases in the recognition of RNA viruses. *Nature,* 441**,** 101-5.

KAUR, S., SASSANO, A., DOLNIAK, B., JOSHI, S., MAJCHRZAK-KITA, B., BAKER, D. P., HAY, N., FISH, E. N. & PLATANIAS, L. C. 2008a. Role of the Akt pathway in mRNA translation of interferon-stimulated genes. *Proceedings of the National Academy of Sciences of the United States of America,* 105**,** 4808-13.

KAUR, S., SASSANO, A., JOSEPH, A. M., MAJCHRZAK-KITA, B., EKLUND, E. A., VERMA, A., BRACHMANN, S. M., FISH, E. N. & PLATANIAS, L. C. 2008b. Dual regulatory roles of phosphatidylinositol 3-kinase in IFN signaling. *J Immunol,* 181**,** 7316-23.

KAWAI, T. & AKIRA, S. 2011. Toll-like receptors and their crosstalk with other innate receptors in infection and immunity. *Immunity,* 34**,** 637-50.

KEATINGS, V. M., COLLINS, P. D., SCOTT, D. M. & BARNES, P. J. 1996. Differences in interleukin-8 and tumor necrosis factor-alpha in induced sputum from patients with chronic obstructive pulmonary disease or asthma. *Am J Respir Crit Care Med,* 153**,** 530-4.

KEICHO, N., ELLIOTT, W. M., HOGG, J. C. & HAYASHI, S. 1997. Adenovirus E1A gene dysregulates ICAM-1 expression in transformed pulmonary epithelial cells. *Am J Respir Cell Mol Biol,* 16**,** 23-30.

KIM, H. P., WANG, X., CHEN, Z. H., LEE, S. J., HUANG, M. H., WANG, Y., RYTER, S. W. & CHOI, A. M. 2008. Autophagic proteins regulate cigarette smoke-induced apoptosis: protective role of heme oxygenase-1. *Autophagy,* 4**,** 887-95.

KIM, J., KUNDU, M., VIOLLET, B. & GUAN, K. L. 2011. AMPK and mTOR regulate autophagy through direct phosphorylation of Ulk1. *Nature cell biology,* 13**,** 132-41.

KIM, S. S., SMITH, T. J., CHAPMAN, M. S., ROSSMANN, M. C., PEVEAR, D. C., DUTKO, F. J., FELOCK, P. J., DIANA, G. D. & MCKINLAY, M. A. 1989. Crystal structure of human rhinovirus serotype 1A (HRV1A). *J Mol Biol,* 210**,** 91-111.

KINIWA, Y., MIYAHARA, Y., WANG, H. Y., PENG, W., PENG, G., WHEELER, T. M., THOMPSON, T. C., OLD, L. J. & WANG, R. F. 2007. CD8+ Foxp3+ regulatory T cells mediate immunosuppression in prostate cancer. *Clin Cancer Res,* 13**,** 6947-58.

KLEIN, K. A. & JACKSON, W. T. 2011. Human Rhinovirus 2 Induces the Autophagic Pathway and Replicates More Efficiently in Autophagic Cells. *J Virol*.

KLIONSKY, D. J., ABDALLA, F. C., ABELIOVICH, H., ABRAHAM, R. T., ACEVEDO-AROZENA, A., ADELI, K., AGHOLME, L., AGNELLO, M., AGOSTINIS, P., AGUIRRE-GHISO, J. A., AHN, H. J., AIT-MOHAMED, O., AIT-SI-ALI, S., AKEMATSU, T., AKIRA, S., AL-YOUNES, H. M., AL-ZEER, M. A., ALBERT, M.

L., ALBIN, R. L., ALEGRE-ABARRATEGUI, J., ALEO, M. F., ALIREZAEI, M., ALMASAN, A., ALMONTE-BECERRIL, M., AMANO, A., AMARAVADI, R., AMARNATH, S., AMER, A. O., ANDRIEU-ABADIE, N., ANANTHARAM, V., ANN, D. K., ANOOPKUMAR-DUKIE, S., AOKI, H., APOSTOLOVA, N., ARANCIA, G., ARIS, J. P., ASANUMA, K., ASARE, N. Y., ASHIDA, H., ASKANAS, V., ASKEW, D. S., AUBERGER, P., BABA, M., BACKUES, S. K., BAEHRECKE, E. H., BAHR, B. A., BAI, X. Y., BAILLY, Y., BAIOCCHI, R., BALDINI, G., BALDUINI, W., BALLABIO, A., BAMBER, B. A., BAMPTON, E. T., BANHEGYI, G., BARTHOLOMEW, C. R., BASSHAM, D. C., BAST, R. C., JR., BATOKO, H., BAY, B. H., BEAU, I., BECHET, D. M., BEGLEY, T. J., BEHL, C., BEHRENDS, C., BEKRI, S., BELLAIRE, B., BENDALL, L. J., BENETTI, L., BERLIOCCHI, L., BERNARDI, H., BERNASSOLA, F., BESTEIRO, S., BHATIA-KISSOVA, I., BI, X., BIARD-PIECHACZYK, M., BLUM, J. S., BOISE, L. H., BONALDO, P., BOONE, D. L., BORNHAUSER, B. C., BORTOLUCI, K. R., BOSSIS, I., BOST, F., BOURQUIN, J. P., BOYA, P., BOYER-GUITTAUT, M., BOZHKOV, P. V., BRADY, N. R., BRANCOLINI, C., BRECH, A., BRENMAN, J. E., BRENNAND, A., BRESNICK, E. H., BREST, P., BRIDGES, D., BRISTOL, M. L., BROOKES, P. S., BROWN, E. J., BRUMELL, J. H., et al. 2012. Guidelines for the use and interpretation of assays for monitoring autophagy. *Autophagy,* 8**,** 445-544.

KNIGHT, Z. A., GONZALEZ, B., FELDMAN, M. E., ZUNDER, E. R., GOLDENBERG, D. D., WILLIAMS, O., LOEWITH, R., STOKOE, D., BALLA, A., TOTH, B., BALLA, T., WEISS, W. A., WILLIAMS, R. L. & SHOKAT, K. M. 2006. A pharmacological map of the PI3-K family defines a role for p110alpha in insulin signaling. *Cell,* 125**,** 733-47.

KONG, D., DAN, S., YAMAZAKI, K. & YAMORI, T. 2010. Inhibition profiles of phosphatidylinositol 3-kinase inhibitors against PI3K superfamily and human cancer cell line panel JFCR39. *Eur J Cancer,* 46**,** 1111-21.

KOTENKO, S. V. 2011. IFN-lambdas. *Curr Opin Immunol,* 23**,** 583-90.

KOTENKO, S. V., GALLAGHER, G., BAURIN, V. V., LEWIS-ANTES, A., SHEN, M., SHAH, N. K., LANGER, J. A., SHEIKH, F., DICKENSHEETS, H. & DONNELLY, R. P. 2003. IFN-lambdas mediate antiviral protection through a distinct class II cytokine receptor complex. *Nat Immunol,* 4**,** 69-77.

KOYASU, S. 2003. The role of PI3K in immune cells. *Nat Immunol,* 4**,** 313-9.

KRANENBURG, A. R., DE BOER, W. I., VAN KRIEKEN, J. H., MOOI, W. J., WALTERS, J. E., SAXENA, P. R., STERK, P. J. & SHARMA, H. S. 2002. Enhanced expression of fibroblast growth factors and receptor FGFR-1 during vascular remodeling in chronic obstructive pulmonary disease. *Am J Respir Cell Mol Biol,* 27**,** 517-25.

LAMBRECHT, B. N. & HAMMAD, H. 2013. Asthma: the importance of dysregulated barrier immunity. *Eur J Immunol*.

LANE, N., ROBINS, R. A., CORNE, J. & FAIRCLOUGH, L. 2010. Regulation in chronic obstructive pulmonary disease: the role of regulatory T-cells and Th17 cells. *Clin Sci (Lond),* 119**,** 75-86.

LAPPALAINEN, U., WHITSETT, J. A., WERT, S. E., TICHELAAR, J. W. & BRY, K. 2005. Interleukin-1beta causes pulmonary inflammation, emphysema, and airway remodeling in the adult murine lung. *Am J Respir Cell Mol Biol,* 32**,** 311-8.

LASITHIOTAKI, I., ANTONIOU, K. M., VLAHAVA, V. M., KARAGIANNIS, K., SPANDIDOS, D. A., SIAFAKAS, N. M. & SOURVINOS, G. 2011. Detection of herpes simplex virus type-1 in patients with fibrotic lung diseases. *PLoS One,* 6**,** e27800.

LAU, C., WANG, X., SONG, L., NORTH, M., WIEHLER, S., PROUD, D. & CHOW, C. W. 2008. Syk associates with clathrin and mediates phosphatidylinositol 3-kinase activation during human rhinovirus internalization. *J Immunol,* 180**,** 870-80.

LAZARUS, S. C., BOUSHEY, H. A., FAHY, J. V., CHINCHILLI, V. M., LEMANSKE, R. F., JR., SORKNESS, C. A., KRAFT, M., FISH, J. E., PETERS, S. P., CRAIG, T., DRAZEN, J. M., FORD, J. G., ISRAEL, E., MARTIN, R. J., MAUGER, E. A., NACHMAN, S. A., SPAHN, J. D. & SZEFLER, S. J. 2001. Long-acting beta2-agonist monotherapy vs continued therapy with inhaled corticosteroids in patients with persistent asthma: a randomized controlled trial. *JAMA,* 285**,** 2583-93.

LE GOFFIC, R., POTHLICHET, J., VITOUR, D., FUJITA, T., MEURS, E., CHIGNARD, M. & SI-TAHAR, M. 2007. Cutting Edge: Influenza A virus activates TLR3-dependent inflammatory and RIG-I-dependent antiviral responses in human lung epithelial cells. *J Immunol,* 178**,** 3368-72.

LEE, H. K., LUND, J. M., RAMANATHAN, B., MIZUSHIMA, N. & IWASAKI, A. 2007. Autophagy-dependent viral recognition by plasmacytoid dendritic cells. *Science,* 315**,** 1398-401.

LEE, W. M., WANG, W. & RUECKERT, R. R. 1995. Complete sequence of the RNA genome of human rhinovirus 16, a clinically useful common cold virus belonging to the ICAM-1 receptor group. *Virus Genes,* 9**,** 177-81.

LEVINE, B., MIZUSHIMA, N. & VIRGIN, H. W. 2011. Autophagy in immunity and inflammation. *Nature,* 469**,** 323-35.

LEVY, D. E., MARIE, I. J. & DURBIN, J. E. 2011. Induction and function of type I and III interferon in response to viral infection. *Curr Opin Virol,* 1**,** 476-86.

LIN, Y. C., KUO, H. C., WANG, J. S. & LIN, W. W. 2012. Regulation of inflammatory response by 3-methyladenine involves the coordinative actions on akt and glycogen synthase kinase 3beta rather than autophagy. *J Immunol,* 189**,** 4154-64.

LOETSCHER, M., GERBER, B., LOETSCHER, P., JONES, S. A., PIALI, L., CLARK-LEWIS, I., BAGGIOLINI, M. & MOSER, B. 1996. Chemokine receptor specific for IP10 and mig: structure, function, and expression in activated T-lymphocytes. *J Exp Med,* 184**,** 963-9.

LOIARRO, M., RUGGIERO, V. & SETTE, C. 2010. Targeting TLR/IL-1R signalling in human diseases. *Mediators Inflamm,* 2010**,** 674363.

LOPEZ, A. D. & MURRAY, C. C. 1998. The global burden of disease, 1990-2020. *Nat Med,* 4**,** 1241-3.

LOPEZ, A. D., SHIBUYA, K., RAO, C., MATHERS, C. D., HANSELL, A. L., HELD, L. S., SCHMID, V. & BUIST, S. 2006. Chronic obstructive pulmonary disease: current burden and future projections. *Eur Respir J,* 27**,** 397-412.

LOUIE, J. K., ROY-BURMAN, A., GUARDIA-LABAR, L., BOSTON, E. J., KIANG, D., PADILLA, T., YAGI, S., MESSENGER, S., PETRU, A. M., GLASER, C. A. & SCHNURR, D. P. 2009. Rhinovirus associated with severe lower respiratory tract infections in children. *Pediatr Infect Dis J,* 28**,** 337-9.

LUND, J. M., ALEXOPOULOU, L., SATO, A., KAROW, M., ADAMS, N. C., GALE, N. W., IWASAKI, A. & FLAVELL, R. A. 2004. Recognition of single-stranded RNA viruses by Toll-like receptor 7. *Proc Natl Acad Sci U S A,* 101**,** 5598-603.

LUPFER, C. & KANNEGANTI, T. D. 2013. The expanding role of NLRs in antiviral immunity. *Immunol Rev,* 255**,** 13-24.

MACNEE, W. 2001. Oxidative stress and lung inflammation in airways disease. *Eur J Pharmacol,* 429**,** 195-207.

MACNEE, W. 2005. Pathogenesis of chronic obstructive pulmonary disease. *Proc Am Thorac Soc,* 2**,** 258-66; discussion 290-1.

MAJO, J., GHEZZO, H. & COSIO, M. G. 2001. Lymphocyte population and apoptosis in the lungs of smokers and their relation to emphysema. *Eur Respir J,* 17**,** 946-53.

MALLIA, P. & JOHNSTON, S. L. 2006. How viral infections cause exacerbation of airway diseases. *Chest,* 130**,** 1203-1210.

MALLIA, P., MESSAGE, S. D., GIELEN, V., CONTOLI, M., GRAY, K., KEBADZE, T., ANISCENKO, J., LAZA-STANCA, V., EDWARDS, M. R., SLATER, L., PAPI, A., STANCIU, L. A., KON, O. M., JOHNSON, M. & JOHNSTON, S. L. 2011. Experimental Rhinovirus Infection as a Human Model of Chronic Obstructive Pulmonary Disease Exacerbation. *Am J Respir Crit Care Med*.

MANNING, B. D. & CANTLEY, L. C. 2007. AKT/PKB signaling: navigating downstream. *Cell,* 129**,** 1261-74.

MANNINO, D. M. & BUIST, A. S. 2007. Global burden of COPD: risk factors, prevalence, and future trends. *Lancet,* 370**,** 765-73.

MANUSE, M. J., BRIGGS, C. M. & PARKS, G. D. 2010. Replication-independent activation of human plasmacytoid dendritic cells by the paramyxovirus SV5 Requires TLR7 and autophagy pathways. *Virology,* 405**,** 383-9.

MARINGER, K. & FERNANDEZ-SESMA, A. 2014. Message in a bottle: lessons learned from antagonism of STING signalling during RNA virus infection. *Cytokine Growth Factor Rev,* 25**,** 669-79.

MATSUMOTO, M., KIKKAWA, S., KOHASE, M., MIYAKE, K. & SEYA, T. 2002. Establishment of a monoclonal antibody against human Toll-like receptor 3 that blocks double-stranded RNA-mediated signaling. *Biochem Biophys Res Commun,* 293**,** 1364-9.

MATSUMOTO, M. & SEYA, T. 2008. TLR3: interferon induction by double-stranded RNA including poly(I:C). *Adv Drug Deliv Rev,* 60**,** 805-12.

MATSUZAKI, S., ISHIZUKA, T., HISADA, T., AOKI, H., KOMACHI, M., ICHIMONJI, I., UTSUGI, M., ONO, A., KOGA, Y., DOBASHI, K., KUROSE, H., TOMURA, H., MORI, M. & OKAJIMA, F. 2010. Lysophosphatidic acid inhibits CC chemokine ligand 5/RANTES production by blocking IRF-1-mediated gene transcription in human bronchial epithelial cells. *J Immunol,* 185**,** 4863-72.

MCMANUS, T. E., MARLEY, A. M., BAXTER, N., CHRISTIE, S. N., O'NEILL, H. J., ELBORN, J. S., COYLE, P. V. & KIDNEY, J. C. 2008. Respiratory viral infection in exacerbations of COPD. *Respir Med,* 102**,** 1575-80.

MCNAMARA, C. R. & DEGTEREV, A. 2011. Small-molecule inhibitors of the PI3K signaling network. *Future Med Chem,* 3**,** 549-65.

MEIJER, A. J. & CODOGNO, P. 2004. Regulation and role of autophagy in mammalian cells. *Int J Biochem Cell Biol,* 36**,** 2445-62.

MELCHJORSEN, J., JENSEN, S. B., MALMGAARD, L., RASMUSSEN, S. B., WEBER, F., BOWIE, A. G., MATIKAINEN, S. & PALUDAN, S. R. 2005. Activation of innate defense against a paramyxovirus is mediated by RIG-I and TLR7 and TLR8 in a cell-type-specific manner. *J Virol,* 79**,** 12944-51.

MILLER, M. D. & KRANGEL, M. S. 1992. Biology and biochemistry of the chemokines: a family of chemotactic and inflammatory cytokines. *Crit Rev Immunol,* 12**,** 17-46.

MIO, T., ROMBERGER, D. J., THOMPSON, A. B., ROBBINS, R. A., HEIRES, A. & RENNARD, S. I. 1997. Cigarette smoke induces interleukin-8 release from human bronchial epithelial cells. *Am J Respir Crit Care Med,* 155**,** 1770-6.

MIZUMURA, K., CLOONAN, S. M., HASPEL, J. A. & CHOI, A. M. 2012. The emerging importance of autophagy in pulmonary diseases. *Chest,* 142**,** 1289-99.

MIZUSHIMA, N. & YOSHIMORI, T. 2007. How to interpret LC3 immunoblotting. *Autophagy,* 3**,** 542-5.

MIZUSHIMA, N., YOSHIMORI, T. & LEVINE, B. 2010. Methods in mammalian autophagy research. *Cell,* 140**,** 313-26.

MIZUSHIMA, N., YOSHIMORI, T. & OHSUMI, Y. 2011. The role of Atg proteins in autophagosome formation. *Annu Rev Cell Dev Biol,* 27**,** 107-32.

MONICK, M. M., POWERS, L. S., WALTERS, K., LOVAN, N., ZHANG, M., GERKE, A., HANSDOTTIR, S. & HUNNINGHAKE, G. W. 2010. Identification of an autophagy defect in smokers' alveolar macrophages. *J Immunol,* 185**,** 5425-35.

MORRIS, G. E., PARKER, L. C., WARD, J. R., JONES, E. C., WHYTE, M. K., BRIGHTLING, C. E., BRADDING, P., DOWER, S. K. & SABROE, I. 2006. Cooperative molecular and cellular networks regulate Toll-like receptor-dependent inflammatory responses. *FASEB J,* 20**,** 2153-5.

MORRIS, G. E., WHYTE, M. K., MARTIN, G. F., JOSE, P. J., DOWER, S. K. & SABROE, I. 2005. Agonists of toll-like receptors 2 and 4 activate airway smooth muscle via mononuclear leukocytes. *Am J Respir Crit Care Med,* 171**,** 814-22.

MORRIS, S., SWANSON, M. S., LIEBERMAN, A., REED, M., YUE, Z., LINDELL, D. M. & LUKACS, N. W. 2011. Autophagy-Mediated Dendritic Cell Activation Is Essential for Innate Cytokine Production and APC Function with Respiratory Syncytial Virus Responses. *J Immunol*.

MURUVE, D. A., PETRILLI, V., ZAISS, A. K., WHITE, L. R., CLARK, S. A., ROSS, P. J., PARKS, R. J. & TSCHOPP, J. 2008. The inflammasome recognizes cytosolic microbial and host DNA and triggers an innate immune response. *Nature,* 452**,** 103-7.

NAKAHIRA, K. & CHOI, A. M. 2013. Autophagy: a potential therapeutic target in lung diseases. *Am J Physiol Lung Cell Mol Physiol,* 305**,** L93-107.

NAKAHIRA, K., HASPEL, J. A., RATHINAM, V. A., LEE, S. J., DOLINAY, T., LAM, H. C., ENGLERT, J. A., RABINOVITCH, M., CERNADAS, M., KIM, H. P., FITZGERALD, K. A., RYTER, S. W. & CHOI, A. M. 2011. Autophagy proteins regulate innate immune responses by inhibiting the release of mitochondrial DNA mediated by the NALP3 inflammasome. *Nat Immunol,* 12**,** 222-30.

NEOTE, K., DIGREGORIO, D., MAK, J. Y., HORUK, R. & SCHALL, T. J. 1993. Molecular cloning, functional expression, and signaling characteristics of a C-C chemokine receptor. *Cell,* 72**,** 415-25.

NEWCOMB, D. C., SAJJAN, U., NANUA, S., JIA, Y., GOLDSMITH, A. M., BENTLEY, J. K. & HERSHENSON, M. B. 2005. Phosphatidylinositol 3-kinase is required for rhinovirus-induced airway epithelial cell interleukin-8 expression. *J Biol Chem,* 280**,** 36952-61.

NEWCOMB, D. C., SAJJAN, U. S., NAGARKAR, D. R., WANG, Q., NANUA, S., ZHOU, Y., MCHENRY, C. L., HENNRICK, K. T., TSAI, W. C., BENTLEY, J. K., LUKACS, N. W., JOHNSTON, S. L. & HERSHENSON, M. B. 2008. Human rhinovirus 1B exposure induces phosphatidylinositol 3-kinase-dependent airway inflammation in mice. *Am J Respir Crit Care Med,* 177**,** 1111-21.

NOORDHOEK, J. A., POSTMA, D. S., CHONG, L. L., MENKEMA, L., KAUFFMAN, H. F., TIMENS, W., VAN STRAATEN, J. F. & VAN DER GELD, Y. M. 2005. Different modulation of decorin production by lung fibroblasts from patients with mild and severe emphysema. *COPD,* 2**,** 17-25.

OHNISHI, K., TAKAGI, M., KUROKAWA, Y., SATOMI, S. & KONTTINEN, Y. T. 1998. Matrix metalloproteinase-mediated extracellular matrix protein degradation in human pulmonary emphysema. *Lab Invest,* 78**,** 1077-87.

OKKENHAUG, K. 2013. Signaling by the phosphoinositide 3-kinase family in immune cells. *Annu Rev Immunol,* 31**,** 675-704.

OLIVER, B. G., JOHNSTON, S. L., BARAKET, M., BURGESS, J. K., KING, N. J., ROTH, M., LIM, S. & BLACK, J. L. 2006. Increased proinflammatory responses from asthmatic human airway smooth muscle cells in response to rhinovirus infection. *Respir Res,* 7**,** 71.

OPPENHEIM, J. J., ZACHARIAE, C. O., MUKAIDA, N. & MATSUSHIMA, K. 1991. Properties of the novel proinflammatory supergene "intercrine" cytokine family. *Annu Rev Immunol,* 9**,** 617-48.

ORDONEZ, C. L., SHAUGHNESSY, T. E., MATTHAY, M. A. & FAHY, J. V. 2000. Increased neutrophil numbers and IL-8 levels in airway secretions in acute severe asthma: Clinical and biologic significance. *Am J Respir Crit Care Med,* 161**,** 1185-90.

OZATO, K., TAILOR, P. & KUBOTA, T. 2007. The interferon regulatory factor family in host defense: mechanism of action. *J Biol Chem,* 282**,** 20065-9.

PALMENBERG, A. C., SPIRO, D., KUZMICKAS, R., WANG, S., DJIKENG, A., RATHE, J. A., FRASER-LIGGETT, C. M. & LIGGETT, S. B. 2009. Sequencing and analyses of all known human rhinovirus genomes reveal structure and evolution. *Science,* 324**,** 55-9.

PAN, H., ZHANG, Y., LUO, Z., LI, P., LIU, L., WANG, C., WANG, H., LI, H. & MA, Y. 2013. Autophagy mediates avian influenza H5N1 pseudotyped particle-induced lung

inflammation through NF-kappaB and p38 MAPK signaling pathways. *Am J Physiol Lung Cell Mol Physiol*.

PAN, Z. K., FISHER, C., LI, J. D., JIANG, Y., HUANG, S. & CHEN, L. Y. 2011. Bacterial LPS up-regulated TLR3 expression is critical for antiviral response in human monocytes: evidence for negative regulation by CYLD. *Int Immunol,* 23**,** 357-64.

PAPADOPOULOS, N. G., BATES, P. J., BARDIN, P. G., PAPI, A., LEIR, S. H., FRAENKEL, D. J., MEYER, J., LACKIE, P. M., SANDERSON, G., HOLGATE, S. T. & JOHNSTON, S. L. 2000. Rhinoviruses infect the lower airways. *J Infect Dis,* 181**,** 1875-84.

PAPI, A., CONTOLI, M., CARAMORI, G., MALLIA, P. & JOHNSTON, S. L. 2007. Models of infection and exacerbations in COPD. *Curr Opin Pharmacol,* 7**,** 259-65.

PAPI, A. & JOHNSTON, S. L. 1999. Rhinovirus infection induces expression of its own receptor intercellular adhesion molecule 1 (ICAM-1) via increased NF-kappaB-mediated transcription. *J Biol Chem,* 274**,** 9707-20.

PARKER, L. C., PRESTWICH, E. C., WARD, J. R., SMYTHE, E., BERRY, A., TRIANTAFILOU, M., TRIANTAFILOU, K. & SABROE, I. 2008. A phosphatidylserine species inhibits a range of TLR- but not IL-1beta-induced inflammatory responses by disruption of membrane microdomains. *J Immunol,* 181**,** 5606-17.

PATEL, A. S., LIN, L., GEYER, A., HASPEL, J. A., AN, C. H., CAO, J., ROSAS, I. O. & MORSE, D. 2012. Autophagy in idiopathic pulmonary fibrosis. *PLoS One,* 7**,** e41394.

PATEL, A. S., MORSE, D. & CHOI, A. M. 2013. Regulation and functional significance of autophagy in respiratory cell biology and disease. *Am J Respir Cell Mol Biol,* 48**,** 1-9.

PAUWELS, R. A., BUIST, A. S., CALVERLEY, P. M., JENKINS, C. R. & HURD, S. S. 2001. Global strategy for the diagnosis, management, and prevention of chronic obstructive pulmonary disease. NHLBI/WHO Global Initiative for Chronic Obstructive Lung Disease (GOLD) Workshop summary. *Am J Respir Crit Care Med,* 163**,** 1256-76.

PAUWELS, R. A., LOFDAHL, C. G., LAITINEN, L. A., SCHOUTEN, J. P., POSTMA, D. S., PRIDE, N. B. & OHLSSON, S. V. 1999. Long-term treatment with inhaled budesonide in persons with mild chronic obstructive pulmonary disease who continue smoking. European Respiratory Society Study on Chronic Obstructive Pulmonary Disease. *N Engl J Med,* 340**,** 1948-53.

PELTIER, D. C., SIMMS, A., FARMER, J. R. & MILLER, D. J. 2010. Human neuronal cells possess functional cytoplasmic and TLR-mediated innate immune pathways influenced by phosphatidylinositol-3 kinase signaling. *J Immunol,* 184**,** 7010-21.

PENGAL, R. A., GANESAN, L. P., WEI, G., FANG, H., OSTROWSKI, M. C. & TRIDANDAPANI, S. 2006. Lipopolysaccharide-induced production of interleukin-10 is promoted by the serine/threonine kinase Akt. *Mol Immunol,* 43**,** 1557-64.

PEROTIN, J. M., DURY, S., RENOIS, F., DESLEE, G., WOLAK, A., DUVAL, V., DE CHAMPS, C., LEBARGY, F. & ANDREOLETTI, L. 2013. Detection of multiple viral and bacterial infections in acute exacerbation of chronic obstructive pulmonary disease: a pilot prospective study. *J Med Virol,* 85**,** 866-73.

PERSSON, H. L., NILSSON, K. J. & BRUNK, U. T. 2001. Novel cellular defenses against iron and oxidation: ferritin and autophagocytosis preserve lysosomal stability in airway epithelium. *Redox Rep,* 6**,** 57-63.

PICHLMAIR, A., SCHULZ, O., TAN, C. P., NASLUND, T. I., LILJESTROM, P., WEBER, F. & REIS E SOUSA, C. 2006. RIG-I-mediated antiviral responses to single-stranded RNA bearing 5'-phosphates. *Science,* 314**,** 997-1001.

PIPER, S. C., FERGUSON, J., KAY, L., PARKER, L. C., SABROE, I., SLEEMAN, M. A., BRIEND, E. & FINCH, D. K. 2013. The role of interleukin-1 and interleukin-18 in pro-inflammatory and anti-viral responses to rhinovirus in primary bronchial epithelial cells. *PLoS One,* 8**,** e63365.

POON, A. H., CHOUIALI, F., TSE, S. M., LITONJUA, A. A., HUSSAIN, S. N., BAGLOLE, C. J., EIDELMAN, D. H., OLIVENSTEIN, R., MARTIN, J. G., WEISS, S. T., HAMID, Q. & LAPRISE, C. 2012. Genetic and histologic evidence for autophagy in asthma pathogenesis. *The Journal of allergy and clinical immunology,* 129**,** 569-71.

POWELL, J. D., POLLIZZI, K. N., HEIKAMP, E. B. & HORTON, M. R. 2012. Regulation of immune responses by mTOR. *Annu Rev Immunol,* 30**,** 39-68.

PRCHLA, E., KUECHLER, E., BLAAS, D. & FUCHS, R. 1994. Uncoating of human rhinovirus serotype 2 from late endosomes. *J Virol,* 68**,** 3713-23.

PUDDICOMBE, S. M., POLOSA, R., RICHTER, A., KRISHNA, M. T., HOWARTH, P. H., HOLGATE, S. T. & DAVIES, D. E. 2000. Involvement of the epidermal growth factor receptor in epithelial repair in asthma. *Faseb Journal,* 14**,** 1362-74.

RAHMAN, I. & MACNEE, W. 1996. Role of oxidants/antioxidants in smoking-induced lung diseases. *Free Radic Biol Med,* 21**,** 669-81.

RAO, N. V., MARSHALL, B. C., GRAY, B. H. & HOIDAL, J. R. 1993. Interaction of secretory leukocyte protease inhibitor with proteinase-3. *Am J Respir Cell Mol Biol,* 8**,** 612-6.

RAPORT, C. J., GOSLING, J., SCHWEICKART, V. L., GRAY, P. W. & CHARO, I. F. 1996. Molecular cloning and functional characterization of a novel human CC chemokine receptor (CCR5) for RANTES, MIP-1beta, and MIP-1alpha. *J Biol Chem,* 271**,** 17161-6.

RAYNAUD, F. I., ECCLES, S., CLARKE, P. A., HAYES, A., NUTLEY, B., ALIX, S., HENLEY, A., DI-STEFANO, F., AHMAD, Z., GUILLARD, S., BJERKE, L. M., KELLAND, L., VALENTI, M., PATTERSON, L., GOWAN, S., DE HAVEN BRANDON, A., HAYAKAWA, M., KAIZAWA, H., KOIZUMI, T., OHISHI, T., PATEL, S., SAGHIR, N., PARKER, P., WATERFIELD, M. & WORKMAN, P. 2007. Pharmacologic characterization of a potent inhibitor of class I phosphatidylinositide 3-kinases. *Cancer Res,* 67**,** 5840-50.

RHEE, S. H., KIM, H., MOYER, M. P. & POTHOULAKIS, C. 2006. Role of MyD88 in phosphatidylinositol 3-kinase activation by flagellin/toll-like receptor 5 engagement in colonic epithelial cells. *J Biol Chem,* 281**,** 18560-8.

RICHETTA, C. & FAURE, M. 2013. Autophagy in antiviral innate immunity. *Cell Microbiol,* 15**,** 368-76.

RIDER, P., CARMI, Y., GUTTMAN, O., BRAIMAN, A., COHEN, I., VORONOV, E., WHITE, M. R., DINARELLO, C. A. & APTE, R. N. 2011. IL-1alpha and IL-1beta recruit different myeloid cells and promote different stages of sterile inflammation. *J Immunol,* 187**,** 4835-43.

RITTER, M., MENNERICH, D., WEITH, A. & SEITHER, P. 2005. Characterization of Toll-like receptors in primary lung epithelial cells: strong impact of the TLR3 ligand poly(I:C) on the regulation of Toll-like receptors, adaptor proteins and inflammatory response. *J Inflamm (Lond),* 2**,** 16.

ROHDE, G., WIETHEGE, A., BORG, I., KAUTH, M., BAUER, T. T., GILLISSEN, A., BUFE, A. & SCHULTZE-WERNINGHAUS, G. 2003. Respiratory viruses in exacerbations of chronic obstructive pulmonary disease requiring hospitalisation: a case-control study. *Thorax,* 58**,** 37-42.

ROYCE, S. G., MOODLEY, Y. & SAMUEL, C. S. 2014. Novel therapeutic strategies for lung disorders associated with airway remodelling and fibrosis. *Pharmacol Ther,* 141**,** 250-260.

RUDD, B. D., BURSTEIN, E., DUCKETT, C. S., LI, X. & LUKACS, N. W. 2005. Differential role for TLR3 in respiratory syncytial virus-induced chemokine expression. *J Virol,* 79**,** 3350-7.

RUSE, M. & KNAUS, U. G. 2006. New players in TLR-mediated innate immunity: PI3K and small Rho GTPases. *Immunol Res,* 34**,** 33-48.

RUSZNAK, C., MILLS, P. R., DEVALIA, J. L., SAPSFORD, R. J., DAVIES, R. J. & LOZEWICZ, S. 2000. Effect of cigarette smoke on the permeability and IL-1beta and sICAM-1 release from cultured human bronchial epithelial cells of never-smokers, smokers, and patients with chronic obstructive pulmonary disease. *Am J Respir Cell Mol Biol,* 23**,** 530-6.

RYTER, S. W., NAKAHIRA, K., HASPEL, J. A. & CHOI, A. M. 2011. Autophagy in Pulmonary Diseases. *Annu Rev Physiol*.

SABBAH, A., CHANG, T. H., HARNACK, R., FROHLICH, V., TOMINAGA, K., DUBE, P. H., XIANG, Y. & BOSE, S. 2009. Activation of innate immune antiviral responses by Nod2. *Nat Immunol,* 10**,** 1073-80.

SABROE, I., DOCKRELL, D. H., VOGEL, S. N., RENSHAW, S. A., WHYTE, M. K. & DOWER, S. K. 2007a. Identifying and hurdling obstacles to translational research. *Nat Rev Immunol,* 7**,** 77-82.

SABROE, I., PARKER, L. C., DOWER, S. K. & WHYTE, M. K. 2007b. Practical and conceptual models of chronic obstructive pulmonary disease. *Proc Am Thorac Soc,* 4**,** 606-10.

SADIK, C. D., BACHMANN, M., PFEILSCHIFTER, J. & MUHL, H. 2009. Activation of interferon regulatory factor-3 via toll-like receptor 3 and immunomodulatory functions detected in A549 lung epithelial cells exposed to misplaced U1-snRNA. *Nucleic Acids Res,* 37**,** 5041-56.

SAETTA, M., MARIANI, M., PANINA-BORDIGNON, P., TURATO, G., BUONSANTI, C., BARALDO, S., BELLETTATO, C. M., PAPI, A., CORBETTA, L., ZUIN, R., SINIGAGLIA, F. & FABBRI, L. M. 2002. Increased expression of the chemokine

receptor CXCR3 and its ligand CXCL10 in peripheral airways of smokers with chronic obstructive pulmonary disease. *Am J Respir Crit Care Med,* 165**,** 1404-9.

SALPETER, S. R., ORMISTON, T. M. & SALPETER, E. E. 2004. Cardiovascular effects of beta-agonists in patients with asthma and COPD: a meta-analysis. *Chest,* 125**,** 2309-21.

SAMUEL, C. E. 2001. Antiviral actions of interferons. *Clin Microbiol Rev,* 14**,** 778-809, table of contents.

SAPEY, E., AHMAD, A., BAYLEY, D., NEWBOLD, P., SNELL, N., RUGMAN, P. & STOCKLEY, R. A. 2009. Imbalances between interleukin-1 and tumor necrosis factor agonists and antagonists in stable COPD. *J Clin Immunol,* 29**,** 508-16.

SARBASSOV, D. D., ALI, S. M. & SABATINI, D. M. 2005. Growing roles for the mTOR pathway. *Curr Opin Cell Biol,* 17**,** 596-603.

SARKAR, S. N., PETERS, K. L., ELCO, C. P., SAKAMOTO, S., PAL, S. & SEN, G. C. 2004. Novel roles of TLR3 tyrosine phosphorylation and PI3 kinase in double-stranded RNA signaling. *Nat Struct Mol Biol,* 11**,** 1060-7.

SATOH, T., KATO, H., KUMAGAI, Y., YONEYAMA, M., SATO, S., MATSUSHITA, K., TSUJIMURA, T., FUJITA, T., AKIRA, S. & TAKEUCHI, O. 2010. LGP2 is a positive regulator of RIG-I- and MDA5-mediated antiviral responses. *Proc Natl Acad Sci U S A,* 107**,** 1512-7.

SCAFFIDI, P., MISTELI, T. & BIANCHI, M. E. 2002. Release of chromatin protein HMGB1 by necrotic cells triggers inflammation. *Nature,* 418**,** 191-5.

SCHALL, T. J., BACON, K., TOY, K. J. & GOEDDEL, D. V. 1990. Selective attraction of monocytes and T lymphocytes of the memory phenotype by cytokine RANTES. *Nature,* 347**,** 669-71.

SCHMEISSER, H., FEY, S. B., HOROWITZ, J., FISCHER, E. R., BALINSKY, C. A., MIYAKE, K., BEKISZ, J., SNOW, A. L. & ZOON, K. C. 2013. Type I interferons induce autophagy in certain human cancer cell lines. *Autophagy,* 9**,** 683-96.

SCHNEIDER, D., GANESAN, S., COMSTOCK, A. T., MELDRUM, C. A., MAHIDHARA, R., GOLDSMITH, A. M., CURTIS, J. L., MARTINEZ, F. J., HERSHENSON, M. B. & SAJJAN, U. 2010. Increased cytokine response of rhinovirus-infected airway epithelial cells in chronic obstructive pulmonary disease. *Am J Respir Crit Care Med,* 182**,** 332-40.

SCHOBER, D., KRONENBERGER, P., PRCHLA, E., BLAAS, D. & FUCHS, R. 1998. Major and minor receptor group human rhinoviruses penetrate from endosomes by different mechanisms. *J Virol,* 72**,** 1354-64.

SCHULZ, C., KRATZEL, K., WOLF, K., SCHROLL, S., KOHLER, M. & PFEIFER, M. 2004. Activation of bronchial epithelial cells in smokers without airway obstruction and patients with COPD. *Chest,* 125**,** 1706-13.

SEEMUNGAL, T., HARPER-OWEN, R., BHOWMIK, A., MORIC, I., SANDERSON, G., MESSAGE, S., MACCALLUM, P., MEADE, T. W., JEFFRIES, D. J., JOHNSTON, S. L. & WEDZICHA, J. A. 2001. Respiratory viruses, symptoms, and inflammatory markers in acute exacerbations and stable chronic obstructive pulmonary disease. *Am J Respir Crit Care Med,* 164**,** 1618-23.

SEEMUNGAL, T. A., HARPER-OWEN, R., BHOWMIK, A., JEFFRIES, D. J. & WEDZICHA, J. A. 2000. Detection of rhinovirus in induced sputum at exacerbation of chronic obstructive pulmonary disease. *Eur Respir J,* 16**,** 677-83.

SETH, R. B., SUN, L. & CHEN, Z. J. 2006. Antiviral innate immunity pathways. *Cell Res,* 16**,** 141-7.

SHA, Q., TRUONG-TRAN, A. Q., PLITT, J. R., BECK, L. A. & SCHLEIMER, R. P. 2004. Activation of airway epithelial cells by toll-like receptor agonists. *Am J Respir Cell Mol Biol,* 31**,** 358-64.

SHAPIRA, S. D., GAT-VIKS, I., SHUM, B. O., DRICOT, A., DE GRACE, M. M., WU, L., GUPTA, P. B., HAO, T., SILVER, S. J., ROOT, D. E., HILL, D. E., REGEV, A. & HACOHEN, N. 2009. A physical and regulatory map of host-influenza interactions reveals pathways in H1N1 infection. *Cell,* 139**,** 1255-67.

SHAPIRO, S. D. 1999. The macrophage in chronic obstructive pulmonary disease. *Am J Respir Crit Care Med,* 160**,** S29-32.

SHEN, M., REITMAN, Z. J., ZHAO, Y., MOUSTAFA, I., WANG, Q., ARNOLD, J. J., PATHAK, H. B. & CAMERON, C. E. 2008. Picornavirus genome replication. Identification of the surface of the poliovirus (PV) 3C dimer that interacts with PV 3Dpol during VPg uridylylation and construction of a structural model for the PV 3C2-3Dpol complex. *J Biol Chem,* 283**,** 875-88.

SHEPPARD, P., KINDSVOGEL, W., XU, W., HENDERSON, K., SCHLUTSMEYER, S., WHITMORE, T. E., KUESTNER, R., GARRIGUES, U., BIRKS, C., RORABACK, J., OSTRANDER, C., DONG, D., SHIN, J., PRESNELL, S., FOX, B., HALDEMAN, B., COOPER, E., TAFT, D., GILBERT, T., GRANT, F. J., TACKETT, M., KRIVAN, W., MCKNIGHT, G., CLEGG, C., FOSTER, D. & KLUCHER, K. M. 2003. IL-28, IL-29 and their class II cytokine receptor IL-28R. *Nat Immunol,* 4**,** 63-8.

SHI, C. S. & KEHRL, J. H. 2008. MyD88 and Trif target Beclin 1 to trigger autophagy in macrophages. *J Biol Chem,* 283**,** 33175-82.

SHI, L., MANTHEI, D. M., GUADARRAMA, A. G., LENERTZ, L. Y. & DENLINGER, L. C. 2012. Rhinovirus-induced IL-1beta Release from Bronchial Epithelial Cells is Independent of Functional P2X7. *Am J Respir Cell Mol Biol*.

SHIMOBAYASHI, M. & HALL, M. N. 2014. Making new contacts: the mTOR network in metabolism and signalling crosstalk. *Nat Rev Mol Cell Biol,* 15**,** 155-62.

SIEDNIENKO, J., GAJANAYAKE, T., FITZGERALD, K. A., MOYNAGH, P. & MIGGIN, S. M. 2011. Absence of MyD88 results in enhanced TLR3-dependent phosphorylation of IRF3 and increased IFN-(beta) and RANTES production. *J Immunol,* 186**,** 2514-22.

SIRIANNI, F. E., CHU, F. S. & WALKER, D. C. 2003. Human alveolar wall fibroblasts directly link epithelial type 2 cells to capillary endothelium. *Am J Respir Crit Care Med,* 168**,** 1532-7.

SLATER, L., BARTLETT, N. W., HAAS, J. J., ZHU, J., MESSAGE, S. D., WALTON, R. P., SYKES, A., DAHDALEH, S., CLARKE, D. L., BELVISI, M. G., KON, O. M., FUJITA, T., JEFFERY, P. K., JOHNSTON, S. L. & EDWARDS, M. R. 2010. Co-ordinated role of TLR3, RIG-I and MDA5 in the innate response to rhinovirus in bronchial epithelium. *PLoS Pathog,* 6**,** e1001178.

SLY, L. M., HAMILTON, M. J., KURODA, E., HO, V. W., ANTIGNANO, F. L., OMEIS, S. L., VAN NETTEN-THOMAS, C. J., WONG, D., BRUGGER, H. K., WILLIAMS, O., FELDMAN, M. E., HOUSEMAN, B. T., FIEDLER, D., SHOKAT, K. M. & KRYSTAL, G. 2009. SHIP prevents lipopolysaccharide from triggering an antiviral response in mice. *Blood,* 113**,** 2945-54.

SMITH, R. E., STRIETER, R. M., PHAN, S. H. & KUNKEL, S. L. 1996. C-C chemokines: novel mediators of the profibrotic inflammatory response to bleomycin challenge. *Am J Respir Cell Mol Biol,* 15**,** 693-702.

SMITH, R. S., SMITH, T. J., BLIEDEN, T. M. & PHIPPS, R. P. 1997. Fibroblasts as sentinel cells. Synthesis of chemokines and regulation of inflammation. *Am J Pathol,* 151**,** 317-22.

SOMMERHOFF, C. P., NADEL, J. A., BASBAUM, C. B. & CAUGHEY, G. H. 1990. Neutrophil elastase and cathepsin G stimulate secretion from cultured bovine airway gland serous cells. *J Clin Invest,* 85**,** 682-9.

SONG, W., ZHAO, J. & LI, Z. 2001. Interleukin-6 in bronchoalveolar lavage fluid from patients with COPD. *Chin Med J (Engl),* 114**,** 1140-2.

SPARRER, K. M. & GACK, M. U. 2015. Intracellular detection of viral nucleic acids. *Curr Opin Microbiol,* 26**,** 1-9.

STANESCU, D., SANNA, A., VERITER, C., KOSTIANEV, S., CALCAGNI, P. G., FABBRI, L. M. & MAESTRELLI, P. 1996. Airways obstruction, chronic expectoration, and rapid decline of FEV1 in smokers are associated with increased levels of sputum neutrophils. *Thorax,* 51**,** 267-71.

STANWAY, G., HUGHES, P. J., MOUNTFORD, R. C., MINOR, P. D. & ALMOND, J. W. 1984. The complete nucleotide sequence of a common cold virus: human rhinovirus 14. *Nucleic Acids Res,* 12**,** 7859-75.

STAUNTON, D. E., MERLUZZI, V. J., ROTHLEIN, R., BARTON, R., MARLIN, S. D. & SPRINGER, T. A. 1989. A cell adhesion molecule, ICAM-1, is the major surface receptor for rhinoviruses. *Cell,* 56**,** 849-53.

STOKES, C. A., ISMAIL, S., DICK, E. P., BENNETT, J. A., JOHNSTON, S. L., EDWARDS, M. R., SABROE, I. & PARKER, L. C. 2011. The role of IL-1 and MyD88-dependent signaling in rhinoviral infection. *J Virol*.

SUN, W., LI, Y., CHEN, L., CHEN, H., YOU, F., ZHOU, X., ZHOU, Y., ZHAI, Z., CHEN, D. & JIANG, Z. 2009. ERIS, an endoplasmic reticulum IFN stimulator, activates innate immune signaling through dimerization. *Proc Natl Acad Sci U S A,* 106**,** 8653-8.

SYKES, A., EDWARDS, M. R., MACINTYRE, J., DEL ROSARIO, A., GIELEN, V., HAAS, J., KON, O. M., MCHALE, M. & JOHNSTON, S. L. 2013. TLR3, TLR4 and TLRs7-9 Induced Interferons Are Not Impaired in Airway and Blood Cells in Well Controlled Asthma. *PLoS One,* 8**,** e65921.

TABETA, K., GEORGEL, P., JANSSEN, E., DU, X., HOEBE, K., CROZAT, K., MUDD, S., SHAMEL, L., SOVATH, S., GOODE, J., ALEXOPOULOU, L., FLAVELL, R. A. & BEUTLER, B. 2004. Toll-like receptors 9 and 3 as essential components of innate immune defense against mouse cytomegalovirus infection. *Proc Natl Acad Sci U S A,* 101**,** 3516-21.

TAKAOKA, A. & YANAI, H. 2006. Interferon signalling network in innate defence. *Cell Microbiol,* 8**,** 907-22.

TAKEUCHI, O. & AKIRA, S. 2010. Pattern recognition receptors and inflammation. *Cell,* 140**,** 805-20.

TAKEYAMA, K., DABBAGH, K., JEONG SHIM, J., DAO-PICK, T., UEKI, I. F. & NADEL, J. A. 2000. Oxidative stress causes mucin synthesis via transactivation of epidermal growth factor receptor: role of neutrophils. *J Immunol,* 164**,** 1546-52.

TAKIZAWA, H., TANAKA, M., TAKAMI, K., OHTOSHI, T., ITO, K., SATOH, M., OKADA, Y., YAMASAWA, F., NAKAHARA, K. & UMEDA, A. 2001. Increased expression of transforming growth factor-beta1 in small airway epithelium from tobacco smokers and patients with chronic obstructive pulmonary disease (COPD). *Am J Respir Crit Care Med,* 163**,** 1476-83.

TANIDA, I., UENO, T. & KOMINAMI, E. 2004. LC3 conjugation system in mammalian autophagy. *Int J Biochem Cell Biol,* 36**,** 2503-18.

THOMAS, B. J., LINDSAY, M., DAGHER, H., FREEZER, N. J., LI, D., GHILDYAL, R. & BARDIN, P. G. 2009. Transforming growth factor-beta enhances rhinovirus infection by diminishing early innate responses. *Am J Respir Cell Mol Biol,* 41**,** 339-47.

TISSARI, J., SIREN, J., MERI, S., JULKUNEN, I. & MATIKAINEN, S. 2005. IFN-alpha enhances TLR3-mediated antiviral cytokine expression in human endothelial and epithelial cells by up-regulating TLR3 expression. *J Immunol,* 174**,** 4289-94.

TRAVES, S. L., SMITH, S. J., BARNES, P. J. & DONNELLY, L. E. 2004. Specific CXC but not CC chemokines cause elevated monocyte migration in COPD: a role for CXCR2. *J Leukoc Biol,* 76**,** 441-50.

TRIANTAFILOU, K., ORTHOPOULOS, G., VAKAKIS, E., AHMED, M. A., GOLENBOCK, D. T., LEPPER, P. M. & TRIANTAFILOU, M. 2005. Human cardiac inflammatory responses triggered by Coxsackie B viruses are mainly Toll-like receptor (TLR) 8-dependent. *Cell Microbiol,* 7**,** 1117-26.

TRIANTAFILOU, K., VAKAKIS, E., RICHER, E. A. J., EVANS, G. L., VILLIERS, J. P. & TRIANTAFILOU, M. 2011. Human rhinovirus recognition in non-immune cells is mediated by Toll-like receptors and MDA-5, which trigger a synergetic pro-inflammatory immune response. *Virulence,* 2**,** 22-29.

TRINCHIERI, G. 2010. Type I interferon: friend or foe? *J Exp Med,* 207**,** 2053-63.

TROUTMAN, T. D., BAZAN, J. F. & PASARE, C. 2012. Toll-like receptors, signaling adapters and regulation of the pro-inflammatory response by PI3K. *Cell Cycle,* 11**,** 3559-67.

UNGER, B. L., FARIS, A. N., GANESAN, S., COMSTOCK, A. T., HERSHENSON, M. B. & SAJJAN, U. S. 2012. Rhinovirus attenuates non-typeable Hemophilus influenzae-stimulated IL-8 responses via TLR2-dependent degradation of IRAK-1. *PLoS Pathog,* 8**,** e1002969.

UNTERHOLZNER, L. 2013. The interferon response to intracellular DNA: why so many receptors? *Immunobiology,* 218**,** 1312-21.

VAN LY, D., KING, N. J., MOIR, L. M., BURGESS, J. K., BLACK, J. L. & OLIVER, B. G. 2011. Effects of beta(2) Agonists, Corticosteroids, and Novel Therapies on

Rhinovirus-Induced Cytokine Release and Rhinovirus Replication in Primary Airway Fibroblasts. *J Allergy (Cairo)*, 2011**,** 457169.

VANHAESEBROECK, B., GUILLERMET-GUIBERT, J., GRAUPERA, M. & BILANGES, B. 2010. The emerging mechanisms of isoform-specific PI3K signalling. *Nat Rev Mol Cell Biol,* 11**,** 329-41.

VESTBO, J., SORENSEN, T., LANGE, P., BRIX, A., TORRE, P. & VISKUM, K. 1999. Long-term effect of inhaled budesonide in mild and moderate chronic obstructive pulmonary disease: a randomised controlled trial. *Lancet,* 353**,** 1819-23.

VLAHOS, C. J., MATTER, W. F., HUI, K. Y. & BROWN, R. F. 1994. A specific inhibitor of phosphatidylinositol 3-kinase, 2-(4-morpholinyl)-8-phenyl-4H-1-benzopyran-4-one (LY294002). *J Biol Chem,* 269**,** 5241-8.

WAJANT, H., PFIZENMAIER, K. & SCHEURICH, P. 2003. Tumor necrosis factor signaling. *Cell Death Differ,* 10**,** 45-65.

WANG, Q., NAGARKAR, D. R., BOWMAN, E. R., SCHNEIDER, D., GOSANGI, B., LEI, J., ZHAO, Y., MCHENRY, C. L., BURGENS, R. V., MILLER, D. J., SAJJAN, U. & HERSHENSON, M. B. 2009. Role of double-stranded RNA pattern recognition receptors in rhinovirus-induced airway epithelial cell responses. *J Immunol,* 183**,** 6989-97.

WARK, P., TOOZE, M., POWELL, H. & PARSONS, K. 2013. Viral and bacterial infection in acute asthma & chronic obstructive pulmonary disease increases the risk of readmission. *Respirology*.

WEDZICHA, J. A. 2004. Role of viruses in exacerbations of chronic obstructive pulmonary disease. *Proc Am Thorac Soc,* 1**,** 115-20.

WEDZICHA, J. A., SEEMUNGAL, T. A., MACCALLUM, P. K., PAUL, E. A., DONALDSON, G. C., BHOWMIK, A., JEFFRIES, D. J. & MEADE, T. W. 2000. Acute exacerbations of chronic obstructive pulmonary disease are accompanied by elevations of plasma fibrinogen and serum IL-6 levels. *Thromb Haemost,* 84**,** 210-5.

WEICHHART, T. & SAEMANN, M. D. 2009. The multiple facets of mTOR in immunity. *Trends Immunol,* 30**,** 218-26.

WILKINSON, T. M., HURST, J. R., PERERA, W. R., WILKS, M., DONALDSON, G. C. & WEDZICHA, J. A. 2006. Effect of interactions between lower airway bacterial and rhinoviral infection in exacerbations of COPD. *Chest,* 129**,** 317-24.

WITKO-SARSAT, V., HALBWACHS-MECARELLI, L., SCHUSTER, A., NUSBAUM, P., UEKI, I., CANTELOUP, S., LENOIR, G., DESCAMPS-LATSCHA, B. & NADEL, J. A. 1999. Proteinase 3, a potent secretagogue in airways, is present in cystic fibrosis sputum. *Am J Respir Cell Mol Biol,* 20**,** 729-36.

WONG, J., ZHANG, J., SI, X., GAO, G., MAO, I., MCMANUS, B. M. & LUO, H. 2008. Autophagosome supports coxsackievirus B3 replication in host cells. *J Virol,* 82**,** 9143-53.

WONG, J. K., CAMPBELL, G. R. & SPECTOR, S. A. 2010. Differential induction of interleukin-10 in monocytes by HIV-1 clade B and clade C Tat proteins. *J Biol Chem,* 285**,** 18319-25.

WOOTTON, S. C., KIM, D. S., KONDOH, Y., CHEN, E., LEE, J. S., SONG, J. W., HUH, J. W., TANIGUCHI, H., CHIU, C., BOUSHEY, H., LANCASTER, L. H., WOLTERS,

P. J., DERISI, J., GANEM, D. & COLLARD, H. R. 2011. Viral infection in acute exacerbation of idiopathic pulmonary fibrosis. *Am J Respir Crit Care Med,* 183**,** 1698-702.

WOS, M., SANAK, M., SOJA, J., OLECHNOWICZ, H., BUSSE, W. W. & SZCZEKLIK, A. 2008. The presence of rhinovirus in lower airways of patients with bronchial asthma. *Am J Respir Crit Care Med,* 177**,** 1082-9.

WU, Q., VAN DYK, L. F., JIANG, D., DAKHAMA, A., LI, L., WHITE, S. R., GROSS, A. & CHU, H. W. 2013. Interleukin-1 receptor-associated kinase M (IRAK-M) promotes human rhinovirus infection in lung epithelial cells via the autophagic pathway. *Virology,* 446**,** 199-206.

WU, Y. T., TAN, H. L., SHUI, G., BAUVY, C., HUANG, Q., WENK, M. R., ONG, C. N., CODOGNO, P. & SHEN, H. M. 2010. Dual role of 3-methyladenine in modulation of autophagy via different temporal patterns of inhibition on class I and III phosphoinositide 3-kinase. *J Biol Chem,* 285**,** 10850-61.

XIA, Y., PAUZA, M. E., FENG, L. & LO, D. 1997. RelB regulation of chemokine expression modulates local inflammation. *Am J Pathol,* 151**,** 375-87.

XIE, S., CHEN, M., YAN, B., HE, X., CHEN, X. & LI, D. 2014. Identification of a role for the PI3K/AKT/mTOR signaling pathway in innate immune cells. *PLoS One,* 9**,** e94496.

YAMAMOTO, M., SATO, S., HEMMI, H., SANJO, H., UEMATSU, S., KAISHO, T., HOSHINO, K., TAKEUCHI, O., KOBAYASHI, M., FUJITA, T., TAKEDA, K. & AKIRA, S. 2002. Essential role for TIRAP in activation of the signalling cascade shared by TLR2 and TLR4. *Nature,* 420**,** 324-9.

YONEYAMA, M. & FUJITA, T. 2010. Recognition of viral nucleic acids in innate immunity. *Rev Med Virol,* 20**,** 4-22.

YORDY, B., TAL, M. C., HAYASHI, K., AROJO, O. & IWASAKI, A. 2012. Autophagy and selective deployment of Atg proteins in antiviral defense. *Int Immunol*.

YUAN, H. X., RUSSELL, R. C. & GUAN, K. L. 2013. Regulation of PIK3C3/VPS34 complexes by MTOR in nutrient stress-induced autophagy. *Autophagy,* 9**,** 1983-95.

YUM, H. K., ARCAROLI, J., KUPFNER, J., SHENKAR, R., PENNINGER, J. M., SASAKI, T., YANG, K. Y., PARK, J. S. & ABRAHAM, E. 2001. Involvement of phosphoinositide 3-kinases in neutrophil activation and the development of acute lung injury. *J Immunol,* 167**,** 6601-8.

ZAHEER, R. S. & PROUD, D. 2010. Human rhinovirus-induced epithelial production of CXCL10 is dependent upon IFN regulatory factor-1. *Am J Respir Cell Mol Biol,* 43**,** 413-21.

ZHANG, T., QI, Y., LIAO, M., XU, M., BOWER, K. A., FRANK, J. A., SHEN, H. M., LUO, J., SHI, X. & CHEN, G. 2012. Autophagy is a cell self-protective mechanism against arsenic-induced cell transformation. *Toxicol Sci,* 130**,** 298-308.

ZHANG, Y., LEE, T. C., GUILLEMIN, B., YU, M. C. & ROM, W. N. 1993. Enhanced IL-1 beta and tumor necrosis factor-alpha release and messenger RNA expression in macrophages from idiopathic pulmonary fibrosis or after asbestos exposure. *J Immunol,* 150**,** 4188-96.

ZHAO, J., BENAKANAKERE, M. R., HOSUR, K. B., GALICIA, J. C., MARTIN, M. & KINANE, D. F. 2010. Mammalian target of rapamycin (mTOR) regulates TLR3 induced cytokines in human oral keratinocytes. *Mol Immunol,* 48**,** 294-304.

ZHAO, W., QI, J., WANG, L., ZHANG, M., WANG, P. & GAO, C. 2012. LY294002 inhibits TLR3/4-mediated IFN-beta production via inhibition of IRF3 activation with a PI3K-independent mechanism. *FEBS Lett,* 586**,** 705-10.

ZHENG, Y., AN, H., YAO, M., HOU, J., YU, Y., FENG, G. & CAO, X. 2010. Scaffolding adaptor protein Gab1 is required for TLR3/4- and RIG-I-mediated production of proinflammatory cytokines and type I IFN in macrophages. *J Immunol,* 184**,** 6447-56.

ZHONG, B., YANG, Y., LI, S., WANG, Y. Y., LI, Y., DIAO, F., LEI, C., HE, X., ZHANG, L., TIEN, P. & SHU, H. B. 2008. The adaptor protein MITA links virus-sensing receptors to IRF3 transcription factor activation. *Immunity,* 29**,** 538-50.

ZHONG, B., ZHANG, L., LEI, C., LI, Y., MAO, A. P., YANG, Y., WANG, Y. Y., ZHANG, X. L. & SHU, H. B. 2009. The ubiquitin ligase RNF5 regulates antiviral responses by mediating degradation of the adaptor protein MITA. *Immunity,* 30**,** 397-407.

ZHOU, D., KANG, K. H. & SPECTOR, S. A. 2012. Production of interferon alpha by human immunodeficiency virus type 1 in human plasmacytoid dendritic cells is dependent on induction of autophagy. *J Infect Dis,* 205**,** 1258-67.

ZHOU, H., LIAO, J., ALOOR, J., NIE, H., WILSON, B. C., FESSLER, M. B., GAO, H. M. & HONG, J. S. 2013. CD11b/CD18 (Mac-1) is a novel surface receptor for extracellular double-stranded RNA to mediate cellular inflammatory responses. *J Immunol,* 190**,** 115-25.

ZHU, L., BARRET, E. C., XU, Y., LIU, Z., MANOHARAN, A. & CHEN, Y. 2013a. Regulation of Cigarette Smoke (CS)-Induced Autophagy by Nrf2. *PLoS One,* 8**,** e55695.

ZHU, S., CAO, L., YU, Y., YANG, L., YANG, M., LIU, K., HUANG, J., KANG, R., LIVESEY, K. M. & TANG, D. 2013b. Inhibiting autophagy potentiates the anticancer activity of IFN1@/IFNalpha in chronic myeloid leukemia cells. *Autophagy,* 9**,** 317-27.

ZHU, Z., TANG, W., GWALTNEY, J. M., JR., WU, Y. & ELIAS, J. A. 1997. Rhinovirus stimulation of interleukin-8 in vivo and in vitro: role of NF-kappaB. *Am J Physiol,* 273**,** L814-24.

ZHU, Z., TANG, W., RAY, A., WU, Y., EINARSSON, O., LANDRY, M. L., GWALTNEY, J., JR. & ELIAS, J. A. 1996. Rhinovirus stimulation of interleukin-6 in vivo and in vitro. Evidence for nuclear factor kappa B-dependent transcriptional activation. *J Clin Invest,* 97**,** 421-30.

ZOLAK, J. S. & DE ANDRADE, J. A. 2012. Idiopathic pulmonary fibrosis. *Immunology and allergy clinics of North America,* 32**,** 473-85.